Université Lille 1

Laboratoire de Mécanique de Lille (UMR CNRS 8107)

Ecole Doctorale régionale Sciences Pour l'Ingénieur Lille Nord-de France

Année 2013 - N° d'ordre : 41294

THESE

pour obtenir le grade de

DOCTEUR DE L'UNIVERSITE DE LILLE I

Discipline : Génie Civil

présentée et soutenue publiquement par

Long CHENG

Date de soutenance : le 11 Décembre 2013

Homogenization of porous media with plastic matrix and non associated flow rule by variational methods

JURY

M. Gărăjeu	Maître de Conférence, HDR, Université d'Aix-Marseille	Rapporteur
V. Monchiet	Maître de Conférence, HDR, Université Paris-Est	Rapporteur
C. Bouby	Maître de Conférence, Université de Lorraine	Examinateur
L. Dormieux	Professeur, ENPC, Champs-sur-Marne	Examinateur
J. Pastor	Professeur, Université de Savoie	Examinateur
D. Weichert	Professeur, RWTH Aachen University, Germany	Examinateur
G. De Saxcé	Professeur, LML, Université de Lille 1	Directeur de thèse
D. Kondo	Professeur, Université Pierre et Marie Curie, Paris VI	Co-directeur de thèse

Mis en page avec la classe thloria.

Acknowledgements

This thesis was realised in Laboratory of Mechanics of Lille (LML). My deepest gratitude goes first and foremost to my supervisor - Professor Géry de Saxcé, and to my co-supervisor - Professor Djimédo Kondo, for their vital encouragement and patient guidance, generous assistance and invaluable advice, all of which have been of inestimable worth to the completion of this thesis.

Secondly, I would like to specially express my heartfelt gratitudes to Mrs. Yun Jia and Mr. Abdelbacet Oueslati, who have helped and taught me immensely during the three years, and who have participated my oral defence presentation as invited committees. I would also like to thank to Professor Jian-Fu Shao and Professor Emmanuel Leriche who have helped me a lot for the posts of Moniteur and ATER.

I would like to particularly thank to Professor Luc Dormieux who did me great honour for chairing the oral defence committees, as weel as Mr. Vincent Monchiet and Mr. Mihail Garajeu for being the rapporteurs of my thesis. I would like to equivalently thank to Professor Joseph Pastor, Professor Dieter Weichert, Mrs. Céline Bouby who have kindly examined this work.

I express my gratitude to the Ministere Francais de l'Enseignment Superieure et de la Recherche who has financed this work by a research allocation.

My gratitude also goes to my friends and colleagues of LML, particularly to Wanqing Shen and Hanbing Bian for their valuable advices and generous help, equivalently to Lifeng, Mingyao, Ramzi, Marie-Christine, Nathalie, Anne-Marie,...

The last but no least, my thanks would also go to my beloved parents and my girlfriend Yue for their boundless love and whole-hearted support over all these past years.

Table des matières

Principales Notations

- **Tensor notations**

T	scalar	.	simple contraction
$\boldsymbol{T}$	tensor of ordre two	:	double contraction
$tr\boldsymbol{T}$	trace du tenseur $\boldsymbol{T}$	$\otimes$	tensor product
$grad\boldsymbol{T}$	gradient of a vector field		
$\mathbf{1}$	identity tensor of order two		

- **Notations for all chapters**

$\boldsymbol{\sigma}$	microscopic stress field
$\boldsymbol{v}$	velocity field
$\boldsymbol{\varepsilon}$	microscopic strain field
$\boldsymbol{d}$	microscopic strain rate field
π	local dissipation
$\boldsymbol{\Sigma}$	macroscopic stress field
$\boldsymbol{E}$	macroscopic strain field
$\boldsymbol{D}$	mAcroscopic strain rate field
Π	macrscopic dissipation
f	porosité
$\dot{f}$	porosité evolution
E	module d'Young
ν	coefficient de Poisson

General introduction

Micromechanical investigation of ductile porous materials starts more than forty years ago with studies by McClintock (1968) and Rice and Tracey (1969) which have been based on variational procedures. These studies have successfully led to establish spherical and cylindrical voids growth law when the solid matrix is von Mises type. They were developed for dilute concentration of voids and do not account for any coupling between the plastic behavior of the matrix and the void growth. Coupled models were initiated by Gurson (1977) who developed for a hollow sphere and a hollow cylinder a kinematical limit analysis approach. The considered cells are made up of a rigid ideal plastic matrix and were subjected to an arbitrary homogeneous strain rate boundary conditions. From this procedure, which required in particular the choice of an appropriate class of trial velocity fields, Gurson derived a macroscopic yield function, exact for the hollow sphere subjected to a hydrostatic external loading and accounting for pressure sensitivity due to the porosity. Owing to the kinematical LA derivation, it was shown later (see for instance (Leblond, 2003)) that the Gurson yield surface constitutes an upper bound for isotropic ductile porous materials, at least for those whose microstructure can be represented by Hashin composite-sphere assemblage.

Several micromechanically-based extensions of Gurson's model have been further proposed in the literature. Improved predictions of the original Gurson model have been obtained by reconsidering the Gurson approach with refined trial velocity fields. For instance, this was done by Gãrãjeu (1995); Gãrãjeu et al. (2000) considered the exact solution of the elastic hollow sphere subjected to an arbitrary loading. Later, Monchiet et al. (2007), Monchiet et al. (2011) used a class of Eshelby-based velocity fields. Notably, important developments in the early 90's aim at accounting for void shape effects (Gologanu et al., 1993, 1994, 1997; Garajeu et al., 1997; Monchiet et al., 2007). They open the way to new applications and issues including for instance the computationnal investigation of the effects of penny shaped cracks on ductile behavior. Still in the context of ductile porous metals another, matrix plastic anisotropy has been taken into account by Benzerga et al. (2001) for spherical voids, and later by Monchiet et al. (2006) for spheroidal cavities (see also (Monchiet et al., 2008)). Mention has to be made also of studies devoted to porous materials with incompressible matrix exhibiting asymmetry between tension and compression (Cazacu and Stewart, 2009).
Another important class of development in the context of classical limit analysis, crucial for applications to polymer and cohesive geomaterials, concerns the consideration of plastic compressibility of the matrix through a Drucker-Prager model (Jeong et al., 1995; Jeong, 2002; Guo et al., 2008), with obviously an associated yielding rule. Application of this class of models has been done in (Lin et al., 2011a,b; Shen et al., 2012). As in Gurson study, a trial velocity field combining the exact solution to the Drucker-Prager hollow sphere an hydrostatic loading and linear terms has been considered. Owing to difficulties to rigorously satisfy the admissibility condition, the authors success to formulate a macroscopic

criterion by relaxing this condition. Numerical limit analysis bounds, provided later by Thoré et al. (2009), have later allowed to rigorously assess the Guo et al criteria. Alternatively to limit analysis approach, by making use of variational techniques in non linear homogenization framework, Ponte-Castañeda (Ponte-Castañeda, 1991)[1] obtained nonlinear Hashin-Shtrikman type upper bounds for von Mises plastic materials containing spherical voids. To improve results predicted by the above mentioned variationnal method, Danas and Ponte-Castaneda (Danas et al., 2008) recently derived accurate yield surfaces for porous materials by using a second order homogenization method. A notable advantage of this second order approach is to predict effects of the stress deviator third invariant for isotropic microtructures. Note also that this effect has also be investigated in recent numerical studies by Thore et al. (2011) and fully predicted by Cazacu et al. (Cazacu et al., 2013) by revisiting the Gurson kinematical approach..

A convex and lower semi-continuous function ϕ, called a superpotential (or pseudo-potential), such that the graph is the one of its subdifferential $\partial\phi$. The function ϕ and its Fenchel conjugate ϕ^* verifies for any couple of dual variables Fenchel's inequality. The dissipative materials admitting a superpotential of dissipation are often qualified as standard (Halphen et al., 1975) and the law is said to be a normality law, a subnormality law or an associated law.

A common point of all the above studies, excepted that of Maghous et al. (2009), is that they consider plastic matrix obeying to normality law (Generalized Standard Materials, GSM, introduced by Halphen et al. (1975))[2] as required by classical limit analysis theory. However, several experimental laws of various engineering materials, particularly in Plasticity, are non-associated. For such laws, de Saxcé proposed in de Saxcé et al. (1991); de Saxcé (1992) a suitable modeling framework based on the concept of Bipotential, a function b of both dual variables (stress and strain), convex and lower semicontinuous in each argument and satisfying a cornerstone inequality saying that for any couple of dual variables the value of the bipotential is greater than or equal to their duality pairing. When equality holds, the couple is said extremal. In a mechanical view point, the extremal couples are the ones satisfying the constitutive law. Materials admitting a bipotential are called Implicit Standard Materials (ISM) because the constitutive law is a subnormality law but the relation between the dual variables is implicit. The classical standard materials corresponds to the particular event of the bipotential being separated as the sum of a superpotential and its conjugate one. In this sense, the cornerstone inequality of the bipotential generalizes Fenchel's one. The existence and construction of a bipotential for a given constitutive law has been recently discussed in Buliga et al. (2008, 2009a, 2010a).

Linked to the structural mechanics and in particular with the Calculus of Variation, the bipotential theory offers an elegant framework for a broad spectrum of non-associated laws. Examples of such non-associated constitutive laws are:

- Non-associated Drucker-Prager (de Saxcé, 1993; Berga et al., 1994; de Saxcé, 2002;

[1] *A similar derivation has been done by Suquet (Suquet, 1992) for cylindrical voids.*

[2] *This class of dissipative materials is known to admit a superpotential of dissipation (or pseudo-potential).*

Bousshine et al., 2001; Hjiaj et al., 2003) and Cam-Clay models (de Saxcé, 1995; Zouain et al., 2007),

- the non linear kinematical hardening rule for cyclic Plasticity (de Saxcé, 1992; Bodovillé et al., 2001) and Viscoplasticity (Hjiaj et al., 2000; Magnier et al., 2006; Bouby et al., 2006, 2009),
- Lemaitre's damage law (Bodovillé , 1999),
- the coaxial laws (de Saxcé, 2002; Vallée et al., 2005),
- Coulomb's friction law (de Saxcé, 1998, 1992, 1993, 1998, 2002; Bousshine et al., 2002; Hjiaj et al., 2002, 2004; Feng et al., 2006b,a; Fortin et al., 1999, 2002; Laborde et al., 2008),
- the blurred constitutive laws (Buliga et al., 2009b, 2010b).

A complete survey of the bipotential approach can be found in (de Saxcé, 2002). In the previous works, robust numerical algorithms were proposed to solve structural mechanics problems.

Let us come now to the Limit Analysis theory which provides a general framework to determine the plastic collapse of structures under proportional loading (Save et al. (1997), de Buhan (1986), Suquet (1982); Salençon (1983), Chen (1975); Chen et al. (1990)), but is restricted to associated plasticity. The classical presentation of the non-associated plasticity is based on a yield function and a plastic potential. The bipotential offers an alternative framework which opens naturally to a variational formulation. This has permitted an extension of limit analysis techniques to non-associated laws (de Saxcé, 2002; Bousshine et al., 2001, 2002; Chaaba et al., 2010; Zouain et al., 2007). Note also extension to the repeated variable loadings, the so-called shakedown theory, to the ISM by the bipotential approach (de Saxcé (2002); Bousshine et al. (2001, 2003); Bouby et al. (2006, 2009)).

The main objective of this thesis is to develop and implement extended limit analysis in the context of ductile porous (geo)materials whose matrix obeys to non associated laws. The final procedure will be based on the bipotential-based variational approach for which a trial stress field and a trial velocity field should be considered. The manuscript is organized into 4 chapters as follows:

The first chapter presents the basic principles of potentials-based modelings in continuum mechanics and limit analysis theory. The later is applied successively to porous materials with a von Mises matrix and then a Drucker-Prager one, delivering respectively the well known Gurson model (Gurson, 1977) and Guo et al. model (Guo et al., 2008). In the first part of the chapter we present the bipotential theory which offers a rigorous mathematical framework for modeling materials with non associated constitutive laws (for instance the Drucker-Prager one). Extension of the classical limit analysis theorems to non associated plasticity is then described on the basis of suitable variational formulations. This will be helpful for several developments in the thesis.

The second chapter is devoted to formulate a new statically based model of ductile porous materials having a von Mises matrix. In contrast to the Gurson's well known kinematical approach applied to a hollow sphere, the proposed study proceeds by means of a statical limit analysis procedure. The established results clearly provide a closed-form expression of the statically-based macroscopic criterion. Due to the relaxed boundary condition resulting from the chosen trial stress field, the criterion will be seen only on as a quasi-lower bound. Interestingly, it will be shown that it depends not only on the macroscopic mean stress and equivalent stress, but also on the sign of the third invariant of the stress deviator.
This stress variational model is extended to non-axisymmetric trial stress formulation case by considering more general stress field. This new macroscopic criterion depends on the macroscopic mean stress, equivalent stress and the Lode angle (or the third invariant of the stress deviator) in three dimensional context.

The third chapter aims at calculating the plastic limit state of a hollow sphere with a non associated Drucker-Prager matrix and subjected to hydrostatic loading. This study can be considered as the first step to propose a macroscopic plastic model for this class of porous materials. It is concluded that for the hydrostatically loaded hollow sphere, the limit load and stress field of the non-associated cases are the same as for the associated one.

The last chapter is devoted to a general macroscopic model for porous materials with non-associated Drucker-Prager matrix, by using the bipotential-based limit analysis method and non-linear homogenization techniques. A trial stress field and a trial velocity field are adopted for the formulation, which allow to obtain a closed-form macroscopic criterion for the new class of materials and a non-associated macroscopic flow rule which has never been introduced in literature. The theoretical results are validated by comparison with numerical ones performed during this thesis.

References

Benzerga, A.A., Besson, J., 2001. Plastic potentials for anisotropic porous solids. European Journal of Mechanics A/Solids, 20, 397-434.

Berga, A., de Saxcé, G., 1994. Elastoplastic Finite Element Analysis of Soil Problems with Implicit Standard Material Constitutive Laws, Revue Européenne des éléments finis, 3, 411-456.

Bodovillé, G., 1999. On damage and implicit standard materials, C. R. Acad. Sci. Paris, Sér. II, Fasc. b, Méc. Phys. Astron., 327, 715-720.

Bodovillé, G., de Saxcé, G., 2001. Plasticity with non linear kinematic hardening : modelling and shakedown analysis by the bipotential approach. Eur. J. Mech., A/Solids, 20, 99-112.

Bouby, C., de Saxcé, G., Tritsch, 2006. A comparison between analytical calculations of the shakedown load by the bipotentiel approach and step-by-step computations for elastoplastic materials with nonlinear kinematic hardening. International Journal of Solids and Structures, 43(9), 2670-2692.

Bouby, C., de Saxcé, G., Tritsch, 2009. Shakedown analysis: comparison between models with the linear unlimited, linear limited and non linear kinematic hardening. Mechanical Research Communication. 36, 556-562.

Bousshine, L., Chaaba, A., de Saxcé, G., 2001. Softening in stress-strain curve for Drucker-Prager non-associated plasticity. Int. J. of Plasticity, 17(1), 21-46.

Bousshine, L., Chaaba, A., de Saxcé, G., 2002. Plastic limit load of plane frames with frictional contact supports. Int. J. Mech. Sci., 44, 2189-2216, 2002.

Bousshine, L., Chaaba, A., de Saxcé, G., 2003. A new approach to shakedown analysis for non-standard elastoplastic material by the bipotential. Int. J. of Plasticity, 19(5), 583-598.

Buliga, M., de Saxcé, G. Vallée, C., 2008. Existence and construction of bipotential for graphs of multivalued laws. Journal of Convex Analysis. J. Convex Analysis, 15(1), 87-104.

Buliga, M., de Saxcé, G. Vallée, C., 2009. Bipotentials for non monotone multivalued operators: fundamental results and applications. Acta Applicandae Mathematicae, 110(2), 955-972.

Buliga, M., de Saxcé, G. Vallée, C., 2009. Blurred constitutive laws and bipotential convex covers. Mathematics and Mechanics of Solid Journal. First on line.

Buliga, M., de Saxcé, G. Vallée, C., 2010. Non maximal cyclically monotone graphs and construction of a bipotential for the Coulomb's dry friction law. J. Convex Analysis, 17(1), 81-94.

Buliga, M., de Saxcé, G. Vallée, C., 2010. Blurred maximal cyclically monotone sets and bipotentials. Analysis and Applications, 8(4), 323-336.

Chaaba, A., Bousshine, L., de Saxcé, G., 2010. Kinematic Limit Analysis of Nonassociated Perfectly Plastic Material by the Bipotential Approach and Finite Element Method. J. Appl. Mech., 77(3), 031016.

O. Cazacu and J. B. Stewart. Plastic potentials for porous aggregates with the matrix exhibiting tension-compression asymmetry. Journal of the Mechanics and Physics of Solids, 57 : 325-341, 2009.

Cazacu, O., Revil-Baudard, B., Lebensohn, R., Garajeu, M., 2013. On the Combined Effect of Pressure and Third Invariant on Yielding of Porous Solids With von Mises Matrix. Journal of Applied Mechanics, DOI: 10.1115/1.4024074.

Chen, W.F., 1975. Limit Analysis and Soil Plasticity. Elsevier, New York.

Chen, W.F., Liu, X.L., 1990. Limit analysis in soil mechanics. Developments in Geotechnical Engineering, Vol. 52.

Danas, K., Idiart, M. I. and Ponte-Castañeda, P. A homogenization-based constitutive model for isotropic viscoplastic porous media. Int. J. Solid. Struct., 45 : 3392-3409, 2008.

de Buhan, P. A fundamental approach to the yield design of reinforced soil structures Chap. 2: yield design homogenization theory for periodic media, Ph.D. Thesis, Univ. Pierre et Marie Curie, Paris VI, 1986.

de Saxcé, G., Feng, Z.Q., 1991. New inequality and functional for contact friction: The implicit standard material approach. Mechanics of Structures and Machines, 19, 301-325, 1991.

de Saxcé, G., 1992. Une généralisation de l'inégalité de Fenchel et ses applications aux lois constitutives. C. R. Acad. Sci. Paris, Sér. II, 314, 125-129, 1992.

de Saxcé, G., Bousshine, L., 1993. On the extension of limit analysis theorems to the non-associated flow rules in soils and to the contact with Coulomb's friction. XI Polish Conference on Computer Methods in Mechanics. Kielce, Poland, 815-822.

de Saxcé, G., 1995. The bipotential method, a new variational and numerical treatment of the dissipative laws of materials. 10th Int. Conf. on Mathematical and Computer Modelling and Scientific Computing, Boston, Massachusetts.

de Saxcé, G., Bousshine, L., 1998. Limit Analysis Theorems for the Implicit Standard Materials: Application to the Unilateral Contact with Dry Friction and the Non Associated Flow Rules in Soils and Rocks. Int. J. Mech. Sci., 40(4),387-398.

de Saxcé, G., Feng, Z.Q., 1998. The bi-potential method: a constructive approach to design the complete contact law with friction and improved numerical algorithms. Mathematical and Computer Modelling, 6, 225-245, 1998.

de Saxcé, G., Bousshine, L., 2002. Implicit standard materials. D. Weichert G. Maier eds. Inelastic behaviour of structures under variable repeated loads, CISM Courses and Lectures 432, Springer, Wien.

I. Ekeland, I., Temam, R., 1975. Convex analysis and variational problems, Amsterdam, North Holland.

Feng, Z.Q., Hjiaj, M., de Saxcé, G., Mróz, Z., 2006. Effect of frictional anisotropy on the quasistatic motion of a deformable solid sliding on a planar surface. Comput. Mech., 37, 349-361.

Feng, Z.Q., Hjiaj, M., de Saxcé, G., Mróz, Z., 2006. Influence of frictional anisotropy on contacting surfaces during loading/unloading cycles. International Journal of Non-Linear Mechanics, 41(8), 936-948.

Fortin, J., de Saxcé, G., 1999. Modlisation numrique des milieux granulaires par lapproche du bipotentiel. C.R. de lAcadmie des Sciences, Srie IIb, 327, 721-724.

Fortin, J., Hjiaj, M., de Saxcé, G., 2002. An improved discrete element method based on a variational formulation of the frictional contact law. Comput. Geotech., 29, 609-640.

Garajeu, M., Suquet, P., 1997. Effective properties of porous ideally plastic or viscoplastic materials containing rigid particles. Journal of the Mechanics and Physics of Solids, 45, 873-902.

M. Gãrãjeu. Contribution à l'étude du comportement non linéaire de milieux poreux avec ou sans renfort. PhD Thesis, University of Marseille, 1995.

M. Garajeu, J.C. Michel, P. Suquet, A micromechanical approach of damage in viscoplastic materials by evolution in size, shape and distribution of voids. *Comput. Methods Appl. Mech. Engrg.*, 183, 223-246, 2000.

Gologanu, M., Leblond, J.-B., Devaux, J., 1993. Approximate models for ductile metals containing non-spherical voids - case of axisymmetric prolate ellipsoidal cavities. J. Mech. Phys. Solids 41 (11), 1723e1754.

Gologanu, M., Leblond, J.B., Perrin, G., Devaux, J., 1994. Approximate models for ductile metals containing non-spherical voids - case of axisymmetric oblate ellipsoidal cavities. J. Engrg. Mat. Tech. 116, 290e297.

Gologanu, M., Leblond, J.B., Perrin, G., Devaux, J., 1997. Recent extensions of Gurson's model for porous ductile metals. P. Suquet (Ed.), Continuum Micromechanics, Springer-Verlag.

Guo, T.F., Faleskog, J., Shih, C.F.2008. Continuum modeling of a porous solid with pressure-sensitive dilatant matrix. Journal of the Mechanics and Physics of Solids, 56, 2188-2212.

Gurson, A.L., 1977. Continuum theory of ductile rupture by void nucleation and growth – part I: Yield criteria and flow rules for porous ductile media, Journal of Engineering Materials and Technology, 99, 2-15.

Halphen, B., Nguyen Quoc, S., 1975. Sur les matériaux standard généralisés. C. R. Acad. Sci. Paris, 14, 39-63.

Hjiaj, M., Bodovillé, G., de Saxcé, G., 2000. Matériaux viscoplastiques et loi de normalité implicites. C. R. Acad. Sci. Paris, Sér. II, Fasc. b, Méc. Phys. Astron., 328, 519-524.

Hjiaj, M., de Saxcé, G., Mróz, Z., 2002. A variational-inequality based formulation of the frictional contact law with a non-associated sliding rule. European Journal of Mechanics A/Solids, 21, 49-59.

Hjiaj, M., Fortin, J., de Saxcé, G., 2003. A complete stress update algorithm for the non-associated Drucker-Prager model including treatment of the apex. International Journal of Engineering Science, 41, 1109-1143.

Hjiaj, M., Feng, Z.Q., de Saxcé, G., Mróz, Z., 2004. Three dimensional finite element computations for frictional contact problems with on-associated sliding rule. Int. J. Numer. Methods Eng., 60, 2045-2076.

Jeong, H.Y., Pan, J., 1995. A macroscopic constitutive law for porous solids with pressure-sensitive matrices and its applications to plastic flow localization. Journal of the Mechanics and Physics of Solids, 39, 1385-1403.

Jeong, H.Y., 2002. A new yield function and a hydrostatic stress-controlled model for porous solids with pressure-sensitive matrices. Journal of the Mechanics and Physics of Solids, 32, 3669-3691.

Laborde, P., Renard, Y., 2008. Fixed points strategies for elastostatic frictional contact problems. Math. Meth. Appl. Sci., 31, 415-441.

J.-B. Leblond, Mécanique de la rupture fragile et ductile. Hermes, 2003.

J. Lin, J.-F. Shao, D. Kondo, 2011. A two scale model of porous rocks with DruckerPrager matrix: Application to a sandstone. Mechanics Research Communications 38 (2011) 602 606

J. Lin, S.Y. Xie, J.F. Shao and D. Kondo. A micromechanical modeling of ductile behavior of a porous chalk: Formulation, identification, and validation. International Journal for Numerical and Analytical Methods in Geomechanics. 36, (2012) 1245-1263.

Maghous, S., Dormieux, L., Barthélémy, J.F., 2009. Micromechanical approach to the strength propoerties of frictional geomaterials. European Journal of Mechanics A/Solids, 28, 179-188.

Magnier, V., Charkaluk, E., Bouby, C., de Saxcé, G., 2006. Bipotential Versus Return Mapping Algorithms: Implementation of Non-Associated Flow Rules, in Proceedings of The Eighth International Conference on Computational Structures Technology (las Palmas de Gran Canaria, sept. 12-15, 2006), B.H.V. Topping, G. Montero and R. Montenegro, (Editors), Civil-Comp Press, Stirlingshire, United Kingdom, paper 68.

McClintock, F.A., 1968. A criterion for ductile fracture by the growth of holes. Journal of Applied Mechanics, Vol.35, 363-371.

V. Monchiet, C. Gruescu, E. Charkaluk, D. Kondo. Approximate yield criteria for anisotropic metals with prolate or oblate voids. C.R. Mcanique. 334(7), 431-439, 2006.

Monchiet, V., Charkaluk, E., Kondo, D., 2007. An improvment of Gurson-type models of porous materials by Eshelby-like trial velocity fields. Comptes Rendus Mécanique, 335, 32-41.

Monchiet, V., Cazacu, O., Kondo, D., 2008. Macroscopic yield criteria for plastic anisotropic materials containing spheroidal voids. International Journal of Plasticity, 24, 1158-1189.

Monchiet, V., Charkaluk, E., Kondo, D., 2011. A micromechanics-based modification of the Gurson criterion by using Eshelby-like velocity fields. Vol 30, 940-949.

P. Ponte-Castañeda. The effective mechanical properties of nonlinear isotropic composites. J. Mech. Phys. Solids, 39 : 45-71, 1991.

Rice, J.R. and Tracey, D.M., 1969. On the ductile fracture enlargement of voids in triaxial stress fields. J. Mech. Phy. Solids, Vol.17, 201-217.

Salençon, Calcul la rupture et analyse limite, Presses de lENPC, 1983.

Save, M.A., Massonnet, C.E., de Saxcé, G., 1997. Plastic limit analysis of plates, shells and disks. Elsevier, New York.

Shen, W.Q., Shao, J-F, Kondo, D., Gatmiri, B., 2012. A micromacro model for clayey rocks with a plastic compressible porous matrix. International Journal of Plasticity, 36, 64-85.

Suquet, P. Plasticité et homogénéisation. Ph.D. Thesis, Univ. Pierre et Marie Curie, Paris VI, 1982.

P. Suquet, On bounds for the overall potential of power law materials containing voids with an arbitrary shape. Mech. Res. Com., 19 : 51-58, 1992.

Thoré, P., Pastor, F., Pastor, J., Kondo, D., 2009. Closed-form solutions for the hollow sphere model with Coulomb and Drucker-Prager materials under isotropic loadings. Comptes Rendus Mécanique, 337, 260-267.

Vallée, C., Lerintiu, C., Fortuné, D., Ban, M., de Saxcé, G., 2005. Hill's bipotential. M. Mihailescu-Suliciu eds. New Trends in Continuum Mechanics, Theta Series in Advanced Mathematics, Theta Foundation, Bucarest, Roumania, 339-351.

Zouain, N., Pontes Filho, I., Borges, L., Mouta da Costa, L., 2007. Plastic collapse in non-associated hardening materials with application to Cam-clay. International Journal of Solids and Structures, 44, 4382-4398.

Chapitre 1

Limit analysis and extension to non associated laws by the bipotential theory

1. Introduction:

This first chapter has several objectives:

- To recall the basic principles of some variational approaches useful for the engineering materials behaviors (linear and non linear).
- To present the framework of classical limit analysis which notably assumes an associated plasticity. An emphasis will be put on the two bounding theorems, namely the kinematical theorem (upper bound) and the statical one (lower bound). for the solid matrix.
- To illustrate the kinematical theorem in section 5.2 for the well known Gurson model corresponding to ductile porous materials with an incompressible (von Mises) matrix. This is completed in section 5.3 by the case of plastically compressible (Drucker-Prager) matrix. A prototype model for this class of porous materials is the one proposed by Guo et al. (Guo et al., 2008) (see also (Jeong et al. , 1995; Jeong , 2002)). It's presentation will allow to show some of the theoretical and computational difficulties related to the consideration of a Drucker-Prager matrix, even in the context of an associated plasticity. These difficulties probably explain why studies of porous materials with a non associated matrix are very seldom, the unique available study being the one recently carried out by Maghous et al. (2009) by means of the so-called modified secant moduli approach of the non-linear homogenization problem.
- To introduce the reader to the bipotential theory, proposed several years ago by G. de Saxcé and co-workers (see (de Saxcé et al., 1991; de Saxcé , 1992)). A noticeable advantage of this theory is that it provides suitable variational theorems for non associated materials, and then allows extension of limit analysis theorems to this class of materials. Derivation in the bipotential framework of the model proposed by (Guo et al., 2008) will be indicated in Chapter 4.
  This will path the way for the final goal of the present thesis which consists in formulating a complete homogenization theory for ductile porous materials with a non associated matrix.

Several scientific questions interestingly raised in the present chapter on the modeling of non-linear porous materials will be addressed in the following chapters.

2. Modeling the constitutive laws

In many theories of Mechanics, one of underlying mathematical structure consists in a constitutive law, that is a graph $M \subset X \times Y$ from a linear space X into its dual one Y. The dual pairing between these spaces will be denoted

$$X \times Y : (\boldsymbol{x}, \boldsymbol{y}) \mapsto \langle \boldsymbol{x}, \boldsymbol{y} \rangle$$

For instance, the dual variables can be the strain and stress tensors and the dual pairing is the double contracted product:

$$\mathbb{S}_3(\mathbb{R}) \times \mathbb{S}_3(\mathbb{R}) : (\boldsymbol{\varepsilon}, \boldsymbol{\sigma}) \mapsto \boldsymbol{\varepsilon} : \boldsymbol{\sigma}$$

Although general, the mathematical structure of graph is poverty-stricken for applications to the science of materials and the continuum mechanics. A fruitful idea is representing a constitutive law by a numerical function. The advantage is double:

- the constitutive laws can be **classified** in a convenient manner for theoretical and numerical purposes,
- but –maybe above all– powerful **variational methods** can be developed for the solving of boundary value problems by building functional from these functions.

For sake of clearness, these variational aspects are discussed latter on and we focuss our attention on the classification of constitutive laws.

2.1. Elasticity and potential

Hooke's elastic law –the queen of the constitutive laws– is a linear relation

$$\boldsymbol{\sigma} = \boldsymbol{C}\,(\boldsymbol{\varepsilon}) \tag{1}$$

A valuable property is the **reversibility**. More precisely, for any loop $\mathcal{C}$ in $X = \mathbb{S}_3(\mathbb{R})$, the stored work is zero

$$\int_{\mathcal{C}} \boldsymbol{\sigma} : d\boldsymbol{\varepsilon} = 0$$

where $\boldsymbol{\sigma} = \boldsymbol{C}\,(\boldsymbol{\varepsilon})$, hence the integrability condition

$$\forall d, \delta, \qquad d\boldsymbol{\varepsilon} : \delta\boldsymbol{\sigma} = \delta\boldsymbol{\varepsilon} : d\boldsymbol{\sigma}$$

which is satisfied if the elastic law is generated by a smooth numerical function π on X

$$\boldsymbol{\sigma} = D\,\pi\,(\boldsymbol{\varepsilon})$$

It is called a **potential** and the law is said to be a **normality law**. Its graph is a differential submanifold of dimension $n = 6$ in the space $X \times Y$ of dimension $2\,n$. Introducing the skew-symmetric bilinear form ω

$$\omega((d\boldsymbol{\varepsilon}, d\boldsymbol{\sigma}), (\delta\boldsymbol{\varepsilon}, \delta\boldsymbol{\sigma})) = d\boldsymbol{\varepsilon} : \delta\boldsymbol{\sigma} - \delta\boldsymbol{\varepsilon} : d\boldsymbol{\sigma}$$

called a **symplectic form**, the integrability condition means that the graph M of the elastic law is a **lagrangian submanifold** of the symplectic manifold $X \times Y$, that is an isotropic submanifold of maximal dimension $n = \frac{1}{2} dim(X \times Y)$. In the language of the analytical dynamics, π is a **generating function** for M. For more details on symplectic mechanics, the reader is refered for instance to Abraham et al. (1980).

The elastic energy stored during a loading along a path $\mathcal{C}$ from $\boldsymbol{\varepsilon}_0$ to $\boldsymbol{\varepsilon}$ is

$$\pi(\boldsymbol{\varepsilon}) = \pi(\boldsymbol{\varepsilon}_0) + \int_{\mathcal{C}} \boldsymbol{\sigma} : d\boldsymbol{\varepsilon}$$

where $\boldsymbol{\sigma}$ is given by (1) and the integral does not depends on the choice of the path (because of the reversibility). Clearly:

$$\pi(\boldsymbol{\varepsilon}) = \frac{1}{2}\,\boldsymbol{\varepsilon} : \boldsymbol{C}\,(\boldsymbol{\varepsilon})$$

Another relevant property of the elastic law is the **convexity** of the potential. For thermodynamical reasons and assuming $\pi(\mathbf{0}) = 0$, the stored energy must be non negative

$$\forall \boldsymbol{\varepsilon} \neq \mathbf{0}, \qquad \pi(\boldsymbol{\varepsilon}) > 0$$

A straighforward consequence is that π is convex and:

$$\forall \boldsymbol{\varepsilon}' \in X, \qquad \pi(\boldsymbol{\varepsilon}') - \pi(\boldsymbol{\varepsilon}) \geq D\,\pi\,(\boldsymbol{\varepsilon}) : (\boldsymbol{\varepsilon}' - \boldsymbol{\varepsilon})$$

2.2. Associated plasticity and superpotential

In plasticity or, more generally, in non smooth mechanics, the law is multivoque. It is represented by a set-valued map

$$X \to 2^Y : \boldsymbol{x} \mapsto M(\boldsymbol{x}) = \{\boldsymbol{y} \quad s.t. \quad (\boldsymbol{x}, \boldsymbol{y}) \in M\}$$

where the section $M(\boldsymbol{x})$ may be empty. There is always a converse law

$$Y \to 2^X : \boldsymbol{x} \mapsto M^*(\boldsymbol{y}) = \{\boldsymbol{x} \quad s.t. \quad (\boldsymbol{x}, \boldsymbol{y}) \in M\}$$

hence the equivalence

$$\boldsymbol{y} \in M(\boldsymbol{x}) \qquad \Leftrightarrow \qquad \boldsymbol{x} \in M^*(\boldsymbol{y}) \qquad \Leftrightarrow \qquad (\boldsymbol{x}, \boldsymbol{y}) \in M$$

The classical theory of plasticity is concerned by a class of materials (typically metals and alloys) for which :

- the elastic domain is a smooth, convex and closed subset K of Y,
- the plastic strain rate $\boldsymbol{d}$ is an exterior normal to K of undetermined intensity.

In convex analysis, the **subdifferential** of a function ϕ in a point $\mathbf{x}$ which is the (possibly empty) set:

$$\partial\phi(\mathbf{x}) = \{\mathbf{y} \mid \forall \mathbf{x}' \in X, \qquad \phi(\mathbf{x}') - \phi(\mathbf{x}) \geq \langle \mathbf{x}' - \mathbf{x}), \mathbf{y} \rangle\} \tag{2}$$

Of course, if ϕ is a smooth and convex function, the law is univalued and

$$\partial\phi(\mathbf{x}) = \{D\phi(\mathbf{x})\}$$

For more details on convex analysis, the reader is refered for instance to (Ekeland et al., 1975; Moreau , 2003; Rockafellar , 1970). On this ground, the concept of potential can be extended in a weak form. We do not require more than the function π to be convex and lower semicontinuous (with possible infinite values) and we consider multivalued laws generated by π according to

$$\boldsymbol{y} \in \partial \pi (\boldsymbol{x}) \tag{3}$$

The function π is called a **superpotential**. And the converse law? It takes a similar form

$$\boldsymbol{x} \in \partial \pi^* (\boldsymbol{y}) \tag{4}$$

where π^* is **Fenchel's transform** (or **conjugate**) of π

$$\pi^* (\boldsymbol{y}) = \sup_{\boldsymbol{x} \in X} (\langle \boldsymbol{x}, \boldsymbol{y} \rangle - \pi(\boldsymbol{x}))$$

As π is convex and lower semicontinuous, π^* so is and $\pi^{**} = \pi$. Consequently, the superpotential π and its Fenchel's conjugate π^* satisfy **Fenchel's inequality**

$$\forall \boldsymbol{x}' \in X, \boldsymbol{y}' \in Y, \qquad \pi(\boldsymbol{x}') + \pi^* (\boldsymbol{y}') \geq \langle \boldsymbol{x}', \boldsymbol{y}' \rangle \tag{5}$$

Moreover, (3) and (4) are equivalent to

$$\pi(\boldsymbol{x}) + \pi^* (\boldsymbol{y}) = \langle \boldsymbol{x}, \boldsymbol{y} \rangle \tag{6}$$

The materials generated by superpotentials are called **generalized standards materials**. For instance, the associated plasticity is obtained by taking π^* as the indicatory function χ_K of the elastic domain K (equal to zero in K and $+\infty$ otherwise) and by considering the **normal flow rule**

$$\boldsymbol{d} \in \partial \pi^* (\boldsymbol{\sigma}) \tag{7}$$

Its Fenchel's conjugate

$$\pi(\boldsymbol{d}) = \sup_{\boldsymbol{\sigma} \in K} (\boldsymbol{d} : \boldsymbol{\sigma}) \tag{8}$$

is called the **support function** of K. It is positively homogeneous of order 1. The converse law reads

$$\boldsymbol{\sigma} \in \partial \pi (\boldsymbol{d})$$

and the elastic domain K is nothing else $\partial \pi (\boldsymbol{0})$. Taking into account (6), the normal yielding rule (7) is satisfied if and only if

$$\boldsymbol{\sigma} \in K \qquad and \qquad \pi(\boldsymbol{d}) = \boldsymbol{d} : \boldsymbol{\sigma} \tag{9}$$

Also, the relation (7) is nothing else **Hill's inequality**

$$\forall \boldsymbol{\sigma}' \in K, \qquad (\boldsymbol{\sigma}' - \boldsymbol{\sigma}) : \boldsymbol{d} \leq 0 \tag{10}$$

The superpotential are useful tools to model a large calls of material behaviour, not only in plasticity but also for instance in viscoplasticity and damage theory but there are

exceptions, the monotone maximal laws and the non associated laws for instance. On the ground of the previous considerations and in order to span a more general family of constitutive laws, we extend the concept of generating object in the following sense. We call **(generalized) generating function** for a graph $M \subset X \times Y$ a numerical function g defined on $X \times Y$ such that

$$\boldsymbol{y} \in \partial g\left(\cdot, \boldsymbol{y}\right), (\boldsymbol{x}) \qquad \Leftrightarrow \qquad \boldsymbol{x} \in \partial g\left(\boldsymbol{x}, \cdot\right), (\boldsymbol{y}) \qquad \Leftrightarrow \qquad (\boldsymbol{x}, \boldsymbol{y}) \in M$$

For instance, **Fenchel's function**

$$g(\boldsymbol{x}, \boldsymbol{y}) = \pi(\boldsymbol{x}) + \pi^*\left(\boldsymbol{y}\right) \tag{11}$$

is a generating function for the subdifferential $\partial\pi$ of the superpotential π.

2.3. Maximal monotone laws and Fitzpatrick's function

For a long time, the mathematicians have been interested in the **monotone graphs** $M \subset X \times Y$ such that

$$\forall (\boldsymbol{x}_1, \boldsymbol{y}_1), (\boldsymbol{x}_2, \boldsymbol{y}_2) \in M, \qquad \langle \boldsymbol{x}_2 - \boldsymbol{x}_1, \boldsymbol{y}_2 - \boldsymbol{y}_1 \rangle \geq 0$$

A **maximal monotone graph** is a monotone graph which does not admit a strict monotone prolongation. For maximal montone graphs M, Fitzpatrick introduced the following function (Fitzpatrick (1988))

$$F_M(\boldsymbol{x}, \boldsymbol{y}) = \sup_{(\boldsymbol{u}, \boldsymbol{v}) \in M} \left\{ \langle \boldsymbol{u}, \boldsymbol{y} \rangle + \langle \boldsymbol{x}, \boldsymbol{v} \rangle - \langle \boldsymbol{u}, \boldsymbol{v} \rangle \right\}$$

that today is named after him and allows to give simpler proofs of hard theorems on monotone graphs. As superior enveloppe of affine functions, it is globally convex with respect to the couple $(\boldsymbol{x}, \boldsymbol{y})$ and, if M is maximal monotone, it is a generating function for it. Similarly, Ghoussoub introduced the **selfdual lagrangians** which are globally convex generating functions. The subdifferential $\partial\pi$ of a superpotential π is maximal monotone. Its Fitzpatrick's function is Fenchel's one (then separated).

Another interesting generalization of the monotony inequality is the following. For $n > 1$, a graph $M \subset X \times Y$ is n-**monotone graphs** if for any finite family of couples $(\boldsymbol{x}_j, \boldsymbol{y}_j) \in M, j = 1, 2, \ldots, n$,

$$\langle \boldsymbol{x}_1 - \boldsymbol{x}_n, \boldsymbol{y}_n \rangle + \sum_{k=1}^{n-1} \langle \boldsymbol{x}_{k+1} - \boldsymbol{x}_k, \boldsymbol{y}_k \rangle \leq 0 \tag{12}$$

the monotone graphs corresponding to $n = 2$. The **Fitzpatrick function of order** n defined by

$$F_{M,n}(\boldsymbol{x}, \boldsymbol{y}) = \sup_{(\boldsymbol{x}_k, \boldsymbol{y}_k) \in M} \left(\sum_{k=1}^{n-2} \langle \boldsymbol{x}_{k+1} - \boldsymbol{x}_k, \boldsymbol{y}_k \rangle + \langle \boldsymbol{x}, \boldsymbol{y}_{n-1} \rangle + \langle \boldsymbol{x}_1, \boldsymbol{y} \rangle - \langle \boldsymbol{x}_{n-1}, \boldsymbol{y}_{n-1} \rangle \right) \tag{13}$$

If M is maximal n-monotone, it is a generating function for it.

If a graph is n-monotone, it is m-monotone for all $m < n$. A graph which is n-monotone for all integer values of n is called a **cyclically monotone graph**. The subdifferential $\partial\pi$ of a superpotential π is maximal cyclically monotone and the sequence of Fitzpatrick's functions $F_{M,n}$ converges pointwise to its Fenchel's function.

3. Brief recall and principles of Variational formulations in Mechanics

3.1. Elasticity

Let V be a solid body of boundary S subjected to imposed stress vector $\bar{\boldsymbol{t}}$ on the part S_t of S and imposed displacement $\bar{\boldsymbol{u}}$ on the remaining part S_u. The set of kinematically admissible (KA) displacement fields is

$$\mathcal{K}_a = \{\boldsymbol{u} \quad s.t. \quad \boldsymbol{u} = \bar{\boldsymbol{u}} \quad on \quad S_u \quad and \quad \boldsymbol{\varepsilon}(\boldsymbol{u}) = grad_s \boldsymbol{u} \quad in \quad V\} \ . \tag{14}$$

The set of the statically admissible (SA) stress fields is

$$\mathcal{S}_a = \{\boldsymbol{\sigma} \quad s.t. \quad div\ \boldsymbol{\sigma} = 0 \quad in \quad V, \quad \boldsymbol{t}(\boldsymbol{\sigma}) = \boldsymbol{\sigma}\boldsymbol{n} = \bar{\boldsymbol{t}} \quad on \quad S_t\} \tag{15}$$

A field couple $(\boldsymbol{u}, \boldsymbol{\sigma})$ is a solution of the boundary value problem (BVP) of the elastostatics if it satisfies together the kinematical condition, the equilibrium equations and Hooke's law

(i) $\boldsymbol{u}$ is KA

(ii) $\boldsymbol{\sigma}$ is SA

(iii) $\boldsymbol{\sigma} = \boldsymbol{C}\,(\boldsymbol{\varepsilon}(\boldsymbol{u}))$ in V

The corresponding displacement variational method is based on the functional

$$\Pi(\boldsymbol{u}) = \int_V \pi(\boldsymbol{\varepsilon}(\boldsymbol{u}))dV - \int_{S_t} \boldsymbol{u} \cdot \bar{\boldsymbol{t}} dS$$

obtained by integrating the potential of the elasticity on V and by substracting the work of imposed external stress vectors $\bar{\boldsymbol{t}}$ on S_t. As π, this function Π is convex, that gives a sense to the variational principle of the displacements

$$\min_{\boldsymbol{u}' \in \mathcal{K}_a} (\Pi(\boldsymbol{u}'))$$

It can be showed that the displacement field $\boldsymbol{u}$ which realizes the minimum is solution of the previous BVP of the elasticity.

On the other hand, the stress variational method is based on the dual functional

$$\Phi(\boldsymbol{\sigma}) = \int_V \pi^*(\boldsymbol{\sigma})dV - \int_{S_u} \bar{\boldsymbol{u}} \cdot \boldsymbol{t}(\boldsymbol{\sigma}) dS$$

obtained by integrating the Fenchel's conjugate of the potential of the elasticity on V and by substracting the work of imposed external displacements $\bar{\boldsymbol{u}}$ on S_u. The stress solution of the BVP of the elasticity can be alternatively obtained as realizing the minimum of the variational principle of the stresses

$$\min_{\boldsymbol{\sigma}' \in \mathcal{S}_a} (\Phi(\boldsymbol{\sigma}'))$$

The two variational principles are dual in the sence that

$$\min_{\boldsymbol{u}' \in \mathcal{K}_a} (\Pi(\boldsymbol{u}')) = \Pi(\boldsymbol{u}) = -\Phi(\boldsymbol{\sigma}) = \max_{\boldsymbol{\sigma}' \in \mathcal{S}_a} (-\Phi(\boldsymbol{\sigma}'))$$

3.2. Associated plasticity

Using the tools of non smooth mechanics and convex analysis, the generalization of the previous method is rather straightforward. The main difference with the elasticity is that the BVP is formulated in velocity instead of displacement. Let V be a solid body of boundary S subjected to imposed stress vector $\bar{\boldsymbol{t}}$ on the part S_t of S and imposed velocity $\bar{\boldsymbol{v}}$ on the remaining part S_v. The set of kinematically admissible displacement fields is

$$\mathcal{K}_a = \{\boldsymbol{v} \quad s.t. \quad \boldsymbol{v} = \bar{\boldsymbol{v}} \quad on \quad S_v \quad and \quad \boldsymbol{d}(\boldsymbol{v}) = grad_s \boldsymbol{v} \quad in \quad V\} \ . \tag{16}$$

while the set of statically admissible stress fields is defined by (15). A field couple $(\boldsymbol{v}, \boldsymbol{\sigma})$ is a solution of the boundary value problem (BVP) of the associated plasticity if it satisfies together the kinematical condition, the equilibrium equations and the normal yielding rule

(i) $\boldsymbol{v}$ is KA

(ii) $\boldsymbol{\sigma}$ is SA

(iii) $\boldsymbol{d}(\boldsymbol{v}) \in \partial\, \pi^* (\boldsymbol{\sigma})$ in V

where π^* is the indicatory function χ_K of the plastic domain. Its Fenchel's conjugate π is the corresponding support function (8). The corresponding velocity variational method is based on **Markov's principle** (Markov (1947))

$$\Pi(\boldsymbol{v}) = \min_{\boldsymbol{v}' \in \mathcal{K}_a} \left(\Pi(\boldsymbol{v}') = \int_V \pi(\boldsymbol{d}(\boldsymbol{v}'))dV - \int_{S_t} \boldsymbol{v}' \cdot \bar{\boldsymbol{t}} dS \right)$$

obtained by integrating the superpotential of the plasticity on V and by substracting the power of imposed external stress vectors $\bar{\boldsymbol{t}}$ on S_t.

On the other hand, the stress variational method is based on **Hill's principle** (Hill (1950))

$$\Phi(\boldsymbol{\sigma}) = \min_{\boldsymbol{\sigma}' \in \mathcal{S}_a} \left(\Phi(\boldsymbol{\sigma}') = \int_V \pi^*(\boldsymbol{\sigma}')dV - \int_{S_v} \bar{\boldsymbol{v}} \cdot \boldsymbol{t}(\boldsymbol{\sigma}')dS \right) \tag{17}$$

obtained by integrating the Fenchel's conjugate of the superpotential of the plasticity on V and by substracting the power of imposed external velocities $\bar{\boldsymbol{v}}$ on S_v. Defining the set of **licit stress fields**:

$$\mathcal{S}_l = \{\boldsymbol{\sigma} \in \mathcal{S}_a \quad s.t. \quad \sigma \in K \quad e.a. \quad in \quad V\} \ ,$$

let us notice that if $\boldsymbol{\sigma}$ is licit, the value of the functional in (17) is finite, infinite otherwise. The minimum being finite, it is realized only for licit fields. Because the superpotential π^* is the indicatory function χ_K of the elastic domain K, it vanishes almost everywhere for the licit fields, hence the variational principle is equivalent to the following on

$$\Phi(\boldsymbol{\sigma}) = \min_{\boldsymbol{\sigma}' \in \mathcal{S}_l} \left(- \int_{S_v} \bar{\boldsymbol{v}} \cdot \boldsymbol{t}(\boldsymbol{\sigma}')dS \right)$$

The two variational principles are dual in the sence that

$$\min_{\boldsymbol{v}' \in \mathcal{K}_a} (\Pi(\boldsymbol{v}')) = \Pi(\boldsymbol{v}) = -\Phi(\boldsymbol{\sigma}) = \max_{\boldsymbol{\sigma}' \in \mathcal{S}_a} (-\Phi(\boldsymbol{\sigma}'))$$

4. Classical limit analysis in associated plasticity: bounding theorems

We suppose now that

- The imposed velocities on S_v vanish
- The imposed stress vector on S_t is controlled by a non negative scalar factor α called **load factor**

$$\bar{\boldsymbol{t}} = \alpha\, \bar{\boldsymbol{t}}^0 \quad on \quad S_t$$

  where $\bar{\boldsymbol{t}}^0$ is a fixed reference load distribution.
- $\mathbf{0} \in K$ then π is non negative (because of (5)).

When the imposed velocities on S_v vanish, Markov's principle is rather puzzling because below a critical value of α called **limit load factor** and denoted α^L, the solution is trivial ($\boldsymbol{v} = \mathbf{0}$) and do not exist beyond it. Only the solution corresponding to α^L are not trivial and represent the **collapse mechanism**. The goal of the limit analysis is to determine at the collapse this mechanism, the corresponding stress field $\boldsymbol{\sigma}$ and the collapse load α^L thanks to two bound theorems of which we shall present here a demonstration based on the variational principles of the plasticity. For more information about the classical limit analysis, the reader is referred for instance to (Salençon (1983), Buhan (1986), Suquet (1982), Save et al. (1997)).

We start with some preliminary remarks.

- If $\boldsymbol{v}$ is solution of the BVP of Subsection 3.2 and $\lambda > 0$, the velocity field $\lambda\boldsymbol{v}$ satisfies (i) because of the linearity of conditions in (16) and (iii) because the normal yielding rule (7) is nothing else Hill's inequality(10). Hence $\lambda\boldsymbol{v}$ is also solution of the BVP. The kinematical solution is defined up to a positive factor.
- For any solution $(\boldsymbol{v}, \boldsymbol{\sigma})$ of the BVP, Eq.(77) holds and, owing to (9), one has

$$\int_V \pi(\boldsymbol{d}(\boldsymbol{v}))dV = \int_V \boldsymbol{d}(\boldsymbol{v}) : \boldsymbol{\sigma} dV = \alpha^L \int_{S_t} \boldsymbol{v} \cdot \bar{\boldsymbol{t}}^0 dS \tag{18}$$

  Hence, if the collapse occurs, $\boldsymbol{v} \neq \mathbf{0}$ and the **external power**

$$P^0_{ext}(\boldsymbol{v}) = \int_{S_t} \boldsymbol{v} \cdot \bar{\boldsymbol{t}}^0 dS > 0$$

  is non negative.

On this ground, we introduce the set of **licit velocity fields**:

$$\mathcal{K}_l = \{\boldsymbol{v} \in \mathcal{K}_a \quad s.t. \quad P^0_{ext}(\boldsymbol{v}) > 0\}$$

Introducing the **internal power**

$$P_{int}(\boldsymbol{v}) = \int_V \pi(\boldsymbol{d}(\boldsymbol{v}))dV \tag{19}$$

the **kinematical factor**

$$\alpha^k = \frac{P_{int}(\boldsymbol{v}')}{P^0_{ext}(\boldsymbol{v}')} \tag{20}$$

associated to any licit velocity field $\boldsymbol{v}'$ bounds the limit factor

$$\alpha^L \leq \alpha^k$$

This is the **kinematical bound theorem**. To prove it, let us remark that because of Markov's principle with the reference loads multiplied by α^L and (18), one has

$$\Pi(\boldsymbol{v}') = P_{int}(\boldsymbol{v}') - \alpha^L P^0_{ext}(\boldsymbol{v}') \geq \Pi(\boldsymbol{v}) = 0$$

On the other hand, (20) leads to

$$\Pi(\boldsymbol{v}') = (\alpha^k - \alpha^L) P^0_{ext}(\boldsymbol{v}')$$

As $\boldsymbol{v}'$ is licit, the external power is non negative, that proves the theorem. As the kinematical solution is defined up to a positive factor, it us usual to fixe it by imposing an additional **normalization condition**

$$P^0_{ext}(\boldsymbol{v}') = 1 \tag{21}$$

hence the kinematical factor is simply the internal power

$$\alpha^k = P_{int}(\boldsymbol{v}') \tag{22}$$

Similarly, for any licit stress field $\boldsymbol{\sigma}'$ with the reference loads multiplied by α^s, the corresponding **static factor** minorizes the limit factor

$$\alpha^s \leq \alpha^L \tag{23}$$

This is the **statical bound theorem**. To prove it, let us remark that Hill's functional in (17) is reduced to

$$\Phi(\boldsymbol{\sigma}) = \int_V \varphi^*(\boldsymbol{\sigma}) dV$$

Hence, because of (iii) in Subsection 3.2

$$\Phi(\boldsymbol{\sigma}') - \Phi(\boldsymbol{\sigma}) = \int_V (\varphi^*(\boldsymbol{\sigma}') - \varphi^*(\boldsymbol{\sigma}) dV \geq \int_V \boldsymbol{d}(\boldsymbol{v}) : (\boldsymbol{\sigma}' - \boldsymbol{\sigma}) dV$$

As $\boldsymbol{v}$ is KA, $\boldsymbol{\sigma}'$ and $\boldsymbol{\sigma}$ are SA with reference loads respectively multiplied by α^s and α^L, (77) leads to

$$(\alpha^s - \alpha^L) P^0_{ext}(\boldsymbol{v}) \leq \Phi(\boldsymbol{\sigma}') - \Phi(\boldsymbol{\sigma})$$

As $\boldsymbol{\sigma}'$ and $\boldsymbol{\sigma}$ are licit, the right hand member vanishes, that proves the theorem.

5. Kinematical limit analysis methods applied to ductile porous materials

5.1. Methodology

Let us consider now a *r.e.v.* Ω of a porous material made up of a solid domain $\Omega_M \subset \Omega$ and voids. The porosity is denoted f. The derivation of the Gurson model which will be presented below is based on the kinematical Limit Analysis approach which has been previously exposed. The reader can found elements of the derivation of the macroscopic strength of ductile porous media in the textbooks Leblond (2001) and Dormieux et al. (2006)[1].

The set of kinematically admissible (KA) velocity fields with a uniform strain rate boundary conditions, $\mathbf{D}$, is defined as:

$$\mathcal{K}_a = \{\boldsymbol{v} \quad s.t. \quad \boldsymbol{v} = \bar{\boldsymbol{v}} = \mathbf{D} \cdot \boldsymbol{x} \quad on \quad S_v \quad and \quad \boldsymbol{\varepsilon}(\boldsymbol{v}) = grad_s \boldsymbol{v} \quad in \quad V\} \ . \tag{24}$$

Let us then consider a microscopic stress field $\boldsymbol{\sigma}(\boldsymbol{x})$ in equilibrium. Hill's lemma states that:

$$\boldsymbol{\Sigma} : \mathbf{D} = \frac{1}{|\Omega|} \int_\Omega \boldsymbol{\sigma} : \mathbf{d} \, dV \tag{25}$$

the macroscopic stress $\boldsymbol{\Sigma}$ corresponding to the average of the microscopic one. The strength of the solid phase is characterized by the convex set F^s of admissible stress states, which in turn is defined by a convex strength criterion $F(\sigma)$:

$$F^s = \{\sigma, F(\sigma) \leq 0\} \tag{26}$$

The dual definition of the strength criterion consists in introducing the support function $\pi(\mathbf{d})$ of F^s, which is defined on the set of symmetric second order tensors $\mathbf{d}$ and is convex with respect to $\mathbf{d}$:

$$\pi(\mathbf{d}) = \sup(\boldsymbol{\sigma} : \mathbf{d}, \boldsymbol{\sigma} \in F^s) \tag{27}$$

$\pi(\mathbf{d})$ represents the local maximum "plastic" dissipation capacity which the material can afford and its macroscopic counterpart is defined as:

$$\Pi^{hom}(\mathbf{D}) = (1-f) \inf_{\boldsymbol{v} \in \mathcal{V}(\mathbf{D})} \frac{1}{\mid \Omega \mid} \int_{\Omega_M} \pi(\boldsymbol{d}) dV \quad \text{with} \quad \mathbf{d} = \frac{1}{2}(\text{grad}\, \underline{v} + {}^t \text{grad}\, \underline{v}) \tag{28}$$

Using Eq. (25) together with the definition Eq. (28), it can be shown that the macroscopic dissipation, denoted here Π^{hom}, is the support function of the domain of macroscopic admissible stresses, F^{hom}:

$$\Pi^{hom}(\mathbf{D}) = \sup(\boldsymbol{\Sigma} : \mathbf{D}, \boldsymbol{\Sigma} \in F^{hom}) \tag{29}$$

The limit stress states at the macroscopic scale are shown to be of the form $\boldsymbol{\Sigma} = \partial \Pi^{hom} / \partial \mathbf{D}$ which corresponds to the previous kinematically-based minimization (see subsection 3.2).

[1] *The present synthesis is inspired from Dormieux and Kondo (2010).*

5.2. The Gurson criterion for ductile porous metals

The classical Gurson approach of porous media has been developed in this standard limit analysis framework and deals with the case of a von Mises solid phase:

$$F(\boldsymbol{\sigma}) = \frac{3}{2}\boldsymbol{s} : \boldsymbol{s} - \sigma_o^2 \tag{30}$$

where $\boldsymbol{s}$ is the deviatoric part of $\boldsymbol{\sigma}$. The support function $\pi(\boldsymbol{d})$ accordingly reads:

$$\begin{aligned} &\operatorname{tr}\mathbf{d} = 0 : \quad \pi(\boldsymbol{d}) = \sigma_o d_{eq} \quad \text{with } d_{eq} = \sqrt{\frac{2}{3}\mathbf{d} : \mathbf{d}} \\ &\operatorname{tr}\mathbf{d} \neq 0 : \quad \pi(\boldsymbol{d}) = +\infty \end{aligned} \tag{31}$$

In the Gurson study two simplifications have been introduced, in order to make the analytical calculation feasible. The first consists in representing the morphology of the porous material by a hollow sphere instead of a *r.e.v.*. Let b (resp. a) denote the external (resp. cavity) radius. The porosity (the volume fraction of the cavity in the sphere) then reads $f = (a/b)^3$. Therefore, instead of seeking the infimum in Eq. (28), $\Pi^{hom}(\mathbf{D})$ is estimated by adopting a particular microscopic velocity field $\underline{v}(\boldsymbol{x})$ which must comply with the boundary conditions. In the solid, this trial velocity field, inspired from Rice and Tracey (1969) is defined as the sum of the solution to an isotropic expansion in the von Mises (plastically incompressible) matrix and a linear part involving the deviatoric part of the macroscopic strain rate tensor $\mathbf{D}$. Note again that the chosen trial velocity field must comply with the boundary conditions. Moreover it must satisfy the local condition (incompressibility) $\operatorname{tr}\mathbf{d} = 0$ for the von Mises material. In spherical coordinates, it takes the form:

$$\underline{v}^G(\boldsymbol{x}) = \frac{D_m}{f}\frac{a^3}{r^2}\underline{e}_r + \mathbf{D}' \cdot \boldsymbol{x} \tag{32}$$

It is worth noticing that this velocity field is entirely determined by the macroscopic strain rate $\mathbf{D}$. As a consequence, no minimization step will be required for the determination of the macroscopic criterion. Recalling Eq. (28), the use of $\underline{v}^G$ (giving strain rate $\mathbf{d}^G$) provides an upper bound of Π^{hom}:

$$\Pi^{hom}(\mathbf{D}) \leq (1-f)\frac{1}{\mid \Omega \mid}\int_{\Omega_M} \pi(\boldsymbol{d}^G) dV \tag{33}$$

Using Eq. (31), the derivation of the right hand side in Eq.(33) requires to determine the average of d_{eq} over Ω_M. In order to obtain a closed form expression, it is convenient to apply the following inequality to $\mathcal{G} = \mathbf{d} : \mathbf{d} = 3d_{eq}^2/2$ Gurson (1977):

$$\int_{\Omega_M} \sqrt{\mathcal{G}(r,\theta,\varphi)} dV \leq 4\pi \int_a^b r^2 \left(< \mathcal{G} >_{\mathcal{S}(r)} \right)^{1/2} dr \tag{34}$$

where $\mathcal{S}(r)$ is the sphere of radius r and $< \mathcal{G} >_{\mathcal{S}(r)}$ is the average of $\mathcal{G}(r,\theta,\varphi)$ over all the orientations:

$$< \mathcal{G} >_{\mathcal{S}(r)} = \frac{1}{4\pi r^2}\int_{\mathcal{S}(r)} \mathcal{G}(r,\theta,\varphi)\, dS \tag{35}$$

This eventually yields the following upper bound of $\Pi^{hom}(\mathbf{D})$:

$$\Pi_G^{hom}(\mathbf{D}) = \sigma_o f D_{eq} \left(\xi \left(\operatorname{arcsinh}(\xi) - \operatorname{arcsinh}(f\xi) \right) + \frac{\sqrt{1+f^2\xi^2}}{f} - \sqrt{1+\xi^2} \right) \tag{36}$$

with $D_{eq} = \sqrt{\frac{2}{3}\mathbf{D}' : \mathbf{D}'}$ and $\xi = 2D_m/D_{eq}$.
The last step consists in the derivation of the limit states $\mathbf{\Sigma} = \partial\Pi_G^{hom}/\partial\mathbf{D}$. It is first observed that $\Pi_G^{hom}(\mathbf{D})$ is in fact a function of $\mathbf{D}$ through D_m and D_{eq}, i.e. through $\xi = \frac{2}{f} D_m/D_{eq}$. the admissible states are given by:

$$\mathbf{\Sigma} = \frac{\partial \Pi_G^{hom}}{\partial D_m} \frac{\partial D_m}{\partial \mathbf{D}} + \frac{\partial \Pi_G^{hom}}{\partial D_{eq}} \frac{\partial D_{eq}}{\partial \mathbf{D}} \tag{37}$$

where

$$\frac{\partial D_m}{\partial \mathbf{D}} = \frac{1}{3}\mathbf{1} \quad ; \quad \frac{\partial D_{eq}}{\partial \mathbf{D}} = \frac{2\mathbf{D}'}{3D_{eq}} \tag{38}$$

The combination of Eqs.(37) and (38) also yields:

$$\operatorname{tr}\mathbf{\Sigma} = \frac{\partial \Pi_G^{hom}}{\partial D_m} \quad ; \quad \Sigma_{eq} = \sqrt{3\mathbf{\Sigma}' : \mathbf{\Sigma}'/2} = \frac{\partial \Pi_G^{hom}}{\partial D_{eq}} \tag{39}$$

In turn, Eq. (36) leads to:

$$\begin{aligned} \operatorname{tr}\mathbf{\Sigma} &= 2\sigma_o \left(\operatorname{arcsinh}(\xi) - \operatorname{arcsinh}(f\xi) \right) \\ \Sigma_{eq} &= \sigma_o \left(\sqrt{1+f^2\xi^2} - f\sqrt{1+\xi^2} \right) \end{aligned} \tag{40}$$

Eliminating ξ between the spherical and deviatoric parts of $\mathbf{\Sigma}$ eventually leads to the well known Gurson strength criterion:

$$\frac{\Sigma_{eq}^2}{\sigma_o^2} + 2f\cosh\left(3\frac{\Sigma_m}{2\sigma_o}\right) - 1 - f^2 = 0 \tag{41}$$

This equation characterizes the boundary of the macroscopic domain F_G^{hom} which support function is Π_G^{hom}. Since the successive approximations preserve the upper bound character of Π^{hom}, the obtained domain is an upper bound of the exact domain F^{hom} of macroscopic admissible stresses, that is, $F^{hom} \subset F_G^{hom}$.

Remark 1: In general, only the kinematical theorem has been applied to porous metals. Mention has to be made of very few attempts that have been made by Sun and Wang (1989); Sun and Wang (1995). Unfortunately, these attempts have not been very successful. we will come back in the next chapter on this point.

Remark 2: It can be also noted that the Gurson criterion, (41) depends only on two

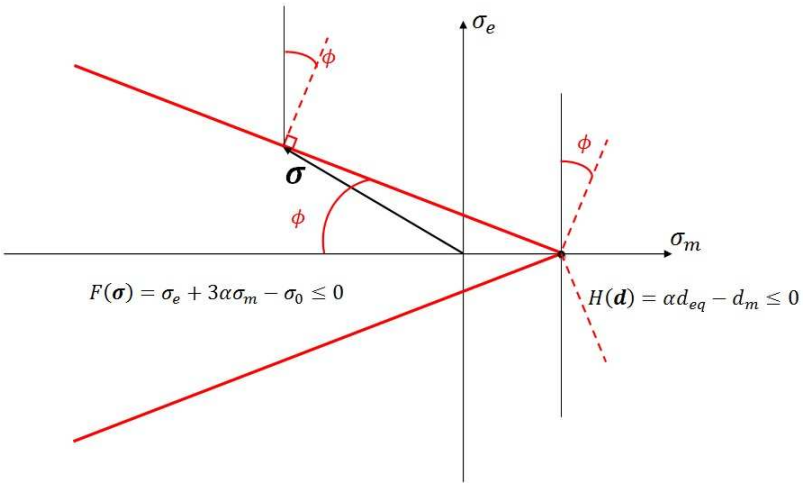

Figure 1: Associated Drucker-Prager model: yield criterion and associated flow rule

stress invariants, Σ_m and Σ_{eq} and not on the third invariant of the stress deviator. As recently recognized and studied by Cazacu et al. Cazacu et al. (2013) (see also Garajeu et al. (2011)), this is a direct consequence of the approximation brought by the inequality (34). We will come back to this point on chapter 3.

5.3. Case of porous materials with an associated Drucker-Prager matrix

Porous materials with an associated Drucker-Prager matrix has been investigated by Guo et al. Guo et al. (2008) by using also classical limit analysis. The approach followed by these authors is methodologically similar to the above one, but shows several difficulties linked to the compressibility of the Drucker-Prager matrix. For instance, let us consider Drucker-Prager model with the yield criterion (Fig. 1):

$$F(\sigma) = \sigma_e + 3\alpha\sigma_m - \sigma_0 \leq 0 \ , \tag{42}$$

where σ_e is the equivalent stress, σ_m the mean stress, $\sigma_0 > 0$ the cohesion stress of the material and α the pressure sensitivity factor. If normality rule is adopted, excepted for the apex of Drucker-Prager cone ($\sigma_e = 0$, $\sigma_m = \sigma_0 \ / \ 3\alpha$) where σ_e is not differentiable, the plastic strain rate is given by the following associated yielding rule:

$$\mathbf{d} = d_{eq}\frac{\partial F}{\partial \sigma} = d_{eq}\left(\frac{3\boldsymbol{s}}{2\sigma_e} + \alpha\mathbf{1}\right), \tag{43}$$

where $\boldsymbol{\sigma}$ is Cauchy stress tensor, $\boldsymbol{s}$ the deviatoric stress, $\mathbf{1}$ the unit tensor. It is recalled that the positive scalar $d_{eq} = \mid \frac{2}{3}\mathbf{d}' : \mathbf{d}' \mid^{1/2}$ with $\mathbf{d}'$ the deviatoric part of $\mathbf{d}$. The volumetric plastic strain is such that:

$$tr\ \mathbf{d} = 3\alpha d_{eq} \tag{44}$$

This suggests introducing:

$$H(\mathbf{d}) = \alpha d_{eq} - d_m$$

The plastic yielding rule (43) is completed at the apex by the condition:

$$H(\mathbf{d}) = \alpha d_{eq} - d_m \leq 0 \tag{45}$$

while, because of (44), $H(\mathbf{d}) = 0$ at the other points of the yielding surface (called regular points). For the above associated Drucker-Prager model, the support function reads (see for instance Salençon (1983):

$$\pi^s(\boldsymbol{d}) = \frac{\sigma_0}{\alpha} d_m \tag{46}$$

when $F(\sigma) \leq 0$ and $H(\mathbf{d}) \leq 0$, equal to $+\infty$ otherwise.
As previously, the determination of the macroscopic dissipation by means of the kinematical method requires the choice of an appropriate velocity field. In the spirit of Gurson model, Guo et al. (Guo et al., 2008) considered a velocity made up of the solution of the hollow sphere with a Drucker-Prager (plastically compressible) matrix and a linear part (generating a homogeneous strain rate field).
In cylindrical coordinates $(\boldsymbol{e}_\rho, \boldsymbol{e}_\phi, \boldsymbol{e}_z)$, the trial velocity field proposed by Guo et al. (2008) which depends on the friction angle ϕ (such that $\tan\phi = 3\alpha$),

$$\boldsymbol{v} = C_0 \left(\frac{b}{r}\right)^{3/s} (\rho \boldsymbol{e}_\rho + z\boldsymbol{e}_z) + C_1 \rho \boldsymbol{e}_\rho + C_2 z \boldsymbol{e}_z \ , \tag{47}$$

with $r = \sqrt{\rho^2 + z^2}$, $s = 1 + 2\epsilon\alpha$, where ϵ is the sign of C_0. The first term is the exact solution for the hydrostatic case Guo et al. (2008) (see also (Thoré et al. , 2009) or (Cheng et al., 2012)). As in Gurson's model Gurson (1977), while the two linear terms aim at capturing the effects of macroscopic shear.
The above trial velocity field complies with the boundary conditions ($\boldsymbol{v} = \boldsymbol{D} \cdot \boldsymbol{x}$) only in an average sense:

$$\boldsymbol{D} = \frac{1}{\mid \Omega \mid} \int_{\partial\Omega} \frac{1}{2} (\boldsymbol{v} \otimes \boldsymbol{n} + \boldsymbol{n} \otimes \boldsymbol{v}) dS$$

Once the microscopic trial velocity field is proposed, the corresponding local strain rate and its macroscopic counterpart can be calculated. It is readily seen that the macroscopic strain rate tensor reads:

$$\boldsymbol{D} = C_0 \mathbf{1} + C_1 (\boldsymbol{e}_\rho \otimes \boldsymbol{e}_\rho + \boldsymbol{e}_\phi \otimes \boldsymbol{e}_\phi) + C_2 \boldsymbol{e}_z \otimes \boldsymbol{e}_z \ , \tag{48}$$

from which it follows that the macroscopic mean strain rate D_m and the equivalent strain rate D_e take the form:

$$\begin{aligned} D_m &= C_0 + \frac{1}{3}(2C_1 + C_2) \\ D_e &= \frac{2}{3} \mid C_1 - C_2 \mid \end{aligned} \tag{49}$$

Moreover, in contrast to the local condition (incompressibility) in the von Mises case, the admissibility condition (45) appears to be very difficult, if not impossible, to satisfy. Indeed, from the considered velocity field, one readily obtains:

$$d_m(r) = \left(1 - \frac{1}{s}\right) C_0 \left(\frac{b}{r}\right)^{3/s} + \frac{1}{3}(2C_1 + C_2) \tag{50}$$

and

$$d_{eq}(r) = \frac{2}{3}\sqrt{(C_1 - C_2)^2 + \frac{3C_0}{s}(C_1 - C_2)(3\cos^2\theta - 1)\left(\frac{b}{r}\right)^{3/s} + \left(\frac{3C_0}{s}\right)^2 \left(\frac{b}{r}\right)^{6/s}} \tag{51}$$

which obviously do not comply with (45) everywhere in the hollow sphere.
Due to the above difficulty, the idea is to relax the admissibility condition in an average sense by imposing

$$\int_{\Omega_M} H(d)\ dV\ = 0 \tag{52}$$

It follows that the normalized macro dissipation, obtained by omitting σ_0 (or taking it equal to 1)[2], is defined by:

$$\Pi^{hom}(\boldsymbol{D}) = \int_{\Omega_M} \frac{d_m}{\alpha} dV \tag{53}$$

under the constraint (52).
After recalling that from the Hill Lemma the minimization problem classically reads

$$\Pi^{hom}(\boldsymbol{D}) - \boldsymbol{T} : \boldsymbol{D} \leq 0 \tag{54}$$

$\boldsymbol{T}$ being the normalized macro stress.
This suggests to introduce the following Lagrangian $\bar{L}$, with $\bar{\Lambda}$ a Lagrange multiplier, assumed constant:

$$\bar{L} = \frac{1}{\Omega}\int_{\Omega_m} \frac{d_m}{\alpha} dV - \mathbf{T} : \mathbf{D} + \bar{\Lambda}[\int_{\Omega_M} (\alpha d_{eq} - d_m) dV] \tag{55}$$

This Lagrangian reads:

$$\bar{L} = \frac{1}{\alpha}[(1-f)D_m - (f^\gamma - f)C_0] + \alpha\bar{\Lambda}\Pi - \bar{\Lambda}[(1-f)D_m - (f^\gamma - f)C_0] - (3T_m D_m + T_e D_e) \tag{56}$$

where $\gamma = 1 - s^{-1}$ and in which

$$\Pi(\boldsymbol{v}) = \frac{1}{|\ \Omega\ |}\int_{\Omega_M} d_{eq}\ dV\ ,$$

[2] *This normalization has been considered in the study by Guo et al. (2008).*

Its expression can be found in Guo et al. (2008) (see also appendix of chapter 4).
Finally, $\bar{L}$ takes the form:

$$\bar{L} = \alpha\bar{\Lambda}\Pi + (\frac{1}{\alpha} - \bar{\Lambda})[(1-f)D_m - (f^\gamma - f)C_0] - -(3T_m D_m + T_e D_e) \tag{57}$$

The following minimization relations then follow:

$$\begin{cases} \dfrac{\partial \bar{L}}{\partial C_0} = \alpha\bar{\Lambda}\dfrac{\partial \Pi}{\partial C_0} - (\dfrac{1}{\alpha} - \bar{\Lambda})(f^\gamma - f) = 0 \\ \\ \dfrac{\partial \bar{L}}{\partial D_m} = (\dfrac{1}{\alpha} - \bar{\Lambda})(1-f) - 3T_m = 0 \\ \\ \dfrac{\partial \bar{L}}{\partial D_e} = \alpha\bar{\Lambda}\dfrac{\partial \Pi}{\partial D_e} - T_e = 0 \end{cases} \tag{58}$$

The first one delivers the optimal expression of $\bar{\Lambda}$

$$\bar{\Lambda} = \frac{\frac{1}{\alpha}(f^\gamma - f)}{f^\gamma - f + \alpha\frac{\partial \Pi}{\partial C_0}} \tag{59}$$

which, when reported in the two last ones, leads to the expression of the macroscopic admissible stress components:

$$3T_m = (1-f)\left[\frac{1}{\alpha} - \frac{\frac{1}{\alpha}(f^\gamma - f)}{f^\gamma - f + \alpha\frac{\partial \Pi}{\partial C_0}}\right] = \frac{(1-f)\frac{\partial \Pi}{\partial C_0}}{f^\gamma - f + \alpha\frac{\partial \Pi}{\partial C_0}} \tag{60}$$

$$T_e = \frac{(f^\gamma - f)\frac{\partial \Pi}{\partial D_e}}{f^\gamma - f + \alpha\frac{\partial \Pi}{\partial C_0}} \tag{61}$$

These are precisely the expressions established by Guo et al. (2008) for the macroscopic criterion of ductile porous materials having an associated Drucker-Prager matrix. The reader interested by the detail of implementation of this criterion may can refer to the above mentioned paper.

6. Modeling constitutive laws in the context of bipotential theory

6.1. Non monotone laws, non associated laws and bipotential

However, many experimental laws proposed these last decades, particularly in Plasticity, are non associated. For such laws, de Saxcé proposed in (de Saxcé et al., 1991; de Saxcé , 1992) a suitable modelization based on more general generating functions called **bipotentials** and defined by the following properties:

(a) b is convex and lower semicontinuous in each argument.
(b) For any $\boldsymbol{x}'$ and $\boldsymbol{y}'$ we have

$$b(\boldsymbol{x}', \boldsymbol{y}') \geq \langle \boldsymbol{x}', \boldsymbol{y}' \rangle \ . \tag{62}$$

(c) For $\boldsymbol{x}$ and $\boldsymbol{y}$ we have the equivalences:

$$\mathbf{y} \in \partial b(\cdot, \boldsymbol{y})(\boldsymbol{x}) \iff \boldsymbol{x} \in \partial b(\boldsymbol{x}, \cdot)(\boldsymbol{y}) \iff b(\boldsymbol{x}, \boldsymbol{y}) = \langle \boldsymbol{x}, \boldsymbol{y} \rangle \ . \tag{63}$$

In a mechanical point of view, the bipotential represents the plastic dissipation power (by volum unit) and (63) is the constitutive law. The couples $(\boldsymbol{x}, \boldsymbol{y})$ for which ones equivalence (63) holds are called **extremal couples**.

First of all, let us show a simple example with $X = Y = \mathbb{R}^n$, the dual pairing being the usual euclidian product. Then we define

$$b(\boldsymbol{x}, \boldsymbol{y}) = \|\boldsymbol{x}\| \ \|\boldsymbol{y}\| \tag{64}$$

The point (a) is obviously satisfied. The point (b) is true by the Cauchy-Schwarz-Bunyakovsky inequality. We have equality in the Cauchy-Schwarz-Bunyakovsky inequality $b(\boldsymbol{x}, \boldsymbol{y}) = \langle \boldsymbol{x}, \boldsymbol{y} \rangle$ if and only if there is $\lambda > 0$ such that $\boldsymbol{y} = \lambda \boldsymbol{x}$ or one of $\boldsymbol{x}$ and $\boldsymbol{y}$ vanishes. This is exactly the statement from the point (c), for the function b under study, hence b is a bipotential called **Cauchy's bipotential**. It is worth to notice the graph M generated by b is the set of pairs of collinear and with same orientation vectors. It is not the subdifferential of a superpotential because it is not monotone (then it is not *a fortiori* cyclically monotone).

A non-empty graph $M \subset X \times Y$ is a **BB-graph** (bi-convex, bi-closed) if for all $\boldsymbol{x}$ and for all $\boldsymbol{y}$ the sets $M(\boldsymbol{x})$ and $M^*(\boldsymbol{y})$ are convex and closed. Given a a non-empty graph $M \subset X \times Y$, there is a bipotential b which is a generating function of M if and only if M is a BB-graph. This bipotential, denoted b_M, is equal to

$$b_\infty(\boldsymbol{x}, \boldsymbol{y}) = \langle \boldsymbol{x}, \boldsymbol{y} \rangle$$

if $(\boldsymbol{x}, \boldsymbol{y}) \in M$ and $+\infty$ otherwise (Buliga et al. (2008)). For a given graph, there is not in general uniqueness of the bipotential because, for instance, considering the graph of Cauchy's bipotential, we obtain a bipotential b_∞ which is clearly different from (64). Another interesting question is: given a graph M, is there a way to construct a bipotential b generating it? The existence result does not give a satisfying bipotential because b_∞ is somehow degenerate because infinite outside M. For example, it would be nice to be able to reconstruct Cauchy's bipotential starting from its graph. An answer to this question is given by the method of the **convex lagrangian covers** (Buliga et al. (2008)) and its generalization of the **bipotential convex covers** (Buliga et al. (2010a)). For a more complete survey on generating functions and bipotentials, the reader is refered to (Buliga et al. (2009a)).

6.2. Non associated plasticity and bipotential

Typical applications of the bipotentials in the mechanics of solids are the non associated plasticity for which the the plastic strain rate is not normal to the elastic domain K. The classical way to formulate such laws is to give a smooth loading function F to represent it:

$$K = \{\boldsymbol{\sigma} \in X \qquad F(\boldsymbol{\sigma}) \leq 0\}$$

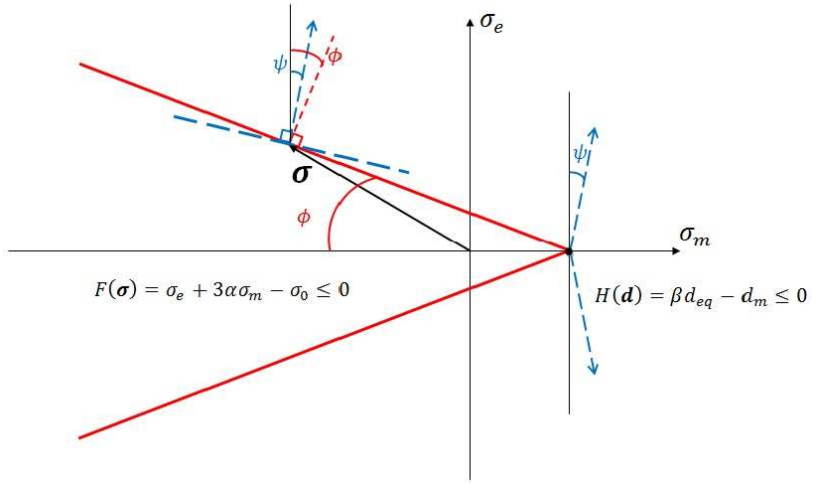

Figure 2: Drucker-Prager model: yield criterion and non associated flow rule

and a plastic potential G to model the plastic flow rule:

$$\boldsymbol{d} = d_{eq}\frac{\partial G}{\partial \boldsymbol{\sigma}}$$

Plastic laws of soils are often non associated. For instance, let us consider Drucker-Prager model with the yield criterion (Fig. 2):

$$F(\sigma) = \sigma_e + 3\alpha\sigma_m - \sigma_0 \leq 0 \ , \tag{65}$$

where σ_e is the effective stress, σ_m the mean stress, $\sigma_0 > 0$ the cohesion stress of the material and α the pressure sensitivity factor related to the friction angle ϕ by:

$$\tan\ \phi = 3\alpha \ .$$

Let us introduce the plastic potential:

$$G(\sigma) = \sigma_e + 3\beta\sigma_m\ - \sigma_0,$$

where β depends on the dilatancy angle ψ through:

$$\tan\ \psi = 3\beta \ .$$

Of course, for the particular event $\psi = \phi$ hence $F = G$, the normality rule is recovered and the plasticity model is associated. Moreover, without loss of generality, we can assume that $0 \leq \beta \leq \alpha$. Excepted for the apex of Drucker-Prager cone ($\sigma_e = 0$, $\sigma_m = \sigma_0\ /\ 3\alpha$) where σ_e is not differentiable, the plastic strain rate is given by the non associated yielding rule:

$$\mathbf{d} = d_{eq}\ \frac{\partial G}{\partial \sigma} = d_{eq}\left(\frac{3\mathbf{s}}{2\sigma_e} + \beta\mathbf{1}\right), \tag{66}$$

where $\boldsymbol{\sigma}$ is Cauchy stress tensor, $\mathbf{s}$ the deviatoric stress, $\mathbf{1}$ the unit tensor and $d_{eq} =\mid \frac{2}{3}\mathbf{e} : \mathbf{e} \mid^{1/2}$ with $\mathbf{e}$ being the deviatoric part of $\mathbf{d}$. The plastic dilatancy is:

$$tr\ \mathbf{d} = 3\beta d_{eq} \tag{67}$$

This suggests introducing:

$$H(\mathbf{d}) = \beta d_{eq} - d_m$$

The plastic yielding rule (66) is completed at the apex by the condition:

$$H(\mathbf{d}) \leq 0 \tag{68}$$

while, because of (67), $H(\mathbf{d}) = 0$ at the other points of the yielding surface (called regular points). Of course, for the particular event $\beta = \alpha$ hence $F = G$, the normality rule is recovered and the plasticity model is associated.

The classical presentation using the plastic potential is recalled only because of its intensive use in the literature but, in actual fact, it is not very relevant for the variational methods. One of the goals of the bipotential method is to give good ideas to find efficient functionals in order to use all the power of the variational tools. For the non associated Drucker-Prager model, let us introduce the function:

$$b(\boldsymbol{d}, \boldsymbol{\sigma}) = \frac{\sigma_0}{\alpha} d_m + (\beta - \alpha)\left(3\sigma_m - \frac{\sigma_0}{\alpha}\right) d_{eq} \tag{69}$$

when $F(\sigma) \leq 0$ and $H(\mathbf{d}) \leq 0$, equal to $+\infty$ otherwise. Indeed, the condition

$$\boldsymbol{d} \in \partial b(\boldsymbol{d}, \cdot)(\boldsymbol{\sigma}) \tag{70}$$

reads

$$\boldsymbol{d} \in (\beta - \alpha) d_{eq}\mathbf{1} + \partial \chi_K(\boldsymbol{\sigma}) \tag{71}$$

If $\boldsymbol{\sigma}$ is a regular point of the boundary of K, introducing a Lagrange multiplier λ, one has

$$\boldsymbol{d} = (\beta - \alpha) d_{eq}\mathbf{1} + \lambda \frac{\partial F}{\partial \boldsymbol{\sigma}} = (\beta - \alpha) d_{eq}\mathbf{1} + \lambda \left(\frac{3\mathbf{s}}{2\sigma_e} + \alpha\mathbf{1}\right)$$

Equaling the deviators of both members leads to $\lambda = d_{eq}$, hence the previous relation is reduced to the yielding rule (66). For the apex, we let the reader to prove that (71) leads to (68). Hence, the non associated yielding rule is described in a compact form by the relation (70) and b generates the corresponding graph.

Let us prove now in three steps that the function (69) is a bipotential.

(i) It is clearly convex and lower semicontinuous.

(ii) To check the condition (62), it is sufficient to verify that, under the conditions (65) and (68), one has

$$b(\mathbf{d}, \sigma) = \frac{\sigma_0}{\alpha} d_m + (\beta - \alpha)\left(3\sigma_m - \frac{\sigma_0}{\alpha}\right) d_{eq} \geq 3\sigma_m d_m + \boldsymbol{s} : \boldsymbol{e} \tag{72}$$

First of all, for any $\boldsymbol{\sigma} \in K$, taking into account Cauchy-Schwarz-Bunyakovsky inequality, the following relation holds

$$-\alpha \left(3\sigma_m - \frac{\sigma_0}{\alpha}\right) d_{eq} \geq \sigma_e d_{eq} \geq \boldsymbol{s} : \boldsymbol{e} \tag{73}$$

On the other hand, under the conditions (65) and (68), one has

$$3\sigma_m \leq \frac{\sigma_0}{\alpha}, \qquad d_m \geq \beta \sigma_m$$

Hence

$$\beta \left(3\sigma_m - \frac{\sigma_0}{\alpha}\right) d_{eq} \geq \left(3\sigma_m - \frac{\sigma_0}{\alpha}\right) d_{eq} d_m \tag{74}$$

Thus condition (72) results from inequalities (73) and (74).

(iii) Finally, we have to check the equivalence (63). If $(\boldsymbol{d}, \boldsymbol{\sigma})$ is an extremal couple,

$$b(\boldsymbol{d}, \boldsymbol{\sigma}) = \boldsymbol{d} : \boldsymbol{\sigma} \tag{75}$$

and, because of (62), for any $\boldsymbol{\sigma}' \in Y$

$$b(\boldsymbol{d}, \boldsymbol{\sigma}') \geq \boldsymbol{d} : \boldsymbol{\sigma}'$$

Hence

$$b(\boldsymbol{d}, \boldsymbol{\sigma}') - b(\boldsymbol{d}, \boldsymbol{\sigma}) \geq \boldsymbol{d} : (\boldsymbol{\sigma}' - \boldsymbol{\sigma})$$

that proves (70). Conversely, if the previous relation is true, let us prove that the couple $(\boldsymbol{d}, \boldsymbol{\sigma})$ is extremal. Indeed, b has a finite value for it, given by the expression (69) or, after some algebraic manipulations

$$b(\boldsymbol{d}, \boldsymbol{\sigma}) = \frac{\sigma_0}{\alpha}(d_m - \beta d_{eq}) + 3\beta \sigma_m d_{eq} + (\sigma_0 - 3\alpha\sigma_m)\, d_{eq}$$

When the plastic strain vanishes, (75) is trivially fulfilled. Otherwise, the stress point is on the boundary of K and $F(\boldsymbol{\sigma}) = 0$ leads to

$$b(\boldsymbol{d}, \boldsymbol{\sigma}) = \frac{\sigma_0}{\alpha}(d_m - \beta d_{eq}) + 3\beta \sigma_m d_{eq} + \sigma_e d_{eq} \tag{76}$$

If it is a regular point, $H(\boldsymbol{d}) = 0$ leads to

$$b(\boldsymbol{d}, \boldsymbol{\sigma}) = 3\sigma_m d_m + \sigma_e d_{eq} = 3\sigma_m d_m + \boldsymbol{s} : \boldsymbol{e}$$

because $\boldsymbol{e}$ and $\boldsymbol{s}$ are collinear. For the apex, $\boldsymbol{s}$ vanishes, $\sigma_m = \sigma_0 \ / \ 3\alpha$ and (76) reads

$$b(\boldsymbol{d}, \boldsymbol{\sigma}) = 3\sigma_m d_m$$

Finally, the equivalence

$$\boldsymbol{\sigma} \in \partial b(\cdot, \boldsymbol{\sigma})(\boldsymbol{d}) \Longleftrightarrow b(\boldsymbol{d}, \boldsymbol{\sigma}) = \langle \boldsymbol{d}, \boldsymbol{\sigma} \rangle$$

is proved in a similar way.

The materials generated by bipotentials are called **implicit standard materials** because the normality law is satisfied in a weak sense of an implicit relation between the dual variables. The bipotentials are generating functions generalizing in a natural way Fitzpatrick's functions and *a fortiori* Fenchel's functions. Athough they were proposed to model the non associated laws, they are also a tool to face the non maximality of a law. For instance, a **non maximal cyclically monotone** law can be generated by a bipotential which is the superior envelop of two Fenchel's functions defined in a suitable way. For more details, the reader is refered to (Buliga et al. (2010a)).

7. Variational formulations for Non associated plasticity and limit analysis

7.1. Formulations

A field couple $(\boldsymbol{v}, \boldsymbol{\sigma})$ is a solution of the boundary value problem (BVP) of the non associated plasticity if it satisfies together the kinematical condition, the equilibrium equations and the implicit normal yielding rule

(i) $\boldsymbol{v}$ is KA

(ii) $\boldsymbol{\sigma}$ is SA

(iii) $\boldsymbol{\sigma} \in \partial b(\cdot, \boldsymbol{\sigma})(\boldsymbol{d}(\boldsymbol{v})) \Longleftrightarrow \boldsymbol{d}(\boldsymbol{v}) \in \partial b(\boldsymbol{d}(\boldsymbol{v}), \cdot)(\boldsymbol{\sigma})$
$\Longleftrightarrow b(\boldsymbol{d}(\boldsymbol{v}), \boldsymbol{\sigma}) = \boldsymbol{d}(\boldsymbol{v}) : \boldsymbol{\sigma}$ in V

The corresponding variational formulation is based on the **bifunctional**

$$B(\boldsymbol{v}, \boldsymbol{\sigma}) = \int_V b(\boldsymbol{d}(\boldsymbol{v}), \boldsymbol{\sigma}) dV - \int_{S_v} \bar{\boldsymbol{v}} \cdot \boldsymbol{t}(\boldsymbol{\sigma}) dS - \int_{S_t} \boldsymbol{v} \cdot \bar{\boldsymbol{t}} dS$$

Indeed, one has:

(i) if $\boldsymbol{v}'$ is KA and $\boldsymbol{\sigma}'$ is SA, $B(\boldsymbol{v}', \boldsymbol{\sigma}') \geq 0$

(ii) if $\boldsymbol{v}$ and $\boldsymbol{\sigma}$ are solution of the BVP, $B(\boldsymbol{v}, \boldsymbol{\sigma}) = 0$

Indeed, if $\boldsymbol{v}'$ is KA and $\boldsymbol{\sigma}'$ is SA, it holds

$$\int_V \boldsymbol{d}(\boldsymbol{v}') : \boldsymbol{\sigma}' dV = \int_{S_v} \bar{\boldsymbol{v}} \cdot \boldsymbol{t}(\boldsymbol{\sigma}') dS + \int_{S_t} \boldsymbol{v}' \cdot \bar{\boldsymbol{t}} dS \tag{77}$$

Hence (i) results from the cornerstone inequality (62) of the bipotential. Besides, if $\boldsymbol{v}$ and $\boldsymbol{\sigma}$ are solution of the BVP, $\boldsymbol{v}$ is KA and $\boldsymbol{\sigma}$ is SA. Consequently, the previous relation is true for $\boldsymbol{v}$ and $\boldsymbol{\sigma}$. Hence (ii) results from (75).

Using (i) with any KA velocity field $\boldsymbol{v}'$ and $\boldsymbol{\sigma}$, and owing to (ii), one has

$$\forall \boldsymbol{v}' \in \mathcal{K}_a, \qquad B(\boldsymbol{v}', \boldsymbol{\sigma}) \geq B(\boldsymbol{v}, \boldsymbol{\sigma}) = 0$$

Similarly, using (i) with $\boldsymbol{v}$ and any SA stress field $\boldsymbol{\sigma}'$, and owing to (ii), one has

$$\forall \boldsymbol{\sigma}' \in \mathcal{S}_a, \qquad B(\boldsymbol{v}, \boldsymbol{\sigma}') \geq B(\boldsymbol{v}, \boldsymbol{\sigma}) = 0$$

In other words, the field couple $(\boldsymbol{v}, \boldsymbol{\sigma})$ solution of the BVP can be obtained as simultaneous solution of the two coupled variational principles

$$\min_{\boldsymbol{v}' \in \mathcal{K}_a} B(\boldsymbol{v}', \boldsymbol{\sigma}) = \min_{\boldsymbol{\sigma}' \in \mathcal{S}_a} B(\boldsymbol{v}, \boldsymbol{\sigma}') = B(\boldsymbol{v}, \boldsymbol{\sigma}) = 0 \tag{78}$$

For the particular event of associated plasticity, the bipotential is Fenchel's function (11) (then separated) and the bifunctional splits into the sum of velocity functional and stress one:

$$B(\boldsymbol{v}, \boldsymbol{\sigma}) = \Pi(\boldsymbol{v}) + \Phi(\boldsymbol{\sigma})$$

and Markov's and Hill's variational principles are decoupled.

7.2. Limit analysis in non associated plasticity

Using the bipotential approach, the classical tools of the limit analysis can be extended to the non associated plasticity (de Saxcé (2002)), according to the following remarks:

- As φ was positively homogeneous of order 1 for plasticity, the partial function $b(., \boldsymbol{\sigma})$ so is. This can be verified for instance on the expression (69).
- Similarly, we can suppose that if $\boldsymbol{v}$ satisfies the BVP of Subsection 7 and $\lambda > 0$, the velocity field $\lambda \boldsymbol{v}$ so is.
- For any solution $(\boldsymbol{v}, \boldsymbol{\sigma})$ of the BVP of Subsection 7, (77) holds and, owing to (iii) of the BVP, one has

$$\int_V b(\boldsymbol{d}(\boldsymbol{v}), \boldsymbol{\sigma}) dV = \int_V \boldsymbol{d}(\boldsymbol{v}) : \boldsymbol{\sigma} dV = \alpha^L P^0_{ext}(\boldsymbol{v}) \tag{79}$$

Introducing the internal power

$$P_{int}(\boldsymbol{v}, \boldsymbol{\sigma}) = \int_V b(\boldsymbol{d}(\boldsymbol{v}), \boldsymbol{\sigma}) dV$$

The kinematical factor associated to a licit velocity field $\boldsymbol{v}'$

$$\alpha^k = \frac{P_{int}(\boldsymbol{v}', \boldsymbol{\sigma})}{P^0_{ext}(\boldsymbol{v}')} \tag{80}$$

depends now on the stress field $\boldsymbol{\sigma}$, exact solution of the BVP and it bounds the limit factor

$$\alpha^L \leq \alpha^k$$

This is the **extended kinematical bound theorem**. To prove it, let us remark that because of the first minimum principle with the reference loads multiplied by α^L, one has

$$B(\boldsymbol{v}', \boldsymbol{\sigma}) = P_{int}(\boldsymbol{v}', \boldsymbol{\sigma}) - \alpha^L P^0_{ext}(\boldsymbol{v}') \geq B(\boldsymbol{v}, \boldsymbol{\sigma}) = 0$$

On the other hand, (80) leads to

$$B(\boldsymbol{v}', \boldsymbol{\sigma}) = (\alpha^k - \alpha^L) P^0_{ext}(\boldsymbol{v}')$$

As $\boldsymbol{v}'$ is licit, the external power is non negative, that proves the theorem.

Similarly, if the exact solution $\boldsymbol{v}$ of the BVP satisfies the normalization condition (21), then for any licit stress field $\boldsymbol{\sigma}'$ with the reference loads multiplied by α^s, the corresponding **static factor** satisfy the following inequality

$$\alpha^s - P_{int}(\boldsymbol{v}, \boldsymbol{\sigma}') \leq \alpha^L - P_{int}(\boldsymbol{v}, \boldsymbol{\sigma}) \tag{81}$$

This is the **extended statical bound theorem**. To prove it, let us remark that because of (iii) in Subsection 7

$$\int_V (b(\boldsymbol{v}, \boldsymbol{\sigma}') - b(\boldsymbol{v}, \boldsymbol{\sigma}) dV \geq \int_V \boldsymbol{d}(\boldsymbol{v}) : (\boldsymbol{\sigma}' - \boldsymbol{\sigma}) dV$$

As $\boldsymbol{v}$ is KA, $\boldsymbol{\sigma}'$ and $\boldsymbol{\sigma}$ are SA with reference loads respectively multiplied by α^s and α^L, (77) leads to

$$(\alpha^s - \alpha^L) P^0_{ext}(\boldsymbol{v}) \leq \int_V (b(\boldsymbol{v}, \boldsymbol{\sigma}') - b(\boldsymbol{v}, \boldsymbol{\sigma}) dV$$

Using (19) the normalization condition (21) proves the theorem.

For the particular event of associated plasticity, the internal power does not depend explicitly on the stress. Then the classical definition (20) of the kinematical factor is recovered from (80). On the other hand, the inequality (81) degenerates into (23).

For more about the limit analysis in non associated plasticity and its extension in presence of unilateral contact with Coulomb's dry friction, the reader is referred to (de Saxcé (2002)). In the next chapters, we shall specialize the previous variational methods and limit analysis approaches to the homogenization problems.

References

Abraham, R., Marsden, J.E., 1980. Foundation of mechanics. 2nd edition, the Benjamin/Cummings Pub. Co.

Buliga, M., de Saxcé, G. Vallée, C., 2008. Existence and construction of bipotential for graphs of multivalued laws. Journal of Convex Analysis. J. Convex Analysis, 15(1), 87-104.

Buliga, M., de Saxcé, G. Vallée, C., 2009. Bipotentials for non monotone multivalued operators: fundamental results and applications. Acta Applicandae Mathematicae, 110(2), 955-972.

Buliga, M., de Saxcé, G. Vallée, C., 2010. Non maximal cyclically monotone graphs and construction of a bipotential for the Coulomb's dry friction law. J. Convex Analysis, 17(1), 81-94.

Cazacu, O., Revil-Baudard, B., Lebensohn, R., Garajeu, M., 2013. On the Combined Effect of Pressure and Third Invariant on Yielding of Porous Solids With von Mises Matrix. Journal of Applied Mechanics, DOI: 10.1115/1.4024074.

Cheng, L., Jia, Y., Oueslati, A., de Saxcé, G, Kondo, D., 2012 Plastic limit state of the hollow sphere model with non-associated Drucker-Prager material under isotropic loading. Computational Materials Science, Vol. 62, 210-215.

P. de Buhan, 1986. A fundamental approach to the yield design of reinforced soil structures (in French), Doctorate Thesis, Paris.

de Saxcé, G., Feng, Z.Q., 1991. New inequality and functional for contact friction: The implicit standard material approach. Mechanics of Structures and Machines, 19, 301-325, 1991.

de Saxcé, G., 1992. Une généralisation de l'inégalité de Fenchel et ses applications aux lois constitutives. C. R. Acad. Sci. Paris, Sér. II, 314, 125-129, 1992.

de Saxcé, G., Bousshine, L., 1998. Limit Analysis Theorems for the Implicit Standard Materials: Application to the Unilateral Contact with Dry Friction and the Non Associated Flow Rules in Soils and Rocks. Int. J. Mech. Sci., 40(4),387-398.

Dormieux L., Kondo D. and Ulm F.J., 2006. Microporomechanics. Wiley.

I. Ekeland, I., Temam, R., 1975. Convex analysis and variational problems, Amsterdam, North Holland.

L. Dormieux, D. Kondo, An extension of Gurson model incorporating interface stress effects, Int. J. Eng. Sci. 48 (2010) 575-581.

Fitzpatrick, S., 1988. Representing monotone operators by convex functions. In: Workshop/Miniconference on Functional Analysis and Optimization, Canberra, 1988, pp. 5965. Proc. Centre Math. Anal. Austral. Nat. Univ., 20, Austral. Nat. Univ., Canberra.

M. Garajeu, 2011. Comportement non linaire des milieux htrognes. Habilitation Thesis, Univ. of Mediterannee, Marseill, France.

Guo, T.F., Faleskog, J., Shih, C.F.2008. Continuum modeling of a porous solid with pressure-sensitive dilatant matrix. Journal of the Mechanics and Physics of Solids, 56, 2188-2212.

A. L. Gurson, 1977. Continuum theory of ductile rupture by void nucleation and growth: part I, yield criteria and flow rules for porous ductile media. *J. Engrg. Mater. Technol.*, 99:2-15

Hill, R., 1950. Mathematical theory of plasticity. Oxford University Press, London.

Jeong, H.Y., Pan, J., 1995. A macroscopic constitutive law for porous solids with pressure-sensitive matrices and its applications to plastic flow localization. International Journal of the Mechanics and Physics of Solids, 39, 1385-1403.

Jeong, H.Y., 2002. A new yield function and a hydrostatic stress-controlled model for porous solids with pressure-sensitive matrices. International Journal of the Mechanics and Physics of Solids, 32, 3669-3691.

J.-B. Leblond, 2001. Mécanique de la Rupture fragile et ductile.

Maghous, S., Dormieux, L., Barthélémy, J.F., 2009. Micromechanical approach to the strength propoerties of frictional geomaterials. European Journal of Mechanics A/Solids, 28, 179-188.

Markov, A.A., 1947. On variational principles on theory of plasticity. Prok. Mat. mekh., 11, 339-350.

Moreau, J.J.,2003. Fonctionnelles convexes. Istituto Poligrafico e Zecca dello Stato, Rome.

Rockafellar, R.T., 1970. Convex Analysis, Princeton University Press, Princeton.

J. R. Rice and D. M. Tracey. On a ductile enlargement of voids in triaxial stress fields. *J. Mech. Phys. Solids*, 17 : 201-217, 1969.

Salençon J., 1983. *Calcul à la rupture et analyse limite*. Presses de l'ENPC.

Save, M.A., Massonnet, C.E., de Saxcé, G., 1997. Plastic limit analysis of plates, shells and disks. Elsevier, New York.

Sun, Y., Wang D., 1989. A lower bound approach to the yield loci of porous materials. Acta Mechanica Sinica, 5, 237-243.

Sun Y., Wang D., 1995. Analysis of shear localization in porous materials based on a lower bound. Int. Journ. Fracture, 71, 71-83.

Suquet, P. Plasticité et homogénéisation. Doctorate Thesis, Univ. Paris VI, 1982.

Thoré, P., Pastor, F., Pastor, J., Kondo, D., 2009. Closed-form solutions for the hollow sphere model

with Coulomb and Drucker-Prager materials under isotropic loadings. Comptes Rendus Mécanique, 337, 260-267.

Chapitre 2

A stress-based variational model for ductile porous materials

International Journal of Plasticity 55 (2014) 133–151

Contents lists available at ScienceDirect

International Journal of Plasticity

journal homepage: www.elsevier.com/locate/ijplas

A stress-based variational model for ductile porous materials

Long Cheng [a], Géry de Saxcé [a], Djimedo Kondo [b,*]

[a] Laboratoire de Mécanique de Lille, UMR 8107 CNRS, Université de Lille 1, Cité scientifique, F59655 Villeneuve d'Ascq, France
[b] Institut Jean Le Rond d'Alembert, UMR 7190 CNRS, Université Pierre et Marie Curie, 4 place Jussieu, F75005 Paris, France

ARTICLE INFO

Article history:
Received 7 July 2013
Received in final revised form 5 October 2013
Available online 26 October 2013

Keywords:
Ductile porous material
von Mises matrix
Statical limit analysis
Homogenization

ABSTRACT

The main objective of this paper is to formulate a very new statically-based model of ductile porous materials having a von Mises matrix. In contrast to the Gurson's well known kinematical approach applied to a hollow sphere, the proposed study proceeds by means of a statical limit analysis procedure. Its development and implementation require the choice of an appropriate trial stress field. The starting point is Hill's variational principle for rigid plastic matrix. The use of a lagrangian multiplier allows to satisfy the plastic criterion in an average sense. The proposed trial stress field, complying with internal equilibrium, is composed of an heterogeneous part (exact solution for the stress field in the hollow sphere under pure hydrostatic loading) to which is added a uniform deviatoric stress field. Owing to this choice, the stress vector conditions on the void boundary are relaxed. By solving the resulting Saddle point problem, we derive closed form formula which depends not only on the first and second invariant of the macroscopic stress tensor but also on the sign of the third invariant of the stress deviator. The obtained results are fully discussed and compared to existing models, available numerical data and to Finite Elements results obtained from cell calculation carried out during the present study. Finally, we provide for the new model the macroscopic flow rule as well as the porosity evolution equations which also show very original features. Some of these features are illustrated.

1. Introduction

To obtain macroscopic criterion of ductile porous materials, Gurson (1977) has proposed a kinematical limit analysis approach of a hollow sphere and a hollow cylinder having a von Mises solid matrix. This approach delivered an upper bound of the searched macroscopic criterion. Several extensions of the Gurson model have been further proposed in the literature. Owing to the observation that Gurson model appears too stiff when compared with finite element unit-cell computations, Tvergaard (1981) and then Tvergaard and Needleman (1984) (see also Tvergaard (1981) and Tvergaard (1990)) proposed a heuristic extension of the Gurson model, known as the GTN model. This extension, widely used in structural computations introduces three parameters, q_1, q_2 and q_3, which have to be determined. A proposition on the dependence of such parameters on porosity has been recently done by Fritzen et al. (2012) based on computations carried out on a representative elementary volume of the ductile porous medium.[1] Applications of ductile fracture models generally concern metallic materials (see for instance Gänser et al. (1998), Han et al. (2013), Khan and Liu (2012) and Khan and Liu (2012)). Further extensions of the Gurson model, probably the most important ones, include those accounting for void shape effects (Gologanu et al., 1997; Garajeu et al., 2000; Monchiet et al., 2007; Monchiet et al., 2013). Matrix plastic anisotropy was also treated for the first time by Benzerga and Besson (2001) in the case of spherical voids, the extension to spheroidal voids being made later by Monchiet et al.

* Corresponding author. Tel.: +33 144275485; fax: +33 144275259.
E-mail address: djimedo.kondo@upmc.fr (D. Kondo).

[1] This study has been extended in Fritzen et al. (2012) to porous materials with Green type matrix.

0749-6419/$ - see front matter © 2013 Elsevier Ltd. All rights reserved.
http://dx.doi.org/10.1016/j.ijplas.2013.10.003

(2006) and Monchiet et al. (2008) (see also Keralavarma and Benzerga (2008) and Keralavarma and Benzerga (2010)). Other recent works concern ductile porous metals with incompressible matrix exhibiting an asymmetry between tension and compression (see for instance Cazacu and Stewart (2009) and Revil-Baudard and Cazacu (2013)). For completeness, mention has to be made of other theoretical extensions taking into account the plastic compressibility of the matrix by considering a Mises–Schleicher or a Drucker–Prager matrix for applications to polymer and cohesive geomaterials (Jeong and Pan, 1995; Jeong, 2002; Lee and Oung, 2000; Zaïri et al., 2008; Canal et al., 2009; Guo et al., 2008). Finally, some very recent works deal with nanoporous materials (Huang and Li, 2005; Li and Huang, 2005; Zhang et al., 2010; Dormieux and Kondo, 2010; Dormieux and Kondo, 2013; Monchiet and Kondo, 2013). Others are devoted to porous materials reinforced by rigid inclusions (Garajeu and Suquet, 1997; Shen et al., 2012; He et al., 2013).

In Gurson's footsteps, all the above limit analysis-based models of ductile porous media are obtained by using kinematical approach which requires the choice of a suitable trial velocity field[2]. On the other hand, few works have been made to develop a theoretical dual stress based model. One may mention the pioneering study of Green (1972), even it has been phenomenologically inspired. A statical limit analysis attempt has been first done for ductile porous media by Sun and Wang (1989) (see also Sun and Wang (1995)) who developed a semi-analytical approach which aimed to deliver a lower bound criterion.[3] Despite the interest of the above approaches by Sun and Wang (1989) and by Landry and Chen (2011), the resulting criteria are in fact obtained by some fitting procedure based on numerical computations. Moreover, although the authors claim a more accurate formability prediction than by the Gurson criterion when compared to experiments, the accuracy of the above criteria (built upon analysis of a hollow sphere subjected to uniform stress boundary conditions) seems not satisfactory in view of rigorous numerical bounds recently obtained by Trillat and Pastor (2005) and Thoré et al. (2011) from statically-based numerical computations and optimization made on the hollow sphere. It clearly appears that a proper theoretical framework based on a statical limit analysis of porous media, and its implementation for the derivation of a macroscopic criterion, are still due. This is the main purpose of the present study.

From a more general point of view, it must be noted that, although the direct and accurate knowledge of the stress field is of great interest in plasticity due to the fact that the yield criterion is often expressed in terms of stress components, the main reason which probably explains the preference in past studies of the kinematical approach (leading to upper bounds) is technical: the dissipation function is non smooth but only for null plastic strains. As it is generally the case for limit analysis of microporous ductile materials, the reference cell (the hollow sphere in the present study) is completely plastified at limit state and the dissipation functional is smooth, differentiable with respect to the trial velocity field parameters. And as it is well known in duality theory, the more a functional is smooth, the more its dual one is non smooth. It is exactly what occurs in plasticity where the stress functional is much more difficult to manage due to its non smoothness concentrated in the satisfaction of the yield criterion.

The principal aim of this paper is to face this difficulty and to open a new way –alternative and complementary to Gurson like models– to build macroscopic yield criteria for ductile porous materials thanks to a stress model leading to a closed form expression of the macroscopic criterion. The developed approach also enters in the framework of limit analysis, well-known as a general method to determine the plastic limit state of structures under proportional loading. The variational formulation of the lower bound theorem is based on Hill's functional (Hill, 1950) (see also Nguyen Dang (1976) or chapter 6 in Save et al. (1997)) which is summarized and adapted to the homogenization problem by applying it to the hollow sphere model. The lower bound character of the results is guaranteed only if the trial stress field is statically and plastically admissible. This is the pitfall because, while the equilibrium equations are linear, the yield criterion is generally non linear, and then difficult to fulfill exactly. Of course, it could seem attractive to use linearised criteria such as Tresca or Mohr–Coulomb ones but they become non linear when expressed with respect to stress components in non principal axes. Still, in the framework of limit analysis, other linearisation were proposed but are not relevant because, to be accurate enough, they require in three dimensions consideration of too numerous linear facets. In the present paper, we follow an alternative approach inspired from numerical works by Nguyen Dang (1976) where the yield criterion is satisfied *'in the mean'* over each finite element. This concept has the following meaning: the yield condition is relaxed and we must expect to obtain only an approximation of the lower bound, sometimes qualified of quasi-lower bound. The idea seems to be relevant also for theoretical models because of the very high difficulty to obtain a closed analytical expression. The key idea is to satisfy only the equilibrium equations, relaxing the plastic criterion with Lagrange's multipliers. Moreover, the stress condition at the void boundary is also difficult to satisfy by simple trial stress fields capturing the shear effects that break the central symmetry; it will be also relaxed. A priori, the final picture could seem too rough but, although the trial stress field is rather simple with a strict number of field parameters able to fit the hydrostatic and deviatoric macro-stress components, the present approach provides a rather accurate model, as it will be shown. Indeed, the lower bound will be lost but, but by comparison to accurate numerical data, the interest and the validity of the new results will be demonstrated. Besides, a salient feature which will be shown for the derived model is that it predicts explicit dependence on all the three stress invariants. This particular point will be fully commented and analysed in relation with very recent results established by Cazacu et al. (2013) based on a kinematical limit analysis approach.

[2] Note that another class of ductile porous models, dealing with representative elementary volume, has been proposed in literature by using nonlinear homogenization techniques (see for instance Ponte-Castañeda (1991), Suquet (1995), Ponte-Castañeda and Suquet (1998), Barthélémy and Dormieux (2003), Danas et al. (2008) and Maghous et al. (2009)). These techniques are not discussed in the present paper.

[3] Note also the more recent study by Landry and Chen (2011) in which has been formulated a plane stress lower bound criterion for porous ductile sheet metals.

The paper is organized as follows. In Section 2, we briefly recall the concepts of statically and plastically admissible stress fields, which allows to define the licit ones. Then, for the formulation of the stress variational model, the limit analysis based homogenization procedure is developed, by simultaneously considering the Hill's variational principle, and introducing a Lagrange's multiplier to solve the resulting saddle-point minimization problem. Section 3 is devoted to the determination of the macroscopic yield function of the porous media. A closed-form expression is established by adopting the hollow sphere model and an appropriate trial stress field which is detailed in Appendix A. In order to underline the interest of the established criterion, a first comparison to Gurson's model is provided in subSection 4.1. For completeness, the predictions of the statically-based criterion obtained by Sun and Wang (1995) will be also included in Appendix C. Other comparisons to numerical solutions (bounds, Finite Elements results) are also reported in the subSection 4.2. Finally, the plastic strain rate equations are given in Section 5 by applying the normality rule, while voids evolution equation is obtained from the mass balance. Some original features of these equations are indicated and illustrated on several figures.

2. A Stress-based variational formulation in the framework of limit analysis

In the perspective of limit analysis application to ductile porous materials, let us consider a reference unit volume or macro-element Ω composed of a void ω and matrix $\Omega_M = \Omega - \omega$. The macro-element Ω is bounded by surface $\partial\Omega$ and the void ω by $\partial\omega$. The matrix is made of a rigid plastic material with a yield criterion:

$$F(\boldsymbol{\sigma}) \leqslant 0, \tag{1}$$

where F is a lower semicontinuous and convex function of the cauchy stress tensor $\boldsymbol{\sigma}$. As classically, the normality law is assumed:

$$\mathbf{d} = \dot{\varepsilon}^p \frac{\partial F}{\partial \boldsymbol{\sigma}}, \tag{2}$$

where $\mathbf{d}$ is the strain rate tensor, while $\dot{\varepsilon}^p$ is the equivalent plastic strain rate. It is worth to notice that, equivalently, the strain rate and stress tensor satisfy Hill's inequality:

$$\forall \boldsymbol{\sigma}' \in K, \quad (\boldsymbol{\sigma}' - \boldsymbol{\sigma}) : \mathbf{d} \leqslant 0, \tag{3}$$

where the plastic domain K is the closed and convex set of stress fields satisfying the yield criterion (1).

From the classical Hill lemma, the macroscopic stress $\boldsymbol{\Sigma}$ and macroscopic strain rate $\mathbf{D}$ are obtained as volume averages of their microscopic counterparts $\boldsymbol{\sigma}$ and $\mathbf{d}$:

$$\boldsymbol{\Sigma} = \frac{1}{|\Omega|}\int_\Omega \boldsymbol{\sigma}\, dV, \quad \mathbf{D} = \frac{1}{|\Omega|}\int_\Omega \mathbf{d}\, dV. \tag{4}$$

The set of kinematical admissible velocity fields classically reads:

$$\mathcal{K}_a = \{\mathbf{v}\ s.t.\ \mathbf{v}(\mathbf{x}) = \mathbf{D}\cdot\mathbf{x} \quad on \quad \partial\Omega\}$$

And, the strain rate field, symmetric part of the velocity gradient, is $\mathbf{d}(\mathbf{v}) = grad_s\mathbf{v}$.

The set of statically admissible stress fields is such as:

$$\mathcal{S}_a = \{\boldsymbol{\sigma}\ s.t.\ div\ \boldsymbol{\sigma} = 0\ in\ \Omega,\ \boldsymbol{\sigma}\cdot\mathbf{n} = 0\ on\ \partial\omega,\ \boldsymbol{\sigma} = 0\ in\ \omega\}.$$

where $\mathbf{n}$ is the unit outward normal vector.

The homogenization problem consists in determining the macroscopic stress for which there exist at least an admissible couple $(\mathbf{v}, \boldsymbol{\sigma}) \in \mathcal{K}_a \times \mathcal{S}_a$ satisfying anywhere in the matrix the yield criterion (1) and the normality rule (2). In general, due to its strongly non linear character, this problem has no closed form solution. This has motivated implementation of an equivalent variational formulation, more appropriate for simple approximations, thanks to relevant choice of trial stress fields and minimization procedure.

Considering an admissible couple $(\mathbf{v}, \boldsymbol{\sigma})$, one has by Hill's lemma,

$$\mathbf{D} : \boldsymbol{\Sigma} = \frac{1}{|\Omega|}\int_\Omega \mathbf{d}(\mathbf{v}) : \boldsymbol{\sigma}\, dV = \frac{1}{|\Omega|}\int_{\Omega_M} \mathbf{d}(\mathbf{v}) : \boldsymbol{\sigma}\, dV.$$

Let us also recall a basic concept of convex analysis, the subdifferential of a function ψ in a point $\boldsymbol{\sigma}$ which is the (possibly empty) set:

$$\partial\psi(\boldsymbol{\sigma}) = \{\mathbf{d} | \forall \boldsymbol{\sigma}', \quad \psi(\boldsymbol{\sigma}') - \psi(\boldsymbol{\sigma}) \geqslant (\boldsymbol{\sigma}' - \boldsymbol{\sigma}) : \mathbf{d}\}. \tag{5}$$

For more details on convex analysis, the reader is referred for instance to Ekeland and Temam (1975), Moreau (2003) and Rockafellar (1970). Hence, introducing the semicontinuous and convex function:

$$\psi(\boldsymbol{\sigma}) = \left\{ \begin{matrix} 0 & \text{if } \boldsymbol{\sigma} \in K \\ +\infty & \text{otherwise} \end{matrix} \right\},$$

Hill's inequality (3) can be recast as:

$$\mathbf{d} \in \partial\psi(\boldsymbol{\sigma}),$$

Since $\boldsymbol{\sigma} \in K$ entails $\psi(\boldsymbol{\sigma}) = 0$, the inequality in (5) degenerates into (3) when $\boldsymbol{\sigma}' \in K$ and is true otherwise, the left hand member being infinite while the left hand one is finite.

This suggests to state Hill's variational principle (Hill, 1950) (see also Nguyen Dang (1976) or chapter 6 in Save et al. (1997)) for a body Ω_M.

Among the statically admissible stress fields, the true one makes the functional

$$\int_{\Omega_M} \psi(\boldsymbol{\sigma})\ dV - \int_{S_v} (\boldsymbol{\sigma}\cdot\mathbf{n})\cdot\mathbf{v} dS, \tag{6}$$

an absolute minimum.

In (6), $\mathbf{v}$ is the imposed velocity on the part S_v of the boundary of Ω_M. Adapted to the context of the present homogenization problem, e.g. the problem of a hollow sphere subjected to uniform strain rate boundary conditions $\mathbf{v}(\mathbf{x}) = \mathbf{D}\cdot\mathbf{x}$ on its boundary $\partial\Omega$, this principle requires to introduce the the following average functional for the hollow sphere:

$$\Phi = \min_{\boldsymbol{\sigma}\in\mathcal{S}_a}\left(\frac{1}{|\Omega|}\int_{\Omega_M}\psi(\boldsymbol{\sigma})\ dV - \mathbf{D}:\boldsymbol{\Sigma}\right), \tag{7}$$

where $\boldsymbol{\Sigma}$ depends on the stress field $\boldsymbol{\sigma}$ through:

$$\boldsymbol{\Sigma} = \frac{1}{|\Omega|}\int_{\partial\Omega}(\boldsymbol{\sigma}\mathbf{n})\otimes\mathbf{x}\ dS,$$

or equivalently (4), provided that the stress field $\boldsymbol{\sigma}$ is statically admissible.

Indeed, let $\mathbf{v}$ and $\boldsymbol{\sigma}$ be the velocity and stress fields at limit state. Taking into account Hill's lemma and $\mathbf{d}(\mathbf{v}) \in \partial\psi(\boldsymbol{\sigma})$, it holds for any statically admissible fields $\boldsymbol{\sigma}'$:

$$\frac{1}{|\Omega|}\int_{\Omega_M}(\psi(\boldsymbol{\sigma}') - \psi(\boldsymbol{\sigma}) - (\boldsymbol{\sigma}'-\boldsymbol{\sigma}):\mathbf{d}((\mathbf{v}))\ dV \geqslant 0,$$

which proves that the limit stress field $\boldsymbol{\sigma}$ realizes the minimum of the functional among all the statically admissible stress fields $\boldsymbol{\sigma}'$. Defining the set of licit stress fields:

$$\mathcal{S}_l = \{\boldsymbol{\sigma}\in\mathcal{S}_a\ s.t.\ F(\sigma)\leqslant 0\ a.e.\ in\ \Omega_M\}, \tag{8}$$

let us notice that if $\boldsymbol{\sigma}$ is licit, the value of the functional in (7) is finite, infinite otherwise. The minimum being finite, it is realized only for licit fields. Because ψ vanishes almost everywhere for the licit fields, the above variational principle (7) is equivalent to the following one:

$$\min_{\boldsymbol{\sigma}\in\mathcal{S}_l}(-\mathbf{D}:\boldsymbol{\Sigma}), \tag{9}$$

The limit analysis approach consists in finding non trivial solutions qualified as failure mechanisms. It is expected that they exist only under an equality condition on $\boldsymbol{\Sigma}$ that can be interpreted as the equation of the macroscopic yield surface.

In the same spirit, as in the work of Guo et al. (2008), a first approximation consists in relaxing the yield criterion (1). Introducing Lagrange's multiplier field $\mathbf{x}\mapsto\dot{\Lambda}(\mathbf{x})$, this constrained minimization problem is transformed into an equivalent saddle-point problem:

$$\max_{\dot{\Lambda}\geqslant 0}\min_{\boldsymbol{\sigma}\in\mathcal{S}_a}\left(\mathcal{L}(\boldsymbol{\sigma},\dot{\Lambda}) = \frac{1}{|\Omega|}\int_{\Omega_M}\dot{\Lambda}F(\boldsymbol{\sigma})\ dV - \mathbf{D}:\boldsymbol{\Sigma}\right),$$

We perform a new approximation by imposing Lagrange's multiplier field to be uniform in Ω_M:

$$\max_{\dot{\Lambda}\geqslant 0}\min_{\boldsymbol{\sigma}\in\mathcal{S}_a}\left(\mathcal{L}(\boldsymbol{\sigma},\dot{\Lambda}) = \dot{\Lambda}\frac{1}{|\Omega|}\int_{\Omega_M}F(\boldsymbol{\sigma})\ dV - \mathbf{D}:\boldsymbol{\Sigma}\right). \tag{10}$$

that is equivalent to minimize the functional Φ under the following condition:

$$\frac{1}{|\Omega|}\int_{\Omega_M}F(\boldsymbol{\sigma})\ dV = 0. \tag{11}$$

Satisfying the condition (1) only in an average sense (Eq. (11)) but not locally anywhere in Ω_M is a strong approximation but required here in order to make the calculation possible. The minimum principle allows then to obtain the "best " solution within the framework imposed by the adopted approximations. Hence, a stress variational macroscopic model (which will be called SVM in the following) can be obtained from Eq. (11). Additionally, it should be emphasized that this model could be seen as a quasi-lower bound due to the adoption of the relaxed licit stress fields which appears as an uncontrollable

approximation in the Hill's variational principle (7). Note that Gurson's kinematically-based model is a true upper bound, all the approximation that it had required being controllable.

The final and crucial step, detailed in the next section, is the choice of a trial stress field depending on some parameters. After expressing it with respect to the invariants of the macro-stress, the macroscopic loading function is:

$$\mathcal{F}(\Sigma) = \frac{1}{|\Omega|}\int_{\Omega_M} F(\boldsymbol{\sigma}(\Sigma))\, dV = 0. \tag{12}$$

Thus, the saddle-point problem (10) reads:

$$\max_{\dot{\Lambda}\geqslant 0}\min_{\Sigma}\Big(\mathcal{L}(\boldsymbol{\Sigma},\dot{\Lambda}) = \dot{\Lambda}\mathcal{F}(\Sigma) - \mathbf{D}:\boldsymbol{\Sigma}\Big),$$

Performing the variation with respect to $\dot{\Lambda}$ provides the macroscopic yield condition:

$$\mathcal{F}(\Sigma) \leqslant 0$$

and with respect to Σ gives the macroscopic plastic flow rule:

$$\mathbf{D} = \dot{\Lambda}\frac{\partial \mathcal{F}}{\partial \boldsymbol{\Sigma}}(\boldsymbol{\Sigma}). \tag{13}$$

where $\dot{\Lambda}$ turns out then to be the plastic multiplier and must satisfy Kuhn–Tucker conditions:

- $\dot{\Lambda} = 0$ *if* $\mathcal{F} < 0$, *or if* $\mathcal{F} = 0$ *and* $\dot{\mathcal{F}} < 0$
- $\dot{\Lambda} > 0$ *if* $\mathcal{F} = 0$ *and* $\dot{\mathcal{F}} > 0$

3. Proposed stress field and formulation of the macroscopic yield criterion

Let us consider a hollow sphere, made up of a spherical void embedded in a homothetic matrix of a rigid-plastic isotropic and homogeneous material with von Mises model:

$$F(\boldsymbol{\sigma}) = \sigma_e(\boldsymbol{\sigma}) - \sigma_0 \leqslant 0,$$

where $\sigma_e = \sqrt{\frac{3}{2}\mathbf{s}:\mathbf{s}}$ is the von Mises equivalent stress defined from the deviatoric part $\mathbf{s}$ of the stress tensor $\boldsymbol{\sigma}$. As usually, the quantity $\sigma_0 > 0$ represents the yield stress of the matrix material. The inner and outer radii of the hollow sphere are respectively denoted by a and b, giving the void volume fraction $f = (a/b)^3 < 1$.

3.1. Proposed trial stress field

Accounting for the symmetry of the hollow sphere model, the trial stress field is considered as the sum of the two following fields:

- A heterogeneous part corresponding to the exact field under pure hydrostatic loadings; it reads, in spherical coordinates with orthonormal frame $\{\mathbf{e}_r, \mathbf{e}_\phi, \mathbf{e}_\theta\}$:

$$\boldsymbol{\sigma}^{(1)} = -A_0\left(\ln\left(\frac{a}{r}\right)\mathbf{1} - \frac{1}{2}(\mathbf{e}_\theta\otimes\mathbf{e}_\theta + \mathbf{e}_\phi\otimes\mathbf{e}_\phi)\right), \tag{14}$$

A_0 being a constant to be determined.
- A homogeneous deviatoric part which is taken in the following form, in the cylindrical coordinates with orthonormal frame $\{\mathbf{e}_\rho, \mathbf{e}_\phi, \mathbf{e}_z\}$:

$$\boldsymbol{\sigma}^{(2)} = A_1(\mathbf{e}_\rho\otimes\mathbf{e}_\rho + \mathbf{e}_\phi\otimes\mathbf{e}_\phi - 2\mathbf{e}_z\otimes\mathbf{e}_z), \tag{15}$$

where $\mathbf{1}$ is the second order unit tensor, while A_1 is also constant parameter. The derivation of the above two stress field contributions is outlined in Appendix A.

Consequently, in the matrix Ω_M, the resultant two parameters-based trial stress field in the matrix can be written as:

$$\boldsymbol{\sigma} = \boldsymbol{\sigma}^{(1)} + \boldsymbol{\sigma}^{(2)}, \tag{16}$$

Note that a vanishing stress field is considered in the void ω.

Remark 1. It is worth to notice that the choice of the above stress field, defined by (16), together with (14) and (15), implies that[4]:

[4] $\sigma_m = tr(\boldsymbol{\sigma})/3$ being the mean stress.

$$\Sigma_m^{void} = \frac{1}{|\Omega|}\int_\omega \sigma_m \, dV = \frac{1}{3|\Omega|}\int_{\partial\omega} \mathbf{x}\cdot(\boldsymbol{\sigma}\mathbf{n}) \, dS = 0. \tag{17}$$

which then appears as a relaxed form of the void boundary condition, difficult to be satisfied by simple stress fields.

As a consequence, the variational principle (9) must then be considered with the following relaxed set of licit stress fields:

$$\mathcal{S}_r = \{\boldsymbol{\sigma} \; s.t. \; div\,\boldsymbol{\sigma} = 0, \; F(\sigma) \leqslant 0 \; in \; \Omega_M, \; \boldsymbol{\sigma} = 0 \; in \; \omega \; and \; \Sigma_m^{void} = 0\}. \tag{18}$$

at the place of $\mathcal{S}_l$ defined by (8).

In cylindrical coordinates, the complete stress field (16) reads:

$$\begin{aligned}\boldsymbol{\sigma} = &\left[\left(-\ln\left(\frac{a}{r}\right)+\frac{1}{2}\cos^2\theta\right)A_0 + A_1\right](\mathbf{e}_\rho\otimes\mathbf{e}_\rho) + \left[\left(-\ln\left(\frac{a}{r}\right)+\frac{1}{2}\right)A_0 + A_1\right](\mathbf{e}_\phi\otimes\mathbf{e}_\phi)\\ &+\left[\left(-\ln\left(\frac{a}{r}\right)+\frac{1}{2}\sin^2\theta\right)A_0 - 2A_1\right](\mathbf{e}_z\otimes\mathbf{e}_z) - \frac{A_0}{2}\sin\theta\cos\theta(\mathbf{e}_\rho\otimes\mathbf{e}_z + \mathbf{e}_z\otimes\mathbf{e}_\rho)\end{aligned} \tag{19}$$

3.2. Derivation of the macroscopic criterion SVM

From (19), it is readily seen that the equivalent stress σ_e in the matrix reads:

$$\sigma_e = \sqrt{\left(\frac{A_0}{2}\right)^2 + \frac{3}{2}A_0A_1(3\cos^2\theta - 1) + (3A_1)^2} \tag{20}$$

A remarkable observation on the above expression of σ_e is that with cylindrical coordinates variables it does not depend on r, but is only function of the variable θ. This remarkable property, which originates from the constance of the deviatoric part of $\boldsymbol{\sigma}^{(1)}$ (exact axisymmetric stress field under hydrostatic loading) in spherical coordinates, will be very useful in the following for the derivation of the macroscopic yield criterion.

The axisymmetric macroscopic stress tensor, resulting from (19), takes the form:

$$\boldsymbol{\Sigma} = -\frac{A_0\ln f}{3}\mathbf{1} + (1-f)A_1(\mathbf{e}_\rho\otimes\mathbf{e}_\rho + \mathbf{e}_\phi\otimes\mathbf{e}_\phi - 2\mathbf{e}_z\otimes\mathbf{e}_z), \tag{21}$$

which readily provides the macroscopic mean stress Σ_m, the macroscopic equivalent stress Σ_e and the third invariant of the macroscopic stress deviator J_3:

$$\Sigma_m = -\frac{A_0\ln f}{3}, \quad \Sigma_e = 3(1-f)|A_1|, \quad J_3 = -2(1-f)^3A_1^3. \tag{22}$$

in which J_3 is the determinant of the deviatoric part of $\boldsymbol{\Sigma}$.

For commodity, let us now introduce the following stress based quantities:

$$\tilde{\Sigma}_e = \frac{\Sigma_e}{1-f}, \quad \tilde{\Sigma}_m = -\frac{3\Sigma_m}{2\ln f}, \quad \tilde{J}_3 = \frac{J_3}{(1-f)^3}, \tag{23}$$

This allows to rewrite (20) in the form:

$$\sigma_e = \sqrt{\tilde{\Sigma}_e^2 + \tilde{\Sigma}_m^2 + sign(J_3)\tilde{\Sigma}_e\tilde{\Sigma}_m(3\cos^2\theta - 1)}$$

for which $sign(J_3)$ is defined by[5]:

$$sign(J_3) = \frac{27}{2}\frac{\tilde{J}_3}{\tilde{\Sigma}_e^3} = -sign(A_1).$$

The macroscopic yield condition (12) then reads:

$$\frac{1}{|\Omega|}\int_{\Omega_M} F(\boldsymbol{\sigma}) \, dV = \frac{2\pi}{|\Omega|}\int_a^b r^2dr\int_0^\pi \sigma_e\sin\theta\, d\theta - (1-f)\sigma_0 = 0$$

and reduces to:

$$\frac{1}{2}\int_0^\pi \sqrt{\tilde{\Sigma}_e^2 + \tilde{\Sigma}_m^2 + sign(J_3)\tilde{\Sigma}_e\tilde{\Sigma}_m(3\cos^2\theta - 1)}\sin\theta\, d\theta = \sigma_0 \tag{24}$$

By considering the notations introduced in (23), the macroscopic criterion takes then the following final form:

[5] This is related to the well known Lode angle in axisymmetric conditions.

$$\mathcal{F}(\boldsymbol{\Sigma},f)=\sqrt{\tilde{\Sigma}_e^2+\tilde{\Sigma}_m^2}\,\mathcal{J}\left(sign(J_3)\frac{2\tilde{\Sigma}_e\tilde{\Sigma}_m}{\tilde{\Sigma}_e^2+\tilde{\Sigma}_m^2}\right)-\sigma_0\ \leqslant 0, \tag{25}$$

Again, the quantities $\tilde{\Sigma}_e, \tilde{\Sigma}_m$ and $\tilde{J}_3$ are defined in (23).

Let us denote:

$$\zeta=sign\,(J_3)\frac{2\tilde{\Sigma}_e\tilde{\Sigma}_m}{\tilde{\Sigma}_e^2+\tilde{\Sigma}_m^2}=sign(J_3)\frac{2\widetilde{T}}{1+\widetilde{T}^2} \tag{26}$$

with

$$\widetilde{T}=\frac{\tilde{\Sigma}_m}{\tilde{\Sigma}_e}=-\frac{3(1-f)}{2lnf}T, \tag{27}$$

T being the stress triaxiality classically defined as $T=\frac{\Sigma_m}{\Sigma_e}$. Note that the definition (26), axisymmetric loading conditions have been used. The quantity ζ obviously depends not only on the sign of the third invariant of the stress deviator but also on that of the stress triaxiality, and on the porosity.

The function $\mathcal{J}$ in Eq. (25) is then defined as:

$$\mathcal{J}(\zeta)=\frac{1}{2}\int_0^{\pi}\sqrt{1+\frac{1}{2}(3\cos^2\theta-1)\zeta}\ \sin\theta\ d\theta. \tag{28}$$

and has the following closed-form expression:

- for $-1\leqslant\zeta\leqslant 0$:

$$\mathcal{J}(\zeta)=\frac{1}{2}\left(\sqrt{1+\zeta}+\frac{2-\zeta}{\sqrt{6|\zeta|}}\arcsin\sqrt{\frac{3|\zeta|}{2-\zeta}}\right), \tag{29}$$

- for $0\leqslant\zeta\leqslant 1$:

$$\mathcal{J}(\zeta)=\frac{1}{2}\left(\sqrt{1+\zeta}+\frac{2-\zeta}{\sqrt{6\zeta}}\ln\frac{\sqrt{3\zeta}+\sqrt{2(1+\zeta)}}{2-\zeta}+\frac{\sqrt{6}}{12}\frac{(2-\zeta)\ln(2-\zeta)}{\sqrt{\zeta}}\right). \tag{30}$$

In addition to the original stress variational methodology introduced in the present study of ductile porous media, Eq. (25) which will be referred as (SVM)[6], together with (29) and (30) constitute probably one of the most important results of the present paper.

Remark 2. It is convenient to indicate that the obtained criterion presents some analogies with that has been derived in the interesting study by Shtern and Cocks (2001) see also a series of papers including Shtern and Cocks (2001), Shtern et al. (2002), Shtern et al. (2002) and Kuz'mov and Shtern (2002)).[7] But in the above studies, the third invariant J3 affects only the macroscopic criterion through the contribution of the Von Mises equivalent stress.

Remark 3. The Gurson's kinematical derivation incorporates an approximation that has been introduced for technical reason and led to the well-known criterion which depends only on the two invariants Σ_m and Σ_e. In contrast to this kinematical derivation, the computing of the analogous integral (24) in our stress variational approach appears to be more simple and has been achieved without any approximation. At this stage, it must be mentioned that in a very recent study, Cazacu et al. (2013) success to obtain a kinematically based criterion without the Gurson approximation. This allowed them to point out and to address the role of the third invariant of the stress deviator. The present criterion (25), derived from a stress-based Limit Analysis, can be viewed as a statical counterpart of these recent results: Eq. (25), together with (29) and (30) also provide a class of yield criteria depending not only on Σ_m and Σ_e (the first and second macroscopic stresses invariants), but also on the sign of the third invariant of the stress deviator, J_3. Indeed, due to the presence of the quantity ζ defined by (26), the criterion is asymmetric respectively with the sign change of Σ_m but also with that of J_3. This kind of dependence has been clearly noted in Cazacu et al. (2013) in the context of the Gurson-like kinematical approach; the following symmetry property of the criterion has been pointed out: $\mathcal{F}(-\Sigma_m,\Sigma_e,-J_3)=\mathcal{F}(\Sigma_m,\Sigma_e,J_3)$. Interestingly, this is fulfilled by the criterion (25) established in the present study.

[6] SVM as Stress Variational Model.

[7] Danas and Castañeda (2012) noted that the effect of the third invariant of the macroscopic stress tensor is introduced by these authors in a somewhat ad hoc manner.

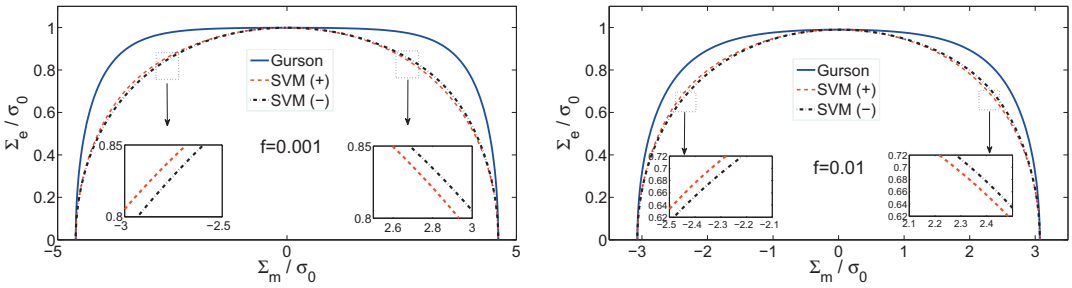

(a) Porosity: $f = 0.001$ (b) Porosity: $f = 0.01$

Fig. 1. Comparison between the yield surfaces obtained from the SVM (this study) and the Gurson criterion (Gurson, 1977) with the values of porosity $f = 0.001$ and $f = 0.01$, respectively.

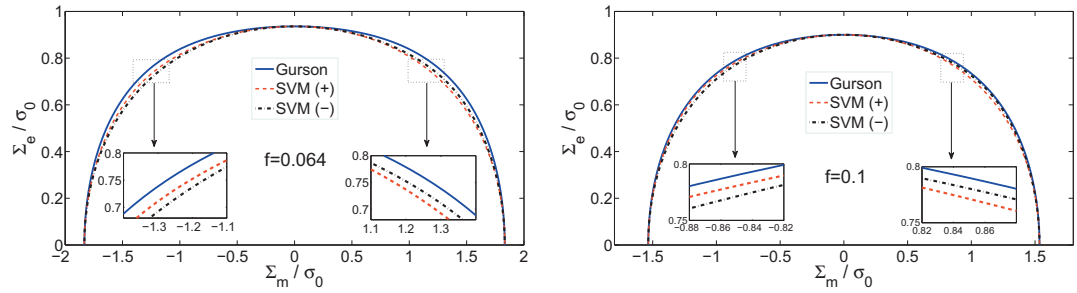

(a) Porosity: $f = 0.064$ (b) Porosity: $f = 0.1$

Fig. 2. Comparison between the yield surfaces obtained from the SVM (this study) and the Gurson criterion (Gurson, 1977) with the values of porosity $f = 0.064$ and $f = 0.1$, respectively.

For the effects of third invariant on the macroscopic behaviour of porous materials, let us also mention the recent study by Brünig et al. (2013) and numerical results by Thoré et al. (2011), Pastor et al. (2012) and Danas and Castañeda (2012).

Remark 4. Noting that the function $\mathcal{J}(\zeta)$ is smooth over $[-1, 1]$ with extreme values $\mathcal{J}_{max} = \mathcal{J}(0) = 1, \mathcal{J}_{min} = \mathcal{J}(1) = 0.976$ over $[0, 1]$ and $\mathcal{J}_{min} = \mathcal{J}(-1) = 0.962$ over $[-1, 0]$, one can be interested to approximate it by unity. This readily leads to a simplified expression of the macroscopic yield function which is then independent of J_3. This simplified criterion, expressed in (B.1), is discussed in Appendix B.

4. Assessment of the predictive capabilities of the statically-based criterion

We aim now at assessing the established macroscopic yield function (SVM) by comparing its predictions first with that of the Gurson criterion (see Figs. 1 and 2). Moreover, the yield surfaces of SVM are shown in these two figures in order to display the asymmetric character of the derived criterion with respect to the sign of the third invariant J_3. Standard Finite Element Method (FEM) based limit analysis computations are also performed and their results allow to assess the theoretical results. For completeness, we also report on Figs. 5–7 the numerical lower and upper bounds of Trillat and Pastor (2005) and Thoré et al. (2011). Finally, the numerical data for all the models and computations of the limit loads are displayed in Appendix D.

4.1. Comparison to analytical criteria and discussion

Due to assumptions on the stress fields which have been introduced for the analytical derivation, the new criterion SVM (25) could be seen just as a quasi-lower bound. However, it still preserves the exact solution of the hollow sphere subjected to a hydrostatic loading, $\Sigma_m/\sigma_0 = -2/3ln(f)$, and leads to the same expression of the limit pure shear load as that given by the Gurson criterion, $\Sigma_e/\sigma_0 = 1 - f$. In addition to the comparison to the Gurson model, we also compare in C the SVM prediction to that of Sun and Wang (1989), in which a statical approach[8] was firstly considered for ductile porous materials.

[8] Even it was for uniform stress boundary conditions.

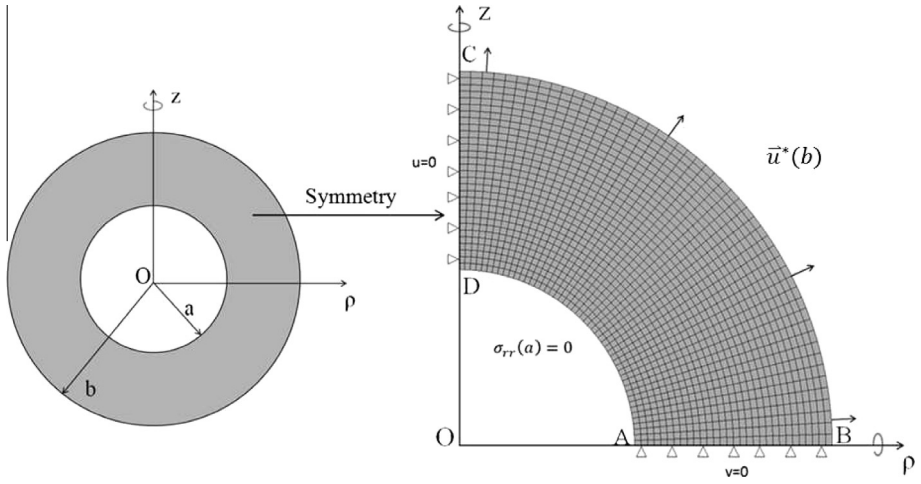

Fig. 3. Hollow sphere model: Geometry of the elementary cell and boundary conditions.

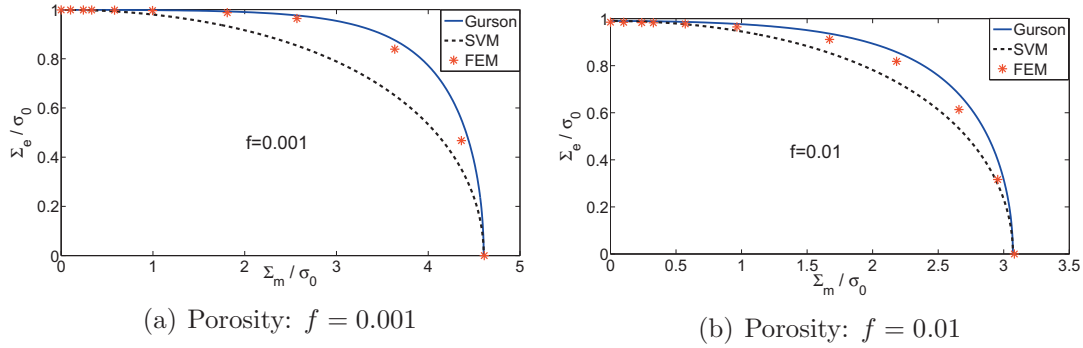

Fig. 4. Comparison between the yield surfaces obtained from the SVM (this study), the Gurson criterion (Gurson, 1977) and the FEM solution with boundary condition of MPC. Porosity: 0.001 and 0.01.

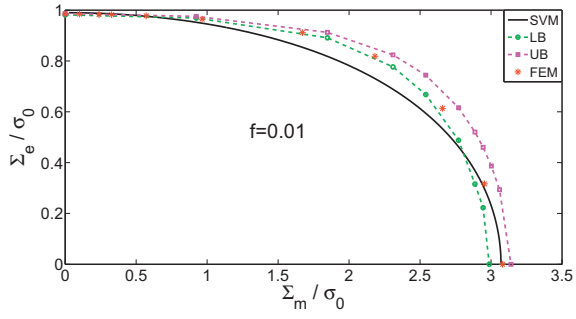

Fig. 5. Comparison between the yield surfaces obtained from the SVM (this study), the numerical bounds (Trillat and Pastor, 2005) and the FEM solution with boundary condition of MPC. Porosity: 0.01.

According to these authors, their approach has led to the so called lower bound criterion, whose closed form expression is valid only for $f \leqslant 0.3$.

Moreover, as mentioned before, due to the presence of the third invariant J_3 in the SVM criterion, the yield surface exhibits an asymmetry about the axis $\Sigma_m = 0$. Hence, the yield surfaces are deliberately plotted on Figs. 1 and 2 for negative and positive Σ_m; the considered porosity values are $f = 0.001, f = 0.01, f = 0.064$ and $f = 0.1$, respectively. These values of the porosity are chosen only for further comparison with the available numerical bounds of Trillat and Pastor (2005) and Thoré et al. (2011) in subSection 4.2 (except for $f = 0.001$ for which the numerical data are not available). It is noted that the SVM

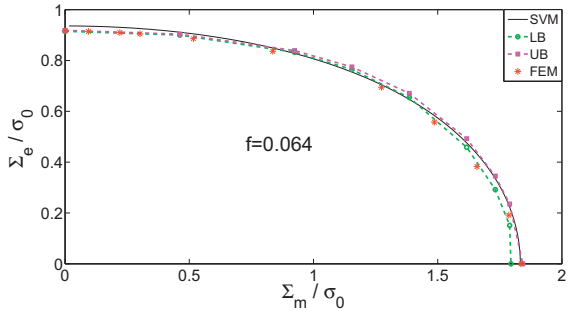

Fig. 6. Comparison between the yield surfaces obtained from the SVM (this study), the numerical bounds (Trillat and Pastor, 2005) and the FEM solution with boundary condition of MPC. Porosity: 0.064.

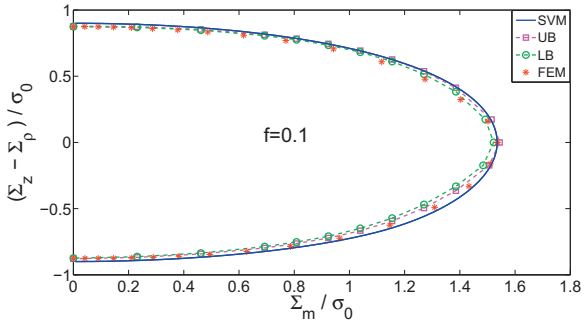

Fig. 7. Comparison between the yield surfaces obtained from the SVM (this study), the numerical bounds (Thoré et al., 2011) and the FEM solution with boundary condition of MPC. Porosity: 0.1.

criterion presents some slight differences with the Gurson one, the surfaces predicted by SVM being strictly "below " the Gurson's ones, simultaneously coincident with them for hydrostatic loading (exact result) and pure deviatoric one (as mentioned before).

Noticeable difference with Gurson criterion is observed for very small porosities. This can be first explained by that the statical and the kinematical approaches of Limit Analysis are fundamentally different in nature: in absence of uncontrolled approximations these two approaches deliver lower and upper bounds, respectively. In the particular context of the SVM, the observed difference may found its origin in the inaccuracy resulting from the relaxation of the yield condition in the matrix, this condition being enforced only in the mean. For small porosities, large plastic strain heterogeneities may occur in the vicinity of the cavities and the above procedure consisting to relax the yield condition should be inaccurate. It is clear that the proposed model can be improved by considering a more refined admissible stress field able to avoid such procedure.

The differences between the surfaces will be more commented in Section 4.2 by means of comparison with numerical bounds which will be presented.

Finally, the slight asymmetry of the SVM yield surfaces can also be observed on Figs. 1 and 2, with the notations of SVM(+) and SVM(−) for the yield surfaces corresponding to $J_3 > 0$ and $J_3 < 0$, respectively. For clarity, and as in Cazacu et al. (2013), a zoom is proposed on a portion of the figure corresponding to moderate stress triaxialities.

4.2. Numerical assessment: comparisons to FEM results and to numerical bounds

In this section, the yield surfaces obtained by means of the stress variational approach will be compared with Finite Element Method (FEM) solutions obtained during the present study. As shown on Fig. 3, the numerical analysis is carried out on an axisymmetric model with a spherical void in its central part. Owing to the geometrical symmetry, only a quarter of this model is considered with 1500 axisymmetric elements. Moreover, an incremental analysis of elastoplastic materials in small deformations is adopted. The computations are carried out by means of ABAQUS/Standard software and a user subroutine MPC (Multi-Points Constraints). The main reason for which we need to enforce MPC conditions in the code is that we have to impose the velocity field $\mathbf{v}$ from $\mathbf{v} = \mathbf{D} \cdot \mathbf{x}$ (on the external boundary of the hollow sphere) such that the constraint of constant macroscopic stress triaxiality ($T = \Sigma_m/\Sigma_e$) be fulfilled. In practice, as in Guo et al. (2008), this is done by applying a constant macroscopic stress ratio Σ_ρ/Σ_z corresponding to the desired Σ_m/Σ_e. Note that the implementation of this procedure is the one that is already described in Cheng and Guo (2007) for the study of voids interaction and coalescence.

As already indicated in subSection 4.1 (See Figs. 1 and 2), the difference between the predictions of the new criterion SVM and the Gurson's one is particularly noticeable for small porosities. For this reason, we first consider in this subsection two values of porosity $f = 0.001$ and $f = 0.01$. The comparisons between the surfaces obtained from the SVM, the Gurson's model and the FEM solutions are illustrated on Fig. 4 only for the first quadrant (the slight asymmetry of the SVM surface is disregarded). We can observe that in these two cases, the FEM solutions are almost between the upper bound (Gurson's model) and the proposed yield criterion (SVM). This fact shows that the SVM could be seemed as a quasi lower bound for the porous materials which have relatively small values of porosity, especially for porous metal materials. Fig. 5 displays the comparisons between the predictions of the SVM criterion and the numerical bounds for $f = 0.01$. It should be noted that, even the FEM solution is between the numerical bounds, the yield surface of SVM is generally below the numerical LB, except for the loadings with high values of stress triaxiality $T = \Sigma_m/\Sigma_e$ for which it interestingly lies between the two bounds and coincides with the exact value of the hydrostatic loading. For the porosity $f = 0.064$ of which results are shown on Fig. 6, a better agreement is obtained between the analytical predictions, the FEM solution and the numerical bounds. Let us recall that the SVM results have been obtained by relaxing stress fields conditions (see Eq. (18)), it is therefore noticeable that it provides the above satisfactory yield surfaces.

For a more detailed discussion of the yield surfaces asymmetry reflecting the effects of the sign of J_3, we will now only consider $f = 0.1$ for which numerical bounds are available in Thoré et al. (2011). It is worthy to point out that the numerical yield surfaces provided by these authors are performed in the first and fourth quadrants. Hence, the SVM yield surface and FEM solutions will be displayed in the same way for this group of comparisons. As shown on Fig. 7, the corresponding results for the loading cases $\Sigma_z - \Sigma_\rho \geqslant 0$ and $\Sigma_z - \Sigma_\rho \leqslant 0$ directly related to the ones of $J_3 > 0$ and $J_3 < 0$, respectively. It is first noted that the locus of the SVM criterion has a good agreement with the UB when $\Sigma_z - \Sigma_\rho \geqslant 0$ (or $J_3 > 0$), while for the corresponding values of $\Sigma_z - \Sigma_\rho \leqslant 0$ (or $J_3 < 0$) with the same value of Σ_m is bigger (in absolute value) than the FEM solution. These observations are more clearly illustrated by comparing them to the FEM solutions in the same quadrant (see Fig. 8). Note that SVM (+) and FEM (+) correspond to the loading cases $\Sigma_z - \Sigma_\rho \geqslant 0$ while SVM (−) and FEM (−) are associated to $\Sigma_z - \Sigma_\rho \leqslant 0$.

For completeness, recalling the notation $T = \Sigma_m/\Sigma_e$ for the stress triaxiality, the values of the FEM solutions, related to the asterisk points in Fig. 7 are reported in Table 1.

5. Plastic flow rule and void growth

Due to the role played by the sign of third invariant in the SVM criterion (25), it is interesting to derive the macroscopic flow rule giving the plastic deformation (through its volumetric and deviatoric parts) by means of normality rule:

$$D_e = \dot{\Lambda}\frac{\partial \mathcal{F}}{\partial \Sigma_e} = \dot{\Lambda}\left[\frac{\mathcal{J}(\zeta)\Sigma_e}{(1-f)^2\sqrt{\tilde{\Sigma}_e^2+\tilde{\Sigma}_m^2}} + \kappa sign(J_3)\frac{d\mathcal{J}(\zeta)}{d\zeta}\frac{\Sigma_m\sqrt{\tilde{\Sigma}_e^2+\tilde{\Sigma}_m^2}}{4(\ln f)^2\Sigma_e^2+9(1-f)^2\Sigma_m^2}\right]$$
$$D_m = \frac{1}{3}\dot{\Lambda}\frac{\partial \mathcal{F}}{\partial \Sigma_m} = \dot{\Lambda}\left[\frac{3\mathcal{J}(\zeta)\Sigma_m}{4(\ln f)^2\sqrt{\tilde{\Sigma}_e^2+\tilde{\Sigma}_m^2}} - \frac{\kappa}{3}sign(J_3)\frac{d\mathcal{J}(\zeta)}{d\zeta}\frac{\Sigma_e\sqrt{\tilde{\Sigma}_e^2+\tilde{\Sigma}_m^2}}{4(\ln f)^2\Sigma_e^2+9(1-f)^2\Sigma_m^2}\right] \quad (31)$$

where $\dot{\Lambda}$ is the plastic multiplier and

$$\kappa = \frac{12(1-f)\ln f\left[4(\ln f)^2 - 9(1-f)^2T^2\right]}{4(\ln f)^2 + 9(1-f)^2T^2} \quad (32)$$

while the expression of $d\mathcal{J}(\zeta)/d\zeta$ can be developed for $-1 \leqslant \zeta \leqslant 0$ as:

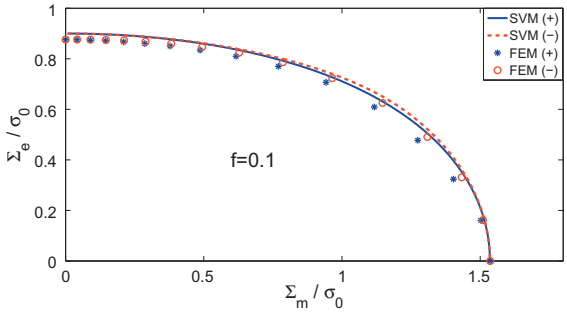

Fig. 8. Comparison between the closed-form yield surface (SVM) and the FEM solution with respect to the influence of the J_3 sign. Porosity: 0.1.

Table 1
Numerical values of Σ_m/σ_0 and $(\Sigma_z - \Sigma_\rho)/\sigma_0$ with respect to different values of $T = \Sigma_m/\Sigma_e$, where $T(+)$ is related to $T \geqslant 0$ and $T(+)$ to $T \leq 0$.

$T(+)$	Σ_m/σ_0	$(\Sigma_z - \Sigma_\rho)/\sigma_0$	$T(-)$	Σ_m/σ_0	$(\Sigma_z - \Sigma_\rho)/\sigma_0$
$+\infty$	1.5358	0.0	$-\infty$	1.5357	0.0
9.3333	1.5022	0.1610	−9.3333	1.5097	−0.1618
4.3333	1.4033	0.3238	−4.3333	1.4330	−0.3307
2.6667	1.2741	0.4778	−2.6667	1.3088	−0.4908
1.8333	1.1169	0.6092	−1.8333	1.1467	−0.6255
1.3333	0.9424	0.7068	−1.3333	0.9646	−0.7235
1	0.7701	0.7701	−1	0.7865	−0.7865
0.7619	0.6171	0.8099	−0.7619	0.6281	−0.8244
0.5833	0.4868	0.8345	−0.5833	0.4941	−0.8469
0.4444	0.3780	0.8504	−0.4444	0.3824	−0.8603
0.3333	0.2867	0.8602	−0.3333	0.2894	−0.8681
0.2424	0.2101	0.8666	−0.2424	0.2116	−0.8727
0.1667	0.1452	0.8711	−0.1667	0.1458	−0.8751
0.1026	0.0896	0.8733	−0.1026	0.0899	−0.8762
0.0476	0.0417	0.8752	−0.0476	0.0417	−0.8764
0.0	0.0	0.8756	0.0	0.0	−0.8761

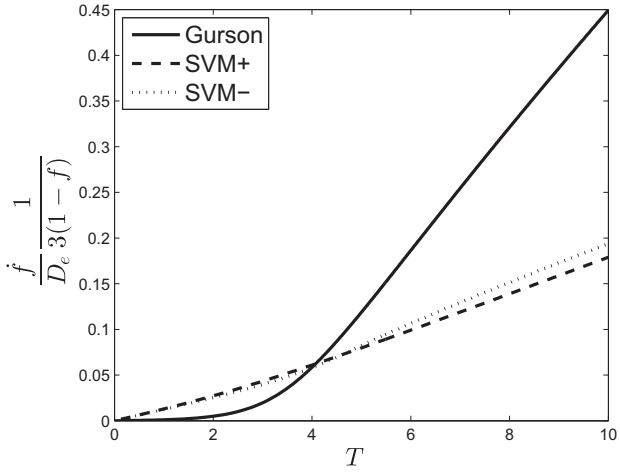

Fig. 9. Evolution of porosity as function of the stress triaxiality for initial porosity $f = 0.001$. Comparison between SVM predictions and that of Gurson model.

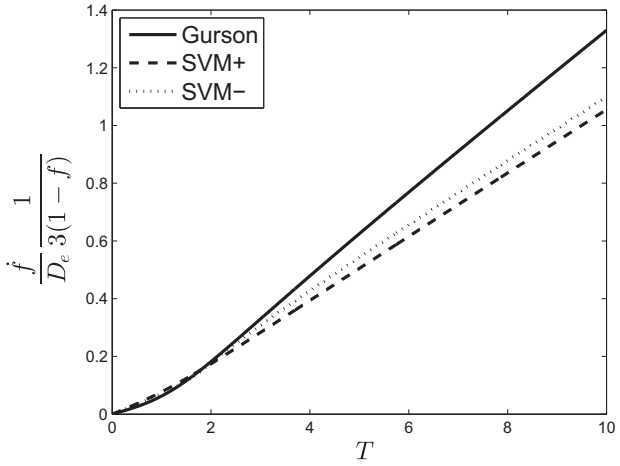

Fig. 10. Evolution of porosity as function of the stress triaxiality for initial porosity $f = 0.064$. Comparison between SVM predictions and that of Gurson model.

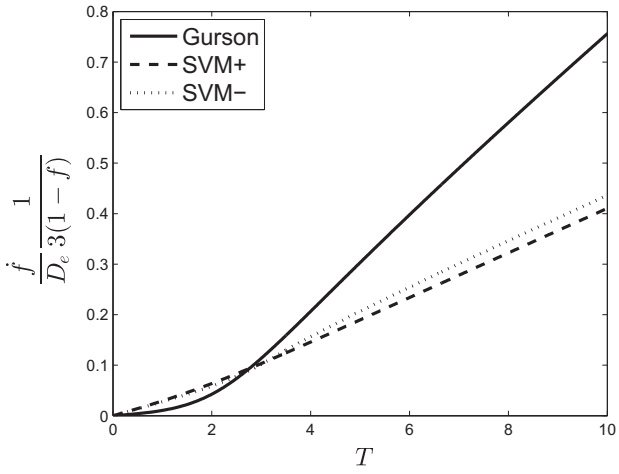

Fig. 11. Evolution of porosity as function of the stress triaxiality for initial porosity $f = 0.01$. Comparison between SVM predictions and that of Gurson model.

$$\frac{d\mathcal{J}(\zeta)}{d\zeta} = \frac{|\zeta|-1}{4|\zeta|\sqrt{1+\zeta}} - \frac{|\zeta|-2}{4|\zeta|\sqrt{6|\zeta|}}\arcsin\left(\sqrt{\frac{3|\zeta|}{2-\zeta}}\right) \tag{33}$$

and for $0 \leqslant \zeta \leqslant 1$ as:

$$\begin{aligned}\frac{d\mathcal{J}(\zeta)}{d\zeta} = {} & \frac{1}{4\sqrt{1+\zeta}} - \frac{\sqrt{6}}{24\zeta^{3/2}}(2+\zeta)\ln\frac{\sqrt{3\zeta}+\sqrt{2(1+\zeta)}}{2-\zeta} - \frac{\sqrt{6}}{48\sqrt{\zeta}}\left[\frac{2+\zeta}{\zeta}\ln(2-\zeta)+2\right] \\ & + \frac{1}{12}\frac{3\sqrt{1+\zeta}(2+\zeta)+\sqrt{6\zeta}(4+\zeta)}{\zeta\sqrt{6\zeta(1+\zeta)}+2\zeta(1+\zeta)}\end{aligned} \tag{34}$$

Remark 5. The plastic flow rule (31) can be rewritten in term of stress triaxiality $\widetilde{T}$ (defined by (27)) and the sign of the third invariant, $sign(J_3)$. One has:

$$\begin{aligned} D_e &= \frac{\dot{\Lambda}}{1-f}\left[\frac{\mathcal{J}(\zeta)}{\sqrt{1+\widetilde{T}^2}} + 2sign(J_3)\frac{d\mathcal{J}(\zeta)}{d\zeta}\frac{\widetilde{T}(\widetilde{T}^2-1)}{(\widetilde{T}^2+1)^{\frac{3}{2}}}\right] \\ D_m &= -\frac{\dot{\Lambda}}{2\ln f}\left[\frac{\mathcal{J}(\zeta)\widetilde{T}}{\sqrt{1+\widetilde{T}^2}} - 2sign(J_3)\frac{d\mathcal{J}(\zeta)}{d\zeta}\frac{\widetilde{T}^2-1}{(\widetilde{T}^2+1)^{\frac{3}{2}}}\right]\end{aligned} \tag{35}$$

Let us recall that ζ has been introduced in (26).

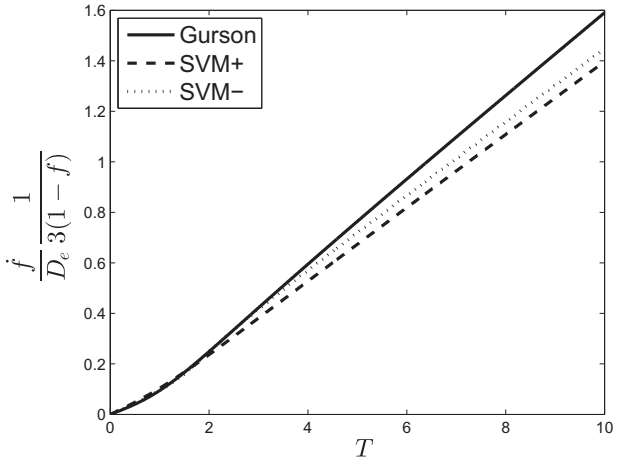

Fig. 12. Evolution of porosity as function of the stress triaxiality for initial porosity $f = 0.1$. Comparison between SVM predictions and that of Gurson model.

Finally, the void growth equation can be also derived as classically from the mass balance equation, $\dot{f} = 3(1-f)D_m$, which can be suitably rewritten in the form:

$$\frac{\dot{f}}{D_e} = 3(1-f)\frac{D_m}{D_e} \tag{36}$$

which is readily given by (31) (or equivalently by (35)) together with (32)–(34). Interestingly, this proved that the void growth is sensitive not only to stress triaxiality but also to the sign of J_3.

Figs. 9–12 illustrate the evolution of porosity given as function of stress triaxiality for three values of initial porosity. It is noted that despite the few influence of the sign of third invariant on the macroscopic criterion, a noticeable effect is noted for the porosity variation. The results are also compared with that predicted by the Gurson model. Clear differences are observed, particularly for high stress triaxialities for which the Gurson model is known to overestimate the variation of the porosity.

6. Conclusion

In this study, we have proposed a stress-based variational methodology of ductile porous materials in the framework of Limit Analysis approach. This has been done by applying homogenization theory combined with the statical limit analysis approach. The stress variational model (SVM), fully described in the paper, takes advantage of Hill's variational principle for which relaxed licit stress fields have been adopted. The established results clearly provide a closed form expression of the statically-based macroscopic criterion. Due to the relaxed internal boundary condition resulting from the chosen trial stress fields, the criterion could be seen only as a quasi-lower bound. An interesting feature of the established criterion is its dependence not only on the two stress invariants Σ_m and Σ_e, but also on the sign of the third invariant of the stress deviator; this leads to specific asymmetries of the macroscopic criterion. From this point of view, and less on the methodological one, the derived criterion appears as a statical counterpart of results recently obtained by Cazacu et al. (2013) in the context of a kinematical limit analysis approach.

The results derived from the obtained criterion are fully assessed by means of comparison with existing analytical criteria, with available numerical bounds and finally with our Finite Elements results. This has allowed to demonstrate the interest of the new theoretical results. For completeness, we also provide voids growth equations which clearly show the effects of the sign of the third invariant in addition to that of the stress triaxiality.[9] The resulting porosity evolution is fully illustrated. Finally, it is convenient to indicate that, besides the original statically-based methodology provided in the present study, an important perspective lies in the possibility now to investigate the case of porous media with a non associated matrix (see studies by Gao et al. (2011)). Clearly enough this can be addressed by means of the Bipotential approach introduced by de Saxcé and Feng (1991), de Saxcé (1992) and Hjiaj et al. (2003) and which has already led to a generalization of classical limit analysis theorems to the context of non associated materials. In this perspective, the interest of the present study lies in that one will need for the implementation of the bipotential theory (for porous media) both the trial velocity and the trial stress fields.

Appendix A. Formulation of the proposed stress field contributions: $^{(1)}$ and $^{(2)}$

Accounting for the central symmetry of the hollow sphere model, the spherical coordinates (r,θ,ϕ) and the cylindrical ones (ρ,ϕ,z) are used for the two adopted stress fields: the hydrostatic component $\boldsymbol{\sigma}^{(1)}$ and the deviatoric one $\boldsymbol{\sigma}^{(2)}$, respectively. ρ and ϕ are the polar radius and angle, z the height with respect to the Oxy plane and $r = \sqrt{\rho^2+z^2}$.

A.1. Formulation of the hydrostatic component $\boldsymbol{\sigma}^{(1)}$

In order to limit the errors due to approximations, we hope the macroscopic model to be exact at least for the pure hydrostatic loading. Let us consider $\hat{\boldsymbol{\sigma}}$ to be the solution for such a particular case in spherical coordinates. Evidently, it has three non-vanishing components $\hat{\sigma}_{rr}$, $\hat{\sigma}_{\theta\theta} = \hat{\sigma}_{\phi\phi}$ and, in absence of body force, satisfies the radial equilibrium equation:

$$\frac{d\hat{\sigma}_{rr}}{dr} + 2\,\frac{\hat{\sigma}_{rr}-\hat{\sigma}_{\theta\theta}}{r} = 0, \tag{A.1}$$

with static boundary condition:

$$\hat{\sigma}_{rr}(a) = 0, \tag{A.2}$$

Furthermore, due to the spherical symmetry, the yield function reads:

$$F(\hat{\sigma}) = \epsilon(\hat{\sigma}_{\theta\theta}-\hat{\sigma}_{rr}) - \sigma_0, \tag{A.3}$$

[9] This topic of the effect of stress states on ductile fracture is a growing and is deserving attention in several recent studies: see for instance Nahshon and Hutchinson (2008), Gao et al. (2009) and Li et al. (2011).

with the following convention:

- $\epsilon = +1$ if $\hat{\sigma}_{rr} \leqslant \hat{\sigma}_{\theta\theta}$,
- $\epsilon = -1$ if $\hat{\sigma}_{\theta\theta} \leqslant \hat{\sigma}_{rr}$.

Combining (A.3) with the equilibrium Eq. (A.1) gives:

$$d\hat{\sigma}_{rr} = \frac{2\epsilon\sigma_0}{r},$$

Hence, considering the boundary condition (A.2) and taking into account (A.3), we obtain the limit state of the pure hydrostatic case:

$$\hat{\sigma}_{rr} = -2\epsilon\sigma_0 \ln\left(\frac{a}{r}\right),$$

$$\hat{\sigma}_{\theta\theta} = \hat{\sigma}_{\phi\phi} = -2\epsilon\sigma_0\left(\ln\left(\frac{a}{r}\right) - \frac{1}{2}\right).$$

Consequently, the hydrostatic part of the stress field can be written as:

$$\boldsymbol{\sigma}^{(1)} = -A_0\left(\ln\left(\frac{a}{r}\right)\cdot\mathbf{1} - \frac{1}{2}(\mathbf{e}_\theta\otimes\mathbf{e}_\theta + \mathbf{e}_\phi\otimes\mathbf{e}_\phi)\right), \tag{A.4}$$

where $\mathbf{1}$ is the unit tensor and A_0 a proportional parameter, while $A_0 > 0$ is corresponding to the general traction loading, and $A_0 < 0$ the general compression one. For this reason, the parameter ϵ is represented implicitly by the sign of A_0.

Next, the corresponding macroscopic stress tensor for $\boldsymbol{\sigma}^{(1)}$ can be obtained:

$$\boldsymbol{\Sigma}^{(1)} = -\frac{1}{3}\ln(f)A_0\cdot\mathbf{1}$$

A.2. Formulation of the component $\boldsymbol{\sigma}^{(2)}$ corresponding to the stress deviator

Let us first note that the formulation of $\boldsymbol{\sigma}^{(2)}$ in the spherical coordinates is very tedious to due to the non-spherically character of the loading. In order to overcome this limitation and keep the formulation simple, it is useful to consider an axisymmetric problem in cylindrical coordinates. We wish then to obtain an axisymmetric trial stress field $\boldsymbol{\sigma}^{(2)}$, which has three non-vanishing components, $\boldsymbol{\sigma}^{(2)}_{\rho\rho} = \sigma^{(2)}_{\phi\phi}, \sigma^{(2)}_{zz}$ and, should also satisfy the equilibrium equation in absence of the body forces:

$$\frac{\partial\sigma^{(2)}_{\rho\rho}}{\partial\rho} + \frac{\sigma^{(2)}_{\rho\rho} - \sigma^{(2)}_{\phi\phi}}{\rho} = 0, \qquad \frac{\partial\sigma^{(2)}_{\phi\phi}}{\partial\phi} = 0, \qquad \frac{\partial\sigma^{(2)}_{zz}}{\partial z} = 0,$$

Owing to the difficulty to obtain an exact field corresponding to the above equations (to be integrated), we propose to adopt a homogeneous deviatoric stress field under axisymmetric conditions:

$$\boldsymbol{\sigma}^{(2)} = A_1(\mathbf{e}_\rho\otimes\mathbf{e}_\rho + \mathbf{e}_\phi\otimes\mathbf{e}_\phi - 2\mathbf{e}_z\otimes\mathbf{e}_z), \tag{A.5}$$

A_1, being a constant parameter. Consequently, the corresponding macroscopic stress field reads:

$$\boldsymbol{\Sigma}^{(2)} = (1-f)A_1(\mathbf{e}_\rho\otimes\mathbf{e}_\rho + \mathbf{e}_\phi\otimes\mathbf{e}_\phi - 2\mathbf{e}_z\otimes\mathbf{e}_z),$$

Appendix B. Approximate criterion (AC)

Following Gurson (1977), the function $\mathcal{J}(\zeta)$ may be taken equal to unity. Consequently, the approximated criterion (AC) can be reduced into the form:

$$\left(\frac{\Sigma_e}{1-f}\right)^2 + \left(\frac{3\Sigma_m}{2\ln f}\right)^2 = \sigma_0^2 \tag{B.1}$$

Both expressions (25) and (B.1) give the same value for the two particular cases:

- *Pure hydrostatic case:* $\Sigma_e = 0, \quad \Sigma_m = -\frac{2\sigma_0\ln f}{3}$
- *Pure shear case:* $\Sigma_e = (1-f)\sigma_0, \quad \Sigma_m = 0.$

As mentioned above, the exact solution of the pure hydrostatic loading, and the same solution as the closed form criterion (SVM) (or Gurson's one) can be obtained from AC. Fig. 13 displays the comparison of the yield loci obtained from the criteria between the Gurson's one, the proposed closed form (SVM) and approximate ones (AC). It should be noted that, due to the fact that the function $\mathcal{J}(\zeta)$ is taken to be unity, the influence of the third invariant J_3 is neglected in the approximate criterion AC. For completeness, the comparisons between the yield loci of Gurson, SVM and AC for four values of porosity ($f = 0.001$, 0.01, 0.064 and 0.1) are displayed on Fig. 13 only in the first quadrant by neglecting the slight asymmetry of the SVM one.

Appendix C. The so called lower bound of Sun and Wang (1989)

The statically-based criterion proposed by Sun and Wang (1989) reads:

$$\frac{\Sigma_e^2}{\sigma_0^2}+\frac{f\left[\beta_1\sinh\left(q\frac{\Sigma_m}{\sigma_0}\right)+\beta_2\cosh\left(q\frac{\Sigma_m}{\sigma_0}\right)\right]}{\left[1+\beta_4 f^2\sinh^2\left(q\frac{\Sigma_m}{\sigma_0}\right)\right]^{\frac{1}{2}}}-\beta_3=0 \tag{C.1}$$

in which $q=\frac{3}{2}$, $\beta_1=0$, $\beta_2=2-\frac{1}{2}\ln f$, $\beta_3=1+f(1+ln(f))$,

$$\beta_4=\left(\frac{\beta_2}{\beta_3}\right)^2 cth^2\left(q\frac{\Sigma_m^0}{\sigma_0}\right)-\frac{1}{f^2\sinh^2\left(q\frac{\Sigma_m^0}{\sigma_0}\right)} \quad with\,\Sigma_m^0=-0.65\sigma_0\ln f$$

Note that the Gurson model corresponds to

$$\beta_1=0,\quad \beta_2=2,\quad \beta_3=1+f^2,\quad \beta_4=0$$

Finally, the comparison of the yield loci obtained from the above yield criterion, the closed form of SVM in Section 3, the Gurson criterion (Gurson, 1977) are performed in Fig. 14 by neglecting the slight asymmetry of the SVM one.

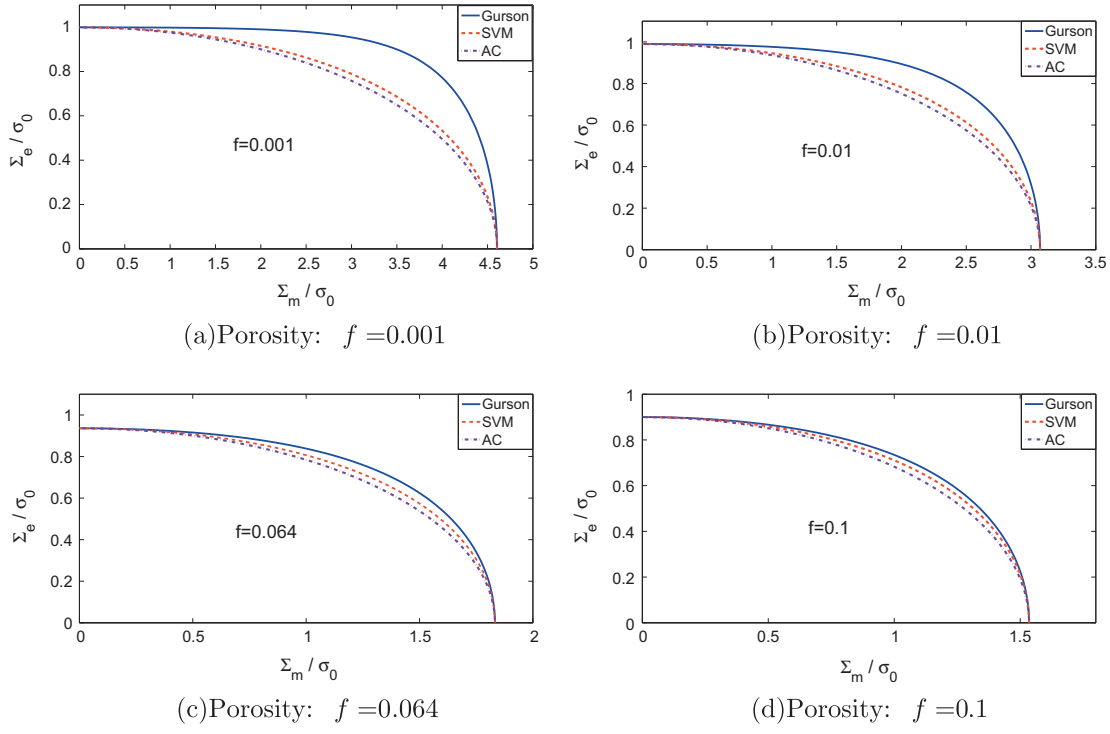

Fig. 13. Comparison between the yield surfaces obtained from the SVM (Section 3), the Gurson criterion (Gurson, 1977) and the approximate one with full-field solutions, with the values of porosity $f = 0.001, f = 0.001, f = 0.064$ and $f = 0.1$, respectively.

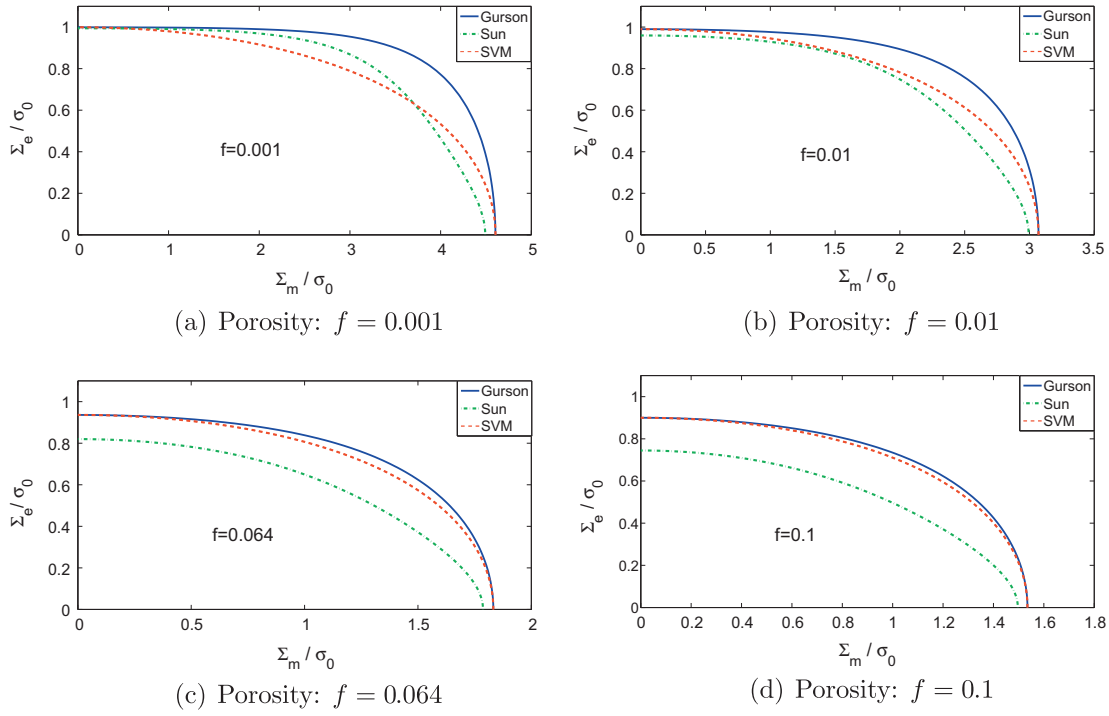

(a) Porosity: $f = 0.001$ (b) Porosity: $f = 0.01$

(c) Porosity: $f = 0.064$ (d) Porosity: $f = 0.1$

Fig. 14. Comparison between the yield surfaces obtained from the SVM (Section 3), the Gurson criterion (Gurson, 1977) and Sun and Wang one (Sun and Wang, 1989) with the values of porosity $f = 0.001, f = 0.001, f = 0.064$ and $f = 0.1$, respectively.

Appendix D. Table of comparison of numerical values

This comparison concerns values of Σ_e/σ_0obtained from Trillat and Pastor (2005), the corresponding analytical ones computed from the established yield criteria (SVM) detailed in Section 3 and the approximate one (AC) detailed in Appendix B, the criterion of Sun and Wang (1989) and the Gurson's model for $f = 0.01, 0.064, 0.1$.

It is worthy to point out that:

- Due to different expressions of von Mises yield criterion, the values of limit stress reported in Trillat and Pastor (2005) are divided by $\sqrt{3}$.

Table D.2
Comparison for $f = 0.01$ and $f = 0.064$.

f	Σ_m/σ_0	SVM	AC	Sun	Gurson	Trillat and Pastor (2005)	
						LB	UB
0.01	0	0.9900	0.9900	0.9596	0.9900	0.9815	0.9865
	0.9238	0.9522	0.9441	0.9342	0.9786	0.9690	0.9754
	1.8475	0.8181	0.7907	0.7963	0.9163	0.8911	0.9125
	2.3094	0.6886	0.6523	0.6150	0.8248	0.7767	0.8239
	2.5403	0.5941	0.5560	0.4805	0.7404	0.6679	0.7441
	2.7713	0.4620	0.4620	0.3128	0.6010	0.4879	0.6160
	2.8868	0.3686	0.3370	0.2068	0.4903	0.3156	0.5204
	2.9445	0.3080	0.2803	0.1365	0.4144	0.2226	0.4599
	3.0022	0.2288	0.2071	–	0.3111	–	0.3867
	3.0600	0.0896	0.0803	–	0.1230	–	0.2935
	$\Sigma_m(max)$	3.0701	3.0701	2.9934	3.0701	2.9876	3.1401
0.064	0	0.9360	0.9360	0.8198	0.9360	0.9150	0.9186
	0.4619	0.9113	0.9058	0.7882	0.9188	0.9000	0.9036
	0.9238	0.8279	0.8084	0.6778	0.8557	0.8324	0.8390
	1.1547	0.7545	0.7268	0.5814	0.7944	0.7645	0.7748
	1.3856	0.6470	0.6126	0.4510	0.6961	0.6541	0.6709
	1.6166	0.4760	0.4408	0.2769	0.5246	0.4585	0.4924
	1.7321	0.3348	0.3057	0.1507	0.3732	0.2920	0.3451
	1.7898	0.2222	0.2011	–	0.2488	0.1512	0.2354
	$\Sigma_m(max)$	1.8326	1.8326	1.7868	1.8326	1.7948	1.8426

Table D.3
Comparison for the case $f = 0.1$.

Σ_m/σ_0	SVM	AC	Sun	Gurson	Thoré et al. (2011)	
					LB	UB
0	0.9000 (−0.9000)	0.9000	0.7447	0.9000	0.8741 (−0.8741)	0.8784 (−0.8784)
0.2309	0.8917 (−0.8098)	0.8898	0.7331	0.8932	0.8631 (−0.8692)	0.8684 (−0.8738)
0.4619	0.8657 (−0.8671)	0.8583	0.6969	0.8718	0.8360 (−0.8481)	0.8427 (−0.8535)
0.6928	0.8186 (−0.8236)	0.8031	0.6327	0.8318	0.7873 (−0.8061)	0.7972 (−0.8134)
0.8083	0.7853 (−0.7932)	0.7651	0.5887	0.8025	0.7522 (−0.7758)	0.7643 (−0.7834)
0.9238	0.7437 (−0.7555)	0.7188	0.5361	0.7650	0.7090 (−0.7350)	0.7221 (−0.7443)
1.0392	0.6918 (−0.7081)	0.6624	0.4744	0.7167	0.6495 (−0.6818)	0.6670 (−0.6933)
1.1547	0.6260 (−0.6456)	0.5930	0.4027	0.6535	0.5721 (−0.6113)	0.5938 (−0.6264)
1.2702	0.5401 (−0.5585)	0.5054	0.3191	0.5683	0.4691 (−0.5154)	0.4959 (−0.5373)
1.3856	0.4200 (−0.4329)	0.3874	0.2159	0.4453	0.3319 (−0.3834)	0.3648 (−0.4129)
1.4843	0.2528 (−0.2578)	0.2295	0.0696	0.2693	0.1732 (–)	– (–)
1.4925	0.2322 (−0.2364)	0.2104	0.0403	0.2473	– (−0.1732)	– (–)
1.5062	0.1922 (−0.1951)	0.1737	–	0.2047	– (–)	0.1732 (–)
1.5148	0.1616 (−0.1636)	0.1457	–	0.1721	– (–)	– (−0.1732)
1.5224	0.1281 (−0.1294)	0.1153	–	0.1364	0 (0)	– (–)
1.5440	– (–)	–	–	–	– (–)	0 (0)

- The numerical results without parenthesis are corresponding to the values of limit stress when $J_3 > 0$, while the ones with parenthesis in the same cells are corresponding to those of $J_3 < 0$.
- There is no value in the cells which are marked by dash "-" because of the non-available information in literature, or due to the fact that there is no real-number solution from the analytical yield functions.

(see Table D.2, D.3)

References

Barthélémy, J.F., Dormieux, L., 2003. Détermination du critère de rupture macroscopique d'un milieux poreux par homogénéisation non linéaire. C.R. Méc. 331, 271–276.

Benzerga, A.A., Besson, J., 2001. Plastic potentials for anisotropic porous solids. Eur. J. Mech. A/Solids 20, 397–434.

Michael Brünig, Steffen Gerke, Vanessa Hagenbrock, 2013. Micro mechanical studies on the effect of the stress triaxiality and the Lode parameter on ductile damage. Int. J. Plast. 50, 49–65.

Cazacu, O., Stewart, J.B., 2009. Plastic potentials for porous aggregates with the matrix exhibiting tension-compression asymmetry. J. Mech. Phys. Solids 57, 325–341.

Cazacu, O., Revil-Baudard, B., Lebensohn, R., Garajeu, M., 2013. On the combined effect of pressure and third invariant on yielding of porous solids with von Mises matrix. J. Appl. Mech.. http://dx.doi.org/10.1115/1.4024074.

Cheng, L., Guo, T.F., 2007. Void interaction and coalescence in polymeric materials. Int. J. Solids Struct. 44, 1787–1808.

Danas, K., Idiart, M.I., Castañeda, P.P., 2008. A homogenization-based constitutive model for isotropic viscoplastic porous media. Int. J. Solids Struct. 45, 3392–3409.

Danas, K., Castañeda, P.P., 2012. Influence of the Lode parameter and the stress triaxiality on the failure of elasto-plastic porous materials. Int. J. Solids Struct. 49, 1325–1342.

de Saxcé, G., Feng, Z.Q., 1991. New inequality and functional for contact friction: the implicit standard material approach. Mech. Struct. Mach. 19, 301–325.

de Saxcé, G., 1992. Une généralisation de l'inégalité de Fenchel et ses applications aux lois constitutives. C.R. Acad. Sci. Paris, Sér. II 314, 125–129.

Dormieux, L., Kondo, D., 2010. An extension of Gurson model incorporating interface stresses effects. Int. J. Eng. Sci. 48, 575–581.

Dormieux, L., Kondo, D., 2013. Non linear homogenization approach of strength of nanoporous materials with interface effects. Int. J. Eng. Sci. 71, 102–110.

Ekeland, I., Temam, R., 1975. Convex Analysis and Variational Problems. North Holland, Amsterdam.

Fritzen, F., Forest, S., Bohlke, T., Kondo, D., Kanit, T., 2012. Computational homogenization of elasto-plastic porous metals. Int. J. Plast. 29, 102–119.

Fritzen, F., Forest, S., Kondo, D., Bohlke, T., 2012. Computational homogenization of porous materials of Green type. Comput. Mech. 52, 121–134.

Gänser, H.-P., Werner, E.A., Fischer, F.D., 1998. Plasticity and ductile fracture of IF steels: experiments and micromechanical modeling. Int. J. Plast. 14, 789–803.

Gao, X., Zhang, T., Hayden, M., Roe, C., 2009. Effects of the stress state on plasticity and ductile failure of an aluminum 5083 alloy. Int. J. Plast. 25, 2366–2382.

Gao, X., Zhang, T.T., Zhou, J., Graham, S.M., Hayden, M., Roe, C., 2011. On stress-state dependent plasticity modeling: Significance of the hydrostatic stress, the third invariant of stress deviator and the non-associated flow rule. Int. J. Plast. 27, 217–231.

Garajeu, M., Suquet, P., 1997. Effective properties of porous ideally plastic or viscoplastic materials containing rigid particles. J. Mech. Phys. Solids 45, 873–902.

Garajeu, M., Michel, J.C., Suquet, P., 2000. A micromechanical approach of damage in viscoplastic materials by evolution in size, shape and distribution of voids. Comput. Methods Appl. Mech. Eng. 183, 223–246.

Gologanu, M., Leblond, J.B., Perrin, G., Devaux, J., 1997. Recent extensions of Gurson's model for porous ductile metals. In: Suquet, P. (Ed.), Continuum Micromechanics. Springer-Verlag.

Green, R.J., 1972. A plasticity theory for porous solids. J. Mech. Phys. Solids 14, 215–224.

Guo, T.F., Faleskog, J., Shih, C.F., 2008. Continuum modeling of a porous solid with pressure-sensitive dilatant matrix. J. Mech. Phys. Solids 56, 2188–2212.

Gurson, A.L., 1977. Continuum theory of ductile rupture by void nucleation and growth – part I: yield criteria and flow rules for porous ductile media. J. Eng. Mater. Technol. 99, 2–15.

Han, X., Besson, J., Forest, S., Tanguy, B., Bugat, S., 2013. A yield function for single crystals containing voids. Int. J. Solids Struct. 50, 2115–2131.

He, Z., Dormieux, L., Kondo, D., 2013. Strength properties of a Drucker–Prager porous medium reinforced by rigid particles. Int. J. Plast. (in press). http://dx.doi.org/10.1016/j.ijplas.2013.05.003.

Hill, R., 1950. Mathematical Theory of Plasticity. Oxford University Press, London.

Hjiaj, M., Fortin, J., de Saxcé, G., 2003. A complete stress update algorithm for the non-associated Drucker–Prager model including treatment of the apex. Int. J. Eng. Sci. 41, 1109–1143.
Huang, M., Li, Z., 2005. Size effects on stress concentration induced by a prolate ellipsoidal particle and void nucleation mechanism. Int. J. Plast. 21 (8), 1568–1590.
Jeong, H.Y., Pan, J., 1995. A macroscopic constitutive law for porous solids with pressure-sensitive matrices and its applications to plastic flow localization. Int. J. Mech. Phys. Solids 39, 1385–1403.
Jeong, H.Y., 2002. A new yield function and a hydrostatic stress-controlled model for porous solids with pressure-sensitive matrices. Int. J. Mech. Phys. Solids 32, 3669–3691.
Keralavarma, S.M., Benzerga, A.A., 2008. An approximate yield criterion for anisotropic porous media. C.R. Mec. 336, 685–692.
Keralavarma, S.M., Benzerga, A.A., 2010. A constitutive model for plastically anisotropic solids with non-spherical voids. J. Mech. Phys. Solids 58, 874–901.
Khan, Akhtar S., Liu, Haowen, 2012. A new approach for ductile fracture prediction on Al 2024-T351 alloy. Int. J. Plast. 35, 1–12.
Khan, Akhtar S., Liu, Haowen, 2012. Strain rate and temperature dependent fracture criteria for isotropic and anisotropic metals. Int. J. Plast. 37, 1–15.
Landry, M., Chen, Z.T., 2011. An approximate lower bound damage-based yield criterion for porous ductile sheet metals. Theor. Appl. Fract. Mech. 55, 76–81.
Lee, J.H., Oung, J., 2000. Yield functions and flow rules for porous pressure-dependent strain-hardening polymeric materials. J. Appl. Mech. 67, 288–297.
Li, Z., Huang, M., 2005. Combined effects of void shape and void size – oblate spheroidal microvoid embedded in infinite non-linear solid. Int. J. Plast. 21 (3), 625–650.
Li, Z., Fu, M.W., Lua, J., Yang, H., 2011. Ductile fracture: experiments and computations. Int. J. Plast. 27, 147–180.
Canal, Luis P., Segurado, Javier, LLorca, Javier, 2009. Failure surface of epoxy-modified fiber-reinforced composites under transverse tension and out-of-plane shear. Int. J. Solids Struct. 46, 2265–2274.
Maghous, S., Dormieux, L., Barthélémy, J.F., 2009. Micromechanical approach to the strength propoerties of frictional geomaterials. Eur. J. Mech. A/Solids 28, 179–188.
Monchiet, V., Gruescu, C., Charkaluk, E., Kondo, D., 2006. Approximate yield criteria for anisotropic metals with prolate or oblate voids. C.R. Mec. 334 (7), 431–439.
Monchiet, V., Charkaluk, E., Kondo, D., 2007. An improvment of Gurson-type models of porous materials by Eshelby-like trial velocity fields. C.R. Méc. 335, 32–41.
Monchiet, V., Cazacu, O., Kondo, D., 2008. Macroscopic yield criteria for plastic anisotropic materials containing spheroidal voids. Int. J. Plast. 24, 1158–1189.
Monchiet, V., Kondo, D., 2013. Combined voids size and shape effects on the macroscopic criterion of ductile nanoporous materials. Int. J. Plast. 43, 20–41.
Monchiet, V., Charkaluk, E., Kondo, D., 2013. Macroscopic yield criteria for ductile materials containing spheroidal voids: an Eshelby-like velocity fields approach. Mech. Mater. (in press). http://dx.doi.org/10.1016/j.mechmat.2013.05.006.
Moreau, J.J. 2003. Fonctionnelles Convexes, Istituto Poligrafico e Zecca dello Stato, Rome.
Nahshon, K., Hutchinson, J.W., 2008. Modification of the Gurson model for shear failure. Eur. J Mech. A/Solids 27, 1–27.
Nguyen Dang, H., 1976. Direct limit analysis via rigid-plastic finite elements. Comput. Methods Appl. Mech. Eng. 8, 81–116.
Pastor, F., Thoré, P., Kondo, D., Pastor, J., 2012. Limit analysis and conic programming for Gurson-type spheroid problems. In: de Saxcé, G., Oueslati, A., Charkaluk, E., Tritsch, J.-B. (Eds.), Limit State of Materials and Structures, Direct Methods 2. Springer, London, pp. 207–218.
Ponte-Castañeda, P., 1991. The effective mechanical properties of nonlinear isotropic composites. J. Mech. Phys. Solids 39, 45–71.
Ponte-Castañeda, P., Suquet, P., 1998. Nonlinear Compos. Adv. Appl. Mech. 34, 171–302.
Revil-Baudard, B., Cazacu, O., 2013. On the effect of the matrix tension-compression asymmetry on damage evolution in porous plastic solids. Eur. J Mech. A/Solids 37, 35–44.
Rockafellar, R.T., 1970. Convex Analysis. Princeton University Press, Princeton.
Save, M.A., Massonnet, C.E., de Saxcé, G., 1997. Plastic limit analysis of plates, shells and disks. Elsevier, New York.
Shen, W.Q., Shao, J.F., Kondo, D., Gatmiri, B., 2012. A micromacro model for clayey rocks with a plastic compressible porous matrix. Int. J. Plast. 36, 64–85.
Shtern, M.B., Cocks, A.C.F., 2001. The structure of constitutive laws for the compaction of metal powders. In: Recent Developments in Computer Modelling of Powder Metallurgy Processes. IOS Press.
Shtern, M.B., Maidanyuk, A.P., Cocks, A., 2002. Effect of a third invariant on the effective reaction ductile porous bodies. I. Behavior of porous material. Unit cell and a generalized rule of normality. Powder Metall. Metals Ceram. 41, 241–248.
Shtern, M.B., Maidanyuk, A.P., Cocks, A., 2002. Effect of a third invariant on the effective reaction ductile porous bodies. II. Loading surface of porous bodies whose prperties are sensitive to a triaxial stressed state. Powder Metall. Metals Ceram. 41, 347–354.
Kuz'mov, A.V., Shtern, M.B., 2002. Effect of a third invariant on the properties and structure of constitutive relationships for powder materials. Powder Metall. Metals Ceram. 42, 329–335.
Sun, Y., Wang, D., 1989. A lower bound approach to the yield loci of porous materials. Acta Mech. Sin. 5, 237–243.
Sun, Y., Wang, D., 1995. Analysis of shear localization in porous materials based on a lower bound. Int. J. Fract. 71, 71–83.
Suquet, P., 1995. Overall properties of nonlinear composites: a modified secant moduli theory and its link with Ponte Castaeda's nonlinear variational procedure. C.R. Acad. Sci. 320, 563–571.
Thoré, P., Pastor, F., Pastor, J., 2011. Hollow sphere models, conic programming and third stress invariant. Eur. J. Mech. A/Solids 30, 63–71.
Trillat, M., Pastor, J., 2005. Limit analysis and Gurson's model. Eur. J Mech. A/Solids 24, 800–819.
Tvergaard, V., 1981. Influence of voids on shear band instabilities under plane strain conditions. Int. J. Frac. 17, 389–407.
Tvergaard, V., Needleman, A., 1984. Analysis of cup-cone fracture in round tensile bar. Acta Metall. 32, 157–169.
Tvergaard, V., 1990. Material failure by void growth and coalescence. Adv. Appl. Mech. 27, 83–151.
Zaïri, F., Naït-Abdelaziz, M., Gloaguen, J.M., Lefebvre, J.M., 2008. Modelling of the elasto-viscoplastic damage behaviour of glassy polymers. Int. J. Plast. 24, 945–965.
Zhang, W., Wang, T.J., Chen, X., 2010. Effect of surface/interface stress on the plastic deformation of nanoporous materials and nanocomposites. Int. J. Plast. 26 (7), 957–975.

Complement to Chapter 2 : Derivation of a Lode angle dependent model for ductile porous materials : an extension of the stress-based variational approach

Derivation of a Lode angle dependent model for ductile porous materials: an extension of the stress-based variational approach

Long Cheng[a], Géry de Saxcé[a], Djimedo Kondo[b]

[a]*Laboratoire de Mécanique de Lille, UMR 8107 CNRS, Université de Lille 1, Cité scientifique, F59655 Villeneuve d'Ascq, France*
[b]*Institut Jean Le Rond d'Alembert, UMR 7190 CNRS, Université Pierre et Marie Curie, 4 place Jussieu, F75005 Paris, France*

Abstract

Recently, a new methodology of macroscopic modeling for ductile porous media has been proposed by the authors, using a statical limit analysis approach (Cheng et al., 2013). Since this model has been derived by considering a hollow sphere under axisymmetric loadings, only the effect of the sign of the stress deviator third invariant (or two values of Lode angle) has been investigated. The aim of the present paper is to extend the above mentioned stress-based model to the general case of non-axisymmetric loadings by introducing a more general trial stress field. The established new yield locus explicitly depends on the effect of the third invariant (equivalently the Lode angle). Finally, non negligible effects of the third stress deviator invariant on the voids growth rate is fully demonstrated. The results are fully illustrated.

Keywords: Ductile Porous material, von Mises matrix, Statical Limit Analysis, Third invariant of stress deviator

1. Introduction

More than thirty years ago, Gurson (1977) proposed a kinematically-based limit analysis approach of a hollow sphere and hollow cylinder having a von Mises rigid plastic matrix. This approach delivered an upper bound of the macroscopic criterion which depends on the pressure and on the von Mises equivalent stress. Very recently, and in contrast to Gurson model, we have introduced in Cheng et al. (2013) a stress-based variational approach of the ductile porous material. The starting point is Hill's variational principle applied to the hollow sphere with rigid perfectly plastic matrix. Implementation of this variational approach requires the choice of a statically and plastically admissible trial stress field. For simplicity, we have resorted in Cheng et al. (2013) an axisymmetric trial stress field. Consequently, the mechanical loadings that can be considered are axisymmetric, and only the sign of the third invariant (or two values of Lode angle) of the stress deviator can then be accounted for the

Email address: `email address` (Djimedo Kondo)

Preprint to be submitted to Elesvier

macroscopic criterion. Note also that the effects of the third invariant sign on the plastic flow rule and on the voids growth rate have been investigated. It is worth noticing that the importance of the above mentioned effects have been fully studied in (Cazacu et al., 2013; Garajeu et al., 2011) based on a kinematical limit analysis method.

The paper is devoted to an extension of the above mentioned stress-based model to the general case of non-axisymmetric loadings by introducing a more general trial stress field. Such extension is based on the consideration and implementation in the context of the SVM approach of an appropriate trial stress field. A macroscopic criterion which explicitly depends on the Load angle (or the third invariant of the stress deviator) is derived. It will be shown that the established new yield locus predicts a slight effect of the third invariant (equivalently the Lode angle). Moreover, the plastic flow rule and void growth functions are given as functions of the mean stress, equivalent stress and the third invariant of the stress deviator.

The outline of the paper is as follows. First, we briefly recall in Section 2 the statically limit analysis approach which aims at formulating a lower bound model, in contrast to the well-known kinematical one. Then, in Section 3, we propose for the hollow sphere model a non-axisymmetric trial stress field. The successful implementation of this new stress field in the stress-based method delivers a macroscopic criterion of the ductile porous medium which is first explicitly formulated in terms of the mean stress, the von Mises equivalent stress and the Lode angle. Finally, in Section 4 are formulated the plastic flow rule and the porosity evolution equation. Section 5 allows to conclude the study.

2. Brief recall of the stress variational limit analysis approach

In the framework of Limit Analysis for the ductile porous media, let us consider a cell Ω composed a void ω and a rigid perfectly plastic matrix $\Omega_M = \Omega - \omega$. The external boundary of the VER and the internal boundary of the void are respectively defined by $\partial\Omega$ and $\partial\omega$. The yield criterion for the matrix takes the form:

$$F(\boldsymbol{\sigma}) \leq 0 \tag{1}$$

where $\boldsymbol{\sigma}$ is the cauchy stress tensor.
The set of plastic admissible stress tensor is defined by

$$\mathcal{S}_p = \{\boldsymbol{\sigma} \quad s.t. \quad F(\boldsymbol{\sigma}) \leq 0\} \tag{2}$$

Considering the normality law, the plastically admissible velocity field reads

$$\mathcal{K}_p = \{\boldsymbol{d} \quad s.t. \quad \boldsymbol{d} = d_{eq} \cdot \frac{\partial F}{\partial \boldsymbol{\sigma}}\} \tag{3}$$

where $\boldsymbol{d}$ is the strain rate tensor and d_{eq} the equivalent strain rate obtained from the strain deviator $\boldsymbol{s}$ through $d_{eq} = \sqrt{\frac{2}{3}\boldsymbol{s} : \boldsymbol{s}}$.

Moreover, the sets of statically admissible stress field and the kinematically admissible velocity ones are respectively defined through

$$\mathcal{S}_a = \{\boldsymbol{\sigma} \quad s.t. \quad div\ \boldsymbol{\sigma} = 0 \quad in \quad \Omega, \quad \boldsymbol{\sigma} \cdot \boldsymbol{n} = 0 \quad on \quad \partial\omega, \quad \boldsymbol{\sigma} = 0 \quad in \quad \omega\} \ . \tag{4}$$

$$\mathcal{K}_a = \{\boldsymbol{v} \quad s.t. \quad \boldsymbol{v}(\boldsymbol{x}) = \boldsymbol{D} \cdot \boldsymbol{x} \quad on \quad \partial\Omega\} \ . \tag{5}$$

$\boldsymbol{n}$ is the unit outward normal vector, and $\boldsymbol{x}$ the position one.

When the cell is subjected to a kinematically admissible velocity field (5), the homogenization problem consists in calculating the minimizing, as implemented in Cheng et al. (2013) of the following functional which is involved to the Hill's variational principal (Hill, 1950)

$$\Psi = \min_{\boldsymbol{\sigma} \in \mathcal{S}_a} \left(\frac{1}{\mid \Omega \mid} \int_{\Omega_M} \psi(\boldsymbol{\sigma}) \ dV - \boldsymbol{D} : \boldsymbol{\Sigma} \right) \ , \tag{6}$$

where $\psi(\boldsymbol{\sigma})$ is an indicator function, which is convex and lower semicontinuous. It vanishes when the stress field is plastically admissible (2), $\psi(\boldsymbol{\sigma}) \mapsto \infty$, otherwise. While the second term on r.h.s. of (6) can be calculated from the microscopic counterpart through the Hill's lemma

$$\boldsymbol{D} : \boldsymbol{\Sigma} = \frac{1}{\mid \Omega \mid} \int_{\Omega} \boldsymbol{d}(\boldsymbol{v}) : \boldsymbol{\sigma} \ dV = \frac{1}{\mid \Omega \mid} \int_{\Omega_M} \boldsymbol{d}(\boldsymbol{v}) : \boldsymbol{\sigma} \ dV \ . \tag{7}$$

For minimization of Ψ (6), in the context of the limit analysis requires to find a licit stress field satisfying

$$\mathcal{S}_l = \{\boldsymbol{\sigma} \in S_a \quad and \quad \boldsymbol{\sigma} \in S_p \quad in \quad \Omega_M\} \ . \tag{8}$$

That is equivalent to the following saddle-point problem by introducing the multiplier of Lagrange $x \mapsto \dot{\Lambda}(\boldsymbol{x})$ and relaxing the yield criterion (1)

$$\max_{\dot{\Lambda} \geq 0} \min_{\boldsymbol{\sigma} \in \mathcal{S}_a} \left(\mathcal{L}(\boldsymbol{\sigma}, \dot{\Lambda}) = \frac{1}{\mid \Omega \mid} \int_{\Omega_M} \dot{\Lambda} F(\boldsymbol{\sigma}) \ dV - \mathbf{D} : \boldsymbol{\Sigma} \right) \ ,$$

Assuming Λ is uniform in the matrix, it follows

$$\max_{\dot{\Lambda} \geq 0} \min_{\boldsymbol{\sigma} \in \mathcal{S}_a} \left(\mathcal{L}(\boldsymbol{\sigma}, \dot{\Lambda}) = \frac{\dot{\Lambda}}{\mid \Omega \mid} \int_{\Omega_M} F(\boldsymbol{\sigma}) \ dV - \mathbf{D} : \boldsymbol{\Sigma} \right) \ . \tag{9}$$

For more information concerning about the statical limit analysis approach, the reader can referred to Salençon (1983); Save et al. (1997), etc..

The macroscopic limit load and the plastic flow can be respectively obtained from the stationarities of (9) with respect to $\dot{\Lambda}$ and $\boldsymbol{\Sigma}$,

$$\mathcal{F}(\Sigma) = \frac{1}{\mid \Omega \mid} \int_{\Omega_M} F(\boldsymbol{\sigma}) \ dV = 0 \ . \tag{10}$$

$$\mathbf{D} = \dot{\Lambda} \frac{\partial \mathcal{F}}{\partial \boldsymbol{\Sigma}} (\boldsymbol{\Sigma}) \ . \tag{11}$$

Obviously, $\dot{\Lambda}$ is simultaneously proved to be the plastic multiplier.

3. Proposed non-axisymmetric trial stress field and 3D macroscopic criterion

In this section, we aim at deriving a new stress variational model for ductile porous media with a non-axisymmetric trial stress field. A macroscopic criterion depending not only on the macroscopic mean and equivalent stresses (Σ_m and Σ_e), but also on the Lode angle θ_L (or third invariant of the stress deviator J_3) is expressed [1]. This stress-based macroscopic modelling is achieved by taking the hollow sphere model having a porosity f. The matrix Ω_M is made up with a rigid perfectly plastic material obeying the von Mises yield criterion

$$F(\boldsymbol{\sigma}) = \sigma_e(\boldsymbol{\sigma}) - \sigma_0 \leq 0 \tag{12}$$

where $\sigma_e = \sqrt{\frac{3}{2}\mathbf{s} : \mathbf{s}}$ is the von Mises equivalent stress defined from the stress deviator part $\mathbf{s}$, while $\sigma_0 > 0$ the matrix shear cohesion.

3.1. Proposed non-axisymmetric trial stress field

Owing to the central symmetry of the hollow sphere model, we propose a trial non-axisymmetric trial stress field, which contains two part as follows,

- A heterogeneous part corresponding to the exact solution under pure hydrostatic loadings, it reads, in spherical coordinates with orthonormal frame $\{\boldsymbol{e}_r, \boldsymbol{e}_\phi, \boldsymbol{e}_\theta\}$:

$$\boldsymbol{\sigma}^{(1)} = -A\left[\ln\left(\frac{a}{r}\right)\mathbf{1} - \frac{1}{2}(\boldsymbol{e}_\theta \otimes \boldsymbol{e}_\theta + \boldsymbol{e}_\phi \otimes \boldsymbol{e}_\phi)\right] , \tag{13}$$

  where $\mathbf{1}$ is the second order unit tensor, A being a constant to be determined.

- A homogeneous part which is non axisymmetric and taken for capturing the shear effect:

$$\boldsymbol{\sigma}^{(2)} = \boldsymbol{B}, \qquad tr\boldsymbol{B} = 0 \tag{14}$$

Hence, the final trial stress field in the matrix can be written as

$$\boldsymbol{\sigma} = \boldsymbol{\sigma}^{(1)} + \boldsymbol{\sigma}^{(2)} \tag{15}$$

which turns to be null in the void ω, and in cylindrical coordinates reads

It follows that the non-axisymmetric macroscopic stress field read:

$$\boldsymbol{\Sigma} = -\frac{1}{3}A\ln f \cdot \mathbf{1} + (1-f)\boldsymbol{B} \tag{16}$$

Next, let us compute that in mechanics, there are three invariants for defining the plastic limit state. From (16) and (14), they can be respectively calculated:

[1] In (Cheng et al., 2013), only the sign of the third invariant is obtained

- Macroscopic mean stress,

$$\Sigma_m = -\frac{1}{3} A \ln f \tag{17}$$

- Macroscopic equivalent stress,

$$\Sigma_e = (1-f)\, B_{eq} \tag{18}$$

where B_{eq} is the equivalent quantity associated to the deviator $\boldsymbol{B}$ (or microscopic stress deviator of $\boldsymbol{\sigma}^{(2)}$):

$$B_{eq} = \sqrt{\frac{3}{2}\boldsymbol{B} : \boldsymbol{B}} \tag{19}$$

- Third invariant of the macroscopic stress deviator,

$$J_3 = (1-f)^3 \det(\boldsymbol{B}) \tag{20}$$

For convenience, Let us introduce the stress based quantities:

$$\begin{aligned} \tilde{\Sigma}_m &= -\frac{3\Sigma_m}{2\ln f} = \frac{A}{2} \\ \tilde{\Sigma}_{eq} &= B_{eq} = \frac{\Sigma_e}{1-f} \\ \tilde{J}_3 &= \frac{J_3}{(1-f)^3} \end{aligned} \tag{21}$$

from which, the macroscopic Lode angle θ_L can be defined as:

$$\cos(3\theta_L) = \frac{27\tilde{J}_3}{2\tilde{\Sigma}_{eq}^3} = \frac{27 J_3}{2\Sigma_e^3}, \qquad 0 \le \theta_L \le 60^\circ \tag{22}$$

3.2. Macroscopic criterion

From Eqs.(13), (14) and (15) the deviator $\boldsymbol{s}$ of the local stress field can be written as:

$$\boldsymbol{s} = \boldsymbol{s}^{(1)} + \boldsymbol{s}^{(2)} = \boldsymbol{s}^{(1)} + \boldsymbol{B} \tag{23}$$

where $\boldsymbol{s}^{(1)}$ is the deviator calculated from (13). Hence, the equivalent stress can be obtained from:

$$\sigma_e = \sqrt{\frac{3}{2}\left[\boldsymbol{s}^{(1)} : \boldsymbol{s}^{(1)} + 2\boldsymbol{s}^{(1)} : \boldsymbol{s}^{(2)} + \boldsymbol{s}^{(2)} : \boldsymbol{s}^{(2)}\right]} \tag{24}$$

It can be calculated from (23) and (24) that

$$\begin{aligned} \boldsymbol{s}^{(1)} : \boldsymbol{s}^{(1)} &= \frac{A^2}{6} \\ \boldsymbol{s}^{(1)} : \boldsymbol{s}^{(2)} &= -\frac{A}{2}\tilde{B} \\ \boldsymbol{s}^{(2)} : \boldsymbol{s}^{(2)} &= \frac{2}{3} B_{eq}^2 \end{aligned} \tag{25}$$

for which expression of $\tilde{B}$ is determined in the following.

Indeed, in order to compute the stress quantity $\tilde{B}$ in spherical coordinates, let us first express the principal stress tensor of $\boldsymbol{B}$ in cartesian coordinates with orthonormal frame $\{\boldsymbol{e}_x, \boldsymbol{e}_y, \boldsymbol{e}_z\}$:

$$\boldsymbol{B} = B_1(\boldsymbol{e}_x \otimes \boldsymbol{e}_x - \boldsymbol{e}_z \otimes \boldsymbol{e}_z) + B_2(\boldsymbol{e}_y \otimes \boldsymbol{e}_y - \boldsymbol{e}_z \otimes \boldsymbol{e}_z), \tag{26}$$

for which the components can be expressed (without loss of generality) in the form:

$$\begin{aligned} B_1 &= -\frac{\Sigma_e}{3}\cos(\theta_L) + \frac{\Sigma_e}{\sqrt{3}}\sin(\theta_L) \\ B_2 &= -\frac{\Sigma_e}{3}\cos(\theta_L) - \frac{\Sigma_e}{\sqrt{3}}\sin(\theta_L) \end{aligned} \tag{27}$$

Consequently, one can then reexpress $\boldsymbol{B}$ in spherical coordinates; it follows immediately that

$$\tilde{B} = \frac{1}{1-f}\left[\frac{\Sigma_e}{3}\cos(\theta_L)(3\cos^2(\theta)-1) + \frac{\Sigma_e}{\sqrt{3}}\sin(\theta_L)\sin^2(\theta)\cos(2\phi)\right] \tag{28}$$

where θ and ϕ are the polar angle and azimuthal one in spherical coordinates system.

As a result, the microscopic equivalent stress (24) can be written as

$$\sigma_e = \sqrt{\frac{A^2}{4} - \frac{3A}{2}\tilde{B} + B_{eq}^2} \tag{29}$$

Taking into account (17), (18) and (25), (29) can be recast in the form:

$$\sigma_e = \sqrt{\tilde{\Sigma}_m^2 - 3\tilde{\Sigma}_m\tilde{B} + \tilde{\Sigma}_e^2} = \sqrt{\frac{9\Sigma_m^2}{4\ln^2 f} + \frac{9\Sigma_m\Sigma_L}{2(1-f)\ln f} + \frac{\Sigma_e^2}{(1-f)^2}} \tag{30}$$

where Σ_L is the macroscopic counterpart of $\tilde{B}$; it reads:

$$\Sigma_L = (1-f)\tilde{B} = \frac{\Sigma_e}{3}\cos(\theta_L)(3\cos^2(\theta)-1) + \frac{\Sigma_e}{\sqrt{3}}\sin(\theta_L)\sin^2(\theta)\cos(2\phi) \tag{31}$$

Hence, the local von Mises yield criterion can be expressed as

$$F(\boldsymbol{\sigma}(\boldsymbol{\Sigma})) = \sigma_e - \sigma_0 = \sqrt{\tilde{\Sigma}_m^2 + \tilde{\Sigma}_e^2 - \frac{3\tilde{\Sigma}_m\Sigma_L}{1-f}} - \sigma_0 \leq 0 \tag{32}$$

Let us recall that for obtaining the macroscopic criterion from (10), one need to integrate (32) over the matrix. However, due to the presence of the azimuth angle ϕ in the expression of Σ_L (31), there is no closed form solution. In order to overcome this difficulty, a simple idea consists in performing a Taylor series expansion (around 0) till the third order, this

leads to the following approximation:

$$\begin{aligned}\sigma_e =& \sqrt{\tilde{\Sigma}_m^2+\tilde{\Sigma}_e^2}\cdot\sqrt{1-\frac{3\tilde{\Sigma}_m\Sigma_L}{(1-f)(\tilde{\Sigma}_m^2+\tilde{\Sigma}_e^2)}}\\ \simeq& \sqrt{\tilde{\Sigma}_m^2+\tilde{\Sigma}_e^2}\cdot\left[1-\frac{3\tilde{\Sigma}_m\Sigma_L}{2(1-f)(\tilde{\Sigma}_m^2+\tilde{\Sigma}_e^2)}-\frac{9\tilde{\Sigma}_m^2\Sigma_L^2}{8(1-f)^2(\tilde{\Sigma}_m^2+\tilde{\Sigma}_e^2)^2}-\frac{27\tilde{\Sigma}_m^3\Sigma_L^3}{16(1-f)^3(\tilde{\Sigma}_m^2+\tilde{\Sigma}_e^2)^3}\right]\end{aligned} \tag{33}$$

Next, the final integration includes the computation of the following integrals:

$$\begin{aligned}&\frac{1}{4\pi}\int_{S(r)}\Sigma_L dS=0\\ &\frac{1}{4\pi}\int_{S(r)}\Sigma_L^2 dS=\frac{4\Sigma_e^2}{45}\\ &\frac{1}{4\pi}\int_{S(r)}\Sigma_L^3 dS=\frac{16\Sigma_e^3}{945}\cos(\theta_L)(4\cos^2(\theta_L)-3)\end{aligned} \tag{34}$$

Finally, from (10), the macroscopic criterion is obtained as:

$$\mathcal{F}\simeq\frac{1}{4\pi}\int_{S(r)}\sigma_e^2 dS-\sigma_0=D\left(1-\frac{C^2\Sigma_e^2}{90D^4}+\frac{C^3\Sigma_e^3}{945D^6}\cos(\theta_L)(4\cos^2(\theta_L)-3)\right)-\sigma_0\leq 0 \tag{35}$$

where we have denoted C and D the following functions of $\mathbf{\Sigma}$

$$\begin{aligned}D(\mathbf{\Sigma})&=\sqrt{\tilde{\Sigma}_m^2+\tilde{\Sigma}_e^2}=\sqrt{\frac{9\Sigma_m^2}{4\ln^2 f}+\frac{\Sigma_e^2}{(1-f)^2}}\\ C(\mathbf{\Sigma})&=-\frac{3\tilde{\Sigma}_m}{1-f}=\frac{9\Sigma_m}{2(1-f)\ln f}\end{aligned} \tag{36}$$

It should be underlined that the established criterion (35) depends not only on the the macroscopic mean stress and equivalent stress, but also explicitly on the Lode angle (or the third invariant of the stress deviator).

3.3. Illustration of the established macroscopic criterion

Next, we provide in this subsection the illustration of the established criterion (35) and its comparison with Gurson model and the Stress Variational Model (SVM) (Cheng et al., 2013). It is worthy to note that the later one has been derived from a closed-form formulation. Two values of porosity $f = 0.001$ and $f = 0.01$ are adopted for the later illustration and comparisons.

First, five yield loci obtained from (35) are illustrated on Fig.1 with different values of Lode angle: $\theta_L = 0$, 15°, 30°, 45° and 60°, while the first and the last ones are corresponding to the macroscopic model obtained from the axisymmetric trial stress field. Consequently,

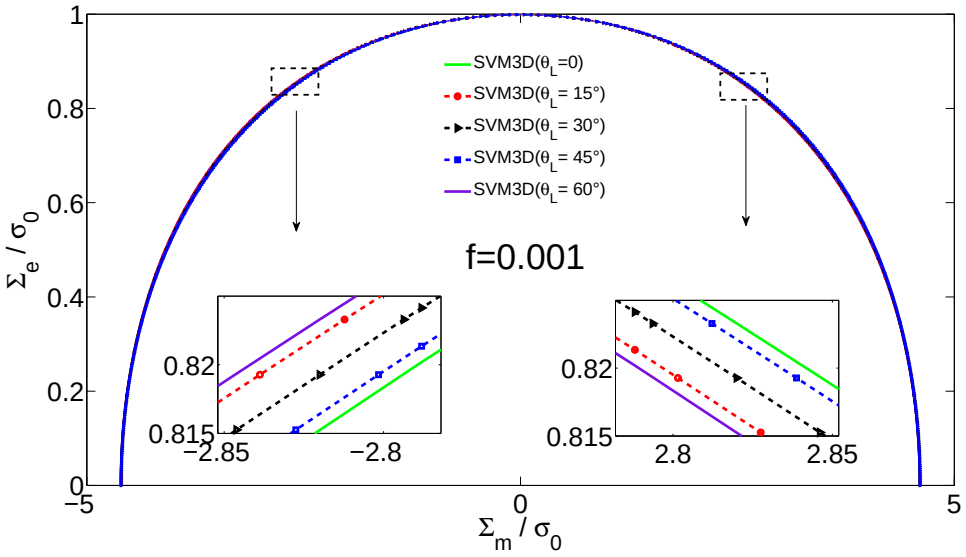

(a) Porosity: $f = 0.001$

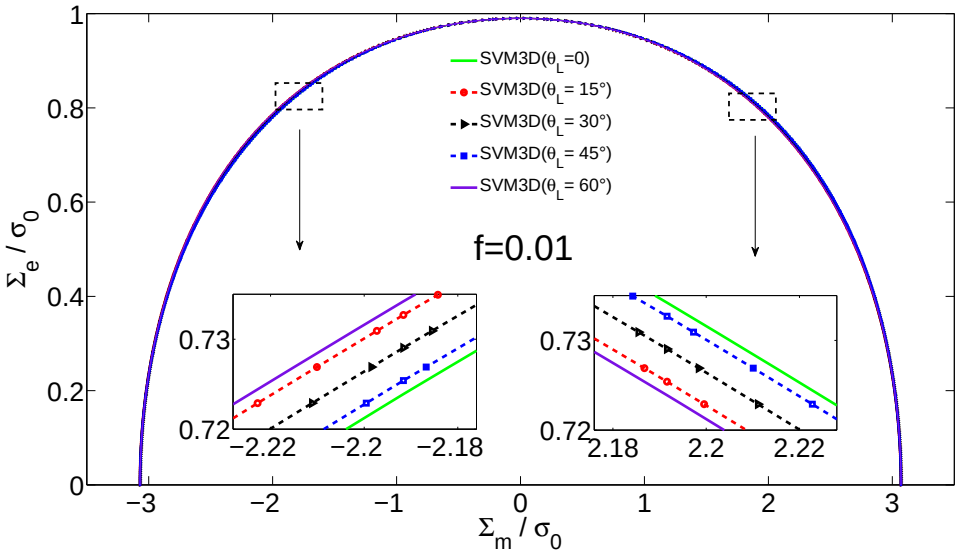

(b) Porosity: $f = 0.01$

Figure 1: Illustrations of the yield surfaces obtained from the new established criterion SVM3D (35) with five values of Lode angle: $\theta_L = 0$, 15°, 30°, 45° and 60°. Porosity: $f = 0.001$ and $f = 0.01$.

the yield surface displays an asymmetry due to the sign of the third invariant (Cheng et al., 2013). It can be observed that the yield surfaces obtained from other values of the Lode angle are absolutely between the above two ones.

For completeness, due to the approximation taken for the derivation of the macroscopic criterion, the new established criterion (35) derived from the axisymmetric trial stress field should perform a difference with respect to the closed-form criterion SVM. To this end, Fig.2 is contributed to the comparison between the SVM, the axismmetric case of SVM3D and the Gurson model. Finally, slight differences between the SVM and the SVM3D is obtained.

4. Plastic flow rule and void growth rate

We aim now at deriving the plastic strain rate from the normality rule. Unlike the conventional modeling, the three invariants of the macroscopic criterion (35) are taken into account. Not only the mean strain rate D_m and the equivalent one D_e have to be computed, but also the contribution D_{III} related to the third invariant of deviator J_3 will be provided. It is worthy to interpret that D_{III} can indicated the influence of the Lode angle upon the π-plane of principal stress space to the macroscopic plastic flow rule. Let us first define the macroscopic stress,

$$\Sigma_{III} = \sqrt[3]{J_3} \tag{37}$$

Hence, the dissipation power Π can be written as

$$\Pi = \boldsymbol{D} : \boldsymbol{\Sigma} = 3\Sigma_m D_m + \Sigma_e D_e + \Sigma_{III} D_{III} \tag{38}$$

Moreover, considering the macroscopic criterion (35), the macroscopic strain rate can be obtained from the associated flow rule

$$\begin{aligned}
D_m &= \frac{1}{3}\dot{\Lambda}\frac{\partial \mathcal{F}_{3D}}{\partial \Sigma_m} \\
&= \frac{1}{3}\dot{\Lambda}\left[\frac{\partial D}{\partial \Sigma_m} - \frac{\Sigma_e^2}{90}\cdot\frac{2CD\frac{\partial C}{\partial \Sigma_m} - 3C^2\frac{\partial D}{\partial \Sigma_m}}{D^4} + \frac{J_3}{70}\left(\frac{729J_3^2}{\Sigma_e^6} - 3\right)\left(\frac{3C^2D^2\frac{\partial C}{\partial \Sigma_m} - 5D^4\frac{\partial D}{\partial \Sigma_m}}{D^7}\right)\right] \\
D_e &= \dot{\Lambda}\frac{\partial \mathcal{F}_{3D}}{\partial \Sigma_e} = \dot{\Lambda}\left[\frac{\partial D}{\partial \Sigma_e} - \frac{C^2}{90}\frac{2D\Sigma_e - 3\frac{\partial D}{\partial \Sigma_e}\Sigma_e^2}{D^4} - \frac{C^3J_3}{70}\left(\frac{5}{D^6}\frac{\partial D}{\partial \Sigma_e}(\frac{729J_3^2}{\Sigma_e^6} - 3) - \frac{6}{D^5}\frac{729J_3^2}{\Sigma_e^7}\right)\right] \\
D_{III} &= \dot{\Lambda}\frac{\partial \mathcal{F}_{3D}}{\partial \Sigma_{III}} = \dot{\Lambda}\left[\frac{C^3}{70D^5}\left(\frac{729J_3^2}{\Sigma_e^6} - 1\right)J_3^{-\frac{2}{3}}\right]
\end{aligned} \tag{39}$$

where

$$\frac{\partial C}{\partial \Sigma_m} = \frac{9}{2(1-f)\ln f}, \quad \frac{\partial D}{\partial \Sigma_m} = \frac{9\Sigma_m}{2D\ln^2 f}, \quad \frac{\partial D}{\partial \Sigma_e} = \frac{2\Sigma_e}{D(1-f)^2}$$

Finally, the plastic void growth rate can be obtained from the mass balance equation. Taking into account the plastic flow rule (39) and eliminating the plastic multiplier $\dot{\Lambda}$, it follows that

$$\frac{\dot{f}}{D_e} = 3\,(1-f)\,\frac{D_m}{D_e} \tag{40}$$

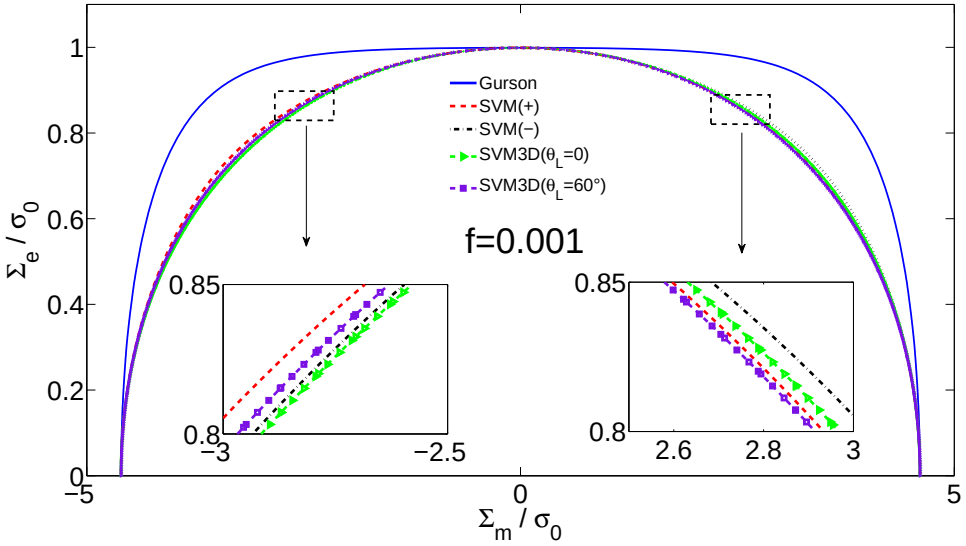

(a) Porosity: $f = 0.001$

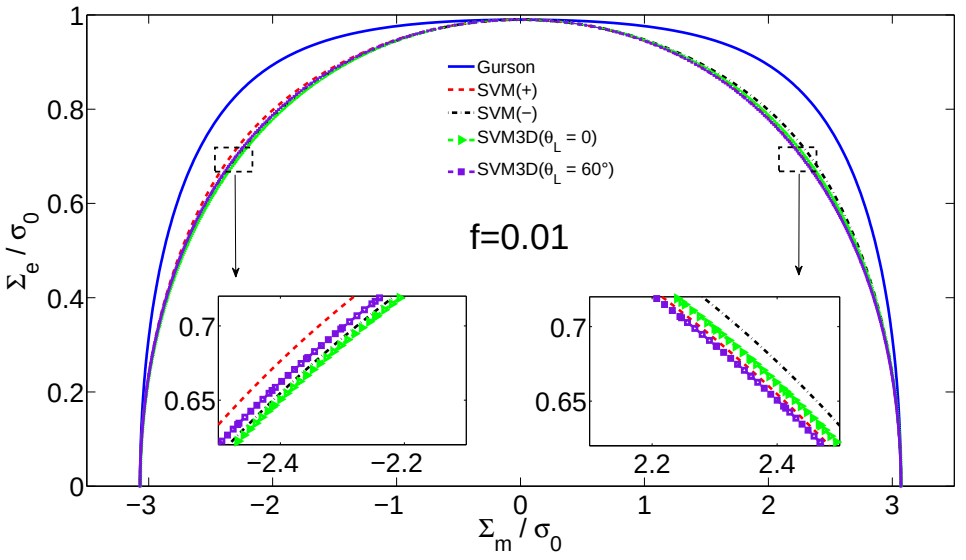

(b) Porosity: $f = 0.01$

Figure 2: Comparison between the yield surfaces obtained from the established criterion SVM3D (35) with axisymmetric trial stress field, the closed form criterion of Stress Variational Model (SVM(+) and SVM(-)) (Cheng et al., 2013) and the Gurson criterion (Gurson, 1977). Porosity: $f = 0.001$ and $f = 0.01$.

It is readily seen from Eqs.(40) and (39) that the void growth rate depends on the third invariant of the stress deviator J_3 (or the Lode angle θ_L).

Fig.3 illustrates the evolution of porosity given as function of stress triaxiality $T = \frac{\Sigma_m}{\Sigma_e}$ for two values of initial porosity. It can be observed that, the ones with axisymmtric loadings ($\theta_L = 0°$ and $60°$) give two extremal values of the void evolution for a fixed value of triaxiality, while for another case with non axisymmetric state ($\theta_L = 30°$) is exactly between the two extremal ones. Slight differences due to the Lode angle (or the third invariant of stress deviator) can be observed.

5. Conclusion

In this study, we applied the statically limit analysis method to derive a Lode angle dependent macroscopic model. To this end, we have proposed a non axisymmetric trial stress field for the porous media whose matrix obeys the von Mises yield criterion. Unlike the conventional macroscopic modelling in literature, the new criterion shows an effect of the three macroscopic invariants: mean stress, equivalent stress and Lode coefficient (or the third invariant of stress deviator). The influence of the last one was specially discussed not only for the macroscopic criterion, but also for the plastic flow rule and the void growth rate.

References

Cazacu, O., Revil-Baudard, B., Lebensohn, R., Garajeu, M., 2013. On the Combined Effect of Pressure and Third Invariant on Yielding of Porous Solids With von Mises Matrix. Journal of Applied Mechanics, DOI: 10.1115/1.4024074.

Cheng, L., de Saxcé, G, Kondo, D.. A stress-based variational model for ductile porous materials. Internal Journal of Plasticity, DOI: http://dx.doi.org/10.1016/j.ijplas.2013.10.003

M. Garajeu, 2011. Comportement non linaire des milieux htrognes. Habilitation Thesis, Univ. of Mediterannee, Marseill, France.

Gurson, A.L., 1977. Continuum theory of ductile rupture by void nucleation and growth – part I: Yield criteria and flow rules for porous ductile media, Journal of Engineering Materials and Technology, 99, 2-15.

Hill, R., 1950. Mathematical theory of plasticity. Oxford University Press, London.

Nahshon, K., Hutchinson, J.W. 2008. Modification of the Gurson Model for shear failure, European Journal of Mechanics, 27, 1-17.

Pastor, F., Kondo, D., Pastor, J., 2013. 3D-FEM formulations of limit analysis methods for porous pressure-sensitive materials, Int. J. Numer. Meth. Engng 2013, 95, 847870.

Salenon, Calcul la rupture et analyse limite, Presses de lENPC, 1983.

Save, M.A., Massonnet, C.E., de Saxcé, G., 1997. Plastic limit analysis of plates, shells and disks. Elsevier, New York.

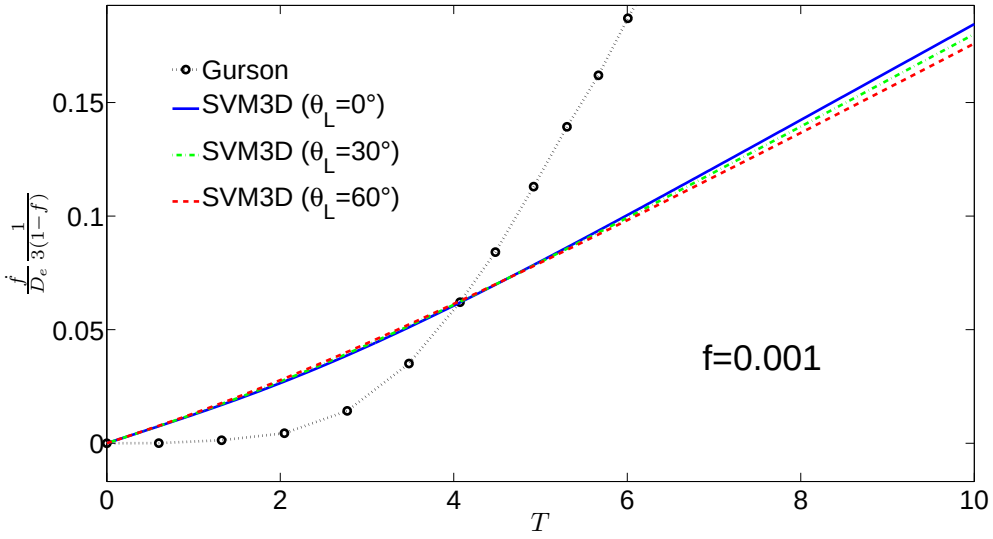

(a) Porosity: $f = 0.001$

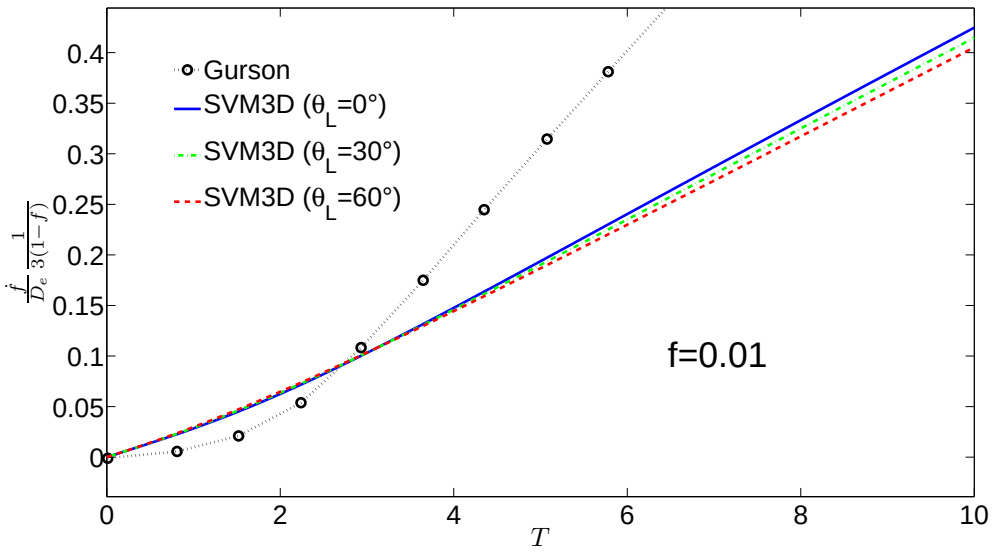

(b) Porosity: $f = 0.01$

Figure 3: Evolution of porosity as function of the stress triaxiality for initial porosity $f = 0.001$ and $f = 0.01$ with three values of Lode angle: $\theta_L = 0$, $30°$ and $60°$.

Chapitre 3

Plastic limit state of the hollow sphere model with non-associated Drucker-Prager material under isotropic loading

Computational Materials Science 62 (2012) 210–215

Contents lists available at SciVerse ScienceDirect

Computational Materials Science

journal homepage: www.elsevier.com/locate/commatsci

Plastic limit state of the hollow sphere model with non-associated Drucker–Prager material under isotropic loading

Long Cheng [a,*], Yun Jia [a], Abdelbacet Oueslati [a], Géry De Saxcé [a], Djimédo Kondo [b]

[a] Laboratoire de Mécanique de Lille, UMR CNRS 8107, Université de Lille 1, Cité scientifique, F59655 Villeneuve d'Ascq, France
[b] Institut Jean Le Rond d'Alembert, UMR CNRS 7190, Université Pierre et Marie Curie, 4 place Jussieu, F75005 Paris, France

ARTICLE INFO

Article history:
Received 23 March 2012
Received in revised form 18 May 2012
Accepted 20 May 2012
Available online 19 June 2012

Keywords:
Porous material
Limit analysis
Bipotential
Drucker–Prager model

ABSTRACT

The paper is devoted to the determination of plastic limit state of a hollow sphere with a Drucker–Prager matrix and subjected to hydrostatic loading. There are two possible plastic regimes corresponding respectively to the tensile and compressive stresses. For the associated case (dilation angle equal to the friction angle), the collapse is complete (the whole sphere is plastified) with a unique regime. For the non-associated cases, we consider weaker solutions (partial collapse and regime change). Nevertheless, we show the collapse is complete and exhibits a single regime. Consequently, the collapse stress field and the limit load do not depend on the value of the dilation angle. This theoretical result is confirmed by numerical simulations.

1. Introduction

The present work can be considered as a first step to propose a macroscopic plastic model for "Porous non-associated Drucker–Prager"-type materials, using homogenization techniques. In a famous paper, Gurson [13] proposed an upper bound limit analysis approach of a hollow sphere and a hollow cylinder having a von Mises solid matrix. Several extensions of Gurson's model have been further proposed in the literature, the probably most important developments being those accounting for void shape effects [11,10,19]. Other extensions are concerned by the plastic anisotropy [2,20]. More extensions take into account the plastic compressibility of the matrix through associated Drucker–Prager model for applications to polymer and cohesive geomaterials [15,16,1,18]. The present paper is a direct extension of a recent paper [23] dedicated to the same problem but with the non-associated yielding rule. It should be emphasized that the ductile porous media with non-associated plastic matrix has not been studied in the literature, except in [18].

Classical bound limit analysis theorems have been generalized to the class of implicit standard materials, i.e. with a non-associated yielding rule represented with a bipotential [7,4]. In Gurson's paper spirit, a trial velocity field is built for homogenization techniques by adding linear terms to the exact one for hydrostatic loading. The goal of the present paper is to determine such an exact field. In limit analysis, the most simple solutions are smooth with a single plastic regime covering the whole body but, generally speaking, it is *a priori* expected that limit state solutions may involve some field discontinuities compatible with the continuum mechanics principles [5,21]. In particular, the collapse may be uncomplete and/or exhibits distinct regimes in subdomains. For non-associated Drucker–Prager model, the collapse stress field is statically and plastically admissible. Then the limit load for the non-associated model is *a priori* less than the limit load for the corresponding associated model (i.e. with the normality rule and the same friction angle). As a matter of fact, although exact solutions do not exist up to now for such class of problems, numerical simulations show that for classical soil mechanics applications (bearing capacity of a strip footing, stability of foundations and tunnels), the limit load of the non-associated case is really strictly less the one of the corresponding associated case [6,3,14]. In the hollow sphere problem, we consider the event of such weaker solutions but we conclude to the impossibility of uncomplete collapse and more than one plastic regime. The paradoxal consequence is the insensitivity of the limit load to the dilation angle.

2. Problem formulation

We consider a hollow sphere, of which the macro-element V is enclosed by surface S, made up of a spherical cavity embedded in a homothetic cell of a rigid-plastic isotropic and homogeneous material with non-associated Drucker–Prager model. The inner and outer radii are respectively denoted a and b, giving the void volume fraction $f = (a/b)^3 < 1$. The hollow sphere is subjected to a uniform hydrostatic stress q upon its external boundary. Accounting for the

* Corresponding author. Tel.: +33 320337166; fax: +33 320337153.
E-mail address: long.cheng@ed.univ-lille1.fr (L. Cheng).

0927-0256/$ - see front matter © 2012 Elsevier B.V. All rights reserved.
http://dx.doi.org/10.1016/j.commatsci.2012.05.048

central symmetry of the problem, the spherical coordinate (r, θ, φ) are used, r being the radius, θ the inclination angle, φ the azimuth one, and all the fields are depending only on r.

In theory of homogenization, the macroscopic stress $\boldsymbol{\Sigma}$ and strain rate $\mathbf{D}$ are defined as volume averages of their microscopic counterparts, $\boldsymbol{\sigma}$ and $\mathbf{d}$:

$$\boldsymbol{\Sigma} = V^{-1}\int_V \boldsymbol{\sigma}\, dV, \qquad \mathbf{D} = V^{-1}\int_V \mathbf{d}\, dV,$$

following the outer boundary conditions on S:

$$\boldsymbol{\sigma}\cdot\mathbf{n} = \boldsymbol{\Sigma}\cdot\mathbf{n} \quad or \quad \mathbf{v} = \mathbf{D}\cdot\mathbf{x} \quad \forall \mathbf{x} \in S.$$

where $\mathbf{v}$ is the surface velocity and $\mathbf{n}$ the unit outward normal vector to S. The global equilibrium and compatibility implies that:

$$\boldsymbol{\Sigma} : \mathbf{D} = V^{-1}\int_V \boldsymbol{\sigma} : \mathbf{d}\, dV. \tag{1}$$

Since the velocity components v_θ and v_φ are null, the strain rate tensor $\mathbf{d}$ has three non-vanishing components given with respect to the radial velocity v_r by:

$$d_{rr} = \frac{dv_r}{dr}, \qquad d_{\theta\theta} = d_{\varphi\varphi} = \frac{v_r}{r}. \tag{2}$$

There is no kinematic boundary conditions but the velocity field $v_r(r)$ must be continuous anywhere.

The stress tensor $\boldsymbol{\sigma}$ also has three non-vanishing components, σ_{rr}, $\sigma_{\theta\theta} = \sigma_{\varphi\varphi}$ and, in absence of body forces, satisfies the radial equilibrium equation:

$$\frac{d\sigma_{rr}}{dr} + 2\,\frac{\sigma_{rr} - \sigma_{\theta\theta}}{r} = 0, \tag{3}$$

with static boundary conditions:

$$\sigma_{rr}(a) = 0, \qquad \sigma_{rr}(b) = q. \tag{4}$$

According to the mechanics of continua, some discontinuities of $\sigma_{\theta\theta}$ and $\sigma_{\varphi\varphi}$ may occur when r varies but the radial stress $\sigma_{rr}(r)$ must be continuous anywhere.

Drucker–Prager model is considered with the yield criterion:

$$F(\sigma) = \sigma_e + 3\alpha\sigma_m - \sigma_0 = 0, \tag{5}$$

where σ_e is the equivalent stress of Von Mises, σ_m the mean stress:

$$\sigma_e = \frac{1}{\sqrt{2}}\sqrt{(\sigma_{rr}-\sigma_{\theta\theta})^2 + (\sigma_{\theta\theta}-\sigma_{\varphi\varphi})^2 + (\sigma_{\varphi\varphi}-\sigma_{rr})^2},$$
$$\sigma_m = \frac{1}{3}(\sigma_{rr} + \sigma_{\theta\theta} + \sigma_{\varphi\varphi}).$$

Due to the spherical symmetry, they could be reduced to:

$$\sigma_e = |\sigma_{rr} - \sigma_{\theta\theta}| = \epsilon(\sigma_{\theta\theta} - \sigma_{rr}), \qquad \sigma_m = \frac{1}{3}(\sigma_{rr} + 2\sigma_{\theta\theta}). \tag{6}$$

With the following convention:

- $\epsilon = +1$ if $\sigma_{rr} \leqslant \sigma_{\theta\theta}$.
- $\epsilon = -1$ if $\sigma_{\theta\theta} \leqslant \sigma_{rr}$.

And $\sigma_0 > 0$ the cohesion stress of the material and α the pressure sensitivity factor related to the friction angle ϕ by:

$$tan\ \phi = 3\alpha.$$

The non-associated yielding rule:

$$\mathbf{d} = \lambda\,\frac{\partial G}{\partial \boldsymbol{\sigma}}, \tag{7}$$

is given by the plastic potential:

$$G(\boldsymbol{\sigma}) = \sigma_e + 3\beta\sigma_m - \sigma_0,$$

where β depends on the dilation angle ψ through:

$$tan\psi = 3\beta.$$

Hence, the strain rate components take the form:

$$d_{rr} = \lambda\left(\beta + \frac{1}{2\sigma_e}(2\sigma_{rr} - \sigma_{\theta\theta} - \sigma_{\varphi\varphi})\right),$$
$$d_{\theta\theta} = \lambda\left(\beta + \frac{1}{2\sigma_e}(2\sigma_{\theta\theta} - \sigma_{\varphi\varphi} - \sigma_{rr})\right),$$
$$d_{\varphi\varphi} = \lambda\left(\beta + \frac{1}{2\sigma_e}(2\sigma_{\varphi\varphi} - \sigma_{rr} - \sigma_{\theta\theta})\right).$$

Considering $(6)_1$ and once again $\sigma_{\theta\theta} = \sigma_{\varphi\varphi}$, they can be reduced to:

$$d_{rr} = \lambda(\beta - \epsilon), \qquad d_{\theta\theta} = d_{\varphi\varphi} = \lambda\left(\beta + \frac{\epsilon}{2}\right). \tag{8}$$

Moreover, the plastic multiplier must be non negative:

$$\lambda \geqslant 0. \tag{9}$$

Of course, for the particular event $\psi = \phi$ hence $F = G$, the normality rule is recovered and the plasticity model is associated. Without loss of generality, we can assume that:

$$0 \leqslant \beta \leqslant \alpha < \frac{1}{2}, \tag{10}$$

or equivalently $0 \leqslant \psi \leqslant \phi < 56°18'$. In practice, these conditions are fulfilled by the geomaterials and other pressure sensitive dilatant materials. Experimental data can be found for polymers, high strength steels and aluminium in [12].

3. Theoretical plastic limit state

In this section, we aim to derive the solution of plastic limit state to the hollow sphere subjected to a hydrostatic loading upon the external boundary, which will be obtained both by statical and kinematical approaches. Let us consider there exist adjoining spherical shells which have distinct plastic regimes corresponding respectively to ϵ and $-\epsilon$. In the present paper we concern the simplest case in which two such adjoining spherical shells exist. The radii at the interface of them is noted as r_0.

3.1. Statical approach

Considering $\sigma_{\theta\theta} = \sigma_{\varphi\varphi}$ and taking into account (6), the Drucker–Prager yield function (5) reads:

$$F(\sigma) = \epsilon(\sigma_{\theta\theta} - \sigma_{rr}) + \alpha(\sigma_{rr} + 2\sigma_{\theta\theta}) - \sigma_0 = 0.$$

Hence, it holds:

$$2(\sigma_{\theta\theta} - \sigma_{rr}) = 3\gamma_\epsilon(H - \sigma_{rr}), \tag{11}$$

where $\gamma_\epsilon = 2\alpha/(2\alpha + \epsilon)$ and $H = \sigma_0/3\alpha = \sigma_0/tan\ \phi > 0$. Due to the condition (10) the sign of γ_ϵ coincides with that of ϵ. Combining (11) with the equilibrium Eq. (3) gives:

$$\frac{d\sigma_{rr}}{dr} + \frac{3\gamma_\epsilon(\sigma_{rr} - H)}{r} = 0.$$

So the radial stress field can be obtained:

$$\sigma_{rr}(r) = H + C_\epsilon \cdot r^{-3\gamma_\epsilon}, \tag{12}$$

where C_ϵ is an integration constant.

The radial stress field of internal shell satisfying the boundary condition $(4)_1$ is:

$$\sigma_{rr}(r) = H\left(1 - \left(\frac{a}{r}\right)^{3\gamma_{-\epsilon}}\right). \tag{13}$$

Since the radial stress should be continuous at the interface ($r = r_0$), from (12) and (13), it follows that in the external shell:

$$\sigma_{rr}(r) = H\left(1 - \left(\frac{r_0}{r}\right)^{3\gamma_\epsilon}\left(\frac{a}{r_0}\right)^{3\gamma_{-\epsilon}}\right). \tag{14}$$

Hence, the limit stress is given by the boundary condition $(4)_2$:

$$q_s = \sigma_{rr}(b) = H\left(1 - \left(\frac{r_0}{b}\right)^{3\gamma_\epsilon}\left(\frac{a}{r_0}\right)^{3\gamma_{-\epsilon}}\right). \tag{15}$$

3.2. Kinematical approach

The kinematical approach consists of minimizing the plastic dissipation power, represented by using the bipotential concept which was proposed in [8,9] to model a large class of non-associated materials called Implicit Standard Materials. In the sense of implicit function theorem, a scalar function b is taken as the bipotential if the following inequality is satisfied:

$$\forall \sigma, \mathbf{d}, \qquad b(\mathbf{d}, \sigma) \geqslant \sigma \cdot \mathbf{d} \tag{16}$$

and a pair $(\mathbf{d}, \sigma)$ is extremal if the equality is achieved in (16):

$$b(\mathbf{d}, \sigma) = \sigma \cdot \mathbf{d}. \tag{17}$$

From a mechanical point of view, such couples are the ones satisfying the constitutive law. Put (8) into (17), and considering (6), one obtains the expression of bipotential for the constitutive law considered in Section 2:

$$b(\mathbf{d}, \sigma) = \lambda(3\beta\sigma_m + \sigma_e). \tag{18}$$

Eliminating the velocity $v_r(r)$ between the two Eq. (2), one obtains:

$$d_{rr} = \frac{d}{dr}(r d_{\theta\theta}). \tag{19}$$

Combining (8) and (19) yields:

$$\frac{d\lambda}{dr} + \frac{3\lambda}{s_\epsilon r} = 0,$$

where we put for convenience $s_\epsilon = 1 + 2\epsilon\beta$. The general solution takes the form:

$$\lambda(r) = \lambda_\epsilon r^{-\frac{3}{s_\epsilon}}. \tag{20}$$

Combining Eqs. (2), (8), and (20) leads to:

$$v_r(r) = K_\epsilon r^{\left(1-\frac{3}{s_\epsilon}\right)}, \tag{21}$$

with

$$K_\epsilon = \left(\beta + \frac{\epsilon}{2}\right)\lambda_\epsilon. \tag{22}$$

Due to the velocity field at the interface of radius r_0 should be continuous, one obtains:

$$K_{-\epsilon} = K_\epsilon r_0^{-3\left(\frac{1}{s_\epsilon} - \frac{1}{s_{-\epsilon}}\right)}.$$

Hence, from (17) and considering (1), the limit load by kinematical approach can be obtained:

$$q_k = \frac{1}{b^2 \cdot v_r(b)}\left[\int_a^{r_0} b(\mathbf{d}, \sigma) r^2 dr + \int_{r_0}^{b} b(\mathbf{d}, \sigma) r^2 dr\right]. \tag{23}$$

Put (18) and (21) into (23), and taking into account (22), q_k can be reduced to:

$$q_k = H\left(1 - \left(\frac{r_0}{b}\right)^{3\gamma_\epsilon}\left(\frac{a}{r_0}\right)^{3\gamma_{-\epsilon}}\right). \tag{24}$$

3.3. Discussion of analytical result

We can observe that $q_s = q_k$, and the limit load by kinematical approach q_k does not depend on the dilation angle ψ. Next the existence of the solution with discontinuities of the shear stress at the interface of radius r_0 will be discussed:

- Assuming K_ϵ and $K_{-\epsilon}$ do not vanish, they should have the same sign, and the plastic multiplier should be positive. However, under the condition (10), $\lambda_\epsilon = K_\epsilon/(\beta + \frac{\epsilon}{2})$ and $\lambda_{-\epsilon} = K_{-\epsilon}/(\beta - \frac{\epsilon}{2})$ have the opposite signs, which is absurd because, accounting for (20), condition (9) would be violated in one of these regimes. Thus no change of regime is allowed at the limit state.
- Let us suppose the collapse is not complete. The plastic multiplier field is identically null in a non plastified spherical shell, hence so is the velocity field because of (20)–(22). It is absurd to assume the existence of a plastic yielding adjoining shell because the continuity of the velocity field at the interface would force the velocity field to vanish in the yielding shell. Hence the collapsed must be complete.

Finally, we can conclude that only one yield shell should be considered in this problem, consequently, $r_0 = a$. The analytical solution of the radial stress field and limit load are respectively:

$$\sigma_{rr}(r) = H\left(1 - \left(\frac{a}{r}\right)^{3\gamma_\epsilon}\right) = \frac{\sigma_0}{3\alpha}\left(1 - \left(\frac{a}{r}\right)^{6\alpha/(2\alpha+\epsilon)}\right) \tag{25}$$

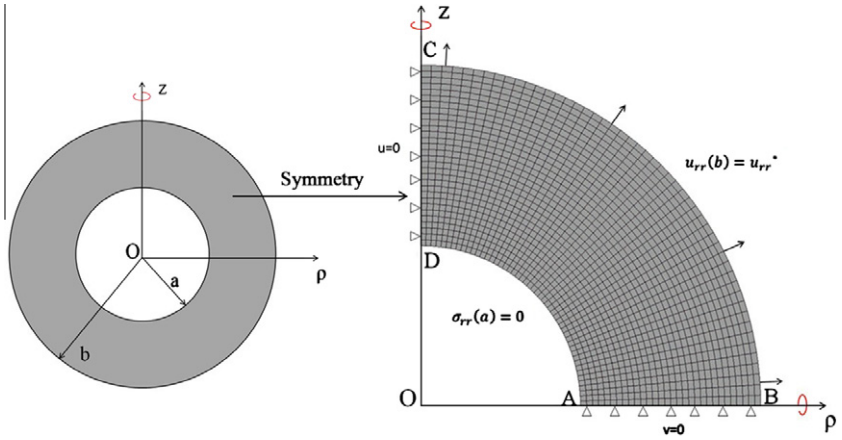

Fig. 1. Hollow sphere model: geometry of the elementary cell and boundary conditions.

Table 1
Comparison between simulation results and the analytical ones.

Case	ψ (°)	f	E (MPa)	Theor.[a] (MPa)		Numer.[b] (MPa)		Error (%)	
				C	T	C	T	C	T
Reference case (Associated case)									
1	30	0.2002	500	−3.007	0.6244	−3.041	0.6183	1.13	0.98
Non-associated case									
2	15	0.2002	500	−3.007	0.6244	−2.995	0.6184	0.40	0.96
3	0	0.2002	500	−3.007	0.6244	−2.980	0.6185	0.90	0.94
Influence of porosity									
4	30	0.1489	500	−3.972	0.7119	−4.054	0.7058	2.06	0.86
5	15	0.1489	500	−3.972	0.7119	−4.023	0.7059	1.28	0.84
6	30	0.2500	500	−2.391	0.5538	−2.376	0.5480	0.63	1.05
7	15	0.2500	500	−2.391	0.5538	−2.370	0.5482	0.88	1.01
Influence of Young's modulus									
8	30	0.2002	1000	−3.007	0.6244	−3.019	0.6186	0.40	0.93
9	15	0.2002	1000	−3.007	0.6244	−3.008	0.6188	0.03	0.90

[a] Analytical results of Section 3.
[b] Results of FEM.

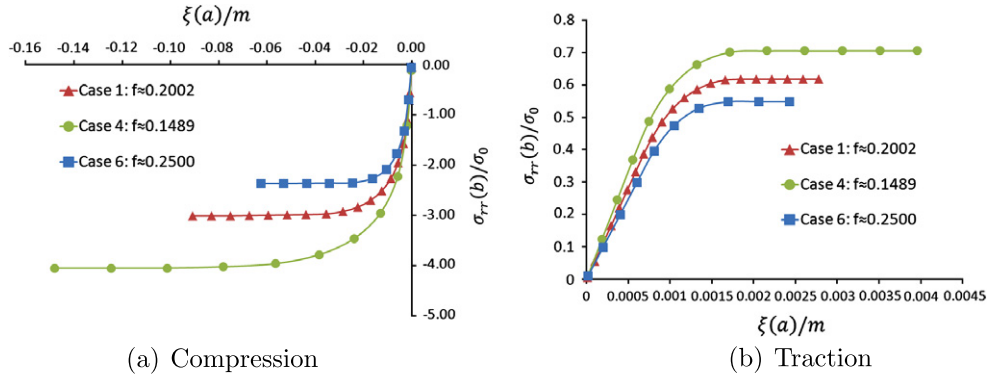

Fig. 2. Comparison of numerical limit loads between the associated Drucker–Prager porous materials ($\psi = \phi = 30^\circ$) with different porosities ($f \approx 0.2002$, $f \approx 0.1489$ and $f \approx 0.2500$).

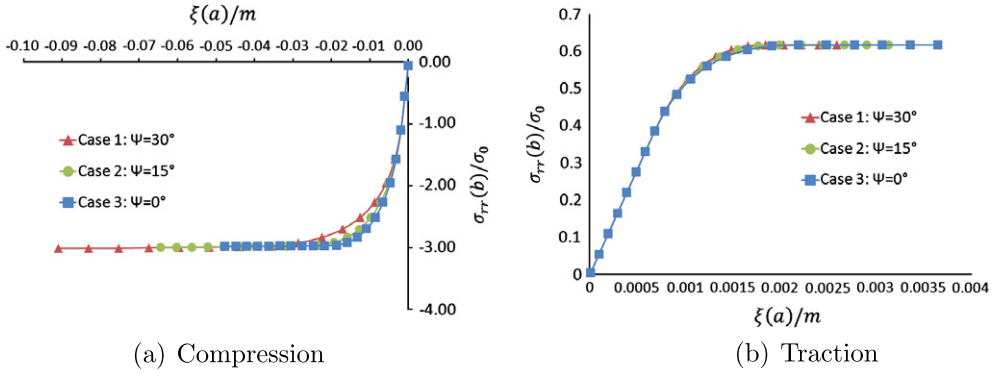

Fig. 3. Comparison of numerical limit loads between associated ($\psi = 30^\circ$) and non-associated cases ($\psi = 15^\circ$ and 0°) with fixed friction angle ($\phi = 30^\circ$) and porosity ($f \approx 0.2002$).

$$q = H(1 - f^{\gamma_\epsilon}) = \frac{\sigma_0}{3\alpha}\left(1 - f^{2\alpha/(2\alpha+\epsilon)}\right). \tag{26}$$

It can be verified that γ_ϵ, σ_{rr} and q have the same sign ϵ. In short, the solution is defined by the limit load (26) and, in the interval $a \leqslant r \leqslant b$, by the collapse fields of plastic multiplier (20), velocity (21), radial stress (12) and yield criterion (11). The stress field and limit loads do not depend on the dilation angle and they are identical to the ones of the associated case with same friction angle, previously obtained in [23]. Only the collapse mechanism is dilation angle dependent. This insensitivity of the limit load to the dilation angle agrees with the model recently proposed in [18].

4. Numerical simulations and comparison

In this section, the analytical solution performed in Section 3 will be compared with the numerical data obtained from the Finite

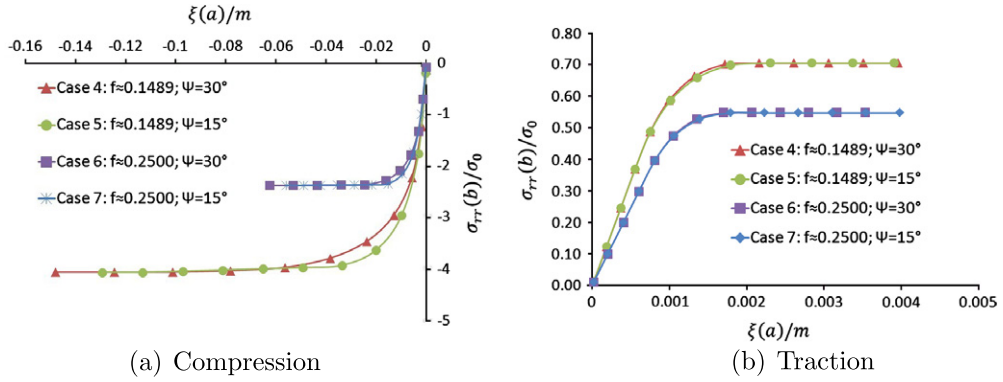

Fig. 4. Comparison of numerical limit loads between associated ($\psi = \phi = 30^\circ$) and non-associated cases ($\phi = 30^\circ$ and $\psi = 15^\circ$) with respect to different porosities ($f \approx 0.1489$ and $f \approx 0.2500$).

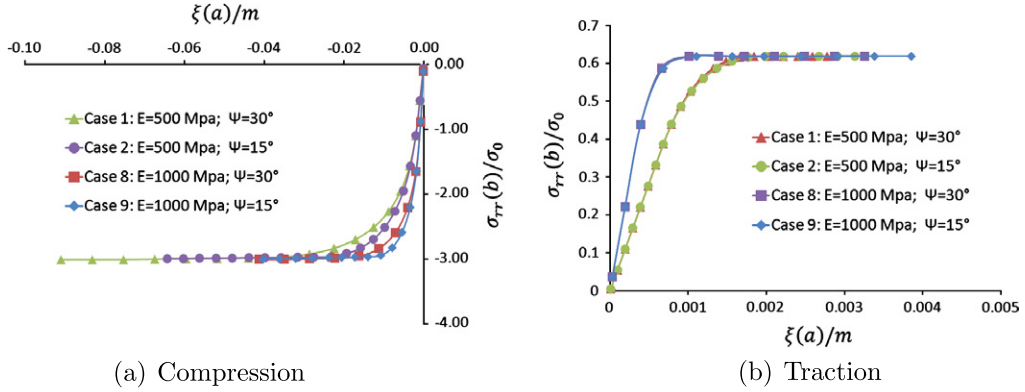

Fig. 5. Comparison of numerical limit loads between associated ($\psi = \phi = 30^\circ$) and non-associated cases ($\phi = 30^\circ$ and $\psi = 15^\circ$) with respect to different Young's modulus ($E = 500$ MPa and $E = 1000$ MPa) and the same porosity ($f \approx 0.2002$).

Element Method (FEM) results. An axisymmetric model of the spherical shell, as shown in Fig. 1, is considered and 1500 quadratic axisymmetric elements are used. Hence, the numerical analysis will be carried out by means of the 2D-FEM code [17,22] developed in LML (*Mechanics Laboratory of Lille, France*) for incremental analysis of elastoplatic materials with non-associated flow rule and in small deformations. The radial displacement is fixed on the plans *ABCD* of symmetry, the vertical and horizontal displacements of the lateral boundaries *AB* and *CD* are also fixed, and a uniform radial displacement is imposed upon the external boundary *BC*, while the internal boundary *DA* is free of stress.

A reference case, denoted Case 1, is firstly defined in which the associated flow rule is applied with the following parameters: $a = 0.585$ m, $b = 1$ m ($f \approx 0.2002$), $\phi = \psi = 30^\circ$, $E = 500$ MPa, $\nu = 0.2$ and $\sigma_0 = 1$ MPa. Then, in order to verify the precision of the proposed model in non-associated cases, two other simulations (denoted Cases 2 and 3) are performed with two different values of ψ (15° and 0°), both under compression (*C*) and traction (*T*) conditions. Finally, two other groups of simulations are carried out to estimate the sensitivity of the proposed model with respect to the porosity and Young's modulus. All of the FEM results and their comparison with the analytical ones are presented in Table 1.

In Case 1, an excellent agreement is obtained between the theoretical value of the limit load established in Section 3 or [23] and the FEM one, both under compression and traction conditions. Furthermore, two other associated cases with different porosities (Cases 4 and 6) are studied. It can be observed that the limit load decreases with an increase of the porosity. This is illustrated in Fig. 2 in which $\xi(r)$ denotes the radial displacement and the limit stress is the asymptotic value. In this group of comparison, an agreement between the theoretical prediction and numerical data is still observed. In conclusion, our FEM code allows to accurately model this hollow sphere problem in the case of associated matrix. We now aim at validating this code in the context of non-associated matrix.

Fig. 3 displays the FEM results of Cases 1 to 3, where the materials possess the same porosity ($f \approx 0.2002$) but different dilation angles. The limit loads of associated case ($\psi = \phi = 30^\circ$) and non-associated ones ($\phi = 30^\circ$, $\psi = 15^\circ$ and 0°), as expected, have almost the same value (Table 1) with small differences of the order 1%. The differences between the reference analytical solution and the finite element ones are rather small and can be attributed to numerical errors due to the discretization. However, the FEM points of these three lines in this figure do not coincide entirely, in other words, as the displacements imposed upon the external boundary being the same, the ones at the internal boundary are not. Therefore, the limit load of non-associated Drucker–Prager porous material does not depend on the dilation angle, whereas the collapse mechanism does.

Next, the Cases 4–7 are contributed to study the influence of the porosity by changing the inner radii *a* from the previous cases. In Cases 4 and 5: $a = 0.530$ m ($f \approx 0.1489$), while in Cases 6 and 7: $a = 0.630$ m ($f \approx 0.2500$). The comparison (see Fig. 4) shows that the limit load of the non-associated case is also the same with the corresponding associated one, do not depend on the porosity.

Finally, the influence of Young's modulus is studied through Cases 8 and 9. Fig. 5 clearly shows that the limit loads are identical

with different values of Young's modulus, only the displacement $\xi(a)$ is changed. Consequently, the limit load is independent of this final parameter.

5. Conclusion

Unlike currently observed in other problems, in the one of the hydrostatically loaded hollow sphere, the limit load and collapse stress field for the non-associated cases are the same as for the corresponding associated one. This event may appear at first glance paradoxal. The key point is the strong condition of central symmetry which is very restrictive and prevents field discontinuities generally allowed by the continuum mechanics. Thus only complete solution with a unique plastic regime is considered and it is necessarily identical to the one of the associated case.

References

[1] J.F. Barthélémy, L. Dormieux, Comptes Rendus Mécanique 331 (2003) 271–276.
[2] A.A. Benzerga, J. Besson, European Journal of Mechanics A: Solids 20 (2001) 397–434.
[3] A. Berga, G. de Saxcé, Revue Européenne des Éléments Finis 3 (1994) 411–456.
[4] L. Bousshine, A. Chaaba, G. de Saxcé, International Journal of Mechanical Sciences 44 (2002) 2189–2216.
[5] W.F. Chen, Limit Analysis and Soil Plasticity, Elsevier, New York, 1975.
[6] W.F. Chen, X.L. Liu, Limit Analysis in Soil Mechanics, Elsevier, Amsterdam, 1990.
[7] G. De Saxcé, L. Bousshine, International Journal of Mechanical Sciences 40 (1998) 387–398.
[8] G. De Saxcé, Z.Q. Feng, Mechanics of Structures and Machines 19 (1991) 301–325.
[9] G. De Saxcé, Comptes Rendus de l'Académie des Sciences – Series II 314 (1992) 125–129.
[10] M. Garajeu, P. Suquet, Journal of the Mechanics and Physics of Solids 45 (1997) 873–902.
[11] M. Gologanu, J.B. Leblond, G. Perrin, J. Devaux, Recent extensions of Gurson's model for porous ductile metals, in: P. Suquet (Ed.), Continuum Micromechanics, Springer-Verlag, 1997.
[12] T.F. Guo, J. Faleskog, C.F. Shih, Journal of the Mechanics and Physics of Solids 56 (2008) 2188–2212.
[13] A.L. Gurson, Journal of Engineering Materials and Technology 99 (1977) 2–15.
[14] M. Hjiaj, J. Fortin, G. de Saxcé, International Journal of Engineering Science 41 (2003) 1109–1143.
[15] H.Y. Jeong, J. Pan, International Journal of the Mechanics and Physics of Solids 39 (1995) 1385–1403.
[16] H.Y. Jeong, International Journal of the Mechanics and Physics of Solids 32 (2002) 3669–3691.
[17] Y. Jia, Contribution à la modélisation thermo–hydro-mécanique des roches partiellement saturées: application au stockage des déchets radioactifs. Thesis of University of Lille 1, 2006.
[18] S. Maghous, L. Dormieux, J.F. Barthélémy, European Journal of Mechanics A: Solids 28 (2009) 179–188.
[19] V. Monchiet, E. Charkaluk, D. Kondo, Comptes Rendus Mécanique 335 (2007) 32–41.
[20] V. Monchiet, O. Cazacu, D. Kondo, International Journal of Plasticity 24 (2008) 1158–1189.
[21] M.A. Save, C.E. Massonnet, G. de Saxcé, Plastic Limit Analysis of Plates, Shells and Disks, Elsevier, New York, 1997.
[22] J.F. Shao, Y. Jia, D. Kondo, A.S. Chiarelli, Mechanics of Materials 38 (2006) 218–232.
[23] P. Thoré, F. Pastor, J. Pastor, D. Kondo, Comptes Rendus Mécanique 337 (2009) 260–267.

Chapitre 4

Bipotential-based limit analysis and homogenization of non-associated porous plastic materials

A bipotential-based limit analysis and homogenization of ductile porous materials with non-associated Drucker-Prager matrix

Long Cheng[a], Yun Jia[a], Abdelbacet Oueslati[a], Géry de Saxcé[a], Djimedo Kondo[b]

[a]*Laboratoire de Mécanique de Lille, UMR CNRS 8107, Université de Lille 1, Cité scientifique, F59655 Villeneuve d'Ascq, France*
[b]*Institut Jean Le Rond d'Alembert, UMR CNRS 7190, Université Pierre et Marie Curie, 4 place Jussieu, F75005 Paris, France*

Abstract

In Gurson's footsteps, different authors have proposed macroscopic plastic models for porous solid with pressure-sensitive dilatant matrix obeying to the normality law (associated materials). The main objective of the present paper is to extend this class of models to porous materials in the context of non-associated plasticity. This is the case of Drucker-Prager matrix for which the dilatancy angle is different from the friction one, and classical limit analysis theory cannot be applied. For such materials, the second last author has proposed a relevant modeling approach based on the concept of bipotential, a function of both dual variables, the plastic strain rate and stress tensors. On this ground, after recalling the basic elements of the bipotential theory, we present the corresponding variational principles and the extended limit analysis theorems. Then, we formulate a new variational approach for the homogenization of porous porous materials with non-associated matrix. This is implemented by considering the hollow sphere model with a non-associated Drucker-Prager matrix. The proposed procedure delivers a closed form expression of the macroscopic bifunctionnal from which is readily obtained the criterion and a non-associated flow rule of the porous material. It is shown that these general results recover several available models as particular cases. Finally, the established results are assessed and validated by comparing their predictions to that of Finite Element computations carried out on a cell representing the considered class of materials.

Keywords: Bipotential theory, Nonlinear Homogenization, Extended Limit analysis, Ductile porous materials, Non associated plasticity, Drucker-Prager matrix
2000 MSC: 74C05, 74L10

1. Introduction

In his famous paper, Gurson (1977) proposed an upper bound limit analysis approach of a hollow sphere and a hollow cylinder having a von Mises solid matrix. Several extensions of

Email address: email address (Djimedo Kondo)

Gurson's model have been further proposed in the literature, the most probably important developments being those accounting for void shape effects (Gologanu et al., 1997; Garajeu et al., 1997; Monchiet et al., 2007; Madou and Leblond , 2012a,b; Monchiet and Kondo , 2013). Plastic anisotropy was treated by (Benzerga et al., 2001; Monchiet et al., 2008; Keralavarma and Benzerga , 2010), while studies by Cazacu et al. (Cazacu and Stewart, 2009) have been devoted to porous materials exhibiting a tension-compression asymmetry. Other extensions take into account the plastic compressibility of the matrix through associated Drucker-Prager model for applications to polymer and cohesive geomaterials (Jeong et al., 1995; Jeong , 2002; Guo et al., 2008; Barthélémy et al., 2003). Application of this class of models has been done in (Lin et al., 2011a,b; Shen et al., 2012). It is worth noticing that, in the spirit of Gurson's paper, the kinematical limit analysis of porous materials with an associated matrix requires the choice of a trial velocity field. The latter is generally built by adding linear terms to the exact one for hydrostatic loading. A notable study concerning the non-associated Drucker-Prager matrix has been done by Maghous et al. (2009) in the context of modified secant moduli approach (see also Ponte-Castaneda (1991); Suquet (1995)).

Coming to a more general point of view, a constitutive law in Mechanics is a relationship between dual variables. The constitutive laws of the materials can be represented, as in Elasticity, by a univalued mapping or, as in Plasticity, can be generalized in the form of a multivalued mapping but this representation is not necessarily convenient. When the graph is maximal cyclically monotone, one can model it thanks to a convex and lower semi-continuous function π, called a superpotential (or pseudo-potential), such that the graph is the one of its subdifferential $\partial\pi$). The function π and its Fenchel conjugate one π^* verifies for any couple of dual variables Fenchel's inequality. The dissipative materials admitting a superpotential of dissipation are often qualified as standard (Halphen et al., 1975) and the law is said to be a normality law, a subnormality law or an associated law.

However, many experimental observations in the last decades have motivated the proposition of non-associated laws, particularly in Plasticity theory. For such laws, the second last author proposed in (de Saxcé et al., 1991; de Saxcé , 1992) a suitable modeling framework based on the bipotential, a function b of both dual variables, convex and lower semicontinuous in each argument and satisfying a cornerstone inequality saying that for any couple of dual variables the value of the bipotential is greater than or equal to their duality pairing. When equality holds, the couple is said extremal. In a mechanical point of view, the extremal couples are the ones satisfying the constitutive law. Materials admitting a bipotential are called implicit standard materials (ISM) because the constitutive law is a subnormality law but the relation between the dual variables is implicit. The classical standard materials correspond to the particular event for which the bipotential is separated as the sum of a superpotential and its conjugate one. In this sense, the cornerstone inequality of the bipotential generalizes Fenchel's one. The existence and construction of a bipotential for a given constitutive law has been recently discussed in (Buliga et al., 2008, 2009a, 2010a).

Linked to the structural mechanics and in particular with the Calculus of Variation, the bipotential theory offers an elegant framework to investigate a broad spectrum of non-associated laws. Examples of such non-associated constitutive laws are:

- in soil mechanics, non-associated Drucker-Prager (de Saxcé , 1993; Berga et al., 1994; de Saxcé , 1998a; Bousshine et al., 2001; Hjiaj et al., 2003) and Cam-Clay models (de Saxcé , 1995; Zouain et al., 2007, 2010),
- the non linear kinematical hardening rule for cyclic Plasticity (de Saxcé , 1992; Bodovillé et al., 2001) and Viscoplasticity (Hjiaj et al., 2000; Magnier et al., 2006; Bouby et al., 2006, 2009),
- Lemaitre's coupled plasticity-damage law (Bodovillé , 1999),
- the coaxial laws (de Saxcé , 2002; Vallée et al., 2005),
- Coulomb's friction law (de Saxcé , 1998b, 1992, 1993, 1998b,a; Bousshine et al., 2002; Hjiaj et al., 2002, 2004; Feng et al., 2006b,a; Fortin et al., 1999, 2002; Laborde et al., 2008),
- the blurred constitutive laws (Buliga et al., 2009b, 2010b).

A complete survey of the bipotential approach can be found in de Saxcé (2002). In the previous works, robust numerical algorithms were proposed to solve structural mechanics problems.

Coming back to the Limit Analysis let us say that a general method to determine the plastic collapse of structures under proportional loading (Suquet, 1982; Salençon , 1983; Save et al., 1997), even particular in soil mechanics (Chen , 1975; Chen et al., 1990), but it is restricted to associated plasticity, then with normality law. The classical presentation of the non-associated plasticity is based on a yield function and a plastic potential. The bipotential offers an alternative formulation which naturally opening to a variational formulation, and then paving the way for an extension of limit analysis techniques to non-associated laws (de Saxcé , 1998a; Bousshine et al., 2001, 2002; Chaaba et al., 2010; Zouain et al., 2007). Extension of limit analysis theory to the repeated variable loading, known as shakedown theory, has been successfully generalized to the ISM[1] by the bipotential approach in (de Saxcé , 2002; Bousshine et al., 2001, 2003; Bouby et al., 2006, 2009).

The aim of the present study is to formulate a macroscopic model for "ductile porous materials with a non-associated Drucker-Prager"-type matrix, using homogenization techniques combined with the bipotential theory. The paper is organized as follows: the non-associated Drucker-Prager plastic model, for which the yield criterion and plastic potential are respectively defined by two functions, is first summarized in Section 2. Next, we introduce in Section 3, the bipotential theory and its two dual fields (stress and velocity fields) based formulation, which allows us to derive the plastic criterion and the non-associated flow rule. An application of the bipotential theory to the non-associated Drucker-Prager plastic model is particularly discussed in subsection 3.3. Section 4 is devoted to the bipotential-based extended limit analysis approach of non-associated porous media. The proposed formulation

[1] *See also the use of Shakedown theory by (Boulbibane and Weichert , 1997) for non-associated soils.*

provides a fundamental variational theory for the macroscopic modeling of a large class of porous media. In Section 5, the proposed bipotential-based theory is implemented in the case of a hollow sphere having a rigid perfectly plastic matrix obeying to a non-associated Drucker-Prager flow rule. This implementation will be performed by adopting simple trial stress and velocity fields. This allows to derive in subsection 5.3 a closed-form expression of the macroscopic criterion and the non-associated plastic flow rule. Furthermore, some special cases, corresponding to existing models previously proposed in literature, are discussed in subsection 6. Finally, in Section 7, the established macroscopic criterion, flow rule and void evolution are respectively assessed and validated by comparison with Finite Element solutions.

2. Brief recall the non-associated Drucker-Prager model

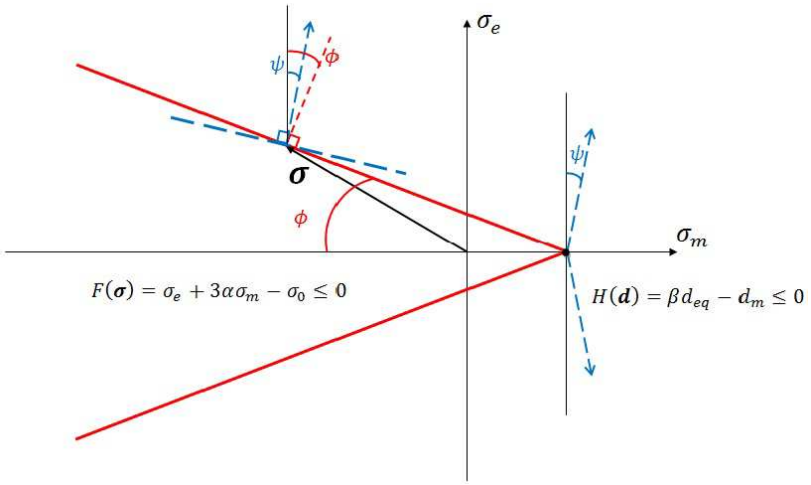

Figure 1: Drucker-Prager model: yield criterion and non-associated flow rule

Drucker-Prager model (Fig.1) requires the consideration of a yield criterion in the form:

$$F(\boldsymbol{\sigma}) = \sigma_e + 3\alpha\sigma_m - \sigma_0 \leq 0 \ , \tag{1}$$

where σ_e is the equivalent stress, σ_m the mean stress, $\sigma_0 > 0$ the shear cohesion stress of the material and α the pressure sensitivity factor related to the friction angle ϕ by:

$$\tan\ \phi = 3\alpha \ .$$

Let us introduce the plastic potential:

$$G(\boldsymbol{\sigma}) = \sigma_e + 3\beta\sigma_m \tag{2}$$

where β ($\beta \leq \alpha$) depends on the dilatancy angle ψ through:

$$\tan\ \psi = 3\beta \ .$$

Except for the apex of Drucker-Prager cone ($\sigma_e = 0$, $\sigma_m = \sigma_0$ / 3α) where σ_e is not differentiable, the plastic strain rate is given by the non-associated yielding rule:

$$\boldsymbol{d} = d_{eq}\,\frac{\partial G}{\partial \boldsymbol{\sigma}} = d_{eq}\left(\frac{3\boldsymbol{s}}{2\sigma_e} + \beta\mathbf{1}\right), \tag{3}$$

where $\boldsymbol{\sigma}$ is Cauchy stress tensor, $\boldsymbol{s}$ the deviatoric stress, $\mathbf{1}$ the unit tensor. $d_{eq} = \mid \frac{2}{3}\boldsymbol{d}' : \boldsymbol{d}' \mid^{1/2}$ with $\boldsymbol{d}'$ being the deviatoric part of $\boldsymbol{d}$. The plastic dilatancy reads:

$$d_m = \frac{1}{3} tr\ \boldsymbol{d} = \beta d_{eq} \tag{4}$$

This suggests to introduce:

$$H(\boldsymbol{d}) = \beta d_{eq} - d_m$$

The plastic yielding rule (3) is completed at the apex by the admissibility condition:

$$H(\boldsymbol{d}) \leq 0$$

while, because of (4), $H(\boldsymbol{d}) = 0$ at the other points of the yielding surface (called regular points). Of course, for the particular event $\psi = \phi$, the normality rule is recovered and the plasticity model is associated. Without loss of generality, we can assume that:

$$0 \leq \beta \leq \alpha < \frac{1}{2}\ , \tag{5}$$

or equivalently $0 \leq \psi \leq \phi < 56°18'$. In practice, these conditions are fulfilled by the geomaterials and other pressure sensitive dilatant materials. Some examples of experimental data concerning the friction angle can be found for polymers, high strength steels and aluminium in (Guo et al., 2008).

3. Bipotential-based formulation of constitutive models

Rigid perfectly plastic model is usually considered to obtain the analytical solution (plastic criterion and potential) for a large class of materials, simultaneously by adopting the Limit Analysis approach, which is extensively discussed in literature . However, this conventional approach can only be rigorously used for Generalized Standard Materials (GSM), that is materials which obey a normality law. the standard limit analysis framework is then not suitable for materials which obey to a non-associated flow rule (for instance, geomaterials). This question has been discussed in several works (Salençon , 1983; Drucker , 1953; Palmer , 1973; Radenkovic , 1961; Telega , 2002; Telega et al. , 2004).

In order to overcome this problem, de Saxcé et al. has proposed in previous papers a new modeling of the non-associated constitutive laws based on the concept of bipotential (de Saxcé et al., 1991; de Saxcé , 1992).

3.1. The bipotential in short

First of all, let us recall a basic concept of convex analysis, the subdifferential of a function π in a point $\boldsymbol{x}$ which is the (possibly empty) set:

$$\partial\pi(\boldsymbol{x}) = \{\boldsymbol{y} \mid \forall \boldsymbol{x'}, \qquad \pi(\boldsymbol{x'}) - \pi(\boldsymbol{x}) \geq (\boldsymbol{x'} - \boldsymbol{x}) : \boldsymbol{y}\} \ . \tag{6}$$

For more details on convex analysis, the reader is refered for instance to (Ekeland et al., 1975; Moreau , 2003; Rockafellar , 1970). Moreover, in mechanics, GSM can represented as a generalized model based on two superpotentials $\pi(\boldsymbol{x'})$ and $\pi^*(\boldsymbol{y'})$, which are depending on a represented strain rate variable $\boldsymbol{x}$ and a stress-like one $\boldsymbol{y}$. Such a couple of superpotentials satisfies the Fenchel's inequality (Fenchel , 1949),

$$\forall(\boldsymbol{x'}, \boldsymbol{y'}) \qquad \pi(\boldsymbol{x'}) + \pi^*(\boldsymbol{y'}) \geq \boldsymbol{x'} : \boldsymbol{y'} \tag{7}$$

where $\pi(\boldsymbol{x'})$ and $\pi^*(\boldsymbol{y'})$ are convex, lower semicontinuous and conjugate each of the other. The r.h.s. of (7) indicates the inner product of $\boldsymbol{x'}$ and $\boldsymbol{y'}$. When the equality is achieved, $(\boldsymbol{x}, \boldsymbol{y})$ is called an extremal couple:

$$\pi(\boldsymbol{x}) + \pi^*(\boldsymbol{y}) = \boldsymbol{x} : \boldsymbol{y}$$

It can be proved that this relation is equivalent to the two following differential inclusions:

$$\boldsymbol{y} \in \partial\pi(\boldsymbol{x}),$$

$$\boldsymbol{x} \in \partial\pi^*(\boldsymbol{y}).$$

It is worth to remark that the convexity properties of π and π^* are essential in order to state and prove minimum variational principles and use the limit analysis approach[2]. When the normality law fails and is replaced by a non-associated flow rule, the classical presentation is based on a yield function (to model the yield criterion) and a plastic potential (to represent the flow rule). Although it is intensively used in the literature, this is, in fact, not very relevant for the variational methods. On the ground of this observation, de Saxcé and collaborators proposed in (de Saxcé et al., 1991; de Saxcé , 1992) a suitable modeling based on more general generating functions called **bipotentials** and defined by the following properties:

(a) b is convex and lower semicontinuous in each argument.

(b) For any $\boldsymbol{x'}$ and $\boldsymbol{y'}$ we have

$$b(\boldsymbol{x'}, \boldsymbol{y'}) \geq \boldsymbol{x'} : \boldsymbol{y'} \tag{8}$$

(c) For $\boldsymbol{x}$ and $\boldsymbol{y}$ we have the equivalences:

$$\mathbf{y} \in \partial b(\cdot, \boldsymbol{y})(\boldsymbol{x}) \iff \boldsymbol{x} \in \partial b(\boldsymbol{x}, \cdot)(\boldsymbol{y}) \iff b(\boldsymbol{x}, \boldsymbol{y}) = \boldsymbol{x} : \boldsymbol{y} \tag{9}$$

In a mechanical point of view, the bipotential represents the plastic dissipation power (by volume unit) and (9) is the constitutive law. The couples $(\boldsymbol{x}, \boldsymbol{y})$ for which ones equivalence (9) holds are called **extremal couples**. The cornerstone inequality (8) clearly generalizes Fenchel's one (7).

[2]Lower and upper bound solutions obtained from the Hill's principle and Markov's one.

3.2. Variational framework of bipotential-based formulations for constitutive laws

Let us now replace the above notations $\boldsymbol{x}$ and $\boldsymbol{y}$ respectively by the strain rate tensor $\boldsymbol{d}$ and the stress tensor $\boldsymbol{\sigma}$. In a mechanical point of view, the corresponding bipotential represents the plastic dissipation power (by volume unit) and from Eq.(9) the constitutive law can be obtained. Accounting for the definition (6) of the subdifferential and the cornerstone inequality (8), the constitutive law reads (Buliga et al., 2009a, 2010a; Laborde et al., 2008; Buliga et al., 2010b):

$$\min_{\boldsymbol{d}'}(b(\boldsymbol{d}',\boldsymbol{\sigma})-\boldsymbol{d}':\boldsymbol{\sigma})=\min_{\boldsymbol{\sigma}'}(b(\boldsymbol{d},\boldsymbol{\sigma}')-\boldsymbol{d}:\boldsymbol{\sigma}')=0\ . \tag{10}$$

It is worth remarking that, with respect to the previous minimization problems, the bipotential has the required convexity properties.

Next, let us show how to recover simply the plastic yielding condition $F(\boldsymbol{\sigma})=0$ by the bipotential formalism. To this end, the first minimization problem in (10) becomes:

$$\min_{H(\boldsymbol{d})\leq 0}(b_0(\boldsymbol{d},\boldsymbol{\sigma})-\boldsymbol{d}:\boldsymbol{\sigma})=0\ , \tag{11}$$

where b_0 is the finite part of the bipotential when the extremal value is taken. Relaxing the kinematical condition $H(\boldsymbol{d})\leq 0$ by use of Lagrange's multiplier λ, this constrained minimization problem is transformed into an equivalent saddle-point problem

$$\max_{\lambda\geq 0}\min_{\boldsymbol{d}}(L(\boldsymbol{d},\boldsymbol{\sigma},\lambda)=b_0(\boldsymbol{d},\boldsymbol{\sigma})-\boldsymbol{d}:\boldsymbol{\sigma}+\lambda H(\boldsymbol{d}))=0\ , \tag{12}$$

where $L(\boldsymbol{d},\boldsymbol{\sigma},\lambda)$ is the lagrangian function. Its stationarity with respect to $\boldsymbol{d}$:

$$\frac{\partial L}{\partial \boldsymbol{d}}=\frac{\partial b_0}{\partial \boldsymbol{d}}(\boldsymbol{\sigma})-\boldsymbol{\sigma}+\lambda\frac{\partial H(\boldsymbol{d})}{\partial \boldsymbol{d}}=0$$

Eliminating the lagrangian multiplier λ in above system of equations, the resultant functional depends only on stress tensor $\boldsymbol{\sigma}$. Let us denote it F; it follows the yield criterion

$$F(\boldsymbol{\sigma})=0$$

In a similar way, it is possible to recover the plastic flow rule (3) at a regular point. The second minimization problem in (10) becomes:

$$\min_{F(\boldsymbol{\sigma})\leq 0}(b_0(\boldsymbol{d},\boldsymbol{\sigma})-\boldsymbol{d}:\boldsymbol{\sigma})=0\ .$$

Relaxing the plastic yielding condition $F(\boldsymbol{\sigma})\leq 0$ by use of Lagrange's multiplier λ^*, this problem is transformed into an equivalent saddle-point problem

$$\max_{\lambda^*\geq 0}\min_{\boldsymbol{\sigma}}(L^*(\boldsymbol{d},\boldsymbol{\sigma},\lambda^*)=b_0(\boldsymbol{d},\boldsymbol{\sigma})-\boldsymbol{d}:\boldsymbol{\sigma}+\lambda^* F(\boldsymbol{\sigma}))=0\ , \tag{13}$$

By calculating the stationarity of the lagrangian $L^*(\boldsymbol{d},\boldsymbol{\sigma},\lambda^*)$ with respect to $\boldsymbol{\sigma}$

$$\frac{\partial L}{\partial \boldsymbol{\sigma}}=\frac{\partial b_0}{\partial \boldsymbol{\sigma}}(\boldsymbol{d})-\boldsymbol{d}+\lambda^*\frac{\partial F(\boldsymbol{\sigma})}{\partial \boldsymbol{\sigma}}=0$$

and eliminating λ^*, the resultant functional (denoted H) depends only on the strain rate tensor $\boldsymbol{d}$. Hence, the flow rule can be obtained

$$H(\boldsymbol{d})=0$$

3.3. Case of the non-associated Drucker-Prager materials

The finite value bipotential of non-associated Drucker-Prager model (see Section 2) takes the form (Hjiaj et al., 2003):

$$b(\boldsymbol{d},\boldsymbol{\sigma}) = \left\{ \begin{array}{cc} \frac{\sigma_0}{\alpha} d_m + (\beta-\alpha)\left(3\sigma_m - \frac{\sigma_0}{\alpha}\right) d_{eq} & \text{if} \quad F(\boldsymbol{\sigma}) \leq 0 \quad and \quad H(\boldsymbol{d}) \leq 0 \\ +\infty \quad \text{otherwise} & \end{array} \right\} , \quad (14)$$

In view of what will be done in subsections 5.2 and 5.3, for the homogenization problem, it is convenient to indicate how the derivation of the non-associated yield criterion can be done from (12) and (14). The lagrangian function reads:

$$L(\boldsymbol{d},\boldsymbol{\sigma},\lambda) = \frac{\sigma_0}{\alpha} d_m + (\beta-\alpha)\left(3\sigma_m - \frac{\sigma_0}{\alpha}\right) d_{eq} - (\sigma_e d_{eq} + 3 d_m \sigma_m) + \lambda(\beta d_{eq} - d_m) \ .$$

Its stationnarity with respect to d_{eq} and d_m gives:

$$\sigma_e = (\beta-\alpha)\left(3\sigma_m - \frac{\sigma_0}{\alpha}\right) + \beta\lambda \ ,$$

$$3\sigma_m = \frac{\sigma_0}{\alpha} - \lambda \ .$$

Eliminating λ between these relations leads to the plastic criterion :

$$F(\boldsymbol{\sigma}) = \sigma_e + 3\alpha\sigma_m - \sigma_0 = 0 \ .$$

Simultaneously, from the second minimization problem of (10), we have the corresponding lagrangian by introducing the multiplier λ^*

$$L^*(\boldsymbol{d},\boldsymbol{\sigma},\lambda^*) = \frac{\sigma_0}{\alpha} d_m + (\beta-\alpha)\left(3\sigma_m - \frac{\sigma_0}{\alpha}\right) d_{eq} - (\boldsymbol{d}' : \boldsymbol{s} + 3 d_m \sigma_m) + \lambda^*(\sigma_e + 3\alpha\sigma_m - \sigma_0) \ .$$

In the same way, the stationnarity with respect to $\boldsymbol{s}$ and σ_m reads,

$$\boldsymbol{d}' = \lambda^* \ \frac{3\boldsymbol{s}}{2\sigma_e} \ , \quad (15)$$

$$(\beta-\alpha) d_{eq} - d_m + \alpha\lambda^* = 0 \ . \quad (16)$$

From (15) one obtains $\lambda^* = d_{eq}$. Eliminating λ^* in (16) leads to the kinematical condition at the regular points upon the yield surface:

$$H(\boldsymbol{d}) = \beta d_{eq} - d_m = 0 \ , \quad (17)$$

That allows to recover the non-associated yielding rule (3):

$$\boldsymbol{d} = \boldsymbol{d}' + d_m \mathbf{1} = d_{eq}\left(\frac{3\boldsymbol{s}}{2\sigma_e} + \beta\mathbf{1}\right) \ .$$

For the treatment of the apex, the reader is refered to (Hjiaj et al., 2003), which is specifically devoted to this question.

4. Extended limit analysis of porous materials with a non-associated matrix

Unlike the classical presentation of the non-associated constitutive laws by means of the yield function and the plastic potential, the bipotential formulation naturally opens into a variational formulation; this is crucial for an extension of limit analysis techniques to the context of non-associated laws. We present here the main elements of this variational framework in the context of porous media.

4.1. Determination of the macroscopic bifunctional and its variational properties

This presentation is directly done in the framework of homogenization of porous material, considering a reference cell Ω composed of a void ω and a matrix $\Omega_M = \Omega - \omega$ made of an Implicit Standard Material. The macro-cell Ω is enclosed by surface $\partial\Omega$ and the void ω by $\partial\omega$. The external boundary of the cell is subjected to a uniform strain rate: $\boldsymbol{v} = \boldsymbol{D} \cdot \boldsymbol{x}$, $\boldsymbol{x}$ being the position vector at the boundary. The macroscopic stress $\boldsymbol{\Sigma}$ and strain rate $\boldsymbol{D}$ are then classically defined as volume averages of their microscopic counterpart $\boldsymbol{\sigma}$ and $\boldsymbol{d}$:

$$\boldsymbol{\Sigma} = \frac{1}{\mid \Omega \mid} \int_{\Omega} \boldsymbol{\sigma} \; dV \; , \qquad \boldsymbol{D} = \frac{1}{\mid \Omega \mid} \int_{\Omega} \boldsymbol{d} \; dV \; . \tag{18}$$

Note that the set of kinematical admissible velocity fields is defined in the following sense:

$$\mathcal{K}_a = \{ \boldsymbol{v} \quad s.t. \quad \boldsymbol{v}(\boldsymbol{x}) = \boldsymbol{D}.\boldsymbol{x} \quad on \quad \partial\Omega \} \; . \tag{19}$$

and the associated strain rate field is given by $\boldsymbol{d}(\boldsymbol{v}) = grad_s \boldsymbol{v} = \frac{1}{2} \left(grad\boldsymbol{v} + grad^T \boldsymbol{v} \right)$.

The set of statically admissible stress fields is:

$$\mathcal{S}_a = \{ \boldsymbol{\sigma} \quad s.t. \quad div \; \boldsymbol{\sigma} = 0 \quad in \quad \Omega_M, \quad \boldsymbol{\sigma} \cdot \boldsymbol{n} = 0 \quad on \quad \partial\omega, \quad \boldsymbol{\sigma} = 0 \quad in \quad \omega \} \; . \tag{20}$$

The set of admissible couples is the product $\mathcal{A} = \mathcal{K}_a \times \mathcal{S}_a$ and the set of extremal ones is defined by:

$$\mathcal{E} = \{ (\boldsymbol{v}, \boldsymbol{\sigma}) \quad s.t. \quad (\boldsymbol{d}(\boldsymbol{v}), \boldsymbol{\sigma}) \quad is \quad extremal \quad in \quad \Omega_M \} \; .$$

The homogenization problem consists in determining the set $\mathcal{A} \times \mathcal{E}$ of admissible and extremal fields. Owing to the non linearity of the problem, no exact solution can be found in general. Due to this difficulty, we present an equivalent variational formulation, more appropriate for simple approximations, thanks to relevant choice of trial fields and minimization procedure. By Hill's lemma, any admissible couple $(\boldsymbol{v}, \boldsymbol{\sigma})$ complies with:

$$\boldsymbol{D} : \boldsymbol{\Sigma} = \frac{1}{\mid \Omega \mid} \int_{\Omega} \boldsymbol{d}(\boldsymbol{v}) : \boldsymbol{\sigma} \; dV = \frac{1}{\mid \Omega \mid} \int_{\Omega_M} \boldsymbol{d}(\boldsymbol{v}) : \boldsymbol{\sigma} \; dV \; , \tag{21}$$

This suggests introducing the following two field macroscopic bifunctional:

$$B(\boldsymbol{v}', \boldsymbol{\sigma}') = \frac{1}{\mid \Omega \mid} \int_{\Omega_M} b(\boldsymbol{d}(\boldsymbol{v}'), \boldsymbol{\sigma}') \; dV - \boldsymbol{D} : \boldsymbol{\Sigma} \; ,$$

As previously indicated, we are interested for homogenization purpose in finding the admissible and extremal couples $(\boldsymbol{v}, \boldsymbol{\sigma})$. In fact, they are solutions of the following simultaneous minimization problems:

$$B(\boldsymbol{v}, \boldsymbol{\sigma}) = \min_{\boldsymbol{v}' \in \mathcal{K}_a} B(\boldsymbol{v}', \boldsymbol{\sigma}) = \min_{\boldsymbol{\sigma}' \in \mathcal{S}_a} B(\boldsymbol{v}, \boldsymbol{\sigma}') = 0 \ . \tag{22}$$

Indeed, if $(\boldsymbol{v}', \boldsymbol{\sigma}')$ is admissible, relation (21) and (8) entail:

$$B(\boldsymbol{v}', \boldsymbol{\sigma}') = \frac{1}{\mid \Omega \mid} \int_{\Omega_M} (b(\boldsymbol{d}(\boldsymbol{v}'), \boldsymbol{\sigma}') - \boldsymbol{d}(\boldsymbol{v}') : \boldsymbol{\sigma}') \ dV \geq 0 \ .$$

In particular, this occurs for admissible couples $(\boldsymbol{v}', \boldsymbol{\sigma})$, $(\boldsymbol{v}, \boldsymbol{\sigma}')$, $(\boldsymbol{v}, \boldsymbol{\sigma})$. Moreover, for the latter, owing to (9):

$$B(\boldsymbol{v}, \boldsymbol{\sigma}) = 0 \ .$$

In short, one has for all admissible fields $\boldsymbol{v}' \in \mathcal{K}_a$ and $\boldsymbol{\sigma}' \in \mathcal{S}_a$:

$$B(\boldsymbol{v}', \boldsymbol{\sigma}) \geq B(\boldsymbol{v}, \boldsymbol{\sigma}) = 0 \qquad and \qquad B(\boldsymbol{v}, \boldsymbol{\sigma}') \geq B(\boldsymbol{v}, \boldsymbol{\sigma}) = 0 \ ,$$

which prove (22).

Now, let us discuss some relevant aspects of the variational principles for a rigid perfectly plastic matrix such as the one described in the previous sections. The set of plastically admissible velocity and stress fields are respectively defined as:

$$\begin{aligned} \mathcal{K}_p &= \{\boldsymbol{v} \quad s.t. \quad H(\boldsymbol{d}(\boldsymbol{v})) \leq 0 \quad in \quad \Omega_M\} \\ \mathcal{S}_p &= \{\boldsymbol{\sigma} \quad s.t. \quad F(\boldsymbol{\sigma}) \leq 0 \quad in \quad \Omega_M\} \ . \end{aligned} \tag{23}$$

while the sets of licit velocity and stress fields are respectively $\mathcal{K}_l = \mathcal{K}_a \cap \mathcal{K}_p$ and $\mathcal{S}_l = \mathcal{S}_a \cap \mathcal{S}_p$. We considered the finite valued bifunctional:

$$B_0(\boldsymbol{v}', \boldsymbol{\sigma}') = \frac{1}{\mid \Omega \mid} \int_{\Omega_M} b_0(\boldsymbol{d}(\boldsymbol{v}'), \boldsymbol{\sigma}') \ dV - \boldsymbol{D} : \boldsymbol{\Sigma} \ . \tag{24}$$

the finite valued bipotential b_0 being introduced in (11).
Hence, the bipotential-based variational homogenization problem becomes:

$$B_0(\boldsymbol{v}, \boldsymbol{\sigma}) = \min_{\boldsymbol{v}' \in \mathcal{K}_l} B_0(\boldsymbol{v}', \boldsymbol{\sigma}) = \min_{\boldsymbol{\sigma}' \in \mathcal{S}_l} B_0(\boldsymbol{v}, \boldsymbol{\sigma}') = 0 \ . \tag{25}$$

Note that the determination of the above macroscopic bifunctional can be done by means of any of the two minimization principles, providing that the exact stress field or exact velocity field is given.

4.2. Application of the variational principle to the plastic porous material

For a rigid perfectly plastic matrix, since b_0 is positively homogeneous of order one in $\boldsymbol{d}$, there is a trivial kinematical solution to the previous problem (equation (25) together with (24)) where $\boldsymbol{v}$ and $\boldsymbol{D}$ vanish. The limit analysis approach consists in finding non trivial solutions qualified as ruin mechanisms. It is expected that these non trivial solutions exist only under an equality condition on $\boldsymbol{\Sigma}$ that can be interpreted as the equation of the macroscopic yielding surface in the model.

It is worth noting that if both $\boldsymbol{D}$ and $\boldsymbol{\Sigma}$ are chosen arbitrarily, there is in general no solution to the problem (25). In a practical point of view, it is more convenient for instance to fix only $\boldsymbol{\Sigma}$ and to find $\boldsymbol{D}$ and $\boldsymbol{v}$ satisfying the first minimization problem in (25). Introducing Lagrange's multiplier field $\boldsymbol{x} \mapsto \Lambda(\boldsymbol{x})$, this constrained minimization problem is transformed into an equivalent saddle-point problem

$$\max_{\Lambda \geq 0} \min_{\boldsymbol{v} \in \mathcal{K}_a} \left(\mathcal{L}(\boldsymbol{v}, \boldsymbol{\sigma}, \Lambda) = B_0(\boldsymbol{v}, \boldsymbol{\sigma}) + \frac{1}{\mid \Omega \mid} \int_{\Omega_M} \Lambda H(\boldsymbol{d}) \, dV \right) .$$

We perform a first approximation by imposing Lagrange's multiplier field to be uniform in Ω_M:

$$\max_{\Lambda \geq 0} \min_{\boldsymbol{v} \in \mathcal{K}_a} \left(\mathcal{L}(\boldsymbol{v}, \boldsymbol{\sigma}, \Lambda) = B_0(\boldsymbol{v}, \boldsymbol{\sigma}) + \Lambda \frac{1}{\mid \Omega \mid} \int_{\Omega_M} H(\boldsymbol{d}) \, dV \right) , \tag{26}$$

that is equivalent to minimize the bifunctional B_0 under the relaxed kinematical condition:

$$\frac{1}{\mid \Omega \mid} \int_{\Omega_M} H(\boldsymbol{d}) \, dV = 0 . \tag{27}$$

Satisfying the kinematical condition only in an average sense but not locally anywhere in Ω_M is a strong approximation but leading to easier calculations. As consequence of this approximation, it is crucial to remark that the minimum of B_0 may not be expected to be zero. Nevertheless, in the spirit of Ladevèze's method of the error on the constitutive law (Ladevèze , 1975; Ladevèze et al. , 1986, 1991, 1997, 2001, 2006a,b), its value for the minimizer can be used as a variational error estimator (Fortin et al., 1999). The minimum principle allows obtaining the "better"solution within the framework imposed by the approximations.

Introducing

$$Y(\boldsymbol{v}, \boldsymbol{\sigma}, \Lambda) = \frac{1}{\mid \Omega \mid} \int_{\Omega_M} b_0(\boldsymbol{v}, \boldsymbol{\sigma}) dV + \Lambda \frac{1}{\mid \Omega \mid} \int_{\Omega_M} H(\boldsymbol{d}) \, dV$$

and considering (24), the Lagrangian function can be recast into

$$\mathcal{L}(\boldsymbol{v}, \boldsymbol{\sigma}, \Lambda) = Y(\boldsymbol{v}, \boldsymbol{\sigma}(\boldsymbol{\Sigma}), \Lambda) - \boldsymbol{D} : \boldsymbol{\Sigma} \tag{28}$$

from which, as it will be shown by introducing the trial stress and velocity fields, one obtains the macroscopic criterion and flow rule.

For now, let us just indicate that the ultimate step is to solve the Saddle-point problem by computing its subdifferentials with respect to parameters $\boldsymbol{D}$:

$$\frac{\partial \mathcal{L}}{\partial \boldsymbol{D}}\left(\Lambda, \boldsymbol{\Sigma}\right) = 0 \tag{29}$$

Eliminating the Lagrangian multiplier Λ in the system of functionals (29), one obtains

$$\mathcal{F}(\boldsymbol{\Sigma}(\phi, \psi, f)) = 0 \tag{30}$$

A priori, the above macroscopic criterion depends not only on the porosity f and the friction angle ϕ, but also on the dilatancy angle ψ of the matrix.

For completeness, the macroscopic non-associated flow rule, with the boundary conditions $\boldsymbol{v} = \boldsymbol{D} \cdot \boldsymbol{x}$, can be directly obtained from the stationnarity of the lagrangian function (28) with respect to the multiplier Λ:

$$\mathcal{G} = \frac{1}{\mid \Omega \mid} \int_{\Omega_M} H(\boldsymbol{d})\, dV = 0\ . \tag{31}$$

5. The hollow sphere model with a non-associated Drucker-Prager matrix

The major objective of this section is to apply the above bipotential-based variational approach and limit analysis technique to the hollow sphere model, which is made up of a spherical void embedded in a homothetic cell of a rigid-plastic isotropic and homogeneous matrix, the latter being described by a non-associated Drucker-Prager model. The inner and outer radii of the hollow sphere are respectively denoted a and b, giving the void volume fraction $f = (a/b)^3 < 1$. The hollow sphere is subjected at its exterior boundary to a uniform strain rate tensor $\boldsymbol{D}$ (see Fig. 2).
Primarily, we aim at deriving a macroscopic criterion for the non-associated porous material and the corresponding flow rule.

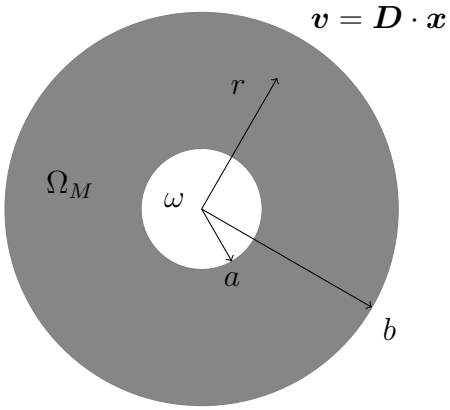

Figure 2: Hollow sphere model

5.1. Proposed trial stress and velocity fields

As mentioned in Section 4, in order to derive the macroscopic model, it is indispensable to propose a couple of trial stress and velocity fields. In order to limit the errors due to approximations, we will consider trial fields for which the macroscopic model is exact at least for pure hydrostatic loadings. In Cheng et al. (2012), we obtain closed analytical formula for the limit hydrostatic stresses. For this case, the stress field and limit load do not depend on the dilatancy angle ψ and they are identical to the ones of the associated case with same friction angle ϕ, previously obtained in Thoré et al. (2009). Only the collapse mechanism is dilatancy angle dependent. This insensitivity of the hydrostatic limit load to the dilatancy angle agrees with the model of Maghous et al. (2009) already mentioned. For this reason, and taking into account the symmetry of the hollow sphere model, the trial stress field is considered as the sum of the two following fields:

- A heterogeneous part corresponding to the exact field under pure hydrostatic loadings (Thoré et al., 2009); it reads, in spherical coordinates with orthonormal frame $\{\mathbf{e}_r, \mathbf{e}_\phi, \mathbf{e}_\theta\}$:

$$\boldsymbol{\sigma}^{(\mathbf{1})} = A_0 \left(\frac{b}{r}\right)^{3\gamma} \left[\boldsymbol{e}_r \otimes \boldsymbol{e}_r + \left(1 - \frac{3\gamma}{2}\right)(\boldsymbol{e}_\theta \otimes \boldsymbol{e}_\theta + \boldsymbol{e}_\phi \otimes \boldsymbol{e}_\phi)\right] \tag{32}$$

  where A_0 is a constant to be determined, $s = 1 + 2\epsilon\alpha$ and $\gamma = 1 - \frac{2\epsilon\alpha}{1+2\epsilon\alpha}$, with a loading parameter $\epsilon = \pm 1$, which will be interpreted later.

- A homogeneous part in the cylindrical coordinates with orthonormal frame $\{\mathbf{e}_\rho, \mathbf{e}_\phi, \mathbf{e}_z\}$:

$$\boldsymbol{\sigma}^{(\mathbf{2})} = A_1 (\boldsymbol{e}_\rho \otimes \boldsymbol{e}_\rho + \boldsymbol{e}_\phi \otimes \boldsymbol{e}_\phi) + A_2 \boldsymbol{e}_z \ \otimes \boldsymbol{e}_z \tag{33}$$

  where A_1 and A_2 are also constant parameters.
  It should be noted that $\boldsymbol{\sigma}^{(2)}$ allows to capture the macroscopic shear effect.

The resultant three parameters based trial stress field is defined in the matrix Ω_M as:

$$\boldsymbol{\sigma} = \boldsymbol{\sigma}^{(\mathbf{1})} + \boldsymbol{\sigma}^{(\mathbf{2})} \tag{34}$$

Note that a vanishing stress field is considered in the void ω.

It is worth to remark that with a stress field is in internal equilibrium, one has:

$$\boldsymbol{\Sigma}^{void} = \frac{1}{\mid \Omega \mid} \int_\omega \boldsymbol{\sigma} dV = \frac{1}{\mid \Omega \mid} \int_{\partial\omega} (\boldsymbol{\sigma}\boldsymbol{n}) \otimes \boldsymbol{x} dS$$

Hence:

$$\Sigma_m^{void} = \frac{1}{\mid \Omega \mid} \int_\omega \sigma_m dV = (3V)^{-1} \int_{\partial\omega} \boldsymbol{x} \cdot (\boldsymbol{\sigma}\boldsymbol{n}) dS$$

As the continuity condition:

$$(\boldsymbol{\sigma}\boldsymbol{n})_- + (\boldsymbol{\sigma}\boldsymbol{n})_+ = 0 \quad on \quad \partial\omega \tag{35}$$

is difficult to satisfy by the very simple chosen trial field, we relax it as follows:

$$(3V)^{-1}\int_{\partial\omega}\boldsymbol{x}\cdot((\boldsymbol{\sigma n})_{-}+(\boldsymbol{\sigma n})_{+})dS=0 \tag{36}$$

which can be equivalently written as:

$$f^{-\gamma}A_0+\frac{2A_1+A_2}{3}=0\ , \tag{37}$$

On the other hand, the macroscopic stress field is:

$$\boldsymbol{\Sigma}=A_0\left(1-f^{1-\gamma}\right)\mathbf{1}+(1-f)\left[A_1\left(\boldsymbol{e}_x\otimes\boldsymbol{e}_x+\boldsymbol{e}_y\otimes\boldsymbol{e}_y\right)+A_2\boldsymbol{e}_z\otimes\boldsymbol{e}_z\right]\ , \tag{38}$$

Taking into account (37), the macroscopic mean stress is:

$$\Sigma_m=A_0(1-f^{-\gamma})\ , \tag{39}$$

while the macroscopic deviatoric stress reads:

$$\Sigma_e=(1-f)\mid A_1-A_2\mid\ . \tag{40}$$

These two last relations allow to express the stress parameters in terms of the macroscopic stress:

$$A_0=\frac{\Sigma_m}{1-f^{-\gamma}}\ ,\quad \mid A_1-A_2\mid=\frac{\Sigma_e}{1-f}\ . \tag{41}$$

Next, following Guo et al. (2008) (see also (Thoré et al., 2009)), we adopt, in cylindrical coordinates, the following trial velocity field which depend on the dilatancy angle ψ, not on the friction angle ϕ,

$$\boldsymbol{v}=C_0\left(\frac{b}{r}\right)^{3/\tilde{s}}(\rho\boldsymbol{e}_\rho+z\boldsymbol{e}_z)+C_1\rho\boldsymbol{e}_\rho+C_2z\boldsymbol{e}_z\ , \tag{42}$$

with $r=\sqrt{\rho^2+z^2}$, $\tilde{s}=1+2\epsilon\beta$, where ϵ is the sign of C_0. The first term is the exact solution for the hydrostatic case (Cheng et al., 2012). As in Gurson's model (Gurson, 1977) and in its extension to pressure sensitive dilatant materials (Guo et al., 2008), this term is completed by two linear terms in order to capture the shear effects.

$\boldsymbol{D}$ being the applied macroscopic strain rate, the trial velocity field (42) must comply with the boundary conditions:

$$\boldsymbol{v}=\boldsymbol{D}\cdot\boldsymbol{x}$$

In the case of axisymmetric macroscopic strain rate ($\boldsymbol{D}=D_{xx}(\boldsymbol{e}_x\otimes\boldsymbol{e}_x+\boldsymbol{e}_y\otimes\boldsymbol{e}_y)+D_{zz}\boldsymbol{e}_z\otimes\boldsymbol{e}_z$), considered in the present study, C_0, C_1 and C_2 are such that:

$$\begin{aligned}D_m&=\frac{1}{3}tr\boldsymbol{D}=C_0+\frac{1}{3}(2C_1+C_2)\\ D_{zz}-D_{xx}&=\frac{2}{3}(C_1-C_2)\end{aligned} \tag{43}$$

from which it follows:

$$D_e=\sqrt{\frac{2}{3}\boldsymbol{D}':\boldsymbol{D}'}=\frac{2}{3}\mid C_1-C_2\mid \tag{44}$$

$\boldsymbol{D}'$ being the deviatoric part of $\boldsymbol{D}$.

5.2. Closed-form expression of the macroscopic bifunctional

In order to derive the non-associated macroscopic model by solving the saddle point problem (26), we aim now at parametrically expressing the macroscopic bifunctional (24) thanks to the proposed trial stress (34) and trial velocity fields (42). It should be pay attention that the bipotential (14) depends on the microscopic mean stress σ_m, mean strain rate d_m and equivalent strain rate d_{eq}. From (34) and (42), and considering (41), these quantities can be respectively calculated as

$$\sigma_m(r) = \frac{\Sigma_m}{1-f^\gamma}\left[1-\frac{f^\gamma}{s}\left(\frac{b}{r}\right)^{3\gamma}\right] , \tag{45}$$

$$d_m(r) = \frac{1}{3}tr\boldsymbol{d} = \left(1-\frac{1}{\tilde{s}}\right)C_0\left(\frac{b}{r}\right)^{3/\tilde{s}} + \frac{1}{3}(2C_1+C_2) \tag{46}$$

$$d_{eq}(r) = \frac{2}{3}\sqrt{(C_1-C_2)^2 + (C_1-C_2)\frac{3C_0}{\tilde{s}}\left(\frac{b}{r}\right)^{3/\tilde{s}}(3\cos^2\theta-1) + \left(\frac{3C_0}{\tilde{s}}\right)^2\left(\frac{b}{r}\right)^{6/\tilde{s}}} \tag{47}$$

for which one must have in mind the relations:

$$d_m(r) = D_m + C_0\left[(1-\frac{1}{\tilde{s}})(\frac{b}{r})^{3/\tilde{s}}-1\right] \tag{48}$$

$$d_{eq}(r) = \frac{2}{3}\sqrt{D_e^2 + sign(C_1-C_2)D_e\frac{3C_0}{\tilde{s}}\left(\frac{b}{r}\right)^{3/\tilde{s}}(3\cos^2\theta-1) + \left(\frac{3C_0}{\tilde{s}}\right)^2\left(\frac{b}{r}\right)^{6/\tilde{s}}} \tag{49}$$

For simplicity, let us introduce the normalized stress tensor

$$\boldsymbol{T} = \frac{\boldsymbol{\Sigma}}{\sigma_0} , \tag{50}$$

and the contribution of the void to average strain rate

$$\boldsymbol{D}(a) = C_0 f^{\tilde{\gamma}}\mathbf{1} + f\left[C_1(\boldsymbol{e}_x\otimes\boldsymbol{e}_x + \boldsymbol{e}_y\otimes\boldsymbol{e}_y) + C_2\boldsymbol{e}_z\otimes\boldsymbol{e}_z\right] , \tag{51}$$

with $\tilde{\gamma} = 1-\tilde{s}^{-1}$.

Combining (14), (22) and (50), the normalized macroscopic bifunctional can be obtained as follows:

$$\bar{B}_0(\boldsymbol{v},\boldsymbol{\sigma}) = \frac{B_0(\boldsymbol{v},\boldsymbol{\sigma})}{\sigma_0} = \frac{1}{3\alpha}tr\left(\boldsymbol{D}-\boldsymbol{D}(a)\right) + \left(1-\frac{\beta}{\alpha}\right)\hat{\Pi}(\boldsymbol{v},\boldsymbol{\sigma}) - \boldsymbol{D}:\boldsymbol{T} \tag{52}$$

with

$$\hat{\Pi}(\boldsymbol{v},\boldsymbol{\sigma}) = \frac{1}{\mid\Omega\mid}\int_{\Omega_M} d_{eq}\ dV\ - \frac{1}{\mid\Omega\mid}\int_{\Omega_M} 3\alpha\frac{\sigma_m}{\sigma_0}d_{eq}dV \tag{53}$$

Hence, it is convenient to introduce

$$\Pi(\boldsymbol{v}) = \frac{1}{\mid\Omega\mid}\int_{\Omega_M} d_{eq}\ dV\ ,$$

which by considering (47) and (43), can be reduced into

$$\Pi(C_0, D_e) = D_e \int_f^1 K(\xi)\sqrt{1+\tau^2 x^{-2/\tilde{s}}}\; dx \;, \tag{54}$$

with

$$\tau = \frac{2C_0}{\tilde{s}D_e}, \qquad x = (\frac{r}{b})^3, \qquad \xi = \frac{2\tau x^{-1/\tilde{s}}}{1+\tau^2 x^{-2/\tilde{s}}}\; sign(C_1 - C_2), \quad |\,\xi\,| \leq 1 \;. \tag{55}$$

$$K(\xi) = \frac{1}{2}\int_0^\pi \sqrt{1+\frac{1}{2}(3\cos^2\theta - 1)\xi}\;\sin\theta\; d\theta \;, \tag{56}$$

Putting (45) into (53), $\hat{\Pi}$ can be recast into the following parametric form

$$\hat{\Pi}(C_0, D_e, T_m) = \left(1 - \frac{3\alpha T_m}{1-f^\gamma}\right)\Pi(C_0, D_e) + \frac{3\alpha T_m}{1-f^\gamma}\frac{f^\gamma}{s} I(D_e) \tag{57}$$

with

$$I(D_e) = D_e \int_f^1 x^{-\gamma} K(\xi)\sqrt{1+\tau^2 x^{-2/\tilde{s}}}\; dx \;. \tag{58}$$

Finally, the closed form expression of the macroscopic bifunctional reads:

$$\begin{aligned}\bar{B}_0(C_0, D_m, D_e, T_m, T_e) =& \frac{1}{\alpha}\left[(1-f)\,D_m - \left(f^{\tilde{\gamma}} - f\right)C_0\right] \\ &+ \left(1 - \frac{\beta}{\alpha}\right)\hat{\Pi}(C_0, D_e, T_m) - (D_e T_e + 3 D_m T_m)\end{aligned} \tag{59}$$

This constitute one of the key practical respect of the study.

5.3. Determination of the macroscopic criterion and of the macroscopic flow rule

Having in hand the bifunctional B_0, we are already now to determine the kinematical admissibility condition (27), written as

$$\beta\Pi(C_0, D_e) - \left[(1-f)\,D_m - \left(f^{\tilde{\gamma}} - f\right)C_0\right] = 0 \tag{60}$$

which plays the role of the macroscopic flow rule.
Concerning the determination of the macroscopic criterion, let us first introduce a normalized multiplier $\bar{\Lambda} = \Lambda/\sigma_0$, the normalized lagrangian can be written as

$$\begin{aligned}\bar{\mathcal{L}}(C_0, D_m, D_e, T_m, T_e, \bar{\Lambda}) =& \frac{\mathcal{L}(C_0, D_m, D_e, T_m, \Lambda)}{\sigma_0} \\ =& \left(\frac{1}{\alpha} - \bar{\Lambda}\right)\left[(1-f)\,D_m - \left(f^{\tilde{\gamma}} - f\right)\right] + \bar{\Lambda}\beta\Pi(C_0, D_e) \\ &+ \left(1 - \frac{\beta}{\alpha}\right)\hat{\Pi}(C_0, D_e, T_m) - (D_e T_e + 3 D_m T_m)\end{aligned} \tag{61}$$

For the minimization of the macroscopic bifunctional (59), one needs to calculate the partial derivatives of the normalized lagrangian (61). Considering

$$\tau = \tau(C_0, D_e), \quad \Pi(C_0, D_e) = \Pi(\tau, D_e), \quad \hat{\Pi}(C_0, D_e, T_m) = \Pi(\tau, D_e, T_m)$$

its stationarity with respect to D_e, D_m and C_0 gives for the normalized stress tensor $\boldsymbol{T} = \frac{\boldsymbol{\Sigma}}{\sigma_0}$:

$$T_e(\tau) = \bar{\Lambda}\beta\Pi_{,D_e}(\tau) + \left(1 - \frac{\beta}{\alpha}\right)\hat{\Pi}_{,D_e}(\tau) \ , \tag{62}$$

$$3T_m(\tau) = \left(\frac{1}{\alpha} - \bar{\Lambda}(\tau)\right) \ (1 - f) \ , \tag{63}$$

$$\bar{\Lambda}\beta\Pi_{,C_0}(\tau) + \left(1 - \frac{\beta}{\alpha}\right)\hat{\Pi}_{,C_0}(\tau) - \left(\frac{1}{\alpha} - \bar{\Lambda}(\tau)\right) \ (f^{\tilde{\gamma}} - f) = 0 \ . \tag{64}$$

from which, we deduce the expression of the normalized multiplier:

$$\bar{\Lambda}(\tau) = \frac{\frac{1}{\alpha}(f^{\tilde{\gamma}} - f) + \left(\frac{\beta}{\alpha} - 1\right)\hat{\Pi}_{,C_0}(\tau)}{f^{\tilde{\gamma}} - f + \beta\Pi_{,C_0}(\tau)} \ .$$

Eliminating $\bar{\Lambda}$ in (62) and (63), delivers the closed-form macroscopic criterion in the form:

$$\begin{aligned} T_e &= \frac{(f^{\tilde{\gamma}} - f)\left[\frac{\beta}{\alpha}\Pi_{,D_e} + \left(1 - \frac{\beta}{\alpha}\right)\hat{\Pi}_{,D_e}\right] + \left(1 - \frac{\beta}{\alpha}\right) \ \beta \ \left(\Pi_{,C_0}\hat{\Pi}_{,D_e} - \Pi_{,D_e}\hat{\Pi}_{,C_0}\right)}{f^{\tilde{\gamma}} - f + \beta\Pi_{,C_0}} \ , \\ 3T_m &= (1 - f) \ \frac{\frac{\beta}{\alpha}\Pi_{,C_0} + \left(1 - \frac{\beta}{\alpha}\right)\hat{\Pi}_{,C_0}}{f^{\tilde{\gamma}} - f + \beta\Pi_{,C_0}} \ . \end{aligned} \tag{65}$$

in which $\hat{\Pi}$ is given by (57), and it is recalled that $\tilde{\gamma} = \frac{2\epsilon\beta}{1+2\epsilon\beta}$.
The explicit expressions for $\Pi_{,C_0}$, $\Pi_{,D_e}$, $\hat{\Pi}_{,C_0}$, $\hat{\Pi}_{,D_e}$ and their antiderivatives Π, $\hat{\Pi}$ are calculated and detailed in Appendix A. It is worthy to noted that the above macroscopic criterion (65) is established in a parametric form which depends on the strain rate ratio τ (55) corresponding to the velocity imposed condtion $\boldsymbol{v} = \boldsymbol{D}\cdot\boldsymbol{x}$. More precisely, the points of plastic limit stress curve can be obtained from the parametric macroscopic criterion (65) for different fixed values of τ. This also allows to deduce the normalized triaxiality $\mathcal{T} = T_m/T_e$.

Finally, the stationarity of the normalized lagrangian (61) with respect to $\bar{\Lambda}$ gives directly the macroscopic flow rule (see (60)).

Note also that, macroscopic associated flow rule is obtained by $\beta = \alpha$, non-associated one otherwise. Let us recall from (55) that

$$C_0 = \frac{\tilde{s}}{2}\tau D_e \tag{66}$$

and introduce

$$\mathcal{P} = \frac{\Pi}{D_e} \tag{67}$$

which only depends on τ. Inserting (66) and (67) into (60) provides a new form of the admissibility condition (60) (flow rule):

$$\frac{D_m}{D_e} = \frac{1}{1-f}\left[\beta\mathcal{P}(\tau) + (f^{\tilde{\gamma}} - f)\frac{\tilde{s}}{2}\tau\right] \tag{68}$$

Hence, the plastic flow direction Υ can be obtained once the value of τ is pre-proposed,

$$\Upsilon = \text{acot}\left[\frac{1}{1-f}\left(\beta\mathcal{P}(\tau) + (f^{\tilde{\gamma}} - f)\frac{\tilde{s}}{2}\tau\right)\right] \tag{69}$$

Finally, owing to the matrix compressibility, the void growth rate readily reads,

$$\dot{f} = 3(1-f)D_m - \frac{1}{\mid \Omega \mid}\int_{\Omega_M} tr\boldsymbol{d}\ dV \tag{70}$$

which, by considering (42), (46) and (66), takes the final expression,

$$\dot{f} = 3(f^{\tilde{\gamma}} - f)C_0 = \frac{3}{2}(f^{\tilde{\gamma}} - f)\tilde{s}\tau D_e \tag{71}$$

Note that (65), (68) and (71) are probably some of the most important and practical results of the study. They are the basic blocks of the non-associated constitutive law of the porous material having a non associated Drucker-Prager matrix.

6. Examination of some special cases

We analyze in this subsection the predictions obtained for some special cases for which results are available in literature. Let us first note that the general problem involves three constants defining the velocity field (42). These constants are linked by the three relations (43), (44) and (60). These equations can be easily explicit in the particular cases examined below.

- Hydrostatic case: $D_e = 0$ and $C_0 \neq 0$
  From (43) and (47), the microscopic equivalent strain rate in this case reads

  $$d_{eq}(r) = \frac{2 \mid C_0 \mid}{\tilde{s}}\left(\frac{b}{r}\right)^{3/\tilde{s}}$$

  It follows from (54) and (58) that

  $$\Pi = \frac{C_0}{\beta}\left(1 - f^{\tilde{\gamma}}\right), \qquad I = \frac{2 \mid C_0 \mid}{\tilde{s}}\frac{1 - f^{\tilde{\gamma}-\gamma}}{\tilde{\gamma} - \gamma}$$

  in which $\tau = \frac{C_0}{D_e}$ has been also considered. Hence, taking also into account (57), the macroscopic stress is given from (65) in the form:

  $$T_e = \frac{\Sigma_e}{\sigma_0} = 0\ , \qquad T_m = \frac{\Sigma_m}{\sigma_0} = \frac{1}{3\alpha}\left(1 - f^{\gamma}\right)\ , \tag{72}$$

which is the plastic limit state for the pure hydrostatic loading $\Sigma_e = 0$ (traction and compression). This result corresponds to the exact solution in non-associated case derived by Cheng et al. (2012), which have also verified that for the hydrostatically loaded hollow sphere, the limit loads for the non-associated case are the same as for the corresponding associated one given by Guo et al. (2008) (see also (Thoré et al., 2009)). Finally, due to $D_e = 0$, (60) readily implies $C_0 = D_m$ and then, by (71), $\dot{f} = 3(f^{\tilde{\gamma}} - f)D_m$.

- $C_0 = 0$ and $D_e \neq 0$
  In this case, from (47), (54) and (58) we have

$$d_{eq} = \frac{2}{3} \mid C_1 - C_2 \mid = \frac{2}{3} D_e$$

$$\Pi = D_e \, (1 - f) \, , \qquad I = D_e \, \frac{1 - f^{1-\gamma}}{1 - \gamma}$$

  The macroscopic limit stresses can be obtained from (65)

$$T_m = \frac{\Sigma_m}{\sigma_0} = 0, \qquad T_e = \frac{\Sigma_e}{\sigma_0} = 1 - f \tag{73}$$

  Similarly, the plastic flow direction can be derived from (68) or (69):

$$\frac{D_m}{D_e} = \beta, \quad or \quad \Upsilon = \operatorname{acot} \beta \tag{74}$$

  In this case, the macroscopic admissibility condition appears as the exact couterpart of the microscopic one. For completeness to this case, the void growth rate can be immediately obtained from (71), that is $\dot{f} = 0$. All of the above results obtained from $C_0 = 0$ reflects and proves that the hollow sphere model is under a pure shear loading (73). They provide the same result as the solution obtained by Gurson (1977) and Guo et al. (2008). Obviously, it leads to the conclusion that no matter the matrix of the porous media take a normality rule or not, solution for pure shear loading depends only on the value of porosity, neither on the friction angle nor the dilatancy one. This is a limitation which comes from the simplicity of the trial fields. Equally important, the plastic flow follows a constant and regularly direction (74), which is independent on the friction angle ϕ. It can be calculated when and only when the dilatancy angle ψ is fixed.

- Case of associated matrix
  When the matrix complies with an associated flow rule, $\psi = \phi$ and $\beta = \alpha$ in Eqs. (1) and (2). It is worthy to indicate that for the pressure-sensitive matrix there is such as $\beta = \alpha \neq 0$. Consequently, one gets from (65) the following macroscopic criterion

$$\begin{aligned} T_e &= \frac{f^\gamma - f}{f^\gamma - f + \alpha \frac{\partial \Pi}{\partial C_0}} \frac{\partial \Pi}{\partial D_e} \\ 3T_m &= \frac{1 - f}{f^\gamma - f + \alpha \frac{\partial \Pi}{\partial C_0}} \frac{\partial \Pi}{\partial C_0} \end{aligned} \tag{75}$$

and from (69) and (71) that the plastic flow direction and the void growth rate, respectively

$$\Upsilon = \operatorname{acot}\left[\frac{1}{1-f}\left(\alpha\mathcal{P}(\tau) + (f^\gamma - f)\frac{s}{2}\tau\right)\right]$$

$$\dot{f} = 3(f^\gamma - f)C_0 = \frac{3}{2}(f^\gamma - f)s\tau D_e$$

which is precisely the so called Upper Bound Model (UBM)[3] proposed in Guo et al. (2008). For completeness, we present in Appendix B the derivation of our methodology in the case of associated matrix.

- von Mises matrix
  For the porous material with an incompressible matrix, for instance the von Mises yield criterion at microscopic level, the pressure-sensitive parameter ϕ and ψ both vanish, or in another word $\alpha = \beta = 0$. In this case, we have

$$\tilde{s} = s = 1, \quad \tilde{\gamma} = \gamma = 0$$

and owing to (60), one obtains $D_m = C_0$. As a result, (47) then takes the form

$$d_{eq} = \frac{2}{3}\sqrt{D_e^2 + 3D_mD_e(3\cos^2\theta)(\frac{b}{r})^3 + (3D_m)^2(\frac{b}{r})^6}$$

and (65) reduced to

$$\begin{aligned} T_e &= \frac{\Sigma_e}{\sigma_0} = \frac{\partial\Pi}{\partial D_e} \\ 3T_m &= 3\frac{\Sigma_m}{\sigma_0} = \frac{\partial\Pi}{\partial D_m} \end{aligned} \tag{76}$$

Considering (54) and (71), we get the following macroscopic criterion

$$T_e^2 + 2f\ \cosh(\frac{3}{2}T_m) - (1+f^2) = 0\ , \tag{77}$$

and the void growth equation

$$\dot{f} = 3(1-f)D_m\ . \tag{78}$$

which are the well-known results of Gurson (1977) obtained by a kinematical limit analysis approach.

[3]It should be emphasized that the macroscopic model proposed by Guo et al. (2008) cannot be seen as an upper bound. For the corresponding demonstration, readers can be referred to Cheng (2013).

7. Illustration and numerical validation of the established criterion

In this section, the predictions of established macroscopic criterion (65) in non-associated cases will be firstly compared with the associated one (75) (see also the so called UBM of Guo et al. (2008)) in subsection 7.1. The expected influence of the non-associated feature is clearly illustrated. Next, Finite Element Method (FEM) based limit analysis computations are performed in subsection 7.2 and their results allow to assess the obtained theoretical criterion. For completeness, due to the fact that the plastic flow rule has been formulated in an implicit form except for the pure shear loading, we will perform in subsection 7.3 the illustration of the analytical plastic flow direction (68) for such a particular case, which will be validated from the corresponding FEM solutions.

7.1. Preliminary illustration of the established criterion

We aim now at illustrating the macroscopic criterion (65) established in subsection 5.3 both in associated and non-associated cases. As mentioned before, the matrix pressure sensitivity is characterized by the friction angle ϕ and the dilatancy one ψ for the Drucker-Prager model (see Eqs.(1) and (2)). These two angles must satisfy the condition $0 \leq \psi \leq \phi < 56°18'$ (see also Eq.(5)). It is convenient to note that porosity values in geomaterials are relatively bigger comparatively to porous metals or polymers, etc.. Accordingly, in this subsection, we provide illustration of the established criterion for a porosity $f = 0.2$ and friction angle $\phi = 30°$. The corresponding associated case $\psi = \phi = 30°$ is denoted AC, while two non-associated cases are considered; they are respectively defined by dilatancy angles $\psi = 15°$ (denoted NAC1) and $\psi = 5°$ (NAC2).

As already mentioned, for hydrostatic loadings (traction and compression), the non-associated cases provide the same predictions as that of the associated one (see Guo et al. (2008); Thoré et al. (2009). Note again that this observation is in full agreement with the theoretical and numerical results already established in Cheng et al. (2012). Furthermore, unlike the previous work of Maghous et al. (2009), as mentioned in sections 4 and 5.3, the non-associated cases show in general different yield loci with respect to the associated one: as expected, the yield surface for a non associated case is lower than for the associated one. Note that a decrease of the dilatancy angle leads to a weaker strength, the difference between the cases $\psi = 15°$ and $\psi = 5°$ being slight. These results will be investigated in subsection 7.2 by means of numerical results.

To simplify the presentation here, additional results are provided in Appendix C.1 (see Figs. C.10 and C.11); they allow to illustrate the effects of porosity ($f = 0.15$, $f = 0.25$) on the macroscopic yield surfaces in the context of the non-associated plastic matrix. In the same appendix, effects of the friction angle ϕ are also provided for a porosity $f = 0.2$.

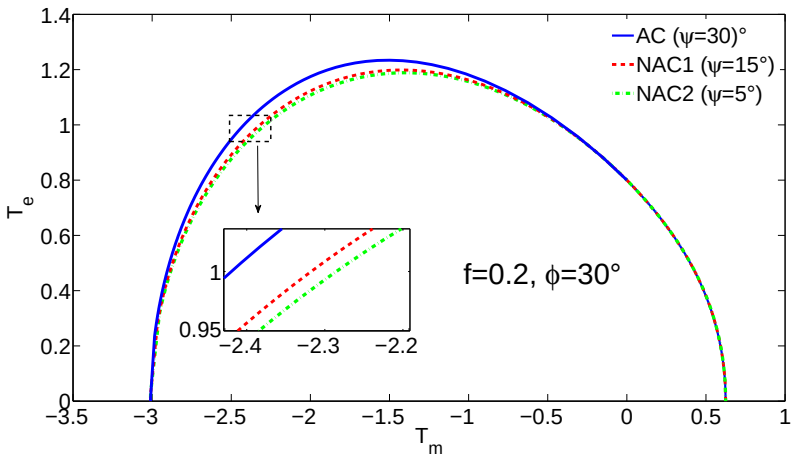

Figure 3: Comparison of yield surfaces between the associated case (denoted AC) with dilatancy angle $\psi = 30°$ and two non-associated cases (65) (denoted NAC1 and NAC2) with $\psi = 15°$ and $5°$, respectively. Porosity: $f = 0.2$; friction angle $\phi = 30°$

7.2. Numerical investigations of the macroscopic yield surface and plastic flow rule in the context of the Druker-Prager non associated matrix

In this subsection, the predictions of the established macroscopic criterion will be compared with the Finite Element Method (FEM) solutions. For the FEM analysis, we consider an axisymmetric model of the spherical shell. Hence, owing to the geometrical symmetry, only a quarter of this model is considered by adopting 1500 quadratic axisymmetric elements (see Fig.4). Moreover, the numerical analysis is carried out in the context of non-associated elastoplasticity and small deformations. The computations are performed by means of ABAQUS/Standard software and a user subroutine MPC (Multi-Points Constraints). The main reason for which we need to enforce MPC conditions in the code is that we have to impose the velocity field $\boldsymbol{v}$ from $\boldsymbol{v} = \boldsymbol{D}\cdot\boldsymbol{x}$ (on the external boundary of the hollow sphere) such that the constraint of constant macroscopic stress triaxiality ($T = \Sigma_m/\Sigma_e$) be fulfilled. In practice, as in Guo et al. (2008), this is done by applying a constant macroscopic stress ratio Σ_ρ/Σ_z corresponding to the desired Σ_m/Σ_e. Note that the implementation of this procedure has been already described by Cheng and Guo (2007) for their study of voids interaction and coalescence in an associated Drucker-Prager matrix.

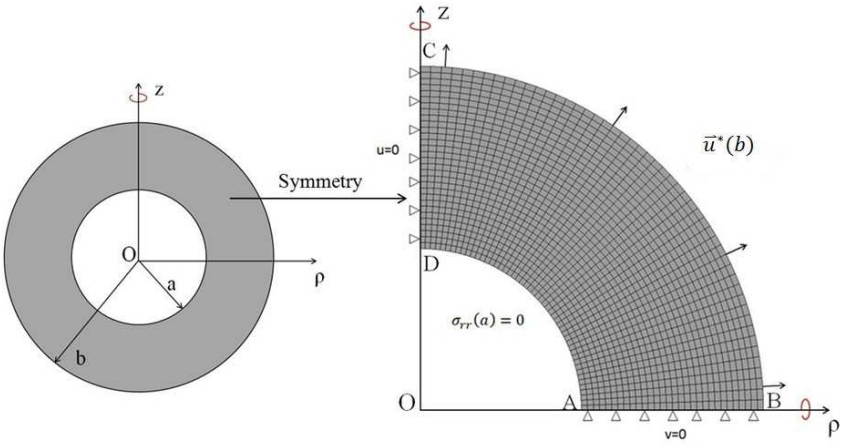

Figure 4: Hollow sphere model: Geometry of the elementary cell and boundary conditions.

Fig.5 displays the FEM results not only for the macroscopic limit stress, but also for the direction of plastic flow. As in subsection 7.1, the values of porosity $f = 0.2$ and friction angle $\phi = 30°$ are considered here. Also, the direction of plastic flow for the associated case and two non-associated cases are denoted DA($\psi = 30°$), DNA1 ($\psi = 15°$) and DNA2 ($\psi = 5°$), respectively. Moreover, the numerical yield surfaces, obtained by connecting each FEM point of plastic limit state, are indicated by SFA($\psi = 30°$), SFNA1($\psi = 15°$) and SFNA2($\psi = 5°$), respectively. Note that each FEM point has been obtained by performing computation at fixed stress triaxialities Σ_m/Σ_e (equivalently at fixed T_m/T_e).

Coming now to the results, an excellent agreement between the DA and SFA is noted (see Fig.5), the plastic flow direction (DA) at each FEM point being normal to the yield surface (SFA). Concerning the plastic flow direction (DNA1 and DNA2) for the cases of non-associated matrix, a lack of normality to the corresponding yield surfaces (SFNA1 and SFNA2) is noted. These FEM results proves the non-associated character of the macroscopic flow rule in the case of a non-associated matrix. It must be noted that the lack of normality is more pronounced when the dilatancy angle ψ is small, that is a material with a pronounced non associated matrix.

For completeness, additional results and validations are provided on Figs. 12(a), 13(a), 14(a) and 15(a) in Appendix C.2. This allows to illustrate the effects of the porosity and friction angle.

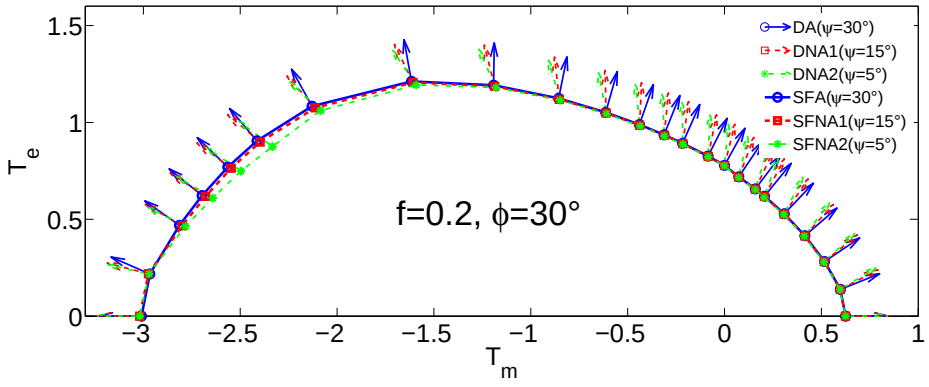

Figure 5: Illustration of FEM results: plastic flow directions (denoted DA for associated case, DNA1 and DNA2 for non-associated ones) and yield surface (denoted SFA for associated case, SFNA1 and SFNA2 for non-associated ones).

7.3. Validations of the established criterion and of the corresponding flow rule

For validation purpose, the analytical yield surfaces for the associated case (AC) as well as the non-associated ones (NAC1 and NAC2) are compared with the corresponding numerical limit stresses on Fig. 6. The FEM results confirm that the limit stresses of non-associated cases (denoted FNAC1 and FNAC2) and the associated one (denote FAC) are very close in the vicinity of traction dominant region $T_m > 0$ (or $\Sigma_m > 0$). In contrary, a slight difference is observed in a part of the compression dominate region $T_m < 0$ (or $\Sigma_m < 0$). The above numerical results validate the predictive capabilities of the analytical criterion.

Let us recall that other validating results showing also the influences of the porosity and friction angle are provided on Fig. 12(b), 13(b), 14(b) and 15(b) in Appendix C.2.

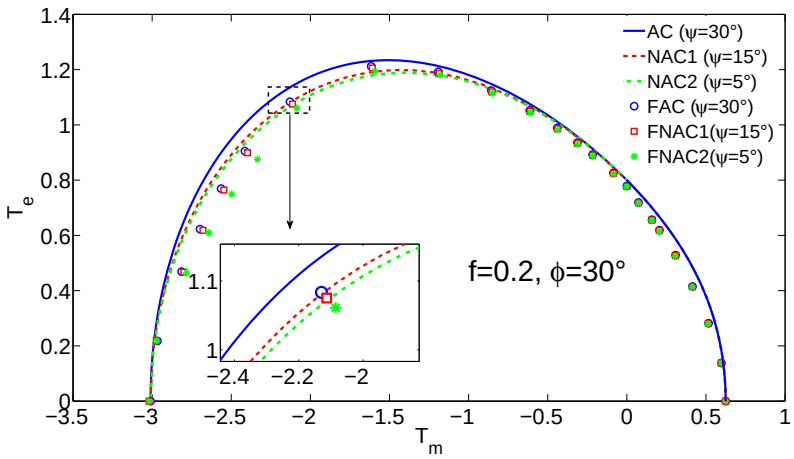

Figure 6: Comparison between the yield surfaces obtained from the established criteria (65) and FEM results (denoted FAC for associated case, FAC1 and FAC2 for non-associated ones).

Concerning the assessment of the obtained macroscopic flow rule (see Eq. (68)). We display on Fig.7 the plastic direction obtained from the analytical function (69) and that numerically computed from the FEM computation. Both of these results are illustrated with respect to the different values of macroscopic stress triaxiality T_m/T_e. The illustrations have been realized for $f = 0.2$ and $\phi = 30°$, $\psi = 30°$, $\psi = 15°$ and $\psi = 5°$. Noticeable difference between the associated case and the non associated ones is obtained, both for the analytical results and for the numerical data. Moreover, for any fixed value of triaxiality, the obtained value of $\mathrm{acot}(D_m/D_e)$ representing the plastic flow direction is smaller when the dilatancy angle ψ diminishes. Finally, very good qualitative agreement is observed between the theoretical predictions and the corresponding numerical data.

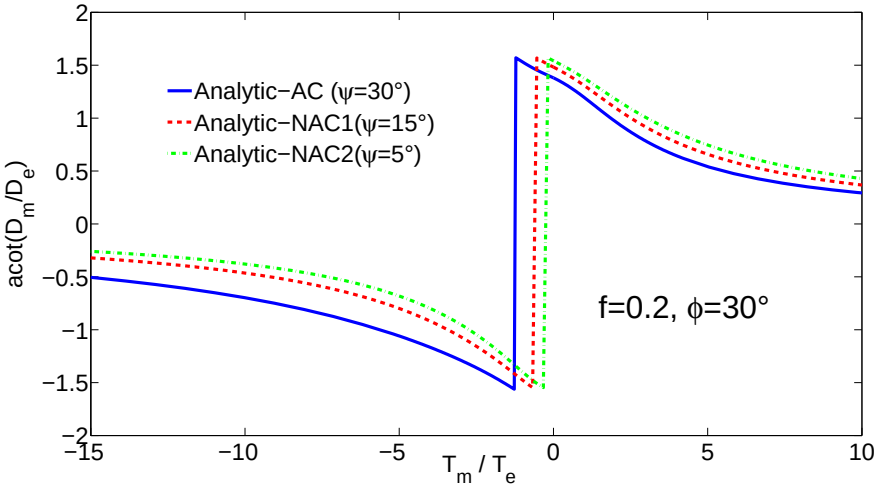

(a) Analytic

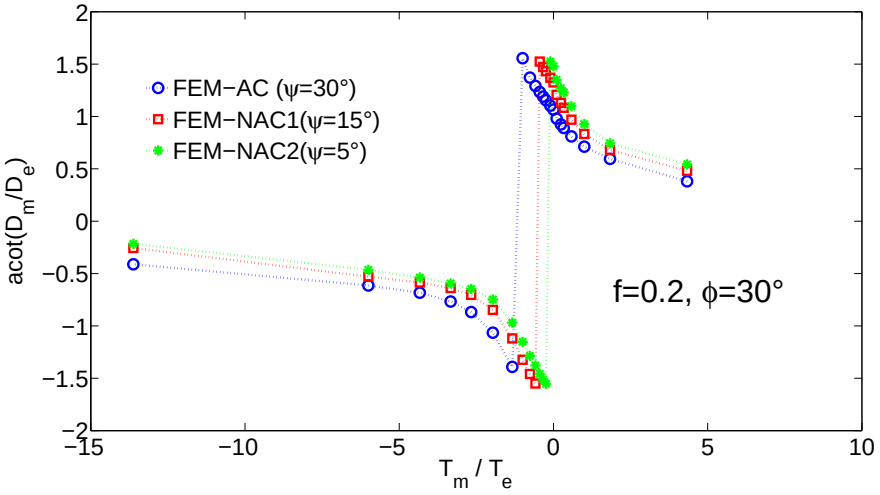

(b) FEM

Figure 7: Analytical result and FEM solutions for plastic flow direction with the fixed values of porosity $f = 0.2$ and friction angle $\phi = 30°$.

At the difference of porous media with an incompressible plastic matrix (Gurson, 1977), void growth (see Eq. (71)) occurs under macroscopic pure shear loading in the case of a pressure-sensitive matrix (as considered in the present work). For this particular shear loading, Eq.(74) indicates that the plastic flow is only influenced by the dilatancy parameter β, but not by the friction one α. Still for the pure shear, we perform on Fig.8 a comparison of the plastic flow direction given by the analytical solution (74) and the FEM computations. The following values of fixed material parameters, $f = 0.2$ and $\phi = 30°$, are considered. An excellent agreement between the analytic and FEM results is obtained.

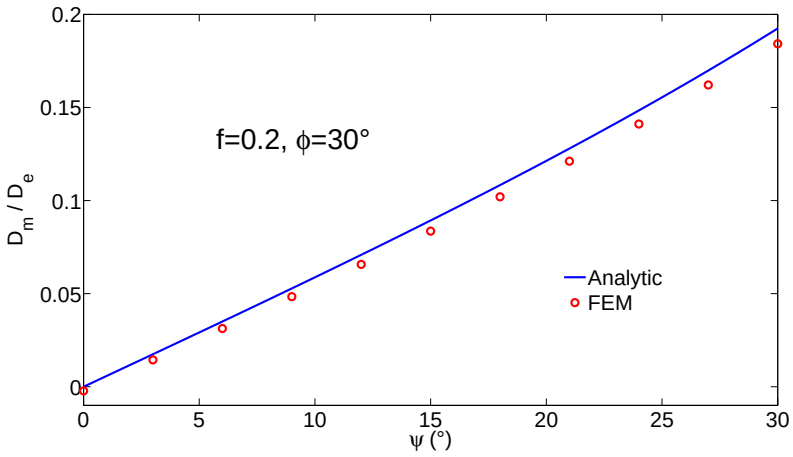

Figure 8: Comparison of plastic flow direction for pure shear loading case obtained from Eq.(68) and FEM solutions with the fixed values of porosity $f = 0.2$ and friction angle $\phi = 30°$.

Finally, Fig. 9 illustrates the variation of porosity with the macroscopic stress triaxiality for a initial porosity $f = 0.2$, a fixed value of friction angle $\phi = 30°$ and for three dilatancy angles $\psi = 30°$, $\psi = 15°$ and $\psi = 5°$. Noticeable difference between the associated case and non-associated ones is observed, particularly for high stress triaxialities.

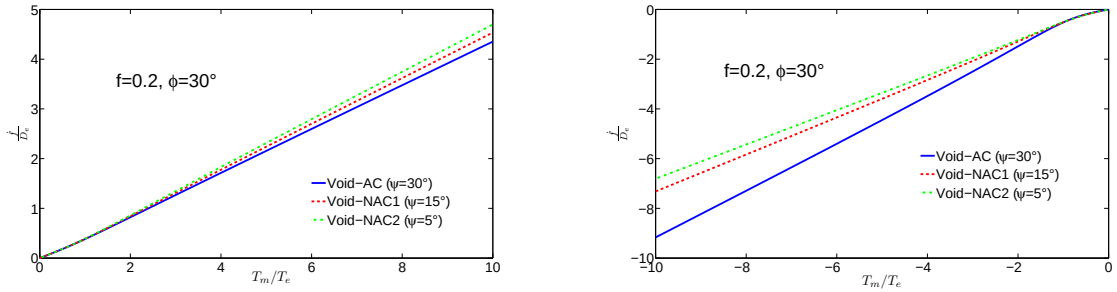

(a) Variation with positive triaxialities

(b) Variation with negative triaxialities

Figure 9: Analytical result of the plastic void growth with a initial value of porosity $f = 0.2$. Friction angle $\phi = 30°$.

8. Conclusion

In this study, a bipotential-based variational framework of ductile porous media has been proposed. It allowed to extend classical limit analysis of porous media to the context of a matrix obeying to a non-associated flow rule. This is generally the case of various porous geomaterials or porous polymers displaying also pressure-sensitivity of the matrix. The proposed variational formulation combines the bipotential theory earlier introduced by de Saxcé et al. (1991) with homogenization techniques. It delivers closed-form expression of the macroscopic criterion for the porous materials, as well as the non-associated flow rule.

As detailed in Section 4, application of the proposed approach to porous materials with non associated plastic matrix (characterized by a friction angle and a dilatancy angle) has led to the formulation of a macroscopic bifunctional. Minimization procedures of the bifunctional have been proposed with respect to a trial kinematically admissible velocity fields (respectively the statically admissible stress fields). This can deliver for the considered class of porous materials an upper bound (respectively lower bound) provided that the exact stress field (respectively the exact velocity field) has been adopted.

Practical implementation of the approach has been done by considering a hollow sphere subjected to uniform strain rate boundary conditions. To this end, a choice of a simple stress field together with a class of trial velocity fields has been made. The whole procedure has allowed to establish a closed form expression of the macroscopic yield function (see equations (65)), as well as the macroscopic flow rule (see equations (68)), in a parametric form. The non-associated character of the matrix (dilatancy angle) affects not only the macroscopic yield surface, but also the macroscopic flow rule which is shown to be non associated. Moreover, due to the suitable choice of the trial fields, the model also preserves the exact solution established in Cheng et al. (2012) for the hollow sphere with the non associated matrix, under pure hydrostatic loadings. It is also worth noticing that the obtained results allow to retrieve (as a particular case) the kinematically-based model proposed by (Guo et al., 2008) for the porous material with an associated Drucker-Prager matrix. This automatically includes the Gurson model for a von Mises matrix (Gurson, 1977). The predictions of the general model are fully assessed, both for the macroscopic yield surfaces and for the flow rule. To this end, numerous Finite Elements computations in non associated plasticity have been carried out on the hollow sphere. A good agreement has been observed between theoretical results and numerical data for various configurations of porosity, friction angle and dilatancy angle.

Finally, it should be noted that some improvements of the basic model are possible, in particular by searching more refined trial velocity and stress fields. The consideration of voids saturation by an internal pressure will also constitute a challenging extension which will pave the way for various applications in geomechanics including non associated poroplasticity.

References

Barthélémy, J.F., Dormieux, L., 2003. Détermination du critère de rupture macroscopique d'un milieux poreux par homogénéisation non linéaire. Comptes Rendus Mécanique, 331, 271-276.

Benzerga, A.A., Besson, J., 2001. Plastic potentials for anisotropic porous solids. European Journal of Mechanics A/Solids, 20, 397-434.

Berga, A., de Saxcé, G., 1994. Elastoplastic Finite Element Analysis of Soil Problems with Implicit Standard Material Constitutive Laws, Revue Européenne des éléments finis, 3, 411-456.

Bodovillé, G., 1999. On damage and implicit standard materials, C. R. Acad. Sci. Paris, Sér. II, Fasc. b, Méc. Phys. Astron., 327, 715-720.

Bodovillé, G., de Saxcé, G., 2001. Plasticity with non linear kinematic hardening : modelling and shakedown analysis by the bipotential approach. Eur. J. Mech., A/Solids, 20, 99-112.

Bouby, C., de Saxcé, G., Tritsch, 2006. A comparison between analytical calculations of the shakedown load by the bipotentiel approach and step-by-step computations for elastoplastic materials with nonlinear kinematic hardening. International Journal of Solids and Structures, 43(9), 2670-2692.

Bouby, C., de Saxcé, G., Tritsch, 2009. Shakedown analysis: comparison between models with the linear unlimited, linear limited and non linear kinematic hardening. Mechanical Research Communication, 36, 556562.

Bousshine, L., Chaaba, A., de Saxcé, G., 2001. Softening in stress-strain curve for Drucker-Prager non-associated plasticity. Int. J. of Plasticity, 17(1), 21-46.

Bousshine, L., Chaaba, A., de Saxcé, G., 2002. Plastic limit load of plane frames with frictional contact supports. Int. J. Mech. Sci., 44, 2189-2216, 2002.

Bousshine, L., Chaaba, A., de Saxcé, G., 2003. A new approach to shakedown analysis for non-standard elastoplastic material by the bipotential. Int. J. of Plasticity, 19(5), 583-598.

Buliga, M., de Saxcé, G. Vallée, C., 2008. Existence and construction of bipotential for graphs of multivalued laws. Journal of Convex Analysis. J. Convex Analysis, 15(1), 87-104.

Buliga, M., de Saxcé, G. Vallée, C., 2009. Bipotentials for non monotone multivalued operators: fundamental results and applications. Acta Applicandae Mathematicae, 110(2), 955-972.

Buliga, M., de Saxcé, G. Vallée, C., 2009. Blurred constitutive laws and bipotential convex covers. Mathematics and Mechanics of Solid Journal. First on line.

Buliga, M., de Saxcé, G. Vallée, C., 2010. Non maximal cyclically monotone graphs and construction of a bipotential for the Coulomb's dry friction law. J. Convex Analysis, 17(1), 81-94.

Buliga, M., de Saxcé, G. Vallée, C., 2010. Blurred maximal cyclically monotone sets and bipotentials. Analysis and Applications, 8(4), 323-336.

O. Cazacu and J. B. Stewart. Plastic potentials for porous aggregates with the matrix exhibiting tension-compression asymmetry. Journal of the Mechanics and Physics of Solids, 57 : 325-341, 2009.

Chaaba, A., Bousshine, L., de Saxcé, G., 2010. Kinematic Limit Analysis of Nonassociated Perfectly Plastic Material by the Bipotential Approach and Finite Element Method. J. Appl. Mech., 77(3), 031016.

Chen, W.F., 1975. Limit Analysis and Soil Plasticity. Elsevier, New York.

Chen, W.F., Liu, X.L., 1990. Limit analysis in soil mechanics. Developments in Geotechnical Engineering, Vol. 52.

Cheng, L., Jia, Y., Oueslati, A., de Saxcé, G, Kondo, D., 2012 Plastic limit state of the hollow sphere model with non-associated Drucker-Prager material under isotropic loading. Computational Materials Science, Vol. 62, 210-215.

Cheng, L., de Saxcé, G, Kondo, D.. A stress-based variational model for ductile porous materials. Vol. 55, 133-151.

Cheng, L. Homogenization of porous media with plastic matrix and non-associated flow rule by variational methods. Ph.D. Thesis, Univ. Lille 1, 2013.

Cheng, L., Guo, T.F., 2006. Void interaction and coalescence in polymeric materials. International Journal of Solids and Structures, 44, 1787-1808.

de Buhan, P. A fundamental approach to the yield design of reinforced soil structures Chap. 2: yield design homogenization theory for periodic media, Ph.D. Thesis, Univ. Pierre et Marie Curie, Paris VI, 1986.

de Saxcé, G., Feng, Z.Q., 1991. New inequality and functional for contact friction: The implicit standard material approach. Mechanics of Structures and Machines, 19, 301-325, 1991.

de Saxcé, G., 1992. Une généralisation de l'inégalité de Fenchel et ses applications aux lois constitutives. C. R. Acad. Sci. Paris, Sér. II, 314, 125-129, 1992.

de Saxcé, G., Bousshine, L., 1993. On the extension of limit analysis theorems to the non-associated flow rules in soils and to the contact with Coulomb's friction. XI Polish Conference on Computer Methods in Mechanics. Kielce, Poland, 815-822.

de Saxcé, G., 1995. The bipotential method, a new variational and numerical treatment of the dissipative laws of materials. 10th Int. Conf. on Mathematical and Computer Modelling and Scientific Computing, Boston, Massachusetts.

de Saxcé, G., Bousshine, L., 1998. Limit Analysis Theorems for the Implicit Standard Materials: Application

to the Unilateral Contact with Dry Friction and the Non Associated Flow Rules in Soils and Rocks. Int. J. Mech. Sci., 40(4),387-398.

de Saxcé, G., Feng, Z.Q., 1998. The bi-potential method: a constructive approach to design the complete contact law with friction and improved numerical algorithms. Mathematical and Computer Modelling, 6, 225-245, 1998.

de Saxcé, G., Bousshine, L., 2002. Implicit standard materials. D. Weichert G. Maier eds. Inelastic behaviour of structures under variable repeated loads, CISM Courses and Lectures 432, Springer, Wien.

de Saxcé, G., Fortin, J., Millet, O. 2004. About the numerical simulation of the dynamics of granular media and the definition of the mean stress tensor. Mechanics of Materials, 36, 1175-1184.

Drucker, D.C. 1953. Limit analysis of two - and three - dimensional soil mechanics problems. J. Mech. Phys.Solids. 1, 217-226.

I. Ekeland, I., Temam, R., 1975. Convex analysis and variational problems, Amsterdam, North Holland.

Fenchel, W., 1949. On conjugate convex functions. Canadian Journal of Mathematics, 1, 73-77.

Feng, Z.Q., Hjiaj, M., de Saxcé, G., Mróz, Z., 2006. Effect of frictional anisotropy on the quasistatic motion of a deformable solid sliding on a planar surface. Comput. Mech., 37, 349-361.

Feng, Z.Q., Hjiaj, M., de Saxcé, G., Mróz, Z., 2006. Influence of frictional anisotropy on contacting surfaces during loading/unloading cycles. International Journal of Non-Linear Mechanics, 41(8), 936-948.

Fine, N.J., 1988. Basic Hypergeometric Series and Applications. Amer. Math. Soc., Providence, RI.

Fortin, J., de Saxcé, G., 1999. Modlisation numrique des milieux granulaires par lapproche du bipotentiel. C.R. de lAcadmie des Sciences, Srie IIb, 327, 721-724.

Fortin, J., Hjiaj, M., de Saxcé, G., 2002. An improved discrete element method based on a variational formulation of the frictional contact law. Comput. Geotech., 29, 609-640.

Garajeu, M., Suquet, P., 1997. Effective properties of porous ideally plastic or viscoplastic materials containing rigid particles. Journal of the Mechanics and Physics of Solids, 45, 873-902.

Gologanu, M., Leblond, J.B., Perrin, G., Devaux, J., 1997. Recent extensions of Gurson's model for porous ductile metals. P. Suquet (Ed.), Continuum Micromechanics, Springer-Verlag.

Guo, T.F., Faleskog, J., Shih, C.F.2008. Continuum modeling of a porous solid with pressure-sensitive dilatant matrix. Journal of the Mechanics and Physics of Solids, 56, 2188-2212.

Gurson, A.L., 1977. Continuum theory of ductile rupture by void nucleation and growth – part I: Yield criteria and flow rules for porous ductile media, Journal of Engineering Materials and Technology, 99, 2-15.

Halphen, B., Nguyen Quoc, S., 1975. Sur les matériaux standard généralisés. C. R. Acad. Sci. Paris, 14, 39-63.

Hjiaj, M., Bodovillé, G., de Saxcé, G., 2000. Matériaux viscoplastiques et loi de normalité implicites. C. R. Acad. Sci. Paris, Sér. II, Fasc. b, Méc. Phys. Astron., 328, 519-524.

Hjiaj, M., de Saxcé, G., Mróz, Z., 2002. A variational-inequality based formulation of the frictional contact law with a non-associated sliding rule. European Journal of Mechanics A/Solids, 21, 49-59.

Hjiaj, M., Fortin, J., de Saxcé, G., 2003. A complete stress update algorithm for the non-associated Drucker-Prager model including treatment of the apex. International Journal of Engineering Science, 41, 1109-1143.

Hjiaj, M., Feng, Z.Q., de Saxcé, G., Mróz, Z., 2004. Three dimensional finite element computations for frictional contact problems with on-associated sliding rule. Int. J. Numer. Methods Eng., 60, 2045-2076.

Jeong, H.Y., Pan, J., 1995. A macroscopic constitutive law for porous solids with pressure-sensitive matrices and its applications to plastic flow localization. Journal of the Mechanics and Physics of Solids, 39, 1385-1403.

Jeong, H.Y., 2002. A new yield function and a hydrostatic stress-controlled model for porous solids with pressure-sensitive matrices. Journal of the Mechanics and Physics of Solids, 32, 3669-3691.

Keralavarma, S.M., Benzerga, A.A. 2010. A constitutive model for plastically anisotropic solids with non-spherical voids. Journal of the Mechanics and Physics of Solids, 58, 874-901.

Laborde, P., Renard, Y., 2008. Fixed points strategies for elastostatic frictional contact problems. Math. Meth. Appl. Sci., 31, 415-441.

Ladevèze, P., 1975. Comparaisons de modèles de milieux continus, Thèse d'Etat, Université Pierre et Marie

Curie, Paris.
Ladevèze, P., Coffignal, G., Pelle, J.P., 1986. Accuracy of elastoplastic and dynamic analysis. in: I. Babuska, J. Gago, E. Oliveira and O.C. Zienkiewicz, eds., Accuracy Estimates and Adaptative Refinements in Finite Element Computations, John Wiley, 181-203.
Ladevèze, P., Pelle, J.P., Rougeot, P., 1991. Error estimation and mesh optimization for classical finite element. Engrg. Comput. 8, 69-80.
Ladevèze, P., Moes, N., 1997. A new a posteriori error estimation for nonlinear time-dependent finite element analysis. Comput. Methods. Appl. Mech. Engrg., 157, 45-68.
Ladevèze, P., Pelle, J.P., 2001. La maîtrise du calcul en mécanique linéaire et non linéaire. Hermes Science.
Ladevèze, P., Florentin, E., 2006. Verification of stochastic models in uncertain environments using the constitutive relation error method. Comput. Methods. Appl. Mech. Engrg., 196, 225-224.
Ladevèze, P., Puel, G., Deraemaeker, A., Romeuf, T., 2006. Validation of structural dynamics models containing uncertainties. Comput. Methods. Appl. Mech. Engrg., 195, 373-393.
J. Lin, J.-F. Shao, D. Kondo, 2011. A two scale model of porous rocks with DruckerPrager matrix: Application to a sandstone. Mechanics Research Communications 38 (2011) 602 606
J. Lin, S.Y. Xie, J.F. Shao and D. Kondo. A micromechanical modeling of ductile behavior of a porous chalk: Formulation, identification, and validation. International Journal for Numerical and Analytical Methods in Geomechanics. 36, (2012) 1245-1263.
Madou, K., Leblond, J.B., 2012. A Gurson-type criterion for porous ductile solids containing arbitrary ellipsoidal voids I: Limit-analysis of some representative cell. Journal of the Mechanics and Physics of Solids, 60, 1020-1036.
Madou, K., Leblond, J.B., 2012. A Gurson-type criterion for porous ductile solids containing arbitrary ellipsoidal voids II: Determination of yield criterion parameters. Journal of the Mechanics and Physics of Solids, 60, 1037-1058.
Maghous, S., Dormieux, L., Barthélémy, J.F., 2009. Micromechanical approach to the strength propoerties of frictional geomaterials. European Journal of Mechanics A/Solids, 28, 179-188.
Magnier, V., Charkaluk, E., Bouby, C., de Saxcé, G., 2006. Bipotential Versus Return Mapping Algorithms: Implementation of Non-Associated Flow Rules, in Proceedings of The Eighth International Conference on Computational Structures Technology (las Palmas de Gran Canaria, sept. 12-15, 2006), B.H.V. Topping, G. Montero and R. Montenegro, (Editors), Civil-Comp Press, Stirlingshire, United Kingdom, paper 68.
Monchiet, V., Charkaluk, E., Kondo, D., 2007. An improvment of Gurson-type models of porous materials by Eshelby-like trial velocity fields. Comptes Rendus Mécanique, 335, 32-41.
Monchiet, V., Cazacu, O., Kondo, D., 2008. Macroscopic yield criteria for plastic anisotropic materials containing spheroidal voids. International Journal of Plasticity, 24, 1158-1189.
Monchiet, V., Kondo, D., 2013. Combined voids size and shape effects on the macroscopic criterion of ductile nanoporous materials. International Journal of Plasticity, 43, 20-41.
Moreau, J.J.,2003. Fonctionnelles convexes. Istituto Poligrafico e Zecca dello Stato, Rome.
Parmer, A.C., 1973. Proceedings of the Symposium on the Role of Plasticity in Soil Mechanics. Cambridge University, Cambridge, England, 314 pp.
Ponte Castaneda, P., 1991. The effective mechanical properties of nonlinear isotropic composites. J. Mech. Phys. Solids, 39, 45-71.
Radenkovic, D., 1961. Limit analysis theorems for a Coulomb material with a non standard dilatation. C. R. Acad. Sci. Paris, 252, 4103-4104.
Rockafellar, R.T., 1970. Convex Analysis, Princeton University Press, Princeton.
Salenon, Calcul la rupture et analyse limite, Presses de lENPC, 1983.
Save, M.A., Massonnet, C.E., de Saxcé, G., 1997. Plastic limit analysis of plates, shells and disks. Elsevier, New York.
Shen, W.Q., Shao,J-F, Kondo, D., Gatmiri, B., 2012. A micromacro model for clayey rocks with a plastic compressible porous matrix. International Journal of Plasticity, 36, 64-85.
Suquet, P. Plasticité et homogénéisation. Ph.D. Thesis, Univ. Pierre et Marie Curie, Paris VI, 1982.
Suquet, P., 1995. Overall properties of nonlinear composites: a modified secant moduli approach and its

link with Ponte Castaneda's nonlinear variational procedure. C. R. Acad. Sc. Paris, IIb, 320, 563-571.
Telega, J.J., 2002. Extremum principles for nonpotential and initial-value problems. Arch. Mech., 54, 565-592.
Telega, J.J., Mohammed, H., Sloan, S.W., 2004. An of Limit Analysis Theorems to Incompressible Material with a Non-Associated Flow Rule. Complementarity, Duality and Symmetry in Nonlinear Mechanics, Advances in Mechanics and Mathematics Volume 6, pp 255-275
Thoré, P., Pastor, F., Pastor, J., Kondo, D., 2009. Closed-form solutions for the hollow sphere model with Coulomb and Drucker-Prager materials under isotropic loadings. Comptes Rendus Mécanique, 337, 260-267.
Vallée, C., Lerintiu, C., Fortuné, D., Ban, M., de Saxcé, G., 2005. Hill's bipotential. M. Mihailescu-Suliciu eds. New Trends in Continuum Mechanics, Theta Series in Advanced Mathematics, Theta Foundation, Bucarest, Roumania, 339-351.
Boulbibane, M., Weichert, D., 1997. Application of shakedown theory to soils with non-associated flow rules. Mechanics Research Communications. 24, 513-519.
Zouain, N., Pontes Filho, I., Borges, L., Mouta da Costa, L., 2007. Plastic collapse in non-associated hardening materials with application to Cam-clay. International Journal of Solids and Structures, 44, 4382-4398.
Zouain, N., Pontes Filho, I., Vaunat, J., 2010. Potentials for the modified Cam-Clay model. European Journal of Mechanics − A/Solids, 29, 327-336.

Appendix A. Explicit expressions of Π, $\hat{\Pi}$ and the derivatives $\Pi_{,C_0}$, $\Pi_{,D_e}$, $\hat{\Pi}_{,C_0}$, $\hat{\Pi}_{,D_e}$

In order to explicitly express the closed-form macroscopic criterion (65), we provide as follows the expressions of Π and $\hat{\Pi}$ and their partial derivatives with respect to C_0 and D_e.

Eqs. (54) for $\Pi(\boldsymbol{v})$ and (58) for $I(\gamma)$ simultaneously contain the term $K(\xi)$, which is smooth over the compactly supported domain with extreme values $K_{max} = K(0) = 1$ and $K_{min} = K(-1) = 0.962$. Following (Gurson, 1977), this function is taken to be unity for simplicity of calculation; that reduces (54) and (58) to:

$$\Pi(\boldsymbol{v}) = D_e \int_f^1 \sqrt{1 + \tau^2 x^{-2/\tilde{s}}}\, dx \ , \tag{A.1}$$

$$I(\gamma) = D_e \int_f^1 x^{-\gamma} \sqrt{1 + \tau^2 x^{-2/\tilde{s}}}\, dx \ . \tag{A.2}$$

Additionally, Eqs.(A.1), (A.2) and the derivatives $\Pi_{,C_0}$, $\Pi_{,D_e}$, $\hat{\Pi}_{,C_0}$ and $\hat{\Pi}_{,D_e}$ can not be calculated into simple forms. Fortunately, they can be expressed by means of the Gauss hypergeometric function (see for example Fine (1988)) defined by:

$${}_2F_1\,(a, b; c; z) = \frac{\Gamma(c)}{\Gamma(b)\Gamma(c-b)} \int_0^1 \frac{t^{b-1}(1-t)^{c-b-1}}{(1-tz)^a} dt$$

This function is a solution of the hypergeometric differential equation

$$z(1-z)y'' + [c - (a+b+1)z]\, y' - aby = 0$$

The regular solution is classically written in the form of the following power series

$$ {}_2F_1\left(a,b;c;z\right)=\sum_{n=0}^{\infty}\frac{(a)_n(b)_n}{(c)_n}\frac{z^n}{n!}\ , \tag{A.3} $$

where $(a)_n$ *is the Pochhammer symbol defined by*

$$ (a)_n=\frac{\Gamma(a+n)}{\Gamma(a)}=a(a+1)...(a+n-1) $$

.

Let us introduce that

$$ \iota=\frac{\tau}{f^{1/\tilde{s}}} $$

Π and I (Eqs. (A.1) and (A.2)) can be indirectly expressed as follows:

$$ \mathcal{P}=\frac{\Pi}{D_e}={}_2F_1\left(-\frac{1}{2},-\frac{\tilde{s}}{2};1-\frac{\tilde{s}}{2};-\tau^2\right)-f\cdot{}_2F_1\left(-\frac{1}{2},-\frac{\tilde{s}}{2};1-\frac{\tilde{s}}{2};-\iota^2\right) \tag{A.4} $$

$$ \begin{aligned}\mathcal{Q}=\frac{I}{D_e}=&s^{-1}\left[{}_2F_1\left(-\frac{1}{2},-\frac{\tilde{s}s^{-1}}{2};1--\frac{\tilde{s}s^{-1}}{2};-\tau^2\right)\right.\\&\left.-f^{s^{-1}}\cdot{}_2F_1\left(-\frac{1}{2},-\frac{\tilde{s}s^{-1}}{2};1--\frac{\tilde{s}s^{-1}}{2};-\iota^2\right)\right]\end{aligned} \tag{A.5} $$

Finally, considering (A.1), (A.2) and (57), the derivatives $\Pi_{,C_0}$, $\Pi_{,D_e}$, $\hat{\Pi}_{,C_0}$ and $\hat{\Pi}_{,D_e}$ can be also computed as follows:

$$ \Pi_{,C_0}=\frac{\tau}{\frac{\tilde{s}}{2}-1}\left[{}_2F_1\left(\frac{1}{2},1-\frac{\tilde{s}}{2};2-\frac{\tilde{s}}{2};-\tau^2\right)-f^{1-2/\tilde{s}}\cdot{}_2F_1\left(\frac{1}{2},1-\frac{\tilde{s}}{2};2-\frac{\tilde{s}}{2};-\iota^2\right)\right] \tag{A.6} $$

$$ \Pi_{,D_e}={}_2F_1\left(\frac{1}{2},-\frac{\tilde{s}}{2};1-\frac{\tilde{s}}{2};-\tau^2\right)-f\cdot{}_2F_1\left(\frac{1}{2},-\frac{\tilde{s}}{2};1-\frac{\tilde{s}}{2};-\iota^2\right)\ , \tag{A.7} $$

$$ \hat{\Pi}_{,C_0}=\Pi_{,C_0}+\frac{3\alpha T_m}{1-f^{\gamma}}\cdot\left(\frac{f^{\gamma}}{s}\cdot I_{,C_0}-\Pi_{,C_0}\right) \tag{A.8} $$

$$ \hat{\Pi}_{,D_e}=\Pi_{,D_e}+\frac{3\alpha T_m}{1-f^{\gamma}}\cdot\left(\frac{f^{\gamma}}{s}\cdot I_{,D_e}-\Pi_{,D_e}\right) \tag{A.9} $$

where $I_{,C_0}$ and $I_{,D_e}$ have the following expressions

$$ \begin{aligned}I_{,C_0}=\frac{2\tau}{\tilde{s}\left(\frac{1}{s}-\frac{2}{\tilde{s}}\right)}\cdot&\left[{}_2F_1\left(\frac{1}{2},-\frac{\tilde{s}}{2}\left(\frac{1}{s}-\frac{2}{\tilde{s}}\right);1-\frac{\tilde{s}}{2}\left(\frac{1}{s}-\frac{2}{\tilde{s}}\right);-\tau^2\right)\right.\\&\left.-f^{\frac{1}{s}-\frac{2}{\tilde{s}}}\cdot{}_2F_1\left(\frac{1}{2},-\frac{\tilde{s}}{2}\left(\frac{1}{s}-\frac{2}{\tilde{s}}\right);1-\frac{\tilde{s}}{2}\left(\frac{1}{s}-\frac{2}{\tilde{s}}\right);-\iota^2\right)\right]\end{aligned} \tag{A.10} $$

$$ I_{,D_e}=s\cdot\left[{}_2F_1\left(\frac{1}{2},-\frac{\tilde{s}}{2s};1-\frac{\tilde{s}}{2s};-\tau^2\right)-f^{\frac{1}{s}}\cdot{}_2F_1\left(\frac{1}{2},-\frac{\tilde{s}}{2s};1-\frac{\tilde{s}}{2s};-\iota^2\right)\right] \tag{A.11} $$

Appendix B. Macroscopic criterion of ductile porous media with an associated Drucker-Prager matrix

We apply here the general procedure proposed in sections 4 and 5 to the particular case of the associated Drucker-Prager matrix ($\psi = \phi \neq 0$ and $\beta = \alpha \neq 0$). This is the case already studied by Guo et al. (2008) by using the classical kinematical limit analysis approach which is retrieve here from the proposed variational formulation.
In this case, the associated flow rule reads:

$$\mathbf{d} = d_{eq}\frac{\partial F}{\partial \sigma} = d_{eq}\left(\frac{3\boldsymbol{s}}{2\sigma_e} + \alpha\mathbf{1}\right), \tag{B.1}$$

The volumetric plastic strain is such that:

$$d_m = \frac{1}{3}tr\mathbf{d} = \alpha d_{eq} \tag{B.2}$$

The plastic flow rule (B.1) is completed at the apex by the condition:

$$H(\mathbf{d}) = \alpha d_{eq} - d_m \leq 0 \tag{B.3}$$

The finite valued bipotential is reduced into:

$$b(\boldsymbol{d}, \boldsymbol{\sigma}) = \left\{ \begin{array}{ll} \frac{\sigma_0}{\alpha} d_m & \text{if} \quad F(\boldsymbol{\sigma}) \leq 0 \quad and \quad H(\boldsymbol{d}) \leq 0 \\ +\infty & \text{otherwise} \end{array} \right\}, \tag{B.4}$$

It should be emphasized that the bipotential in this case takes the same expression as the support function for the associated Drucker-Prager model (see for instance by Salençon (1983)). Moreover, considering the velocity field (42) in the case of associated matrix (see Guo et al. (2008))

$$\boldsymbol{v} = C_0\left(\frac{b}{r}\right)^{3/s}(\rho\boldsymbol{e}_\rho + z\boldsymbol{e}_z) + C_1\rho\boldsymbol{e}_\rho + C_2 z\boldsymbol{e}_z\ , \tag{B.5}$$

the microscopic mean strain rate (46) and the equivalent one (47) can be recast into:

$$d_m(r) = \left(1 - \frac{1}{s}\right)C_0\left(\frac{b}{r}\right)^{3/s} + \frac{1}{3}(2C_1 + C_2) \tag{B.6}$$

and

$$d_{eq}(r) = \frac{2}{3}\sqrt{(C_1 - C_2)^2 + (C_1 - C_2)\frac{3C_0}{s}\left(\frac{b}{r}\right)^{3/s}(3\cos^2\theta - 1) + \left(\frac{3C_0}{s}\right)^2\left(\frac{b}{r}\right)^{6/s}} \tag{B.7}$$

which obviously do not comply with (B.3) everywhere in the hollow sphere.
Due to this difficulty, the idea is to relax the admissibility condition in an average sense by imposing

$$\int_{\Omega_M} H(d)\ dV\ = \int_{\Omega_M}(\alpha d_{eq} - d_m)dV = 0 \tag{B.8}$$

Next, by introducing (B.6) and (B.4) into (24), the macroscopic bifunctional in the case of an associated matrix can be written as:

$$B_0(\boldsymbol{v},\boldsymbol{\sigma}) = \frac{1}{\mid \Omega \mid}\int_{\Omega_M}\frac{\sigma_0}{\alpha}d_m dV - \boldsymbol{D}:\boldsymbol{\Sigma}\ . \tag{B.9}$$

with the relaxed admissibility constraint (B.8): $\int_{\Omega_M} d_m dV = \int_{\Omega_M} \alpha d_{eq} dV$.
For the first minimization problem of (25), as for the non associated case, it is suggested to introduce the normalized Lagrangian $\bar{\mathcal{L}}$ by omitting σ_0 (or taking it equal to 1), with $\bar{\Lambda}$ the Lagrange multiplier which is assumed constant:

$$\bar{\mathcal{L}} = \frac{1}{\mid \Omega \mid}\int_{\Omega_m}\frac{d_m}{\alpha}dV - \mathbf{T}:\mathbf{D} + \bar{\Lambda}[\int_{\Omega_M}(\alpha d_{eq} - d_m)dV] \tag{B.10}$$

Putting (B.6) and (B.7) into (B.10) leads to:

$$\bar{L} = \alpha\bar{\Lambda}\Pi + (\frac{1}{\alpha} - \bar{\Lambda})[(1-f)D_m - (f^\gamma - f)C_0] - (3T_m D_m + T_e D_e) \tag{B.11}$$

The following minimization relations are obtained:

$$\begin{cases} \frac{\partial \bar{L}}{\partial C_0} = \alpha\bar{\Lambda}\frac{\partial \Pi}{\partial C_0} - (\frac{1}{\alpha} - \bar{\Lambda})(f^\gamma - f) = 0 \\ \\ \frac{\partial \bar{L}}{\partial D_m} = (\frac{1}{\alpha} - \bar{\Lambda})(1-f) - 3T_m = 0 \\ \\ \frac{\partial \bar{L}}{\partial D_e} = \alpha\bar{\Lambda}\frac{\partial \Pi}{\partial D_e} - T_e = 0 \end{cases} \tag{B.12}$$

The first equation of (B.12) delivers the optimal expression of $\bar{\Lambda}$

$$\bar{\Lambda} = \frac{\frac{1}{\alpha}(f^\gamma - f)}{f^\gamma - f + \alpha\frac{\partial \Pi}{\partial C_0}} \tag{B.13}$$

which, when reported in the two last ones, leads to the expression of the macroscopic admissible stress components, the parametric expression of the macroscopic criterion then reads:

$$3T_m = (1-f)\left[\frac{1}{\alpha} - \frac{\frac{1}{\alpha}(f^\gamma - f)}{f^\gamma - f + \alpha\frac{\partial \Pi}{\partial C_0}}\right] = \frac{(1-f)\frac{\partial \Pi}{\partial C_0}}{f^\gamma - f + \alpha\frac{\partial \Pi}{\partial C_0}} \tag{B.14}$$

$$T_e = \frac{(f^\gamma - f)\frac{\partial \Pi}{\partial D_e}}{f^\gamma - f + \alpha\frac{\partial \Pi}{\partial C_0}} \tag{B.15}$$

which corresponds to the result obtained by Guo et al. (2008). It is worth noticing that, due to the relaxation of the admissibility condition, (B.14) and (B.15) do not guarantee the upper bound character of the result.

Appendix C. Complementary results concerning the effects of the porosity, friction angle and dilatancy angle on the macroscopic criterion

In this section, we will illustrate the influences of the porosity f and the friction angle ϕ, together with that of the dilatancy angle ψ. The analytical results described in Appendix C.1 will be validated from the FEM computations shown in Appendix C.2.

Appendix C.1. Analytical results

Fig.C.10 displays the yield surfaces with a relatively smaller porosity $f = 0.15$ and a bigger one $f = 0.25$, both for the associated case (AC) and two non-associated cases (NAC1 and NAC2). Moreover, the same values of material parameters as described in subsection 7.1 (for the case $f = 0.2$) are respectively adopted for the three cases. As observed through this figure, the yield loci of non-associated cases are lower than the corresponding associated one. It is interesting to point out that the difference between the yield surfaces of the associated case and non-associated one becomes smaller when the porosity is bigger.

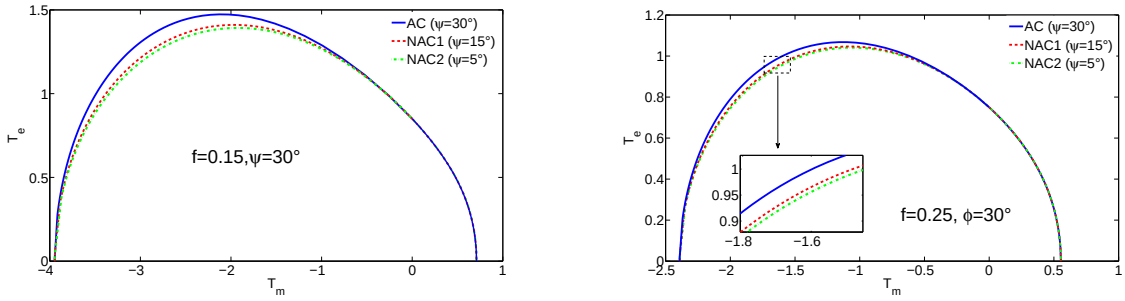

(a) Porosity: $f = 0.15$, friction angle $\phi = 30°$ (b) Porosity: $f = 0.25$, friction angle $\phi = 30°$

Figure C.10: Comparison of yield surfaces illustrated from (65) between the associated case (denoted AC) with dilatancy angle $\psi = 30°$ and two non-associated cases (denoted NAC1 and NAC2) with $\psi = 15°$ and $5°$, respectively.

Next, in order to estimate the influence of the friction angle ϕ on the proposed macroscopic criterion (65), two groups of comparisons with a fixed value of porosity $f = 0.2$ but different friction angles $\phi = 20°$ and $40°$, are reported on Fig.C.11. More specifically, for $\phi = 20°$, the non-associated case NAC1 and NAC2 are defined by $\psi = 15°$ and $\psi = 10°$. For the case of $\phi = 40°$, the values $\psi = 30°$ and $\psi = 20°$ are considered. As shown on figure (65), it is observed that the yield locus of non-associated case decreases with the decrease of ψ. Additionally, from this group of comparisons, it is observed that the difference between the associated yield surface and the non-associated one diminishes when the value of friction angle ϕ is smaller[4].

[4]For the same reductions of dilatancy angle ψ with respect to the associated one.

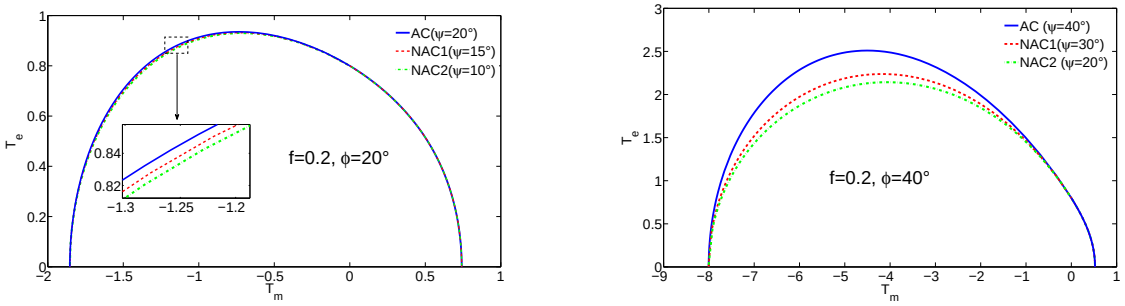

(a) AC: $\phi = \psi = 20°$; NAC1: $\phi = 20°$, $\psi = 15°$; NAC2: $\phi = 20°$, $\psi = 10°$

(b) AC: $\phi = \psi = 40°$; NAC1: $\phi = 40°$, $\psi = 30°$; NAC2: $\phi = 20°$, $\psi = 20°$

Figure C.11: Comparison of plastic flow direction for pure shear loading case obtained from Eq.(69) and FEM solutions.

Appendix C.2. Assessment of analytical results with FEM computations

The influence of the porosity f on the plastic limit states (directions of plastic flow and limit stresses) are reported on Figs.C.12 and C.13. It is observed that the difference between the non-associated case and the associated one is more significant for $f = 0.15$ in the compression zone ($T_m = \Sigma_m/\sigma_0 < 0$) than for the case $f = 0.25$. This fact numerically confirms that, as in Appendix C.1, the difference of the yield locus between the associated case and the non associated one is smaller with the decrease of the friction angle ϕ.

Finally, the influence of friction angle ϕ is assessed through Figs.C.14 and C.15 by adopting a fixed value of porosity $f = 0.2$ and two values of friction angle $\phi = 20°$ and $40°$, respectively. From the illustrations on Figs. 14(b) and 15(b) [5], it is validated that the difference between non-associated case with a fixed dilatancy angle ψ and corresponding associated one is negligible when the friction angle ϕ is adequately smaller.

It is important to point out that for the case $\phi = 40°$, the FEM yield surfaces are relatively higher than the analytical one; this probable results from the proposed stress fields, for which the internal boundary condition is relaxed because of its homogeneous part.

[5]For the non-associated cases with material parameters $\phi = 40°$, $\psi = 30°$ and $20°$, there are not enough FEM results to represent the plastic flow and to construct the yield surface due to the so strong non-linearity of the non-associated model that the corresponding FEM plastic limit states cannot be obtained in this paper.

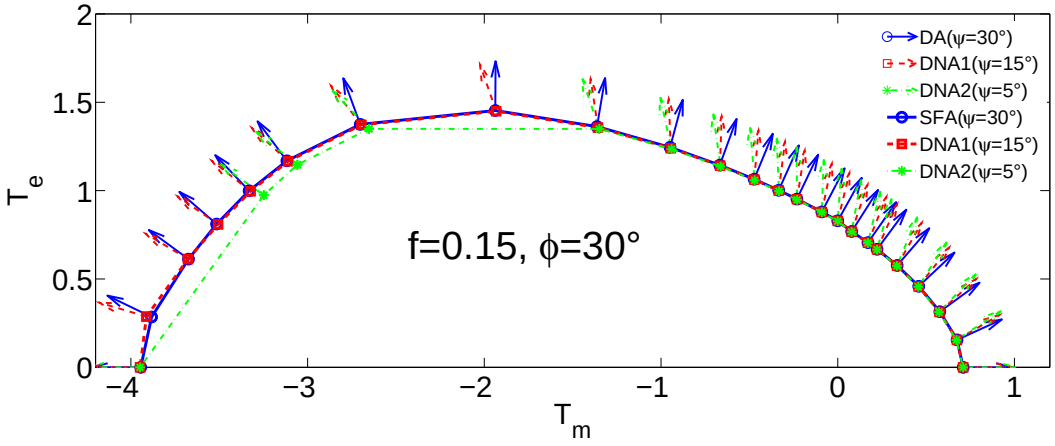

(a) Illustration of FEM results: plastic flow directions (denoted DA for associated case, DNA1 and DNA2 for non-associated ones) and yield surface (denoted SFA for associated case, SFNA1 and SFNA2 for non-associated ones).

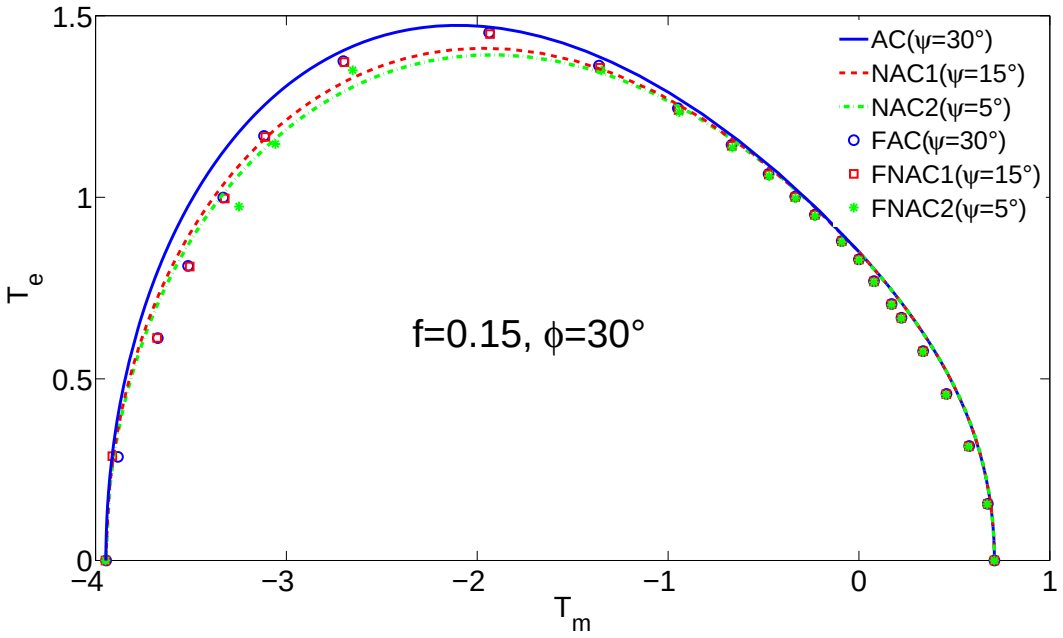

(b) Comparison between the yield surfaces obtained from the established criteria (65) and FEM results (denoted FAC for associated case, FAC1 and FAC2 for non-associated ones).

Figure C.12: Numerical validation for the established model with fixed porosity $f = 0.15$ and friction angle $\phi = 30°$.

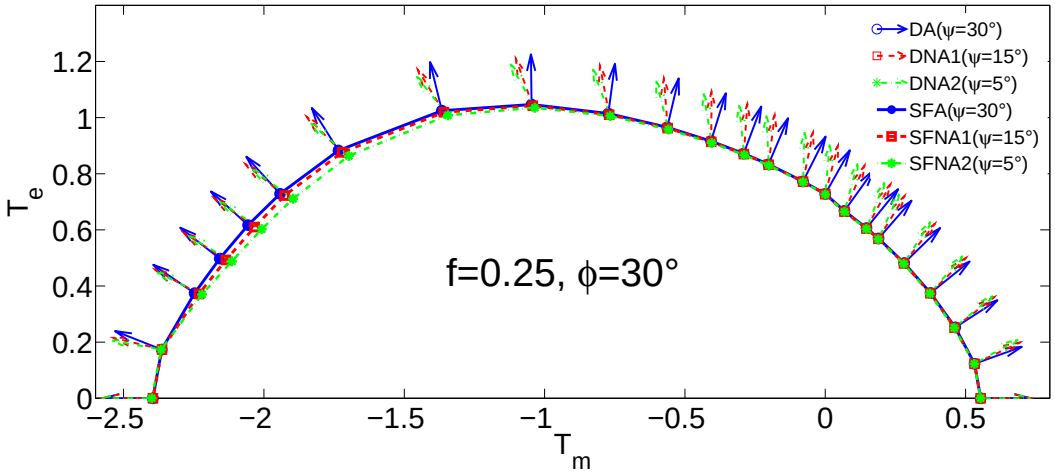

(a) Illustration of FEM results: plastic flow directions (denoted DA for associated case, DNA1 and DNA2 for non-associated ones) and yield surface (denoted SFA for associated case, SFNA1 and SFNA2 for non-associated ones).

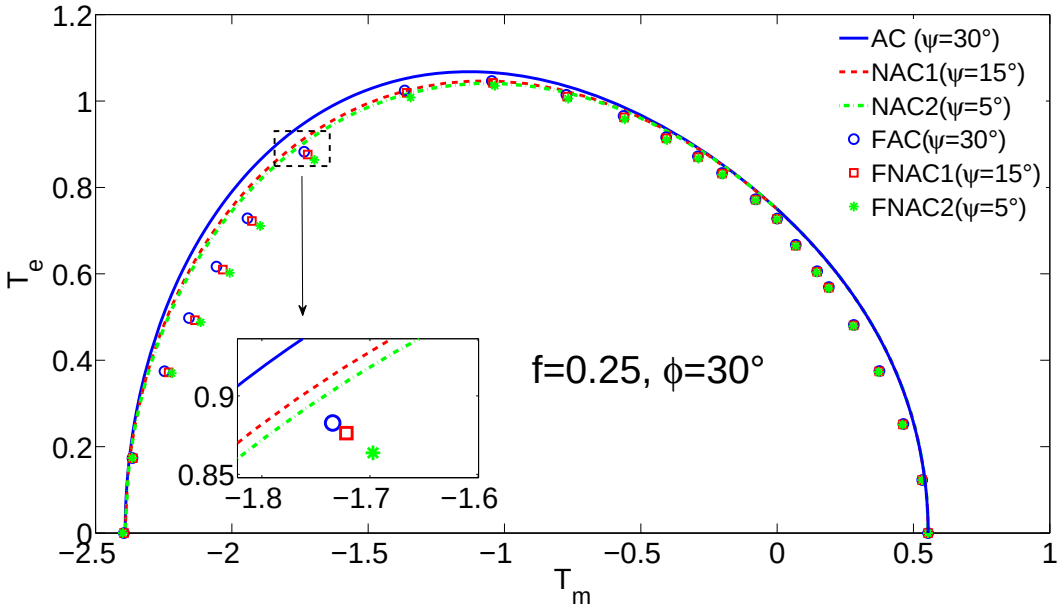

(b) Comparison between the yield surfaces obtained from the established criteria (65) and FEM results (denoted FAC for associated case, FAC1 and FAC2 for non-associated ones).

Figure C.13: Numerical validation for the established model with fixed porosity $f = 0.25$ and friction angle $\phi = 30°$.

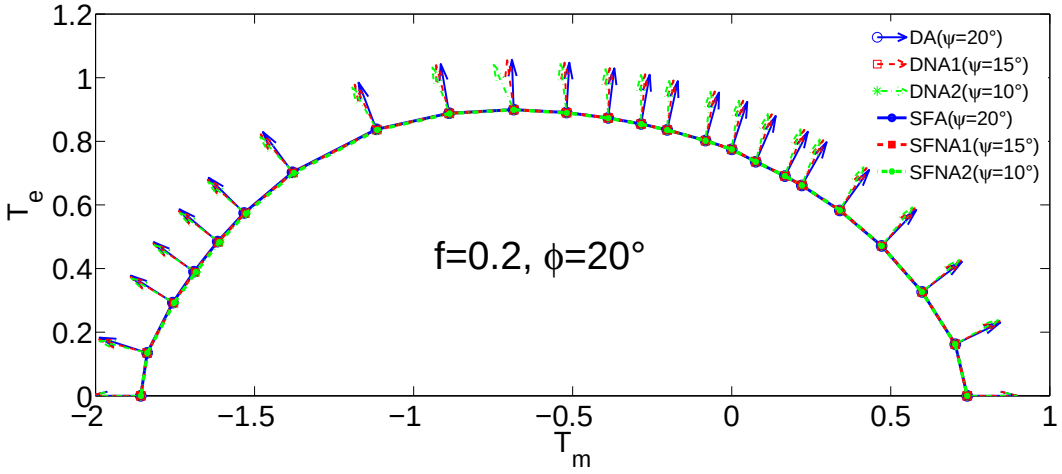

(a) Illustration of FEM results: plastic flow directions (denoted DA for associated case, DNA1 and DNA2 for non-associated ones) and yield surface (denoted SFA for associated case, SFNA1 and SFNA2 for non-associated ones).

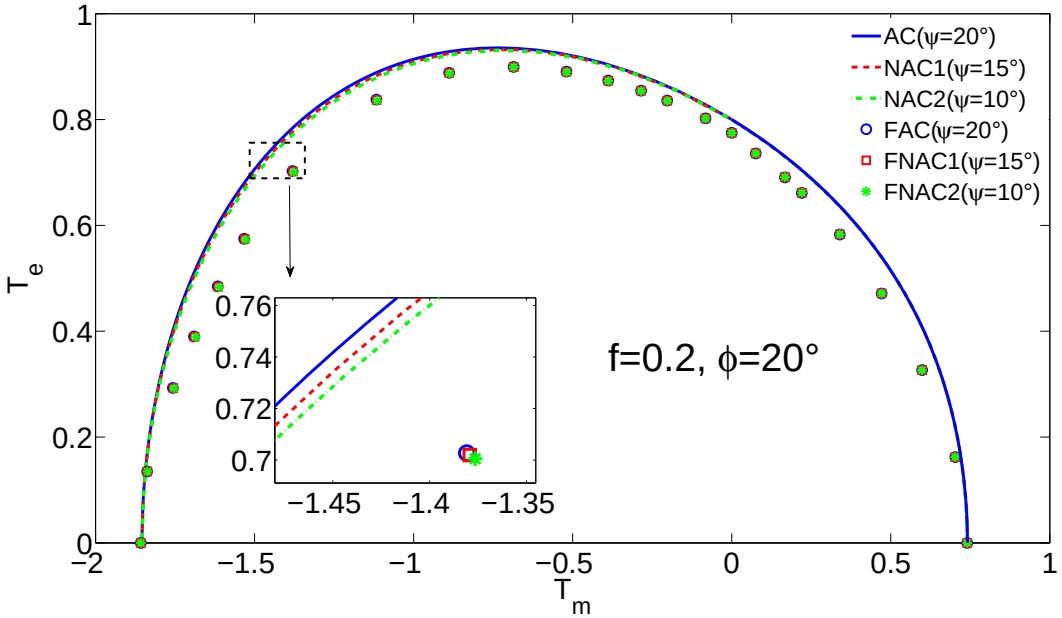

(b) Comparison between the yield surfaces obtained from the established criteria (65) and FEM results (denoted FAC for associated case, FAC1 and FAC2 for non-associated ones).

Figure C.14: Numerical validation for the established model with fixed porosity $f = 0.2$ and friction angle $\phi = 20°$.

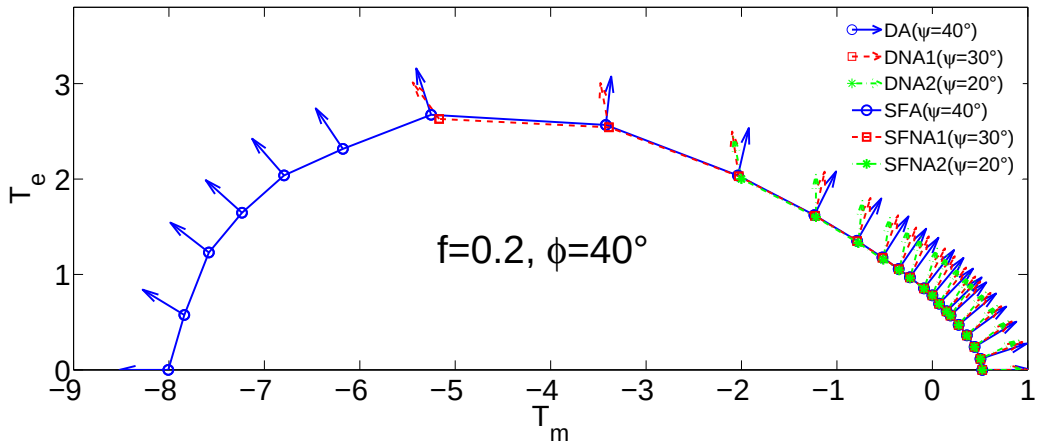

(a) Illustration of FEM results: plastic flow directions (denoted DA for associated case, DNA1 and DNA2 for non-associated ones) and yield surface (denoted SFA for associated case, SFNA1 and SFNA2 for non-associated ones).

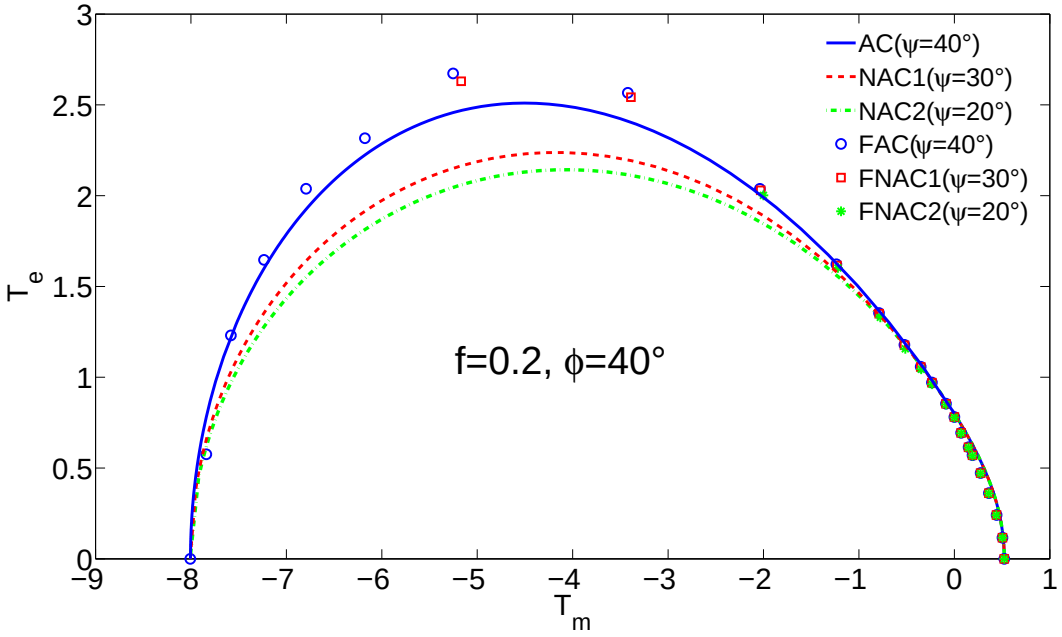

(b) Comparison between the yield surfaces obtained from the established criteria (65) and FEM results (denoted FAC for associated case, FAC1 and FAC2 for non-associated ones).

Figure C.15: Numerical validation for the established model with fixed porosity $f = 0.2$ and friction angle $\phi = 40°$.

Appendix D. Complementary results concerning the effects of the porosity, friction angle and dilatancy angle on the macroscopic flow rule and on the porosity evolution

In Figs.D.16 to D.19 we aim to illustrate the influences of porosity f and friction angle ϕ on the plastic flow rule with respect to the variation of macroscopic stress triaxiality T_m/T_e, both from the established law (69) and the FEM computations. It can be observed again that the difference between the associated case and the non-associated ones increases with the decrease of the porosity, and with the increase of friction angle. The same conclusion can be deduced from the Figs.D.20-D.23, which illustrate the void growth rate also with repsect to the macroscopic stress triaxiality.

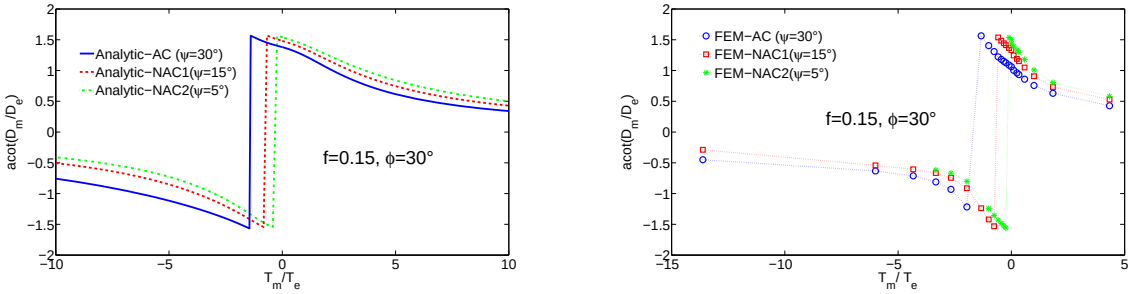

(a) Analytic (b) FEM

Figure D.16: Analytical result and FEM solutions for plastic flow direction with the fixed values of porosity $f = 0.15$ and friction angle $\phi = 30°$.

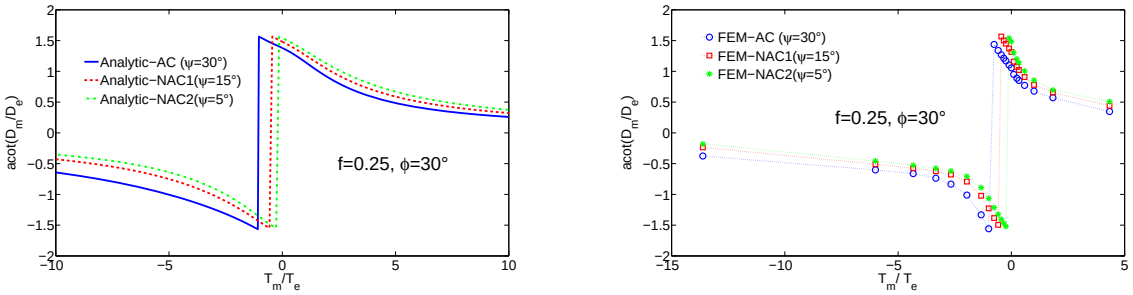

(a) Analytic (b) FEM

Figure D.17: Analytical result and FEM solutions for plastic flow direction with the fixed values of porosity $f = 0.25$ and friction angle $\phi = 30°$.

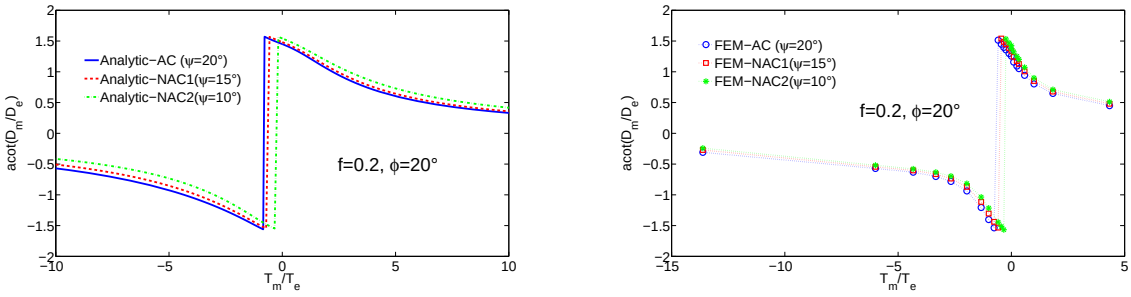

(a) Analytic (b) FEM

Figure D.18: Analytical result and FEM solutions for plastic flow direction with the fixed values of porosity $f = 0.2$ and friction angle $\phi = 20°$.

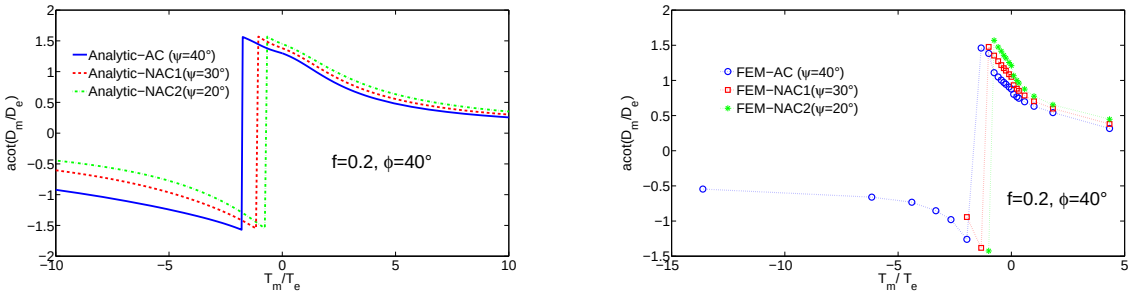

(a) Analytic (b) FEM

Figure D.19: Analytical result and FEM solutions for plastic flow direction with the fixed values of porosity $f = 0.2$ and friction angle $\phi = 40°$.

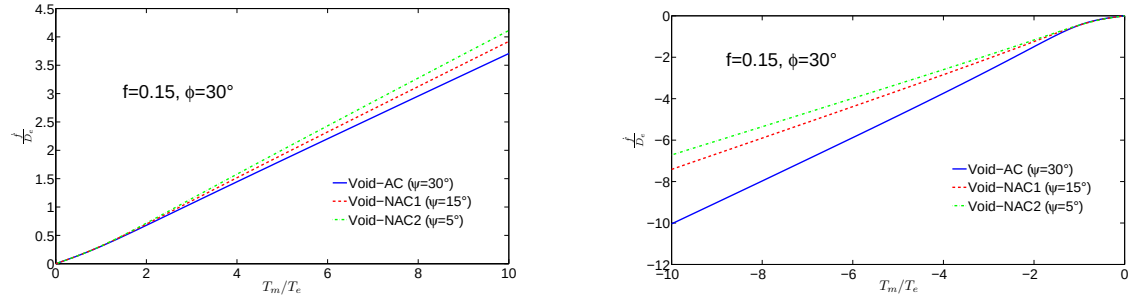

(a) Variation with positive triaxialities (b) Variation with negative triaxialities

Figure D.20: Analytical result of the plastic void growth with a initial value of porosity $f = 0.15$. Friction angle $\phi = 30°$.

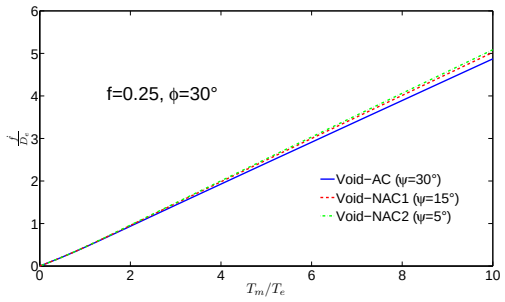

(a) Variation with positive triaxialities

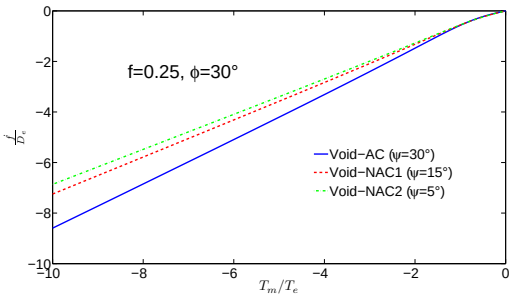

(b) Variation with negative triaxialities

Figure D.21: Analytical result of the plastic void growth with a initial value of porosity $f = 0.25$. Friction angle $\phi = 30°$.

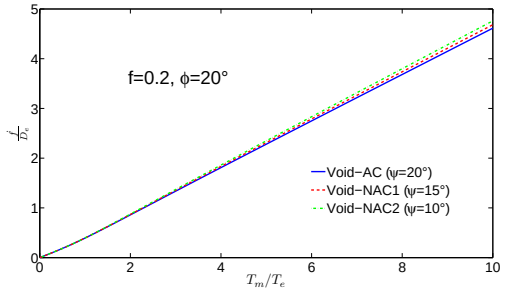

(a) Variation with positive triaxialities

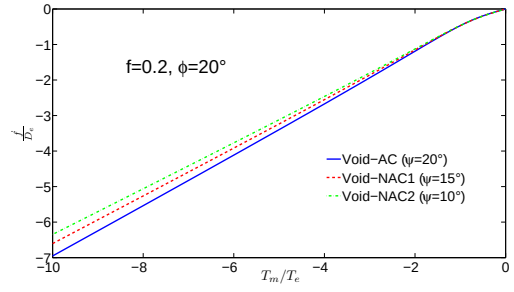

(b) Variation with negative triaxialities

Figure D.22: Analytical result of the plastic void growth with a initial value of porosity $f = 0.2$. Friction angle $\phi = 20°$.

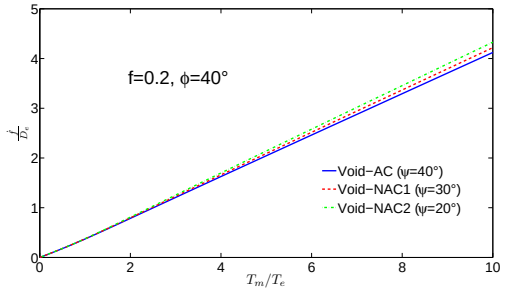

(a) Variation with positive triaxialities

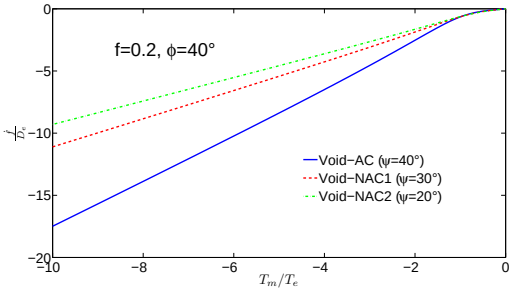

(b) Variation with negative triaxialities

Figure D.23: Analytical result of the plastic void growth with a initial value of porosity $f = 0.2$. Friction angle $\phi = 40°$..

General conclusions and perspectives

The main objective of this thesis was to formulate a micro-macro approach for a large class of porous plastic materials whose matrix obeys to non-associated flow rules. It was conducted by applying the bipotential theory which allows to extend Limit Analysis theory considering dual fields (stress field and strain rate field), simultaneously in the homogenization problem. A crucial point for the extended variational limit analysis approach is the simultaneous choice of the trial stress field and velocity field.

Specifically speaking:

- In the first chapter, we have firstly recalled the basic variational principals and presented the framework of classical limit analysis and the resulting upper bound and lower bound theorem for associated plasticity. Moreover, it has also been recalled that the conventional kinematical Limit Analysis theory (upper bound theorem) and its applications in literature proposed by Gurson (1977) to the von Mises type porous materials, and by Guo et al. (2008) to the associated Drucker-Prager one. Finally, the bipotential theory and the corresponding variational formulations for non associated plasticity was detailed.

- Before solving the main problem of this thesis (non-associated macroscopic modelling), we proposed in Chapter 2 a stress-based variational methodology of ductile porous materials in the framework of statical Limit analysis approach (Lower bound theorem). Due to the relaxed void boundary condition resulting from the axisymmetric trial stress field, the criterion could be seen as a quasi-lower bound. Nevertheless, an interesting feature has been analytically obtained for the established criterion that it depends not only on the two stress invariant - macro mean stress and macro equivalent stress - but also on the sign of third invariant of stress deviator. The general contribution of the third invariant has been also provided from the completeness of this Chapter by adopting the same variational approach, but with a non-axisymmetric trial stress field. For the porous material with a von Mises matrix, our study provides for the first time a general 3D criterion including the effects of all stress invariants.

- Next, before proposing a macroscopic model for porous material with non-associated Drucker-Prager matrix we investigated in Chapter 4. The plastic limit state of a hollow sphere with non-associated plastic matrix subjected to hydrostatic loadings. To this end and in order to establish the exact solution, upper bound and lower bound theorems are both applied. It has been demonstrated that for the non associated case, the limit load and stress field of the hollow sphere under hydrostatic loadings have the same expression as the associated one. This fact has been validated from the numerical solutions.

- Finally, we have proposed a new general methodology to derive the macroscopic model for non-associated porous materials thanks to the bipotential-based limit analysis method, combined with homogenization techniques. The choice of trial stress field and trial velocity one has been detailed. The variational formulation proves that the macroscopic criterion of the non-associated case expresses a different form, and the illustrated yield locus is lower with respect to the associated one (except for the pure hydrostatic loading and the pure shear one). The formula of the macroscopic flow for non associated porous materials has also been established.

Additionally, some improvements to the study may be brought through additional works in the future. First, the SVM models (see Chapter 2 and its complement) can be suitably improved by searching and implementing more refined trial stress fields. Other important perspectives lie in the possibility now to propose a lower bound model for the considered class of non-associated porous materials by formulating more refined couple of trial stress field and a trial velocity one. Extensions to saturated porous materials will be also of primary importance for several application in geomechanics.

References

A. L. Gurson, 1977. Continuum theory of ductile rupture by void nucleation and growth: part I, yield criteria and flow rules for porous ductile media. *J. Engrg. Mater. Technol.*, 99:2-15

Guo, T.F., Faleskog, J., Shih, C.F.2008. Continuum modeling of a porous solid with pressure-sensitive dilatant matrix. Journal of the Mechanics and Physics of Solids, 56, 2188-2212.